UNIVERSITY OF CALIFORNIA,
IRVINE

Hydrogen's Role in Power Markets and Freight Transportation to Achieve Carbon Neutrality

DISSERTATION

Submitted in partial satisfaction of the requirements
for the degree of

DOCTOR OF PHILOSOPHY

In Civil and Environmental Engineering

By

Clinton Thai

Dissertation Committee:
Professor Jacob Brouwer, Chair
Professor Steven Davis
Professor Vince McDonnell

2023

DEDICATION

I dedicate this to my parents and wife for their unconditional love and support.

TABLE OF CONTENTS

LIST OF FIGURES

LIST OF TABLES

LIST OF ACRONYMS

Acronym	Description
BAU	Business as usual
BESS	Battery energy storage system
BG	Nominal locational marginal price node
BOP	Balance of Plant
BP	Nominal locational marginal price node
BTMPV	Behind the meter photovoltaic
CAISO	California Independent System Operator
CAP	Climate action plan
CARB	California Air Resources Board, an agency
CCA	Community choice aggregation
CEC	California Energy Commission, an agency
CF	Capacity factor
CI	Carbon Intensity
DAM	Day-ahead market
EAC	Equivalent annual cost
EIA	Energy Information Administration, an agency
EO	Executive order
EOL	End-of-life
EPA	Environmental Protection Agency, an agency
EPRI	Electric Power Research Institute, an agency
GHG	Greenhouse gas
GREC	Gaseous renewable energy certificate, novel term of this work
GT-CC	Gas-turbine combine-cycle
HDV	Heavy-duty vehicle
H-S	High-demand solar-dominant scenario, nominal scenario of this work
H-W	High-demand wind-dominant scenario, nominal scenario of this work
IOU	Investor-owned utility
LCFS	Low-carbon fuel standard, a state program
LCOE	Levelized cost of electricity
LCOT	Levelized cost of transmission
LDV	Light-duty vehicle
LMP	Locational marginal price
L-S	Low-demand solar-dominant scenario, nominal scenario of this work
L-W	Low-demand solar-dominant scenario, nominal scenario of this work
MDV	Medium-vehicle duty
Mt	Million metric ton, a unit of mass measure
MTCO2e	Million metric ton of equivalent carbon dioxide, a unit of mass measure
MWh	Megawatt-hour, a unit of energy measure
NREL	National Renewable Energy Laboratory, an agency

OOS	Out-of-state
P2G	Power-to-gas
P2G2P	Power-to-gas-to-power
P2G-FC	P2G using fuel cell for electrification, nominal pathway of this work
P2G-GT	P2G using gas turbine for electrification, nominal pathway of this work
PDP	Physical disposition pathway, novel term of this work
PG&E	Pacific Gas and Electric Company, an investor-owned utility
PLEXOS	Commercial energy market power system simulation software
PPA	Power purchase agreement
PV	Photovoltaic
REC	Renewable energy certificate
RES%	Renewable energy supply percentage
ROI	Return on investment
RTM	Real-time market
SCE	Southern California Edison Company, an investor-owned utility
SCG	Southern California Gas Company, an investor-owned utility
SDG&E	San Diego Gas and Electric Company, an investor-owned utility
SOC	State-of-charge
T&D	Transmission and distribution
UC	University of California
UCI	University of California, Irvine
VDP	Virtual disposition pathway, novel term of this work
WL	Nominal locational marginal price node
ZEV	Zero-emission vehicle

ACKNOWLEDGEMENTS

I would like to thank Dr. Prof. Jack Brouwer, who is an amazing mentor and role model. I would like to thank Dr. Prof. McDonell who oversaw the start of my time at APEP and who is now serving on my defense committee. I would also like to acknowledge Professor Davis, who has emphatically supported my academic endeavors. Further, the staff at APEP have spurred my academic and professional development, namely: Dr. Reed, Dr. Flores, Dr. Mastropasqua, and, in addition, the many students who have come before me and those who have embarked on this journey alongside me. With great gratitude, thank you to everyone who has made this journey possible.

VITA

Education

University of California, Irvine | Irvine, CA

Ph.D. in Civil and Environmental Engineering — December 2019 - March 2023
M. S. in Mechanical Engineering (3.86/4.00) — June 2018 - December 2019
B.S. in Mechanical Engineering (3.78/4.00) — September 2015 - June 2018

Experience

Advanced Power & Energy Program | Irvine, CA

Graduate Applied Energy Researcher — June 2018 – March 2023

- Develop and optimize 2050 California spatially-resolved power generation model to meet cross-sector hydrogen demand, minimizing total system costs.
- Calculate statewide distributed electrolyzer injection potential through geospatial analysis to estimate carbon reductions with local renewable gas production.
- Lead team of 9 engineers in supply chain feasibility study of statewide hydrogen adoption for California freight transportation as a killer application
- Develop novel low-carbon fuel standard pathway utilizing hydrogen injection to advise policy which facilitates increasing gas grid renewable contents.
- Execute cost-benefit analyses for both retail and wholesale settings using utility tariffs, system price nodes, and relevant technological cost assumptions:
    - Dispatch of local energy resources with technical potential of distributed PV and energy storage in different campus settings
    - Implementation of energy storage at congested PV farm considering multiple storage technologies and usage of the LCFS program
- Coordinate with industry partners for site visits and prepare deliverable reports.
- Perform cash flow analysis for emerging zero-emission technologies to establish sound assumptions in other modeling work.
- Investigate locational price changes for marginally congested utility-scale solar PV farms by conducting analysis of variance statistical study.

Advanced Power & Energy Program | Irvine, CA

Undergraduate Researcher — *January 2017 - June 2018*

- Evaluate seasonal shifting storage dynamics and magnitude considering hydropower, wind, solar, and load dynamics in Pacific Northwest.
- Perform cost savings analysis, design and installation of micro-scale Mazda rotary engine natural gas cogeneration demonstration project.

Publications

C. Thai and J. Brouwer, "Comparative Levelized Cost Analysis of Transmitting Renewable Solar Energy," Energies (Basel), vol. 16, no. 4, p. 1880, Feb. 2023, doi: 10.3390/en16041880.

C. Thai and J. Brouwer, "Injecting Hydrogen Into Natural Gas Pipelines at Congested Solar Farms for Transportation Fuel," in PSIG Annual Meeting Proceedings, May 2022.

C. Thai and J. Brouwer, "Challenges estimating distributed solar potential with utilization factors: California universities case study," Appl Energy, vol. 282, no. PB, p. 116209, 2021

Z. Heydarzadeh, M. Mackinnon, C. Thai, J. Reed, and J. Brouwer, "Marginal methane emission estimation from the natural gas system," Appl Energy, vol. 277, p. 115572, Nov. 2020.

Z. Heydarzadeh, M. Mackinnon, C. Thai, and J. Reed, "Comprehensive Study of Major Methane Emissions Sources from Natural Gas System and Their Dependency to Throughput," Applied Energy Symposium: Mit A+B, Cambridge, USA, 17-19 May, 2020.

Z. Heydarzadeh, D. McVay, R. Flores, C. Thai, and J. Brouwer, "Dynamic Modeling of California Grid-Scale Hydrogen Energy Storage," ECS Trans, vol. 86, no. 13, p. 245, Jul. 2018

C. Thai, L. Mastropasqua, A.H. Mejia, A. Saeedmanesh, E. Dailey, et al., "Cleaning up freight transportation in California," Submitted to Nature Communications (under review).

C. Thai and J. Brouwer, "Is hydrogen optimal for power generation?" Submitted to Scientific Reports (under review).

C. Thai and J. Brouwer, "Limitations in Decarbonizing University Campus Microgrid," Submitted to Energy Conversion and Management (under review).

Conference Presentations

C. Thai, "Injecting Hydrogen Into Natural Gas Pipelines at Congested Solar Farms for Transportation Fuel." *Pipeline Simulation Interest Group Annual Meeting*. San Diego, CA, 2022.

C. Thai, "PV Solar Potential and Integration to Reach Carbon Neutrality at UCI." *International Colloquium on Environmentally Preferred Advanced Power Generation*. Irvine, CA, 2021.

ABSTRACT OF THE DISSERTATION

Hydrogen's Role in Power Markets and Freight Transportation to Achieve Carbon Neutrality

By

Clinton Thai

Doctor of Philosophy in Mechanical and Aerospace Engineering

University of California, Irvine, 2023

Professor Jack Brouwer, Chair

Hydrogen is a flexible form of chemical storage and fuel for both power generation and transportation applications. In the context of decarbonization, hydrogen is the key technology at the highest renewable penetration percentages in the power generation sector. The transportation sector will likely be the primary driver for hydrogen demand due to the difficulty of decarbonizing heavy-payload long-distance freight applications. Hydrogen-based technology complementing other renewable resources must be well understood.

Techno-economic analyses comparing power-to-gas (P2G) and battery energy storage systems (BESS) are carried out in both wholesale and retail settings. In addition, novel low-carbon fuel standard (LCFS) pathways are developed that utilize injecting hydrogen to promote increasing the gas grid's renewable contents. Further, a feasibility analysis for a completely renewable fuel supply chain meeting a bottom-up estimated completely decarbonized freight demand in 2050 is executed. Finally, a spatially-resolved hourly annual California state power generation model is optimized to meet massive hydrogen demand.

Assuming zero power-to-gas (P2G) capital costs, current market signals do not promote seasonal energy storage despite the need for at least 72 and 115 TBtu for an 87% and 90% renewable energy supply (RES%). Deploying P2G systems in distributed settings enables distributed PV resulting in similar increases to RES% compared to BESS. A LCFS pathway that promotes injecting hydrogen into the gas grid is the most profitable means of deploying electrolyzers in the short term. Distributed electrolyzers are found to only be able to inject in roughly 10% of distributed pipeline mains, suggesting significant investment is required on the transmission level. This is especially true as total transportation hydrogen demand in 2050 spans from 9-20 MMT/yr. Meeting 4.25 MMT/yr as opposed to 1.25 MMT/yr of hydrogen demand would result in an 8% increase in power generation sector cost, with the benefit of reducing carbon emissions by 73%, equivalent to a carbon abatement of 34 $/MTCO2e. A zero-carbon constraint on society would only further increase system costs by requiring more hydrogen production within the state, but hydrogen remains the only extensible renewable solution in completely decarbonizing both the power generation and transportation sectors due to the limitations of BESS.

1 Introduction

1.1 Motivation: California and renewable energy

The low price at which solar PV could bid into the market midday in cohesion with an electric demand peak in the evening results in the notorious "duck curve," a figure that graphs load after solar dispatch throughout the day. The biggest challenge with the duck curve is that NGCC power plants are the primary resource for meeting load as solar PV generation declines proportionally, often imagined to be the steep neck of the duck. In 2020, 40% of California's load was met by renewables [35], but many questions arise regarding what the future of the grid looks like moving toward higher renewable contents given this limitation. Local limitations have also become more prevalent, specifically where there are many solar PV power plants in rural areas with transmission lines previously installed without the consideration of such a resource. The congestion at this level results in price signals that suggest additional solar should not be installed. As a result, developing solar power plants with on-site battery energy storage at utility-scale power plants is becoming increasingly common.

California has the goal of 100% renewable electricity by 2045 [36] with a 50% checkpoint by 2030. Similarly, executive order (EO) B-55-18 aims for the state to be carbon neutral by 2045, largely impacting the transportation sector. EO B-16-12 [37] calls for 1.5 and 5 million ZEV sales in 2025 and 2030, respectively. EO N-78-20 aims for 100% of new drayage, LDV, and off-road vehicles sales to be ZEV. The same bill aims for 100% of new MDV and HDV be ZEV by 2030 [38]. EO N-19-19 [39] calls for aggressive investment and action to combat climate change proceeded by SB129 which explicitly dedicates almost 4 billion dollars over three years for ZEV

investments, infrastructure, and clean transportation equity programs [40]. This is largely to bolster the current progress toward meeting the goal established by EO B-48-18 [41], which aims to have 200 hydrogen fueling stations and 250,000 electrical vehicle chargers. The simultaneous push for decarbonizing the transportation sector provides major synergistic potential as the excess renewable generation throughout the day can be used for renewable fuels.

Utilizing hydrogen as a form of chemical energy storage is possible through the usage of electrolyzers which use electricity to split water molecules into hydrogen and oxygen. Hydrogen can then be used for the reverse electrochemical reaction using a fuel cell. This effectively is a battery in which the storage of energy as a gas is resistant to leakage or parasitic losses. Though this process is less energy efficient than simply storing electricity in a lithium-ion battery, hydrogen has the flexibility to be mixed into the existing gas infrastructure or used to synthesize renewable hydrocarbon fuels. This option is popularly discussed when accommodating greater amounts of renewable generation as it is one way to manage the dynamics of renewable generation.

1.2 Research Goals

The goal of this research is to assess technological advancements and policy necessary to facilitate high renewable penetration future. A central focus is on capturing power-to-gas energy storage's value to the electricity grid and the resulting limitations of hydrogen injection in existing gas grids in present time and its evolution into 2050. Adoption of energy storage technology including battery-based technology for various zero carbon applications are considered: power generation, industrial freight, emergency backup power, and electric grid transmission relief.

1.3 Objectives

Objective 1. Review literature on modeling energy storage system deployments, power grid markets, policy impacting technology costs and operation of an increasingly renewable utilities infrastructure.

Objective 2. Model and simulate energy storage operation complementing a utility-scale solar PV power plant facing electricity transmission congestion.

Objective 3. Evaluate role of energy storage in high renewable penetration in distributed suburban microgrid campus setting.

Objective 4. Evaluate the vehicle hydrogen demand for freight for zero-emissions powertrains and the feasibility of the fuel supply chain.

Objective 5. Evaluate the distributed potential and identify candidate sites for electrolyzer systems injecting electrolytic hydrogen to the gas grid increasing the renewable attributes of the gas systems.

Objective 6. Model electrolyzers integrated in California's grid and meeting state hydrogen demands in a unit commitment economic dispatch optimization in 2050 using PLEXOS.

1.4 Approach

Regarding the research goal of understanding the value of hydrogen storage compared to battery energy storages, the following tasks are established, corresponding to the objectives presented in Section 1.3 where: the first four systematically evaluate the role energy storage in different sectors and the last two focus on the overall of role of power-to-gas on a system level.

Task 1. Background (Chapter 2).

- Distinguishing taxonomy of renewable energy scopes (Section 2.1)
- Conduct technological overview of energy storage options (Sections 2.2 & 2.3)
- Address dynamical challenges in energy conversion in practice (Section 2.3)
- Review studies oriented toward accommodating renewable resources and capacity planning (Section 2.4)
- Identify remaining economic and sociopolitical pressures (Sections 2.5 & 2.6)

Task 2. Investigate energy storage operation complementing a utility-scale solar PV power plant (Chapter 3).

- Establishing scenario for congested and uncongested PV power plant using locational marginal price nodes (Section 3.1)
- Energy arbitrage via battery energy storage system and power-to-gas-to-power (Sections 3.1.1 & 3.1.2)
- Develop potential low-carbon fuel standard scenarios as a revenue stream for power-to-gas (Sections 3.1.3 & 3.1.4)
- Conduct cost-benefit analysis with established strategies and low-carbon fuel standard pathways (Section 3.2)
- Identify sensitivity changes to energy arbitrage impacting factors as contingencies for future economic viability (Section 3.3)

Task 3. Evaluate role of energy storage in distributed suburban campus setting (Chapter 4).

- Identify campus resources to meet electric demand (Section 4.1)
- Evaluate the potential of energy storage to achieve carbon neutrality status (Section 4.2)
- Investigate value of implementing energy storage when also doubling as emergency backup generators and when used exclusively for the latter (Sections 4.3 & 4.4)
- Quantify emission and air pollutant reduction potential (Section 4.5)

Task 4. Evaluate the freight hydrogen demand and fuel supply chain feasibility (Chapter 5).

- Characterize freight trade volume and routes for ships, heavy-duty trucks, and rail (Section 5.2)
- Identify feasibility of battery-based and fuel cell-based powertrains for routes mentioned above (Section 5.2)
- Identify powertrain and supply chain process efficiencies to calculate total hydrogen demand (Sections 5.2 & 5.3)

- Evaluate necessary renewable capacity and land requirements for fuel procurement and estimate resulting costs (Section 5.4)

Task 5. Identify electrolytic hydrogen high-pressure distribution and transmission injection sites and investigate their contribution to maximizing renewable hydrogen on the gas grid (Chapter 6).

- Procure utilities infrastructure and parcel-level land-use data (Section 6.2.1)
- Establish algorithm to identify and treat distributed electrolyzer sites (Section 6.2.2)
- Investigate development potential of distributed electrolyzer sites (Section 6.2.3)
- Identify and treat the selection of transmission electrolyzer sites (Section 6.2.4)
- Calculate and contextualize distributed electrolyzer contribution to the overall gas system (Section 6.3.1)
- Investigate electrolyzer sites injecting into transmission system and identify key differences (Section 0)

Task 6. Investigate electrolyzers role in the power grid when co-optimized with meeting renewable fuel demands in 2050 (Chapter 7).

- Use PLEXOS to establish representative California electric network (Sections 7.1.1 & 7.1.3)
- Develop operational profile for energy storage to participate in markets (Section 7.1.2).
- Characterize power generation plants (Sections 7.1.4 & 7.1.5)
- Evaluate high installation levels of electrolyzer and renewable generation capacity to meet state fuel demands and renewable standards. (Sections 7.2.1 & 7.2.2)
- Investigate the seasonal dynamics power generation and storage (Sections 7.2.3 & 7.2.4)
- Identify challenges with transmission and general flow of power. (Section 7.2.5)

2 Background

2.1 Renewable primary energy

In the 21st century, renewable energy is a prominent term in social and political conversations, yet what might be considered renewable is often not universally agreed on. Though the definition of what is renewable is debatable, this work is established and discussed in the context of the California energy grid. However, even as policy is evolving, different stakeholders can often have slightly different definitions or terms for categories for what might be considered renewable. This discrepancy is even more present when comparing local and national approaches or perspectives to those overseas.

2.1.1 Types of renewable power

A brief background of the different types of renewable power generation technologies are provided—each with their strengths and weaknesses in certain settings. The sun provides instantaneous energy in the form of electromagnetic radiation. As such it provides light and heat, which historically has been harnessed by different means. The visible light has historically been reflected and concentrated to provide thermal heating in concentrated solar power plants [1]. This contrasts the now more commonly understood type of solar generation post-2011 when solar photovoltaic panels saw major cost reductions and installations throughout. Solar photovoltaic cells utilize the energy from the light form to move electrons and is primarily an electrochemical reaction. These panels, unlike the CSP predecessor, have the strength of being highly modular and scalable, allowing them to be installed on rooftops, rather than requiring major amounts of

dedicated land. A positive feedback cycle for cost reductions is created with technological improvements and policy favoring adoption. Ultimately, installing solar PV became a largely economic choice as utility-scale power plants quickly became one of the cheapest sources of power generation on an energy basis. A major factor that working against this is local congestion and the generation dynamics which will be further explored in Chapter 3.

Simultaneously, wind energy has rapidly grown in the United States with a cumulative total of 136 GW in 2021 [2]. It is especially prevalent in midwestern united states where land is more abundant and wind speeds are more favorable for power generation.

While hydropower is perhaps the oldest form of renewable power generation, its ability to be procured as an asset is largely limited by its geographical requirements. In some jurisdictions and definitions, hydropower's consideration to be a renewable source of power is size dependent [3]. It has been a critical grid asset as it is a flexible generator with low operating costs. Its operation is limited by the available amount of water in the reservoirs. Some hydropower plants are run-of-the-river and do not have this flexibility, but generally hydropower plants with head pond and tail pond forming a closed system, as typical of in California, is assumed in this work when referring to hydropower.

Geothermal power plants are another baseline renewable power generator but have more geographic constraints than hydropower plants, slowing growth [4]. As such, geothermal power plants have historically provided relatively minor power capacities in California thought to be maximized around 3 GW by 2050 [5].

California does not consider nuclear as a source of renewable power, so the last power plant in the state rated at 2.2 GW is set to close by 2025 which some studies will look to convert to be renewable like Temiz and Dincer [6] for Bouma et al. [7] to produce heat, power, clean water, and hydrogen. As a contributor to electric load, new renewable generation would need to be procured and to fill the void left by decommissioning this massive power plant.

2.1.2 Retail versus wholesale power generation

Of the previously mentioned resource types of renewable energy, solar PV is unique in that it is seen in both distributed and centralized in utility-scale settings. Distributed PV systems are at the crux of microgrids and have been found to have massive benefits to society in terms of decarbonization and lower emissions. Even when considering the lifecycle emissions, Peng and Lu [8] find that emissions are an order of magnitude lower than fossil fuels. This is in addition to the benefit of circumventing energy transmission necessary for utility-scale power plants. As a result, there are lower ohmic losses associated with the transmission of electricity. The disadvantage of distributed PV electricity is the misalignment of generation and load and controlling the excess can be challenging for system operators. Commercial batteries are becoming an increasingly common solution in distributed settings. Utility-scale solar faces the same problem, but the availability of land to install energy storage systems and local transmission capacity are both higher. In addition, other dispatchable generators are connected to the transmission grid, such as natural gas combined cycle plants to help with balance load and generation. This contrasts the distributed transmission networks that lack generation diversity and have limited transmission flexibility [9].

Distributed PV is valuable in that it can produce low-cost electricity close to loads and despite the challenges that may arise managing the grid stability and excess production, many researchers are investigating the technical potential for distributed PV. Assouline et al. [10] use a random forest machine learning algorithm to quantify the monthly and yearly rooftop PV electricity production for Switzerland. The data is evaluated at 200 x 200 m^2 159,105 groups and they find 25.3% of the yearly demand could be met with rooftop PV (64.4 TWh/yr). Margolis et al. [11] use lidar data and building footprints to identify rooftop capability to host PV. Important factors that go into the percentage of local city demand met by PV are rooftop suitability, household footprint per-capita, solar resource, and electricity consumption. The authors find as a result, some cities can meet 88% of demand whereas some cities can only meet 16% from rooftop PV. Parking lot PV canopies were not considered in this work.

Another difference between distributed and centralized resources is ownership. Distributed ownership is simpler than the latter. In distributed ownership, the building owner often hires a commercial seller and installer. Its operation is then dependent on the setting—in California there is net metering. Net metering allows for generation to be exported and offsets any imports in an established timeframe, often the utility billing cycle. However, in the utility setting, the developer may differ from the operator and even then, may have a contract in place where the energy put on the grid is claimed by a load at a remote location. This arrangement is known as a power purchase agreement. Wholesale power generators make offers to the energy market where buyers bid in the marketplace. This in addition to physical transmission limitations

and losses result in a geospatially resolved electricity market price, often aggregated, and represented by locational marginal prices.

2.1.3 Quantifying solar potential in distributed setting

The amount of distributed PV that can be deployed depends upon how much rooftop space is available and their performance corresponds with solar irradiance potential. Freitas et al. [12] have conducted a review of methods modeling the irradiance aspect and is recommended for the performance aspect. On the other hand, a 2013 NREL report [11] reviews rooftop suitability methods and patents for commercial software. According to this report, rooftop suitability evaluations generally fall into three categories: constant-value, manual selection, and GIS-based methodologies.

These three categories have some differences compared to a similar set of three categories suggested by Schallenberg-Rodríguez [13]: extrapolating from a single sample, extrapolating from multiple samples, and complete census databases. Both sets of three methods essentially address varying ranges of external validity, computational intensity, and available data. In other words, when databases have a detailed count and sizes of rooftops it is easy to make good estimations, but this data is not always available. As a result, the remaining methods are a balance of computational rigor and replicability.

Many works in the literature try to identify the total potential or limit to which PV can be deployed. These vary in scope from as small as a single building to as large as entire nations. Work from Strzalka et al. [14] is of interest as they consider a single building case analysis and evaluate a greater region by different means in the same paper. Many other attempts exist for quantifying

the solar capacity for campuses [15] [16], small towns [3] [17] [18] [19], large cities [8][20] [21] [22] [23], provinces [24], and entire countries [25] [26] [27].

Bergamasco and Asinari [28] attempt to address several estimation uncertainties with coefficients in their analysis. In addition, they acknowledge a difference in residential and industrial buildings. This is of interest because other studies find differences in hosting capacity between commercial and residential buildings with additional differences depending on the climate [29]. More details can be captured when considering smaller areas in which the characteristics are more locally valid. Most of the works consider residential settings or urban settings. Works that focus on the residential side are typically done so in aggregation over large scales. Kabir et al. [22] use satellite images and analyze the brightness of the rooftop as rooftop hosting capacity. Additional challenges arise in urban settings [23] in which adjacent buildings spacing, size and shapes may play a large role. Several other works that address solar potential from a urban development perspective include those of Lobaccaro et al. [30] and Kanters and Wall [31]. In addition, local ordinances may have local building codes that further impact the capacity in the studies previously listed.

Identifying the number of viable solar panel sites is a much greater challenge because one could also account for shading from rooftop obstacles and other panels. Architecture designs for single buildings [14],[16] to address this aspect are highly detailed and have been but are only suitable on a building-to-building basis-- not practically scalable. On the opposite end of the spectrum, fixed rooftop utilization is sometimes used for entire regions. This is by far the simplest method in estimating PV potential. However, these fixed utilization approaches have varied

significantly from work to work. Peng and Lu [8] find that a utilization factor of 0.6-0.7 is more accurate for Hong Kong and Byrne et al. [11] find a value of 0.7 for rooftop utilization is fitting for the city of Seoul. An IEA report [32] finds that a ratio of 0.4 for central western Europe is fit. Helm and Burman [18] consider the potential of an Hawaiian island and assume a fixed power rating per rooftop area but only consider commercial rooftops to circumvent the challenges with rooftop obstacles and shading. Vardimon [27] considers a range to represent the adoption of panels and suggests 0.3 as the base case and up to 0.5 as an economic case where the panels are cheap enough to justify marginal installations. Both these values are on the lower end due to the local specific design of having water heaters on the roof in Israel. An NREL report [33] finds that utilization factors for commercial flat rooftop buildings are roughly 0.6 in warm climates and 0.65 for cool climates. For residential buildings, the utilization factors are as low as 0.24 for warm climates and lowers to 0.18 in cool climates.

These constant rooftop utilization factors are difficult for accurate estimates when addressing larger scopes. This is especially true when the buildings are not homogenous. Several works exist that try to address the shading of nearby buildings by generating 3D models [14] [15] [17] [34]. Several other works use 2D imaging to capture large areas and building footprints, also referred to as land areas, and are used to calculate the capacity to host PV systems with constant rooftop viability assumptions to account for rooftop obstacles.

2.1.4 Delivering electricity

This dissertation will largely focus on utilizing electricity and managing renewable energy sources as compared to understanding the physics of electricity generation. Though electricity is

the flow of electrons with measurable velocity, it is often practically modeled to be instantaneous. For this reason, electric generation and load are balanced in real time. For a fundamental review of electricity generation, the reader is referred to Tiwari and Dubey [42], focused on electrochemical process (via photovoltaics), and Smythe [43], focused on the historically dominant electromechanical processes. One major aspect of instantaneous load and generation balance is the constraint due to the transmission line capacity. Lines that operate at capacity are referred to as congested, implying there is little room for additional transfer capacity in the direction it is. When this occurs, system operators can capture this phenomenon and through their simulation, returning price signals to incentivize unloading the line. These price signals are elaborated in Section 3.1 and are independent of the capital cost of building such lines.

Gorman et al. [44] calculate an average capital cost for transmission projects (LCOT, delivered MWh) is 0-10 $/MWh with individual projects spanning 0-40 $/MWh. This difference in range depends upon if the renewable resource has low-capacity factor and if the line is shared or serves multiple purposes beyond delivering a single project's electricity. Interconnection studies focus more on system results holistically, providing lower costs for bulk transmission. Bulk transmission costs can be a tenth of LCOE, but comparable to the utility-scale LCOE if only the LCOT individual projects are considered. For reference, Gorman et al. find the LCOE of wind to be between 29-56 $/MWh and 36-46 $/MWh for solar.

Many academic papers and agency planning reports analyze the cost-benefit of proposed projects, whether it be transmission upgrades or deferrals. This type of evaluation contrasts budget proposals that investor-owned utilities make to state agencies to justify changing customer

rates to “support load and distributed energy resources growth, transmission grid reliability, and renewable generation” [45] which largely report total capital and operating expenditures.

2.2 Energy storage

2.2.1 Types of energy storage

The frequency of energy storage accompanying renewable storage is becoming increasingly typical and so a brief discussion of popular energy storage technologies is provided. Arabkooshar and Nami [46] provide a comprehensive description and discussion of pumped hydropower storage. They iterate that among the mechanical energy storage technologies, it has one of the highest roundtrip efficiencies as high as 85% and has the capability of having very large storage capacities – dependent on the head and tail pond. Hydropower energy storage operates by pumping water from the lower elevation pond to the higher one and allow at times electricity is cheap. Tarroja et al. [47] conclude that with weather variability from climate change that the overall levelized cost of electricity does not change significantly. However, a greater amount of natural gas generators is relied upon to meet the grids ramping requirements as the pumped hydropower plants are one of the key critical dispatchable generators in California. Newer papers like that from Zheng and Sahraei-Ardakani [48] push for novel developments to expand hydropower capacity in California. Zheng and Sahraei-Ardakani [48] introduce and evaluate the possibility of retrofits around the state at water and wastewater infrastructure to mimic existing large, pumped hydropower energy storage. They find that this method of distributed pumped hydro has the capacity to add 280 MWh of energy storage for the state.

CAES, like pumped hydropower storage, is a relatively mature storage technology, so there are various papers that evaluate the limits of their application. Luo et al. [49] briefly covers the fundamentals of CAES systems and provides a review of some technical and economic characteristics alongside fitting applications. The authors conclude that large CAES systems are apt for energy management and arbitrage, whereas smaller systems still can provide valuable ancillary services. Drury et al. [50] consider CAES operation in several American electricity markets and Foley and Lobera [51] does similarly in Ireland. Drury et al. is of interest as they consider an adiabatic system and co-optimize for additional revenue streams beyond energy arbitrage. They find an average value of 23 $/kW-yr for energy arbitrage versus an average of 28 $/kW-yr for the adiabatic system. Donadei and Schneider [52] briefly discuss the potential underground storage features such as depleted oil and gas fields, aquifers, salt caverns, and abandoned mines. Guo et al. provide a very focused review and field tests specifically for aquifers to evaluate their suitability for CAES. These developments may prove critical for California, as the state currently has several natural gas storage fields spread throughout the state. If not used for CAES, Heydarzadeh et al. [53] consider their usage for integrated renewable hydrogen gas to reach 100% renewable gas usage.

There is no shortage of energy storage options as review papers for them are frequent occurrences and comprehensive. Cho et al. [54] published a paper in in 2015 reviewing battery technologies specifically focused on commercial and research purposes, including lead-acid, sodium-sulfur, lithium-ion, and vanadium redox flow batteries. The shift to contextualize the batteries in a sustainability framework is evident and well-represented by a 2018 [55] review paper

by Zhang et al. which focuses on lithium-ion batteries and ancillary equipment to complement renewable generators. Even more recently in 2019, Dehghani-Sanij et al. [56] once again review the gamut of energy storage technologies contextualizing their impact on sustainability by focusing on their carbon footprint. The technological fundamentals as well as their operation is well-researched to be able to evaluate their potential value and role in a renewable future. This is of importance as the economics justify adoption independent of simply pursuing renewable goal numbers.

2.2.2 Energy arbitrage

Many papers in the literature identify energy arbitrage as the primary revenue stream to justify energy storage installments. Terlouw et al. [57] model an aggregation of home batteries as a larger size utility-scale battery. Six battery technologies are considered to compare the carbon footprint of production and operation in this residential setting. The best economic and environmental performance case among them is the lithium-nickel-manganese-cobalt battery. A MILP is used to evaluate a peak-shaving optimized and a cost and emission combination reduction optimization is done using aggregated community energy storage. Both Lithium-ion and vanadium redox flow batteries are also found to be profitable. Both the production and operation cost of the batteries are included. Similarly, Varghese and Sioshansi [58] consider six battery technologies for several retail and wholesale tariff structures. The ideal energy capacity to power capacity ratios is of interest when including capacity payments as an additional revenue stream. In some scenarios, the battery set in the Mojave Desert yields better profits than those set in Los Angeles. This is because there is higher solar yield in the desert as compared to in the city. The authors find that

ITC, electricity price, and capacity payments are sensitive variables to the return of a battery system. Though without much policy intervention, the authors determine that energy storage maximizes profit through focusing on energy arbitrage. Vafamehr and Moslemi [59] focus on the value added for industrial and commercial customers by reducing demand charges. In addition, with sufficient aggregation, they can increase revenue by offering ancillary services. Cheng and Powell [60] develop a control scheme to optimize energy storage specifically to co-optimize frequency response and energy arbitrage. They demonstrate that with this method, the revenue is higher than an asset operating purely for frequency response.

The focus on installing energy storage is of interest even in places with differing meteorological conditions than California. For example, Wankmuller et al. [61] use MISO wholesale prices and find the NPV is found to be 358 $/kWh for battery storage (1c scenario and 194-314 $/kWh when degradation is accounted for. The authors introduce an energy throughput-based penalty cost to account for degradation to slow cycling. When end-of-life (EOL) is defined as 80% of initial capacity (80%EOL), EOL occurs before 10 years in the 1c and c/2 scenarios. In the c/3 and c/4 scenarios, EOL is met at the 10 year mark. With a 10% interest rate—1c is 225 $/kWh (80%EOL) and 306 $/kWh (65%EOL). Bradbury et al. [62] identify cost reductions needed to be profitable in when only operating based on energy arbitrage. 14 ESS technologies in seven regional markets are considered with pumped hydro, CAES, and ZEBRA ESS having the highest IRR. The majority of the technologies are optimally sized at 4 or less hours of storage. This paper is of interest as it precedes many recent papers that seem to all agree lithium-ion based energy storage is the recommended approach.

Dowling et al. [63] find that total system costs do not vary significantly between 0.11 $/kWh and 0.12 $/kWh with over 39 years of solar and wind data. Simulating over a longer multiple year timeframe resulted in a greater reduction in renewable capacity. One notable finding is that the system cost over the studied timeframe would be 0.14 $/kWh with batteries only, 0.13 $/kWh if only using long duration storage, and 0.12 $/kWh when using both. The authors find that the long-duration cost and energy capacity is the most sensitive to longer simulation time frames as seasonal storage becomes more likely. Narayanan et al. [64] model both solar PV panels and wind turbines are adopted with BESS. The authors find that only 63% of the load could be met at a small Belgian city. A 40% reduction in production cost would reach parity with non-renewable energy sources. The average cost of electricity from the considered systems ranged from 0.372 to 0.452 euros/kWh.

Abdin and Merida [65] evaluate a scenario in which solar only, wind only, and a combination is then mixed with having a fuel cell, or not, and battery or not. In all cases an electrolyzer is there to make hydrogen. They find a range of 0.50 to 0.66 $/kWh for the scenarios with wind and solar that typically including a battery lowers the average cost of electricity, unsurprisingly.

Walawalkar et al. [66] conduct a study in 2007 on regional price nodes around New York and note that at the time, most energy storage solutions are not cheaper than gas peakers. At the time sodium-sulfur high temperature and flywheel energy storage seemed the most economically competitive choice. Locational marginal prices are considered around 11zones in New York state with sensitivities to efficiency, energy storage capacity time, costs, and revenue. Among battery

types considered by Fares and Webber [67], the NPV of the battery increases when extending calendar life 6-20 $/kWh whereas for increasing by cycle life is only 0-3 $/kWh. Despite this, the authors find none of the NPV are positive from providing energy arbitrage in the ERCOT market. Considered technologies include advanced lead-acid, lithium-ion, NaS, and vanadium-redox. Gundogdu et al. [68] develop control strategy to provide EFR, DFFR, SFFRhigh, SFFRlow ancillary services in the UK market with a 1 MW/1MWh battery and find that revenue can be maximized by providing both energy arbitrage and ancillary services, echoed in these types of papers. Denholm et al. [69] evaluate the potential for energy storage to provide peaking capacity in the U.S. energy market. They find that roughly 28 GW of energy storage capacity would likely help current supply and demand energy balances. Further, this amount of energy storage capacity would enable greater PV deployment which would then extend the potential of 4-h energy storage to be up to 50 GW to accommodate excess solar generation and increase the competitiveness of longer-duration energy storage.

Using 2012 CAISO data, Eichman et al. [70] determine that energy arbitrage (despite long-duration storage as only the price differential offset by the roundtrip efficiency matters) is not as good of a revenue stream compared to selling the hydrogen outright as a transportation fuel. As found in the other energy arbitrage studies, the optimal way to increase revenue streams is to have it also participating in the ancillary services market. The low roundtrip efficiency deters even weekly energy shifting. Yet energy storage could enable greater renewable energy generation deployment as well. This is seen in Cuz Goransson and Johnsson [71], where the authors develop a model to dispatch thermal generators with the installation of 34% wind in Denmark. In general,

they find that the largest thermal plants, despite having low running costs, have slightly lower capacity factors. In return, the smaller generators have increased capacity factors too as their start-up costs are lower penalties to accommodate variable wind generation. Despite the increase in thermal plant start-ups, the emissions are still found to be significantly lower in the 34% wind case compared to without wind and could be furthered with storage accounting for higher amounts of wind.

Further, there often is another subset of papers which add value by focusing on the mathematical approach to optimizing energy storage deployments. Babacan et al. [72] solve a convex problem and the optimization accounting for TOU charges and demand charges. 53 residential customers with co-located solar and storage are considered. They show peak demand can be reduced by 46-64%. They introduced a supply charge concept to prevent backflow on the distribution system. Bassett et al. [73] utilize a Fourier transform analysis that identifies that two to four charge/discharge cycles are available throughout a day providing ancillary services. Black start and voltage control ancillary services can also be provided.

Bynre and Gyuk [74] run an optimization of ESS at 2200 nodes with three historical years of data to compare spatial difference in revenue. Then, different simulations in which the operation is based on price thresholds and day-ahead market (DAM) prices rather than optimizing with foresight were run. When participating in both DAM and real-time market (RTM), the increase in revenue could be as high as 441% for some nodes. Energy arbitrage revenue is found to be highly location dependent, with the RTM cases having 2.83 times better revenue than on average. The authors suggest that DAM market prices are not a good indicator for RT arbitrage potential

with simple price threshold operation being more profitable than maximum revenue operation using DAM market prices.

One of the biggest challenges with energy arbitrage analyses in wholesale settings is assuming the locational marginal price (LMP) remains unchanged with the inclusion of the subject operating energy storage system. Some works like Yan et al. [75] consider a distribution network and investigate energy storage's role in congestion relief. The resulting difference in LMP is found and illustrates the value of energy storage on select busbars rather than simply evaluating the intrinsic value to the asset owner. Though it is not a comprehensive analysis on the value that energy storage could provide to the whole system, the concept of energy storage operation affecting LMP is important for long-term operation, especially with potential co-optimization of energy storage systems on the same busbar or price node. The difference between RTM and DAM prices is a metric that Zarnikau et al. [76] evaluate by conducting a linear regression on wholesale prices to help guide policy-making implications. They find that more wind generation would lower the price due to merit order effects and trading efficiency (the gap between RTM and DAM prices) would decrease if wind forecasting error were reduced. This concept will likely become more relevant as the production of renewable fuels will often use electricity as feedstock.

2.3 Renewable fuels

2.3.1 Renewable natural gas

Natural gas is a largely a fossil fuel, but recent advancements have been made to produce renewable natural gas. Renewable natural gas, biomethane, and biogas are often used interchangeably to describe largely methane gas produced by multiple organic pathways. The

most popular include using manure, food waste, landfill gas, wastewater treatment sludge, forest residues, agricultural residues, and the organic fraction of municipal solid waste. This is done taking the feedstock and undergoing the anerobic digestion or biomass gasification processes and then methanation to meet heating standards. To this end, Parker et al. [77] evaluate these pathways to predict the potential renewable gas that could be procured in California. They find that 68 bcf per year is possible given the current policy framework that incentivizes producing such fuel for the transportation fuel market through a credit system. This work by Park et al. is well-complemented by a technology and research review by Assunção et al. [78] which help identify and propose a roadmap to support current growing biogas upgrading technological developments. This is relevant as Murray et al. [79] assess the market potential of biogas in the United States and find that policy incentives are necessary to spur growth and achieve significant market share.

In the same vein, is a paper by Lane et al. [80] which forecasts the renewable hydrogen production in California given the multiple pathway feedstock potential and cost reductions. In this work, the authors find that the initial cost of gasifiers cost the market share distribution in 2050. In addition, the share from electrolytic hydrogen continually grows starting from 2025. A comprehensive roadmap for the deployment and building out hydrogen production plans throughout California sponsored by the CEC [81] is publicly available which covers the supply, demand, and physical siting of the production plants.

2.3.2 Renewable hydrogen gas

Both renewable natural gas and renewable hydrogen are widely evaluated to help decarbonize the gas and in doing so many aspects are considered for their integration.

Haeseldonckx and D'haeseleer [82] consider the possibility of using existing natural gas pipelines to carry hydrogen. Several attributes of the mixture are explored: linepack energy in pipelines, energy flow relative to natural gas without hydrogen, and Wobbe index. The author champions popular beliefs such as 17% vol mixture will not significantly impact end-use and that hydrogen volumetrically leaks faster than natural gas. However, Hormaza Mejia et al. [83] investigates hydrogen leakage in a distributed setting where the gas is typically at low pressures and finds that it leaks at the same rate as natural gas. Aw

Some of the papers in this realm focus on existing system limitations. Hafi et al. [84] simulate a steady state flow CFD model consisting of three nodes is simulated to evaluate the effects from injecting hydrogen. The pressure, velocity, and mass flow rate are tracked along the length of the pipelines and compared to other works. In addition, the evolution of pressure at the node upon injecting hydrogen is simulated. The authors confirm that higher than 30% mass of hydrogen mixture will surpass the allowable circumferential stress of existing X52 steel natural gas pipelines. Wang et al. [85] use a MILP model to determine which pipelines in an existing natural gas network need to be upgraded, new lines built, and where compressor stations would need to be added to handle 5% vol and 10% vol hydrogen injected to be delivered to three different nodes. The authors argue this method of balancing expansion and upgrading existing lines is appropriate for the reformation schemes of natural gas networks to handle hydrogen.

Gondal [86] finds compressors are the limiting factor in transmission network, with a limiting value of 10% vol hydrogen. This contrasts with distribution network and storage elements that are as high as 50% vol and end use appliances being between 20% vol and 50% vol. A

secondary portion of the study finds that a 2% vol injection has negligible effects but a 10% vol mixture affects the calorific value of the gas supply. Gondal further concludes injection into a distribution network in a mountainous town in Pakistan results in heating values too low for 10% vol whereas 2% vol is unaffected. This largely contrasts, Ekhtiari et al. [87] who cite that distribution lines can be 50-100% hydrogen. Though this study does not optimize for the lowest costs, it investigates a network of 28 pipelines and 25 nodes with three injection points fed by wind electrolysis. These hydrogen injection points are complemented by three natural gas supply nodes to simulate gas flow in Ireland with focus on the hydrogen quality throughout the system.

Guandalini et al. [88] model pipelines as a discretized numerical model. Similarly, the authors' interest is to track the properties of the gas mixture along the pipeline after injecting hydrogen. Primary attributes are composition, flow rate, pressure, Wobbe Index, as well as density. One notable finding in their dynamic simulation is that if there is a large load outlet, then much more hydrogen is pulled out and as a result more could be injected at the offtake. Vice versa, if there is a lack of load then hydrogen can build up and injecting more could violate the concentration limit. Quarton and Samsatli [89] propose a feed in tariff for injecting hydrogen. Both complete conversion of natural gas pipelines and injected mixtures of hydrogen with natural gas pipelines are considered in a Value Web Model (VMW) building upon S. Samsatli and N. Samsatli [90], a UK cast study for injected hydrogen. Transmission and distribution are added to the VWM and the cost breakdown for the entire value chain is conducted. Seasonal storage shift is evident in meeting all the heating loads.

2.3.3 Inter-sector synergy

Hydrogen as a transportation fuel has the potential to become a major driver for increased demand. Gray et al. [91] have recently provided a review for alternative fuels for specifically the haulage sector, considering the application specification requirements and how different renewable fuels compare. It is identified that the renewable fuels, as opposed the batteries, are advantageous for long-haul trips, typical in the freight industry. Mao et al. [92] evaluate a set of historical shipping routes taken between the United States and China. Authors identify the fueling requirements if the ships were powered by hydrogen fuel and the frequency at which ships would stop to refuel. In addition, replacing some cargo space with fuel allows even more ships powered by hydrogen to be able to make longer trips and be serviced by theoretical refueling stations. Average attainment rate across all TEU rating ships is 79% for legs and 43% for total voyage. Reducing cargo space by a maximum of 5% increases both these values to 99%.

Pratt et al. [93] conduct a case study analysis for a 150-passenger ferry boat that travels across the San Francisco Bay. The authors find 1.5-2 times increase in capital cost and 3-10 times increase in operating cost if built at the time of writing. The authors suggest there is societal health benefits of have a zero-emission vehicle amounting to about 50% of the lower capital cost estimate. The authors determine that there are no policy or technological infeasibilities that would preclude the procurement and operation of such a vehicle-- only cost as a barrier for this relatively high-speed mid-size passenger ferry. While some of the cost numbers have decreased since writing, this paper was one of the earlier ones that evaluated using hydrogen power train to decarbonize a marine vehicle.

CleanTech [94] conduct a supply chain analysis to determine the cost of producing hydrogen through two pathways: natural gas reformation and renewable energy electrolysis were considered. The case for fueling three different types of vessels were considered: a car-ferry, high speed vessel, and a platform supply vehicle. The authors determine that the size of the demand of liquid hydrogen in Europe is too small and thus costs too high to serve the Norwegian maritime market. The transport to Norway only increased the cost.

OECD/ITF [95] conduct a study considering technological measures including lighter materials, slender design, propulsion improvements, bulbous bow, air lubrication, hull surface and heat recovery and how they impact carbon emission reductions. Operating measures that can change are the speed, ship size, ship-port interface, and onshore power with the first two making potentially up to 90% and the latter two up to 4%. Finally, fuels could be some form of advanced biofuel (25-100% renewable), liquid natural gas (LNG) (up to 20%), hydrogen, ammonia, electricity up to 100%. The paper, however, only considers fuel cell usage for auxiliary loads. Study establishes 4 pathways to achieve 82-95% reduction of the projected 2035 level of emissions in shipping. Regarding alternative energy carriers, Patonia and Poudineh [96] suggest that green ammonia will only be able to be implemented in extremely low-cost or surplus renewable energy production under current policies.

Outside of shipping, Liu et al. [97] detail the recent operations of the hydrogen fuel cell bus fleet in Foshan and Yunfu, China. Starting in 2016 a handful of buses has grown proven to be reliable. The authors state that by 2020 20 fueling stations are thought to be installed in Foshan with more than 1000 buses running. They highlight that the energy consumption has a linear

relationship with increasing vehicle weight with a better slope than petrol vehicles. List of buses with over 46 thousand km, one with almost 80 km at the time. Foshan, has a factory capable of producing 500 MW of fuel cell units per year. Mariani [98] conduct a bottom-up cost analysis of liquid natural gas stations for both LNG and C-LNG. Some scenarios result in 1-2 euro/kg depending on outlet and product, useful for trucking goods.

On the commercial side, the behavior of consumers charging their cars can contribute to the changing electricity grid needs. Hu et al. [99] propose a mathematical formulation which models the decisions of EV owners, fleet operators, and distributed system operators to manage distributed congestion. They find that by using the spot prices, rather than day-ahead prices, a more accurate shadow price can be provided to incentivize congestion relief. Without this measure, the cost to charge the fleet of vehicles could be as much as 85% more. Staudt et al. [100] Break down Germany into 5 major regions in which 2 to 8 million EV's are considered and their impact on grid congestion and their ability to reduce redispatch costs are evaluated. In the base case where there is no vehicle to grid flexibility, the redispatch cost of the grid to manage congestion is 147 million euro for the year. This number can be reduced by roughly 77% with 2 million EVs participating, providing a potential incentive for individual owners to participate. Sun et al. [101] simulate a high renewable 2030 California scenario in which batteries in vehicles are used as energy storage. The developed scenarios identify how the fleet of vehicles would help balance the California grid if vehicles are capable of bi-directional charging as well as unidirectional charging. The equivalent stationary storage cost equivalent is found to be roughly 16 billion and 26 billion U.S. dollars for the unidirectional and bidirectional charging scenarios, respectively.

Using the aggregate of light-duty vehicles as energy storage assets only further complicates the degradation investigation. For example, Schmidt et al. [102] consider the design of light-duty vehicles that would result in the least degradation. They compare the tradeoffs when optimizing fuel cell and battery capacity in fuel-cell electric vehicles for different objectives. Designs optimized for one of the three objectives (i.e., fuel consumption, lifetime, and cost per mile) still perform well for the others. When optimized for fuel consumption the difference between optimal and the worst of the three is 2.8%, for lifetime the reduction is a 4.5% from optimal, and for relative cost it is 8.2% increase from the optimal.

Produced hydrogen can also be used for power generation. Colombo et al. [103] model a flexible solid-oxide electrolyzer to manage the excess PV generation in a university microgrid setting. This installation doubles the amount of solar that can be installed, and the excess can be used for the on-site gas turbine to reduce up to 16% of CO2 emissions. Salvo and Mei [104] find that synthetic biogas can replace 19% of 2016 levels of industrial natural gas demand in California and P2G can replace 7%.

2.4 Modeling efforts

2.4.1 System modeling

Beyond simply adding additional energy generation and storage, much effort goes toward optimizing existing assets and increasing energy efficiency. Sanstad et al. [105] break down major commercial and residential end-uses to check how demand-side management could reduce load in various utility jurisdictions in WECC. The authors suggest an approach for forecasting load by using both econometric and technology end-use elements and techniques captures greater detail

of peak demand rather than either one alone. Energy efficiency for regions like SMUD, PG&E, PGE, SCE, and others in WECC as a starting point for regional planning.

By splitting the Europe in 50 different regions, Goransson et al. [106] identify three different types of system-level congestion. Congestion can occur due to high loads, high level of wind production during low loads, and a mismatch of supply profiles. The authors find that demand-side management load reduction is helpful for high load congestion but does not aid in the other types. Despite this, demand-side management can still help with relieving local marginal congestion and defer transmission investments.

Modeling the electric grid system is possible at many spatial, temporal, and technical resolutions. While accurately simulating the grid is ideal, there is a computational cost to model more nodes as well as nonlinear AC power flow, to capture voltage magnitude and stability. Layered along with the possibility to run the model for timesteps ranging from every minute to hourly, can result in long simulation times. To this end, researchers and engineers are consistently looking for sound assumptions and novel approaches to increase simulation efficiency.

Yang et al. [107] simulate a linear power flow model which includes reactive power and phase is developed by formulating them as independent variables. The authors find that the linearization error of treating the voltage magnitude squared as an independent variable is smaller when the unsquared voltage magnitude is treated as an independent variable. The authors attribute this to special properties of the distribution of voltage angle in power grids. Dashtdar et al. [108] develop a genetic algorithm that utilizes generating scaling factors to solve nonlinear optimal power flow problems. The authors demonstrate that the dispatch resulted in lower losses

and generation costs compared to other works that evaluated the subject circuit. An economic dispatch and Lagrangian formulation that still utilized the generation scaling factors is introduced and compared to the genetic algorithm version. Li et al. [109] propose a method of distributed optimal power flow which circumvents a full system centralized simulation. This method involves a distributed economic dispatch and distributed state estimate to predict generation and load change. In addition to observing line constraints, this method is suggested to be more suitable for a grid system that has an increasing number of distributed resources.

A DC optimal power flow problem formulation typically does not account for ohmic transmission losses but runs quicker as there are less variables involved than an AC optimal power flow. Cain et al. [110] conduct a review on formulation for solving ACOPF and is recommended as a primer for OPF and further understanding the difference between common power flow problems and formulations. Litvinov et al. [111] utilize loss distribution factors to create a load-based distribution of losses for a more realistic model and to better quantify the value of firm transmission rights. Purchala et al. [112] analyze how much error there might be in using simplified DCOPF models. In general, they use the historical voltage measurements of a Belgian transmission line to evaluate the assumption of the flat voltage profile DCOPF models are based on and find 94% of the line differences are less than a two-degree voltage angle difference. In addition, the line reactance to resistance ratio (X/R) is evaluated for four different voltage levels and it is determined that an X/R ratio greater than four would likely result in negligible error. Castillo and Gayme [113] augment a DCOPF model to also account for losses and integrate an energy storage system. The authors find that a simplified DCOPF model without losses results in suboptimal siting

and dispatch of a storage unit, whereas the DCOPF model with losses and energy storage integrated is closer to the results of an ACOPF model with storage.

2.4.2 Capacity expansion

Capacity expansion modeling is a common approach to planning for future grid resources. However, the computational requirements for a model which captures a multitude of generators, and transmission lines can often become a massive problem numerically, especially when optimizing over a horizon with many steps (i.e., over a year at an hourly resolution). This can become a challenge as the most economic technology for meeting a marginal unit of demand may not necessarily be the best choice in a further-looking timeframe. This idea might be the basis for the heated debate between highly-electrified end use society versus maintaining the symbiotic electric and gas systems in California. In both cases, the possibility of being renewable is technically possible but the co-optimized system can be challenging to model.

Capacity expansion modeling often incorporates modeling the system evolving over time, which allows the opportunity to model changing technology costs. Heuberger et al. [114] model a learning curve integrated endogenously from local adoption meeting renewable energy and emission goals. They account for local cost learning curve and find that without local learning installed capacity offshore wind capacity, for example, is 32% lower than the optimal amount found in 2050. It is 50% lower than the optimal amount if only the global portion of learning is omitted. This suggests the sensitivity of the endogenous cost learning curves used to help identify optimal investment timings and realistic build rates in capacity expansion planning models. While this is fair point, it can be tricky as renewable technologies can be incentivized in various ways to

promote adoption. This interaction is further convoluted when one desires to consider the degree to which the local incentivizes can alter local adoption rates and how it may impact the global progression and adoption of a technology. These types of minor differences in inputs used in models can propagate differing results. Mai et al. [115], despite using the same inputs for three different commercial capacity expansion models (NREL, EIA, EPRI), find that each model has some slight differences in results including the capacity of renewable energy capacity installed, the portfolio, regional buildouts, curtailments, and least-cost optimized portfolios.

On the gas side, one key variable to consider for the gas grid is the prominence of the renewable fuel market. Johnson and Ogden [116] input hydrogen demands, generation sites, and candidate pipeline routes to develop buildout of gas network to accommodate growing fuel cell vehicle market. Rollout of new pipelines for hydrogen generation and pipeline sizing with growing hydrogen demand for fuel cell vehicles is presented. Kluschke and Neumann [117] is an interesting work that combines both the gas and electric grids. They consider hydrogen refueling stations with on-site electrolyzers that can add 72 TWh of demand to the 463 TWh in the base case. The authors find roughly a 2% total system cost reduction if planned with the hydrogen refueling stations in mind because they can cause or relieve congestion. Because of this there is also a slight regional difference in fuel price throughout the country dependent on the type of electricity generation and availability of transmission. This paper accounts for renewable fuel demand to be part of the power system capacity expansion model, showing the potential impact on electric nodal prices representing feedstock prices.

2.4.3 Deep decarbonization

There is more and more uncertainty when modeling in further out years, but many works are dedicated to evaluating the feasibility of what future systems in 2050 might look like. Goop et al. [118] consider an hourly dispatch to cost minimization dispatch model for the European grid following the European Commission's Roadmap scenario to reach 95% RES by 2050. One focus of this work is that the authors compare a base case with the high renewable constraints compared to if net metering is enabled for residential customers. They find that in the latter case, a greater amount of solar is deployed to the point that midday marginal costs are near-zero and congestion typically follows 6-9 hours after peak solar generation. In the summer of the net metering case, congestion occurs largely due to the solar. On the other hand, in the base case where wind makes a larger portion of the mix, congestion occurs more often in the winter. Battery storage becomes competitive after greater than 20% solar power penetration. Wind power still causes congestion over week time-scales and solar does as well with a time delay from peak generation.

Jentsch et al. [119] utilize an electrolyzer to handle up to 85% renewable energy supply nodal model of Germany. Transmission line capacity is modeled and the cost-benefit of varying electrolyzer capacity prices is modeled to identify the optimal capacity to deploy. Results for where most of energy exchange between regions occurs to identify candidate power-to-gas plant locations. Optimal electrolyzer capacity found to be between 6-12 GW mostly located in the north of Germany to reduce power flows. Similarly, Rose and Neumann [120] consider a zero carbon German power system in addition to meeting local heavy-duty vehicle traffic fuel demands, assuming they all use hydrogen. In this work, the authors still find some degree of congestion on

the transmission grid using their optimistic assumptions of maintaining current demand, doubling existing transmission capacity, and omitting international HDV traffic.

In general, Rose and Neumann call for a greater need to investigate the potential impact of optimizing multiple sectors, as the value provided to several sectors may overlap. S. Samsatli and N. Samsatli [90] conduct a geospatial optimization to locate on-shore and off-shore wind complemented with electrolyzers for long-duration storage to meet all the Great Britain's heat demand. A base case is conducted to evaluate what types of investments are needed to handle the dynamics of power generation and load. Secondary scenarios are conducted to evaluate a sensitivity on only using off-shore wind turbines and a reduction in off-shore wind capacity price. In general, the authors find that the optimal portfolio to meet heat demand is roughly 80% electricity and 20% hydrogen.

2.4.4 California case studies

California as a state is often time the focus many studies due to their aggressive renewable goals. The works in the literature that focus on a single technological vector (e.g., hydrogen) and those that have more holistic approaches both are generally motivated by a zero-carbon sustainable future. Denholm and Margolis [69] find that enormous GW amounts of battery would be needed to reduce peak demand with increasing solar installments. Higher solar makes a "peakier" demand in which storage has greater value reducing peak load than if either technology was alone. Roy and Sinha [121] model a 50 MW solar PV paired with 4-hour battery and find that it can provide 98% up time for the 3-hour window that gas peaker plants typically operate in. Overall, the lifetime cost of operation is lower when accounting for tax incentives and fuel costs

of a gas peaker. The gap widens as battery costs decrease moving forward. A 50 MWac solar and 60 MW/240 MWh storage can replace a 70 MW combustion turbine power plant that typically works as a peaker and is found to be cheaper as well. Colbertaldo et al. evaluate what 100% RES with different mixes of solar, wind, electrolyzer, and fuel cell amounts in the California grid would look like. Their focus is on identifying the required amount of renewable generation and capacity without the physical siting of the assets.

There also is a subset of works that focus on the challenges associated with the anticipated growth in renewables. Cohen and Callaway [122] focus on distributed load and PV. Some instances of backflow of power at the substation where they would sooner need a replacement. Geographic diversity reduced backflow due to non-coincident backflow. This study also finds 15-min temporally resolved data is sufficient compared to 1-min available data. Torroja et al. [47] suggest that climate induced variability makes greater generation capacity (up to 6.3%) available necessary yet does not significantly impact renewable penetration. This variability also increases natural gas power plant and downtime and startup frequency, which has high emissions relative to operating at a steady level, but there is minimal change to system-wide costs. Tian et al. [123] compare operational carbon offset of BESS accounting for upstream emissions and find that BESS at capacities absorbing 38-76% of daily generation has diminishing returns of carbon reduction in a scenario with 80% of electric supply being from solar and wind. Cases as early as 105% of daily average renewable generation would result in zero marginal environmental benefit.

Coignard et al. [124] assume an average of one EV per household and find that 60% of residential feeder circuits need to be reinforced due to rapid EV charging at 6.6 kW. Even with an

optimized approach of controlled charging times, peak demand would still increase by 8%. They also suggest that adoption would not be uniformly distributed but have a leaning toward higher income households. Cohen et al. [125] evaluate the PV avoided wholesale energy expenditure and voided distribution upgrades with load growth. They find that there is little value in most distribution circuits but massive value (60 $/kW-year) on small portion, 1%, of circuits where PV penetration is much lower. On average, there is a $6/kW-year benefit when averaged across PG&E service territory. The authors do not anticipate large expansion toward distributed because the gain is not massive over central. Still works like Zhang et al. [126] attempt to address distributed solar forecasting uncertainty to ease local grid balancing via a multiple linear regression model, a machine learning gradient boosting approach, and a random forest ensemble data mining approach.

Then still regarding California, there are studies that are more carbon emission-oriented. Wang et al. [127] find that excess renewable for transportation fuels is the most cost-effective way to reduce emissions. Excess electricity sent to energy storage for stationary electric loads have less emission reduction because current transportation fuels are more GHG intensive than fuel for power generation. However renewable gas for industrial usage provides greatest cost reduction at higher levels of renewable penetration and provides more grid flexibility due to dispatchable operation of electrolyzer-- effectively enabling higher renewable deployment. They identify that the approach to minimize emissions is different than that that minimizes costs. In the same vein, Zhao et al. [128] establish two scenarios to compare to a BAU. One is driven by air quality and health benefit (favoring slightly higher degree of end-use electrification) and the other is driven

by cost optimization (more combustible renewable fuels). Both have slightly different results in terms of geospatial distribution of air pollutants and emissions, but both achieve 80% GHG reduction.

2.5 Economic factors

2.5.1 Power markets

Some studies give extra focus toward the economic drivers for capacity expansion and deployment to meet renewable goals. Shawhan et al. [129] conduct an economic optimization cost dispatch model that endogenously model economic decisions to retire existing and build new power plants. The authors also endogenously model the effect of policy on fuel prices and consequently its consumption for power generation. Asadinejad et al. [130] use a reduced WECC model that employs a demand response tariff of 10 $/MWh in addition to regular customer electricity price. This in return reduces price volatility in the wholesale market and benefit is seen by both customers and the LSE. In 2017 Brown and O'Sullivan [131] identify that CAISO is the exception for increasing solar capacity penetration with falling costs. In 2017, CAISO's solar capacity penetration is at 27.8% followed by ISONE at 5.4% and the other system territories less than 2.3%. At the time, a carbon and health tax were needed in addition to the energy and capacity value of utility solar to breakeven and reach a NPV of zero. The authors suggest existing CO2 and SO2 emission cap-trade programs are undervalued, and the floor should be raised, or caps lowered.

Other studies step away from the technical modeling and lean more toward the policy philosophy. Tierney [132] suggest a two-part strawman proposal to handle the evolution of the

California electric grid given the recent challenges and foreseeable obstacles. The proposal is broken down as a resource-adequacy construct and an energy-production construct. In summary, the resource-adequacy suggests a shift away from the existing definition purely dependent on monthly and annual peak load and instead be dynamic and encapsulate system needs such as operational flexibility, local capacity, or complementing zero-emission assets. The energy-production construct shifts away from a pure bid-offer market and considers whether the bidding generator is also providing RA resources. The same for ancillary service market is suggested as the expectation is that many of the high variable cost generators would have significant market power. Ideally, prices paid for energy procurement will more accurately reflect the cost of production and are expected to vary from location to location as the bidding markets today do not necessarily facilitate the adoption of assets needed in the long-term.

Orvis and Aggarwal [133] advocate for renewable generators with zero or negative marginal cost to be subject to bidding into the market and submitting a curve rather than self-scheduling. The authors believe this is required to create appropriate price signals for investors and flexible resources. The authors also suggest greater flexibility could be allowed if gas-electric market intervals are smaller, as the gas market interval clears ahead of the electricity market intervals.

2.5.2 Risk tolerance

Adoption risk tolerance is another large driver when discussing the economics of renewable development. Egli [134] investigate risk factors of technology, policy, curtailment, financing price, and resource availability and how they have changed from 2009 and 2017. In

general, technology and financing risks have decreased but curtailment, price and policy depend on the country. New technological design risk is small compared to the overall technology risk reduction. Market creation and maturing attracts new service providers and leads to service improvements, which is better for investors. Policies to handle variable generation and better assessment tools to improve technology risk outlook are also key. If this can be improved, adoption is expected to increase but the increasing number of curtailments have slowed adoption. Flor and Haansen [135] model firms with investment opportunities that return perpetual earnings. Earnings are modeled to stochastically have a chance of increasing due to technological advancements. The firms' problem is to have the optimal investment time relative to the technological advancement. The authors consider technological advances to be random and occur in spikes to propel cost reductions and adoption essentially suggesting the investment threshold is not constant and the option value is sensitive to advancements.

He et al. [136] establish a non-linear relationship model showing there is a dual threshold effects from green-credit that occurs in stages: promoting, restraining, promoting in this order. The authors suggest financial institutions should be combined with already existing green credits paradigms to promote green technology growth. The barrier for smaller companies should be addressed to help them adopt new technologies because the risk is more easily managed by larger companies. He et al. [137] conduct a follow-up work in response to the concerns established previously in [136]. They bring up that green financing is not uniformly defined in academia, as such governments need to play a role in building and consolidating such structures in financial institutes, shown to promote efficient renewable energy investments. Similarly, Guo et al. [138]

suggest governments can support by expanding credit market and establishing "appropriate fiscal and taxation mechanisms".

Masini and Menichetti [139] suggest in 2013 that private investment pathways are not prevalent enough for renewable energy technologies and suggest it biases perceptions and preference to maintaining status instead of addressing price signals. They surveyed about 300 contacts in various European countries: banks, investment funds, energy companies. They find that the effectiveness of policy can be one of the biggest influences on investors including renewable energy technology in their portfolios. Boute [140] emphasizes regulatory stability is important. Changes in policy are typically needed to protect end-users from subsidizing renewable energy investments but deters regulatory volatility deters investors. Many lawsuits are pending as of Feb 2019, especially versus Spain. The major items that are proposed for a stable regulatory model are things like: specificity of stability guarantees, competitive selection, quantity limits and locational signals, commitment to tariff stability, tariff changes over time, and stable access to interconnection. Overall, the trend calling for improvements to regulatory stability is key to maintaining healthy investor growth.

Liu et al. [141] consider 236 companies between 2000 and 2017. Civil law systems versus common law systems can be beneficial or adverse in overcoming the financial constraints that come with high levels of renewable energy investments. This is because the legal system can largely shape business ethos and regulation. Common law is based on historical decisions whereas civil law puts more weight on what is already written. Common law countries have higher constraints and even when subsidized, investors are hesitant due to the actual unreliable

economics. Civil factor in the long-term value and thus have lower fiscal constraints. Business "ethos" can market or put more weight on the social good of environmentally friendly decisions. Common law countries typically have volatile support and consumers often bear the burden of subsidizing the cost. Foregoing opportunity cost is essentially in conflict with long-term environmental investments; thus, this can be helped with financial incentives, societal engagement and green financing. In another work, Liu et al. [142] suggest NPV is not a good enough metric due to uncertainty regarding renewable energy, thus real option approach is more suitable. In review, they find some works combine this type of approach with the deterministic approach employed by the DOE.

Sinsel et al. [143] conduct a review of 130 studies that can be broken down as focused on either market and policy challenges or technological challenges. The authors also conduct interviews with various experts in the field. Results summarize and categorize the issues as power quality, flow, stability, or balance. Some solutions are provided for the challenges and is a recommended reference for review regarding renewable energy technology adoption.

2.5.3 Adoption

Hansen et al. [144] review 180 100% RES energy system studies since 2004. The authors suggest more recent studies focus more on the pathway toward 100% renewable energy system and are adopting a holistic framework, considering sectors outside of power generation. The authors also suggest lack of research in other countries and regions may be bottleneck for effective policy-making.

Ang et al. [145] sample 25,000 over 33 European and find there is a 2% increase in adoption rate for those that have individualistic values. In addition, the authors find that those with individualistic values tend to purchase energy efficiency appliances and cleaner personal transportation options. As a result, the authors suggest in individualistic societies, marketing should be placed on uniqueness and novelty of technology whereas in collectivistic society, marketing should be focused on the normalization of adoption.

Lukanov and Krieger [146] discuss the recent growth in distributed PV contributing up to 6.6% of in-state generation in 2018, up from 3% in 2014, in the context of environmental justice. Authors use CalEnviroScreen to identify areas that are disadvantaged and conduct linear regression analysis to find statistically significant and correlated factors such as kW per capita, education, housing burden, linguistic isolation, median household income, poverty, and unemployment. Rode and Weber [147] use an epidemic model to analyze the spatial-temporal diffusion of household PV rooftop installations in Germany. In general, the authors find a decreasing influence on adoption rates beyond 1 km. However, within the first band of the seed installations, an incidence ratio of 1.3 per year and incidence ratio of 1.11 per year in the second band is found. The authors confirm their hypothesis that imitation in household PV is localized.

2.5.4 Cost reductions

When it comes to modeling the price of certain technologies, learning curves are often used to represent an increase in production efficiency and thus lower costs. Hayward and Graham [148] consider learning curve of many electric generation technologies. Authors suggest a penalty price for installing too much of one technology to prevent establishing a feedback loop that locks

in that technology as the most dominant is necessary. This is a major point they make that should be considered conducting cost reduction analyses. Huenteler et al. [149] suggest some portion of the technological learning rate can be split between local and global. This depends on the sourcing of material often time. The authors suggest that because of this government should consider adopting technology with the mindset of increasing capacity locally in a developing country to take advantage of this. After all the authors continue to re-emphasize the importance of the price is based on existing capacity, the learning rate, and the availability of local components.

Schmidt et al. conduct a thorough review of electricity storage technologies and evaluates their cost projection from 2015 to 2050. They find that lithium-ion battery solutions become the most dominantly deployed and suggest it is due to a higher experience rate due to their use in other sectors. A standard normalization to evaluate the levelized cost of storing electricity is detailed to help aid transparency in future work. The various technologies are also considered in various grid applications in which they can increase their benefit beyond energy arbitrage [150].

This is very much aligned with the findings from studies that focus on the gas side. Hassan et al. [151] consider scenarios in which P2G systems use wind, solar, grid, and combinations of each as feedstock. It is found that the cost to produce renewable methane with captured carbon dioxide is in the range of 200 -300 euros/MWh (thermal HV) for a large-scale system, whereas a smaller system on the magnitude of 1 MW or less could be a factor of two to three more. The authors find that the price of the feedstock electricity is the greatest factor, in some cases as much as 85% of the cost. As such, the authors suggest that while cost reductions in P2G systems would help, improvement in renewable energy capacity production costs and efficiency will likely be

critical. Wei et al. [152] evaluate the learning curves of micro-scale CHP fuel cell power systems used for residential application in Japan and larger SOFC CHP fuel cell systems used for commercial application in the U.S. The authors find that in the 2007-2015 timeframe, the learning rate for SOFC systems under the California SGIP was nearly zero while the micro-CHP systems in Japan was roughly 18%. The authors suggest that the difference can be attributed to the difference in development, market, technology, and policy. One notable difference is the Japan set a deployed system goal whereas California simply subsidized the system costs. Other potential factors the authors highlight is that the Japanese system suppliers are large and collaborate with utilities, and U.S. MW-scale fuel cell system producers do not have domestic competitors.

Another study that simply focuses in on cost reductions with a bottom-up approach is that from Battelle Memorial Institute [153]. They conducted a study where they found PEM stacks were 50% of overall system cost for all sizes and production volumes. Less than 15% at higher production volumes. DC/DC was the largest BOP cost with the next biggest cost being the high-pressure regulators. Life cost analysis was done to compare the emission difference between backup power generation options. At the highest volume it was approaching 1000 $/kW at 50,000 units/yr whereas this figure changes to 1215 $/kW for 10kW at 50,000 and 1876 $/kW for 5,000.

2.6 Sociopolitical factors

2.6.1 Social discussions

Beyond the economics the way discussions are framed at a consumer level can play a major role. Schmidt-Costa et al. [154] develop a Bass Diffusion Model which includes six feedback loops that generate dynamic behavior regarding consumer decisions. They highlight that if the state

would develop a second edition of a state program to deploy rooftop PV solar, installing 1750 MW would only take 44.26% of the original budget and occur 10% faster than the first time. Further, installed capacity would increase by another 1050 MW with an 15.79% increase in budget. The authors attribute this to the product-service system business model providing avenues to PV adoption and the "word of mouth effect" generates a positive feedback loop among other factors to further adoption. Hazboun et al. [155] conduct a survey-based study which found that when the adoption of renewable energy was framed as energy security, energy diversification, resource conservation and air pollution reduction, the response was much more positive. Conversely, when it is presented in the context of climate change or a religious duty to preserve nature, the response was much more negative.

Tzankova [156] highlights the contributions of private governance toward renewable energy transition. Tzankova's findings can be summarized as two-fold: 1) direct demand for increasing renewable capacity and as a result 2) engaged in an active role in calling for and shaping public policy. This framework suggests that private, market-based governance has the ability to positively influence the green energy transition rather than being assumed to be an antagonist.

Education and cultivating environmental justice can go hand in hand with adoption. NREL report by O'Shaughnessy et al. [157] summarize community choice aggregation (CCA) contributions in each state in the United States. This report explains how CCA fits into both unregulated and regulated markets. In this work, the authors highlight the challenges associated with CCA such as: the need to maintain cost savings for customers, balancing the scales of aggregation to maintain the adoption of renewables, and keeping them informed. More

specifically, Vogel [158] suggests that California is a leader in adopting "innovative and stringent environmental standards" because it has appealing environmental amenities that citizens have wanted to protect, and business interests benefit from protecting. By reviewing the leadership that communities and agencies had in the past, the author highlights what is necessary for strong political support for public policies: 1) a significant community adversely affected by a particular commercial practice and 2) an alternative to the destructive environmental practice. Differences between states can be seen more clearly by referring to Hess and Lee [159], which narrates the evolution of CCA and community solar in both California and New York. Due to different policies and agency decisions both have seen an increase in solar in a decentralized manner with greater contention between CCA and utilities.

Tying in environmental justice in line with economic mobility can be another strong driving force as seen by Topcu and Tugcu [160], which analyzes the 1990-2014 timeframe to evaluate the effects on renewable energy consumption and its effects on society. They find that increasing renewable energy consumption correlates significantly with decreasing income inequality, especially in developed countries. However, this is contradicted by Monyei et al. [161] which point to trends of increasing electricity cost and increasing amounts of renewable. In general, transitioning to more renewables should be done by reconsidering the entire energy framework to "create more equitable, egalitarian, pro-poor, low-carbon transition policies."

2.6.2 Forecasting and policy planning

While Reyna and Chester [162] find that between 2020 and 2060 electric load is thought to increase as much as 87% but can be kept to as low as 28% if aggressive energy efficiency policies

are enacted, ultimately, additional renewable resources will be necessary. For one, there are many who would argue the usage of importing renewable electricity from other states is productive [163] and optimal [164] for reaching such a goal, and still there are others that suggest independence from other states holds greater renewable integrity and maintain equity [165]. Those who are of this latter mindset typically address the feasibility of doing so with the usage of seasonal storage [64], [166]. Whereas those who are of the prior mindset like Bistline et al. [167] use EPRI's REGEN model to determine the impact of flexible regional REC trading on the geospatial rollout of renewable power generation. They find that the NPV through to 2050 would be 148 billion without REC trading and 68 billion with REC trading. While this suggests inter-regional trading would be beneficial, the local siting of generation capacity is not evaluated and the authors find that only half of local renewable requirements are met within state and the remainder through REC trading with other regions (e.g., California with Texas or SE-Central).

Lo et al. [168] suggest retail electricity structures do not reflect capacity constraints necessarily. Even TOU structures end up creating peaks before and after the time window. The authors suggest that activating loads (e.g., water heaters, thermostats, and electric vehicle chargers) can help underutilized generation assets and even real time pricing (so that individual customers can respond to price but are exposed to more risk and closing the open feedback system) but ultimately suggest a more customer-involved framework for establishing rates. The authors suggest that the current electricity grid is becoming increasingly like telecommunications infrastructure in that it is high capital cost and low operational costs. As such, utilities should consider selling service based on some guiding questions, such as "what is the minimum amount

of power capacity that customers' needs during times of grid congestion?". This idea is echoed by Ossenbrink et al. [169] which propose a template framework for analyzing policy and using energy storage in California as an example topic. The authors suggest that policy can be analyzed initially by considering a top-down framework which focuses on the strategic intent of a certain policy and then a bottom-up framework which focuses on the outcomes of the policy.

This in addition to other demand response willingness and desired decarbonization and local generation availability help utilities with forward looking rate planning rather than basing new rates on historical activity. Lo et al. suggest forward-looking customer engaged rate structures should more accurately reflect congestion pricing. Forward planning can help ease the transition of resources and has always been of concern as seen from a 2007 study by Cramton and Stoft [170] which also encourages long-term forward contracts that help reduce volatility and risk by hedging fuel prices.

3 Wholesale Perspective Case Study: Burford Giffen

Since the overall project is to understand the role energy storage could fulfill at Burford Giffen and utility-scale solar farms in general, this step serves to:

1) Investigate the value of integrating energy storage at UC's Giffen solar site.
2) Considering an alternative pathway which utilizes the Low Carbon Fuel Standard (LCFS) policy framework that currently exists in California.

Burford Giffen is a 20 MW solar site developed by Clēnera Renewable Energy roughly 40 miles west-southwest of Fresno, California. The site sells electricity to the University of California (UC) via a purchase power agreement (PPA) and is connected to the grid at the end of a 60-kV transmission line as seen in the Figure 1 below. In conjunction with other local solar developments, the transmission line is often constrained and has resulted in a permanent curtailment schedule effective 2019—limiting the amount of exported power to 12 MW nearly year-round. This curtailment slows the amount of renewable energy put on the grid and consequently slows the number of RECs that the UC can generate and claim. More importantly, the recent operation of the solar site has been a financial burden to all parties and implementation of energy storage for long-term economic viability is of interest.

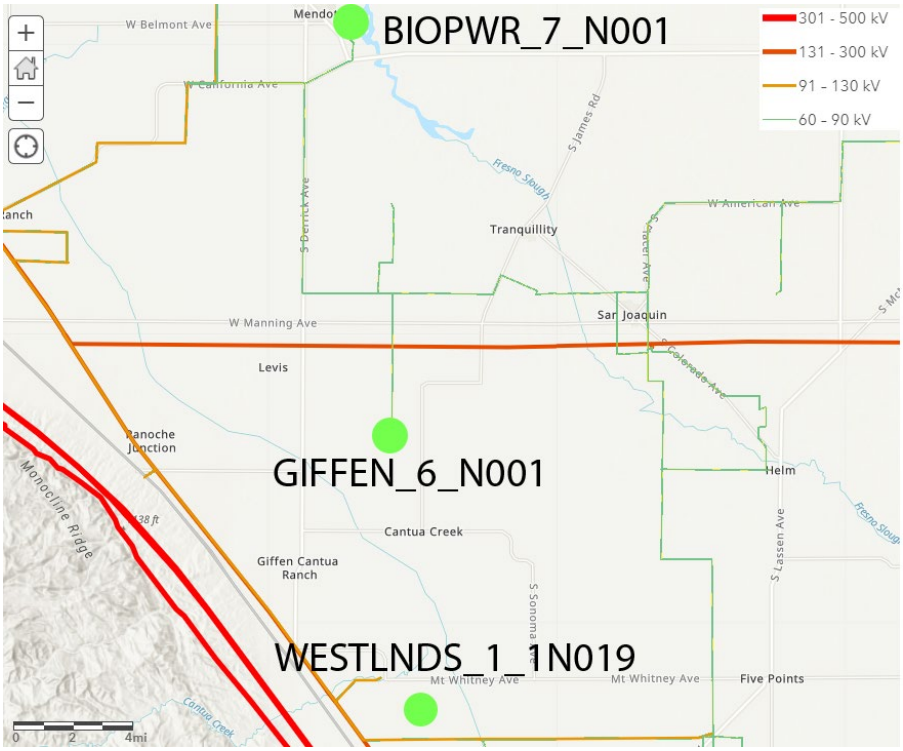

Figure 1 – The Burford Giffen solar site is co-located with the GIFFEN_6_N001 price node. The 60 kV line runs north but is not connected with the 230 kV line that runs east/west.

3.1 Approach

Of the many California Independent System Operator (CAISO) price nodes, there are three considered relevant to this study: BIOPWR (BP), GIFFEN (BG), and WESTLNDS (WL) [172]. The BG node is the locational marginal price (LMP) that the Burford Giffen solar site trades at. The BP node which is about 15 miles north of the solar site, is co-located with a substation that switches multiple higher voltage lines including the one that the Giffen site is connected to. Due to its connection with the 115-kV transmission line, this price node sees higher prices compared to the BG node from lack of congestion. The E3 Burford Giffen analysis assumes that if congestion is alleviated, the LMP at BG increases to match BP. This is a fair assumption as the marginal cost of congestion (MCC) will be the most significantly different component of their LMP—the other two

being the dominant marginal cost of energy (MCE) which is the same across all system nodes for a given hour and marginal cost of losses (MCL) which varies with distance from a reference node. Five Points is another UC site and trades on the WL price node. Being located along a 115-kV transmission line, local congestion is minimal and the historic wholesale prices are more typical of a solar farm in the region. Historic metered electric production for 2018 up to April 2019 is provided by the UCOP to model generation. May to October values from 2018 are repeated in 2019 as representative values.

3.1.1 Battery Energy Storage System

A lithium-ion based battery energy storage system (BESS) is modeled with a 275 $/kWh capital cost [173]. A fixed 4 to 1 power to energy capacity ratio is assumed. The charging efficiency is based on the normalization of the open-current voltage with respect to state of charge. This charging efficiency ranges from 84% at 10% state-of-charge (SOC) to 99% at 100% SOC [174]. Similarly, the discharge efficiency curve is based on a voltage versus discharge capacity graph from Yang et al. [175]. The discharge efficiency ranges from 89% at 10% SOC to 73% at 100% SOC.

The BESS is set to charge from 12-4PM and discharges from 6-10PM as done in the E3 study. The BESS charges with as much electricity produced from the solar farm as possible and imports electricity so that it can operate at full capacity—improving its capacity factor and utilizing its energy arbitrage potential. This assumption differs from the E3 work which only charges the energy storage only with storage that would have been curtailed. This E3 assumption results in less energy shifted and the value realized from energy arbitrage is lower in conjunction with a less utilized asset. The E3 work assumes such operation of the energy storage system in conjunction

with change in activity at other solar sites connected to the same transmission line will relieve the constraint allowing for the constrained BG price node to converge to the BP node. On the other hand, this work assumes importing electricity is an indicator of congestion relief but even then, is a whimsical assumption as existing curtailment at other solar sites could be relaxed and reinstate congestion. Therefore, much of this analysis is conducted assuming multiple price nodes. By doing so, each node reflects varying levels of local congestion, and the results are bounded.

3.1.2 Power-to-Gas-to-Power

An alkaline electrolyzer system is modeled with a 1,100 $/kW capital cost [176] and a PEM fuel cell system with a 1,200 $/kW capital cost [177]. In addition, 11 $/kWh [178] on-site gas cylinders are utilized for storing hydrogen produced. Unlike the BESS, the number of gas cylinders, size of the electrolyzer and fuel cell can all be varied independently. The part load efficiency of the fuel cell follows a typical parabolic current-voltage curve as seen in Salva et al. [179]. This translates to a 13% efficiency at 10% rated power capacity and 55% at full capacity with peak efficiency of 63% at roughly 80-90% of rated power in the model. The electrolyzer part load efficiency is derived from Gibson and Kelly [180] with an efficiency range spanning from 71% at rated power to 78% at the lower fraction of rated power.

Unlike the BESS, the energy storage capacity corresponding with the number of hydrogen gas cylinders and the charging and discharging power rating corresponding with the electrolyzer and fuel cell size can be altered independently. In conjunction with a negligible gas leakage rate analogous with self-discharge in the BESS case, the power-to-gas-to-gas (P2G2P) scenario can shift energy seasonally with the marginal cost of additional gas cylinders. Regarding energy arbitrage

value, much literature already suggests the higher roundtrip efficiency of BESS make them a better candidate for daily energy-shifting. The potential value of using hydrogen for long-duration energy-shifting by sending power to the electrolyzer when the hourly price node value falls below user-defined threshold value, a price ceiling, and the fuel cell consumes hydrogen to produce electricity when the price surpasses another user-defined value, a price floor, is explored. In general, the lower prices occur when curtailment of excess solar is needed (i.e., frequently in Spring) and the higher prices occur when the system requires additional generators to meet system demand (i.e., during Fall after limited PHES resources are depleted).

3.1.3 Low Carbon Fuel Standard (LCFS) Credit

A second set of scenarios depending on power-to-gas is considered in which the produced hydrogen is injected into the existing natural gas infrastructure or delivered to a hydrogen fueling station rather than converted back to electricity via a fuel cell. These scenarios not only explore the potential value of improving transmission line congestion as done in previous scenarios, but also investigate how using the low-carbon fuel standard credit (LCFS) system as an additional revenue stream compares. The associated costs are primarily the electrolyzer, any imported electricity, and transportation. The hourly CI for grid electricity is taken from CARB's 2020 update [181]. Some scenarios consider injecting hydrogen produced at Burford Giffen at a gas grid compressor site roughly 10 miles away, while other scenarios aim to deliver hydrogen directly to a hydrogen fueling station 30 miles away (distance to Fresno outskirts). When hydrogen is trucked away from the solar site, a fixed fee for cylinders and transporting them is considered, whereas for the pipeline case, an adequately sized pipeline is designed, and cost is annualized.

A core procurement gas price of 34.73 cents per therm was used to quantify revenue for wholesale gas sales when injected at the compressor station in the indirect pathways. A much larger portion of revenue is from the amount of LCFS credits generated and is based on a CARB equation which depends on the reference fuel carbon intensity (CI) and the CI of the alternative fuel pathway in consideration shown below. The amount awarded by the LCFS program can be calculated with the following equation.

$$\frac{\$}{\boldsymbol{kg}}\boldsymbol{Hydrogen}$$

$$= [(\boldsymbol{CI_{Gasoline}} * (\boldsymbol{EER}) - \boldsymbol{CI_{H2}})]\frac{\boldsymbol{g_{CO2}}}{\boldsymbol{MJ}} * \mathbf{120}\ \frac{\boldsymbol{MJ}}{\boldsymbol{kg_{H2}}} * \mathbf{10^{-6}}\frac{\boldsymbol{MTCO_2}}{\boldsymbol{g_{CO2}}}$$

$$* \boldsymbol{LCFS\ Price}\ \frac{\$}{\boldsymbol{MTCO_2}} \qquad \boldsymbol{Eq.(1)}$$

Where EER for light and medium-duty hydrogen fuel cell vehicles is 2.5 and for heavy-duty and off-road application fuel cell vehicles is 1.9. $CI_{Gasoline}$ is used as the reference for light and medium-duty vehicles and CI_{Diesel} is used for heavy-duty and off-road applications. A table for both fuel's benchmark CI can be found for 2019 to 2030 and onwards is found on the CARB website. The amount of revenue from LCFS in this report is relative to the prevalent SMR pathway which makes the portion realizable to the injecting party irrelevant of whether it displaces gasoline or diesel. It is calculated as the difference of awarded LCFS credit amount from the considered pathways and the amount awarded from the HYF. By doing this, one can evaluate the maximum realizable value from coordinating with a third-party SMR plant in the indirect pathways and establishes the opportunity cost for all pathways.

In other words, any reduction in CI for the pathway translates into higher LCFS revenue rewarded per produced kilogram hydrogen. This provides an opportunity to justify using RECs to claim any feedstock electricity used in the pathway is 100% renewable and carbon-free. It is found that at current LCFS prices, buying RECS modeled in this work as 17 $/MWh falls into the green region of benefitting the LCFS credit awardee seen in Figure 2.

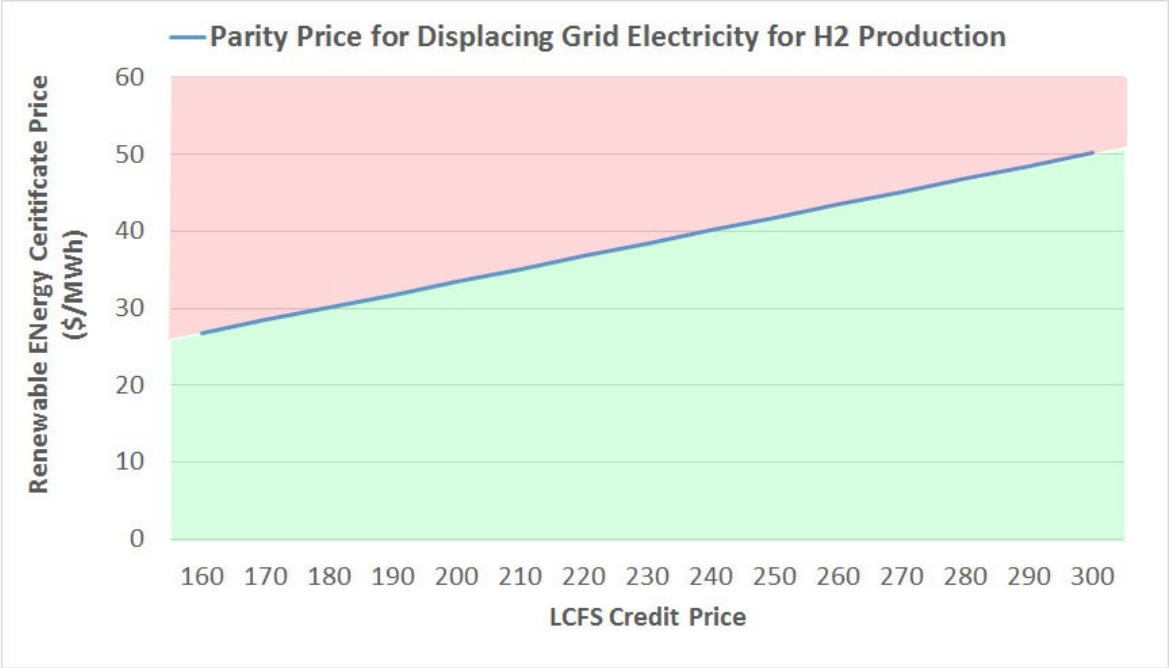

Figure 2 – Comparing the price at which RECs for renewable electricity would be beneficial for reducing electricity feedstock emissions in an LCFS pathway.

3.1.4 Considered Pathways

In this work, eight downstream LCFS pathways in addition to the electrolysis CI is considered. Two pathways correspond to the direct delivery of electrolytic hydrogen to a hydrogen fueling station and six pathways novelly suggest the possibility of a steam methane reformation (SMR) plant producing hydrogen with methane from the gas grid whilst claiming the renewable attributes of hydrogen being injected into the at a remote location (i.e., Burford Giffen). This is

done to provide a pathway to decarbonize the California gas grid whilst producing renewable fuel for the transportation sector. A pathway producing hydrogen by steam reformation plant and then compressed for transport to a fueling station already exists, known as the HYF pathway, and is often referenced in the following. These indirect pathways depend on how the renewable attributes of injecting hydrogen into the gas grid are accounted for. Three approaches are presented referred to as the 1) physical disposition pathway (PDP), 2) virtual disposition (VDP), and 3) gaseous renewable energy certificate (GREC). Each of these indirect pathways also have a slightly different CI, dependent on whether the hydrogen is piped or trucked away from the solar site. Figure 3 provides a visualization of all the considered pathways along some existing ones.

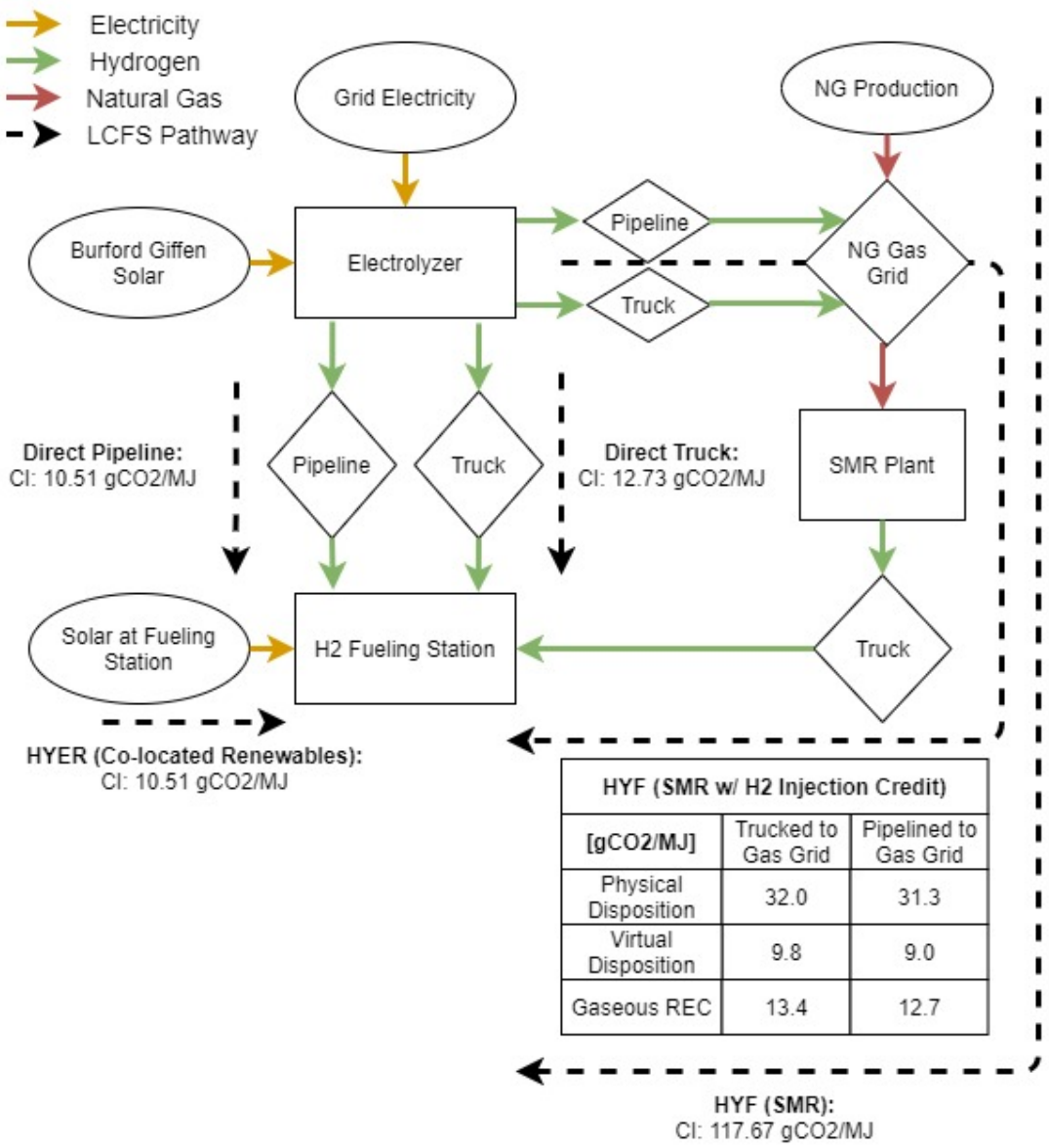

HYF (SMR w/ H2 Injection Credit)		
[gCO2/MJ]	Trucked to Gas Grid	Pipelined to Gas Grid
Physical Disposition	32.0	31.3
Virtual Disposition	9.8	9.0
Gaseous REC	13.4	12.7

Figure 3 – Depicting the two existing LCFS pathways, HYER and HYF, alongside two direct and six indirect considered in this work.

For all three indirect pathways, injecting hydrogen results in a reduction of system fugitive greenhouse gas emissions. Assuming 2% system leakage would result in about 360 milligrams of methane leaked to the atmosphere per MJ heating value throughput. When applying the 100-year global warming potential of methane [182], this mass of methane is equivalent to 10.8 gCO2e per

MJ throughput. The 100-year GWP of hydrogen is 5.8 gCO2e/MJ [183]. At the same 2% leakage rate, this would result in 0.82 gCO2e per MJ throughput hydrogen. This would be a reduction of 10.0 grams of CO2e from avoided fugitive emissions per MJ throughput. This would be considered a lower bound reduction, since one could propose that system leakage is not entirely dependent on throughput but rather continuous with time or based on events [184]. The assumption that all system leakage is not throughput based, implies the lower energy density of hydrogen compared to natural gas is an advantage, since venting events would relieve pressure with a higher volumetric fraction of hydrogen.

The PDP treats the injection of hydrogen into the gas grid as a parallel to the physical SMR process. Because of this, the existing HYF pathway is effectively used but the implication of injecting hydrogen is considered. This includes the prior reduction in fugitive emissions in addition to a reduced carbon potential of the fuel in end-use. The reduction in carbon potential follows the carbon potential of methane as quantified in GREET pathway documentation. The transport component of the fuel is increased by 25% to represent the interstate movement of hydrogen in pipelines (250 miles) compared to imported natural gas (1000 miles). In this approach, 1.4 MJ is injected into the gas grid, 1.4 MJ is withdrawn for SMR resulting in a 14.4 gCO2e fugitive reduction per 1 MJ energy of hydrogen delivered to the fueling station. Note that in Figure 4 and Figure 5 the MMBtu unit can be interchanged with MJ as the efficiency of the SMR plant remains the same.

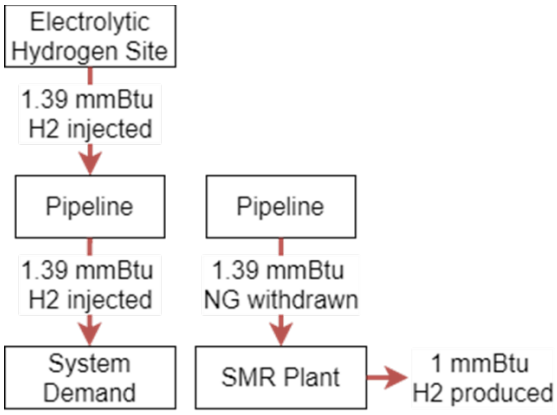

Figure 4 – Physical disposition pathway depicting injection of hydrogen occurs in parallel with steam methane reformation process.

The VDP considers the gas grid system as an intermediary. This approach follows similarly to the existing biomethane pathway. In addition to accounting for the production (zero for electrolytic hydrogen) and transport emissions (250 miles as done in the PDP); it is suggested that the amount of injected gas is 100% renewable. If so, the equivalent amount of withdrawn energy can be thought to be renewable, and the carbon emissions discounted. This suggests a carbon-free SMR process and the remainder of the carbon intensity from this pathway is due to transporting the final product and compressing at the fueling station, as done in all pathways. The fugitive emissions reduction is the same as the PDP.

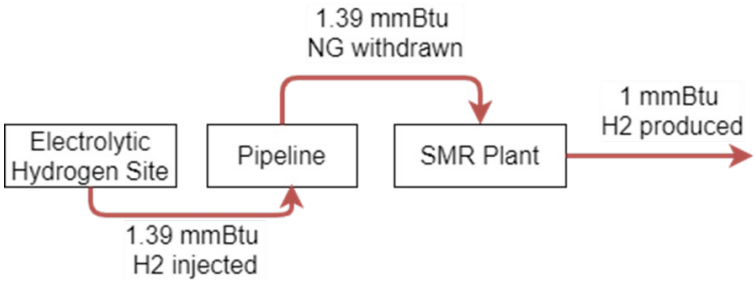

Figure 5 – Virtual disposition pathway depicting a systemwide accounting basis of renewable content rather than local reductions.

The GREC pathway is akin to the electric grid RECs, in which a unit of renewable electricity is put onto the grid and an equivalent unit at the end-use is deemed renewable. However, in this scenario the SMR plant is thought to be part of the natural gas infrastructure as a vehicle to promote hydrogen injection. One could potentially make the case that the SMR plant is like a renewable transformer analogous to a distribution transformer in the electric system. Following this, only 1 MJ of hydrogen is injected (and withdrawn) per 1 MJ of hydrogen produced. This results in a near-identical pathway emission as the VDP except the fugitive emission reduction is less as only 1 MJ of natural gas is being displaced as compared to 1.4 MJ.

The CI of trucking is assumed to be 0.07405 gCO2e/MJ per mile [185]. On the other hand, the electrolyzer outlet pressure is sufficiently high enough so that additional compression to transport the hydrogen to the compressor station or fueling station is unwarranted. Recent literature suggests a tube trailer can carry a load of 150,000 standard cubic foot (scf) [186] or about 700 kilograms of hydrogen at 165 bar [187] which is an improvement predicted by the Yang and Ogden [188]. Based on their results, a 1.10 $/kg trucking fee is assumed. The pipeline cost is calculated as done in the HDSAM. A 6-inch pipe is calculated to be able to handle the highest hydrogen flows from a 20 MW electrolyzer, but a 8-inch pipeline is considered as this effectively

doubles the throughput capacity and achieves slight economies of scale. This represents a scenario in which, if the situation warranted building out a pipeline and was profitable, another future solar PV farm would and could operate identically to share half of the pipeline cost.

3.2 Results

Many following graphs are stacked columns graphs of monthly costs and revenues relative to the business as usual (BAU) case. The BAU case assumes a maximum export of 12 MW for the 20 MW solar farm at Burford Giffen using the BG price node for wholesale electricity sales. By doing this, the benefit of implementing energy storage compared to doing nothing is considered, so investing in energy storage as beneficial can be determined. In some cases, values become negative indicating a decrease in quantity relative to the BAU case. Across the BESS, P2G2P, and LCFS scenarios many of the costs and revenues are from the same sources. Resource adequacy obtainable by the fuel cell and BESS is modeled to be 40 $/kW per month and RECs are valued at $17/MWh as done in the E3 study. The direct energy revenue stream represents the electricity sold directly whereas energy arbitrage revenue is electricity sold from stored energy. Note that a large enough energy storage system will sufficiently relieve congestion on the transmission line is assumed, translating to the 12 MW export limit being lifted. Then, wholesale energy sales increase due to an increase in direct sales in conjunction with energy arbitrage from the storage system. This detail should be considered along with the price node at which wholesale electricity is sold when reviewing the result graphs below.

The cost columns include the equipment equivalent annual cost (EAC) split into equal monthly payments. The EAC is calculated using an annuity factor assuming a 5% rate per year over

the assumed lifespan of the component. In addition, a 60 $/MWh PPA cost associated with non-curtailed electricity is considered to capture the perspective of the UCOP, who purchases power from the solar site. Electricity purchased from the grid at the hourly wholesale price to send to the BESS or electrolyzer is labeled as imported electricity.

Many of the results will vary with the assumed wholesale price node which is used to determine the price when selling or buying electricity. In general, the congested transmission lines cause lower prices to occur due to peak solar generation. Most of the time the LMP is the same among the three nodes as MCE is often the largest chunk of the three components more attributable to the CAISO system as a whole and the differences seen at the lower price end in Figure 6 is due to local constraint differences resulting in different MCC. This is further evident when considering the capacity factor of solar in California and the percentage of the time the duration curves vary. The selection of the price node drives a significant difference in profitability of each energy arbitrage scenario. The selection of which price node used reflects the degree to which the integrated energy storage strategy truly relieves local transmission line constraints. In some sense, the BG price node reflects the most locally constrained node considered and the WL node is representative of typical solar without local transmission constraints.

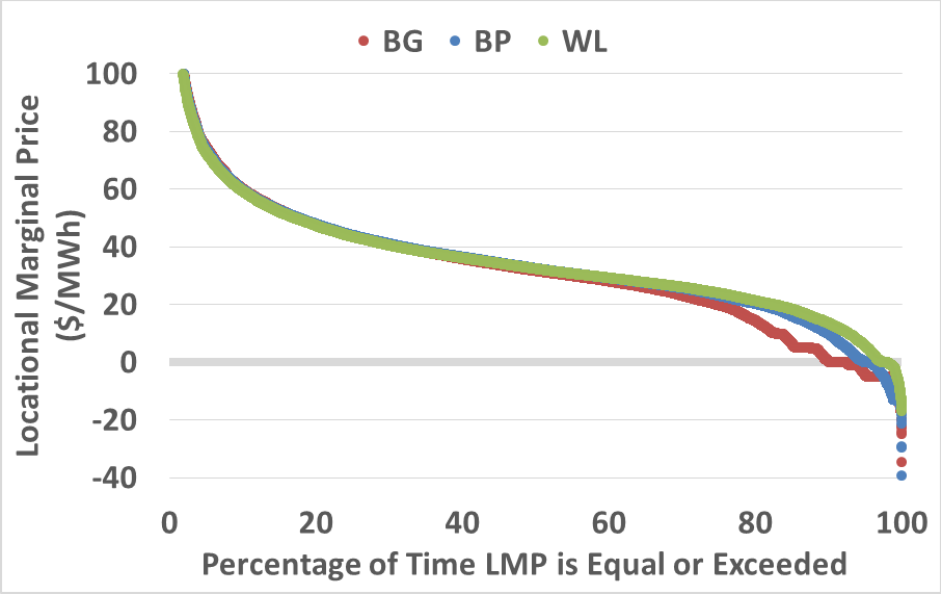

Figure 6 – Hourly locational marginal price duration curve for three relevant price nodes for the time period of January 2018 to November 2019

The results utilize a return on investment (ROI) metric. This is calculated by the following equation for each considered time period.

$$ROI = \frac{Revenue - Cost}{Cost} * 100\%$$

Where the revenue is the difference between the total revenue from integrating an energy storage system and the revenue in the BAU case. The cost is the difference between the cost associated with installing and operating an energy storage system and the BAU associated costs.

3.2.1 Battery Energy Storage System

The BESS is modeled to have an energy capacity of 20 MWh and power rating of 5 MW. This size is selected to be slightly lower than the 8 MW that the Burford Giffen solar farm is forced to be curtailed. A 40 MWh and 10 MW BESS is considered subsequently to reflect the higher end of the 8 MW peak curtailment. By assuming the battery charges during peak generation and

prevents the line from being congested, there are additional direct electricity sales in addition to energy being sent to storage. Results are presented with all three price nodes as much uncertainty exists regarding the degree that the energy storage system relieves congestion. The importance that congestion is relieved is a critical basis for results in this report because as an extreme example, a 1 kW BESS will effectively have no effect on alleviating the congestion therefore invalidate the assumption that export limit would be lifted. Figure 7 illustrates how a 20 MWh, and 5 MW BESS would fair over the previous 22 months resulting in an ROI of -51%, -31%, -36% when using BG, WL, and BP price nodes, respectively.

a)

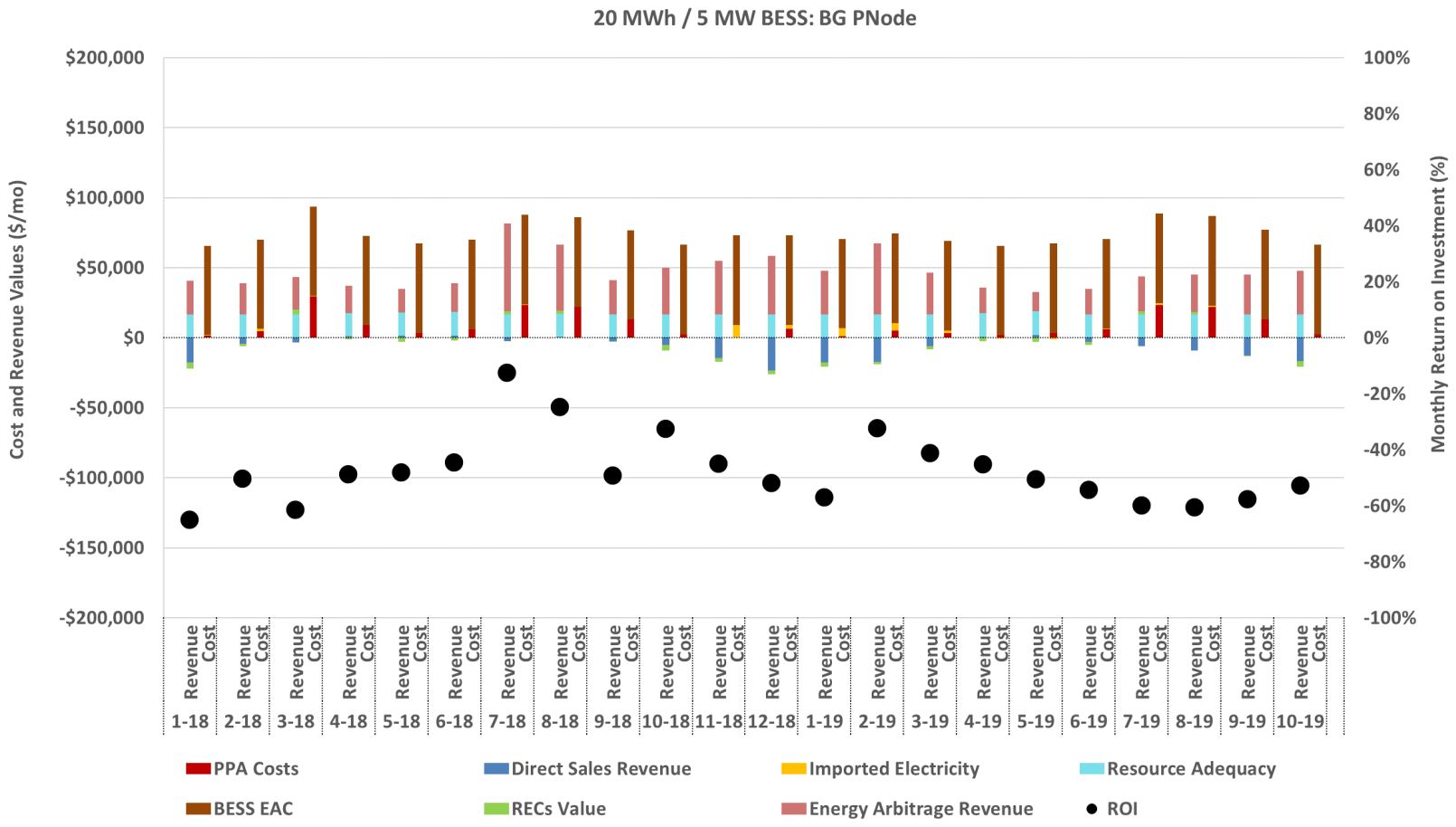
20 MWh / 5 MW BESS: BG PNode
Cost and Revenue Values ($/mo)
Monthly Return on Investment (%)
$200,000
$150,000
$100,000
$50,000
$0
-$50,000
-$100,000
-$150,000
-$200,000
100%
80%
60%
40%
20%
0%
-20%
-40%
-60%
-80%
-100%
Revenue
Cost
1-18
2-18
3-18
4-18
5-18
6-18
7-18
8-18
9-18
10-18
11-18
12-18
1-19
2-19
3-19
4-19
5-19
6-19
7-19
8-19
9-19
10-19
PPA Costs
Direct Sales Revenue
Imported Electricity
Resource Adequacy
BESS EAC
RECs Value
Energy Arbitrage Revenue
ROI

b)

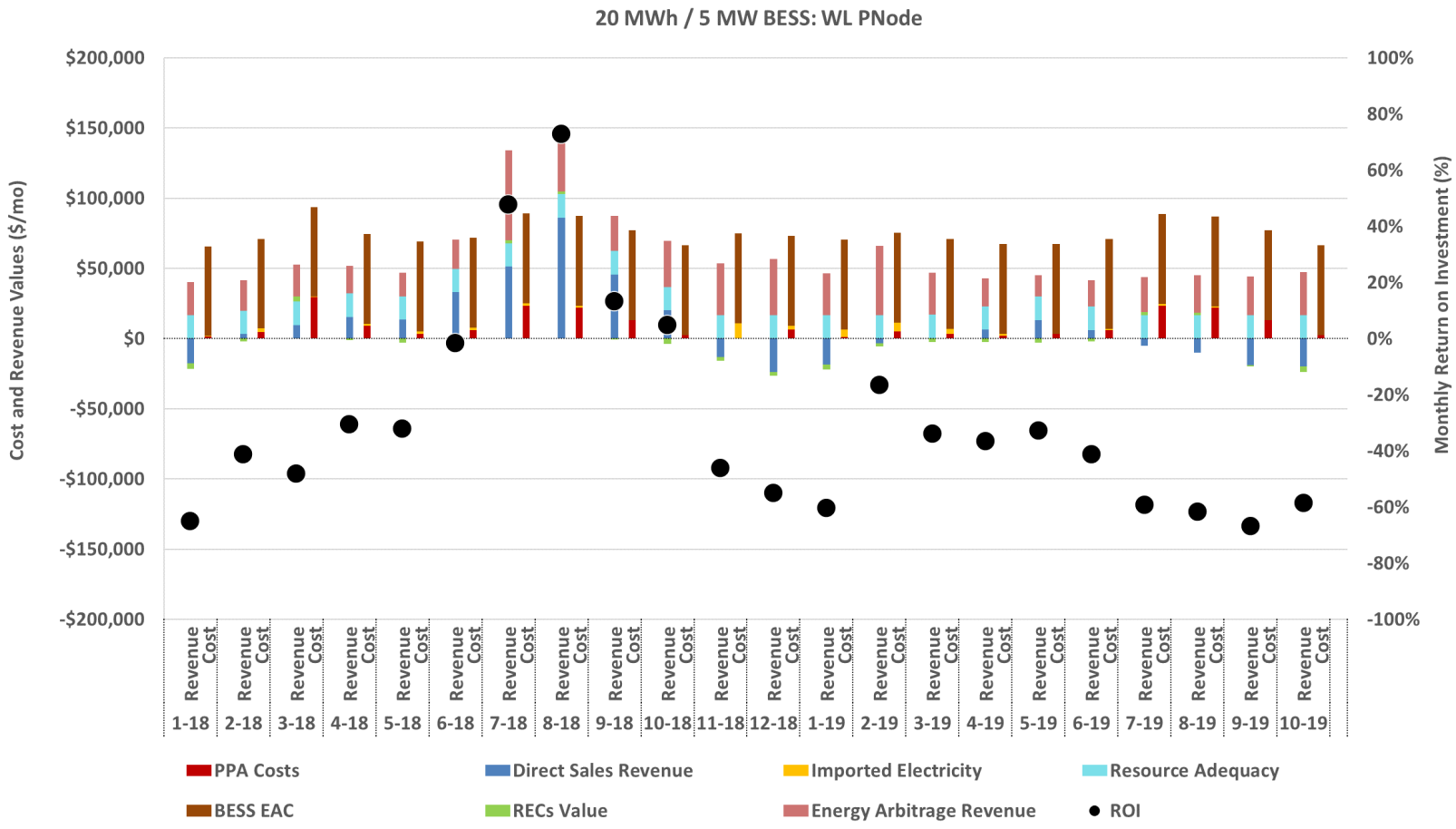
20 MWh / 5 MW BESS: WL PNode
Cost and Revenue Values ($/mo)
Monthly Return on Investment (%)
$200,000
$150,000
$100,000
$50,000
$0
-$50,000
-$100,000
-$150,000
-$200,000
100%
80%
60%
40%
20%
0%
-20%
-40%
-60%
-80%
-100%
Revenue
Cost
1-18
2-18
3-18
4-18
5-18
6-18
7-18
8-18
9-18
10-18
11-18
12-18
1-19
2-19
3-19
4-19
5-19
6-19
7-19
8-19
9-19
10-19
PPA Costs
Direct Sales Revenue
Imported Electricity
Resource Adequacy
BESS EAC
RECs Value
Energy Arbitrage Revenue
ROI

c

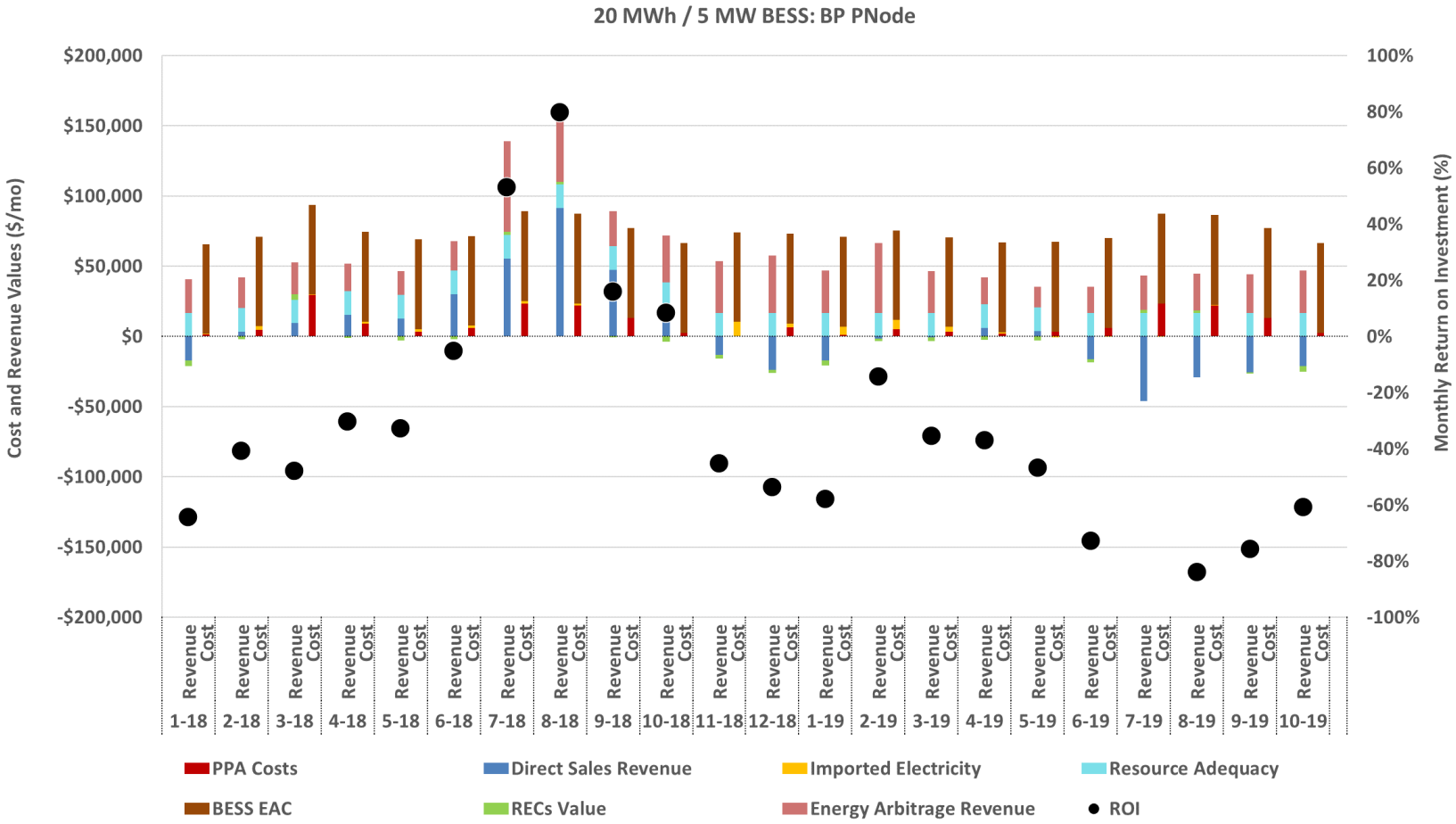

Figure 7 – Monthly costs and revenue from implementing 20 MWh, 5 MW BESS at Burford Giffen assuming a) BG price node b) WL price node and c) BP price node.

The BESS operates daily, charging and discharging at prescribed times each day. Some months see greater wholesale energy sales that are not entirely attributable to lower buy and sell prices but also due to the amount of previous curtailment. When considering July of 2018, the increase in revenue from wholesale energy sales from curtailed energy is roughly 90% for the BG price node. This metric changes when considering the WL and BP node as the amount of revenue from electricity that has been curtailed is closer to 50%. Note that the revenue from the BESS when discharging in the evening will be similar for all three nodes but the BAU wholesale energy revenue is lower for the BG node due to the historically negative prices during peak generation. At the current BESS sizes considered, most of the electricity is being sold directly rather than sent to storage. The amount of energy that would be curtailed and the wholesale revenue received is summarized in Figure 8.

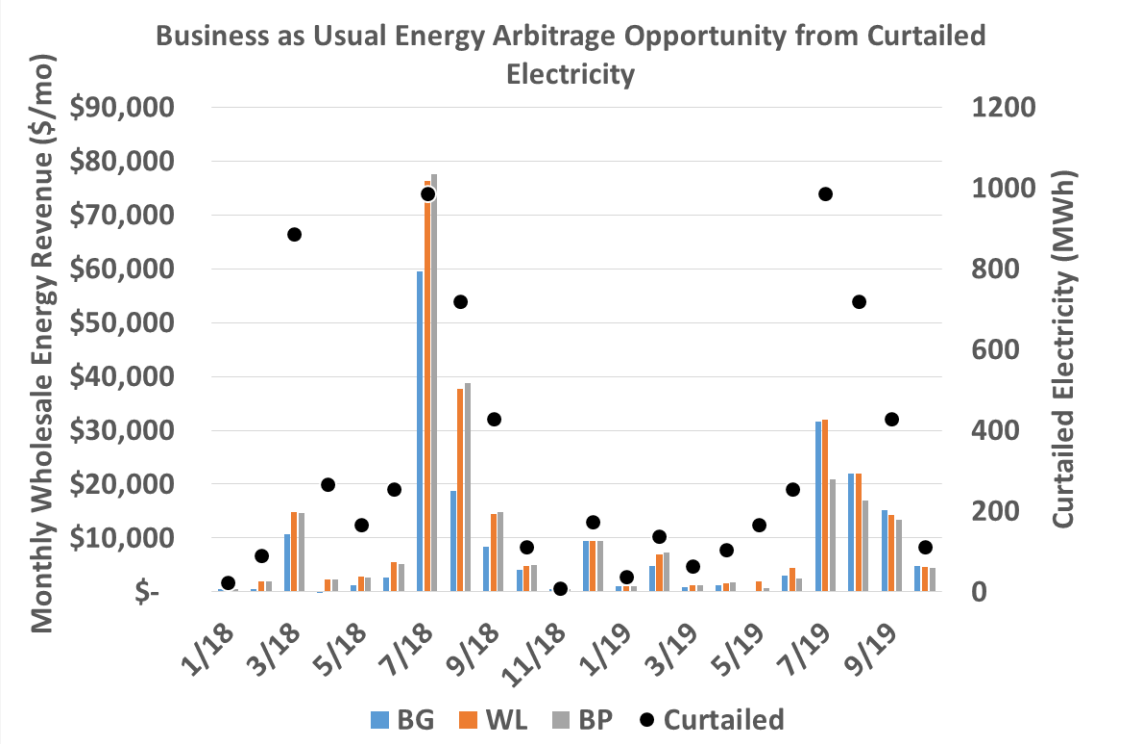

Figure 8 - Wholesale energy revenue from directly selling curtailed electricity assuming historic price node values.

Implementing a larger BESS exaggerates each of the cost and revenue streams presented previously, in Figure 7. The BESS EAC grows slightly faster than the value gained from arbitrage and resource adequacy. Meanwhile the PPA cost remains the same and more electricity can be sent to storage compared to the smaller BESS case. This results in a greater amount of imported electricity when generation from the solar panels is less than the maximum power rating of the BESS. In addition, there are less RECs generated compared to the smaller BESS and BAU cases because the roundtrip efficiency of the BESS lowers the amount of renewable electricity exported. The amount of electricity imported is accounted for by the portion of electricity dispatched from storage that should be awarded RECs. Figure 9 illustrates how over the previous 22 months this analysis results in an ROI of -49%, -54%, -44% when using BG, WL, and BP price nodes, respectively.

a)

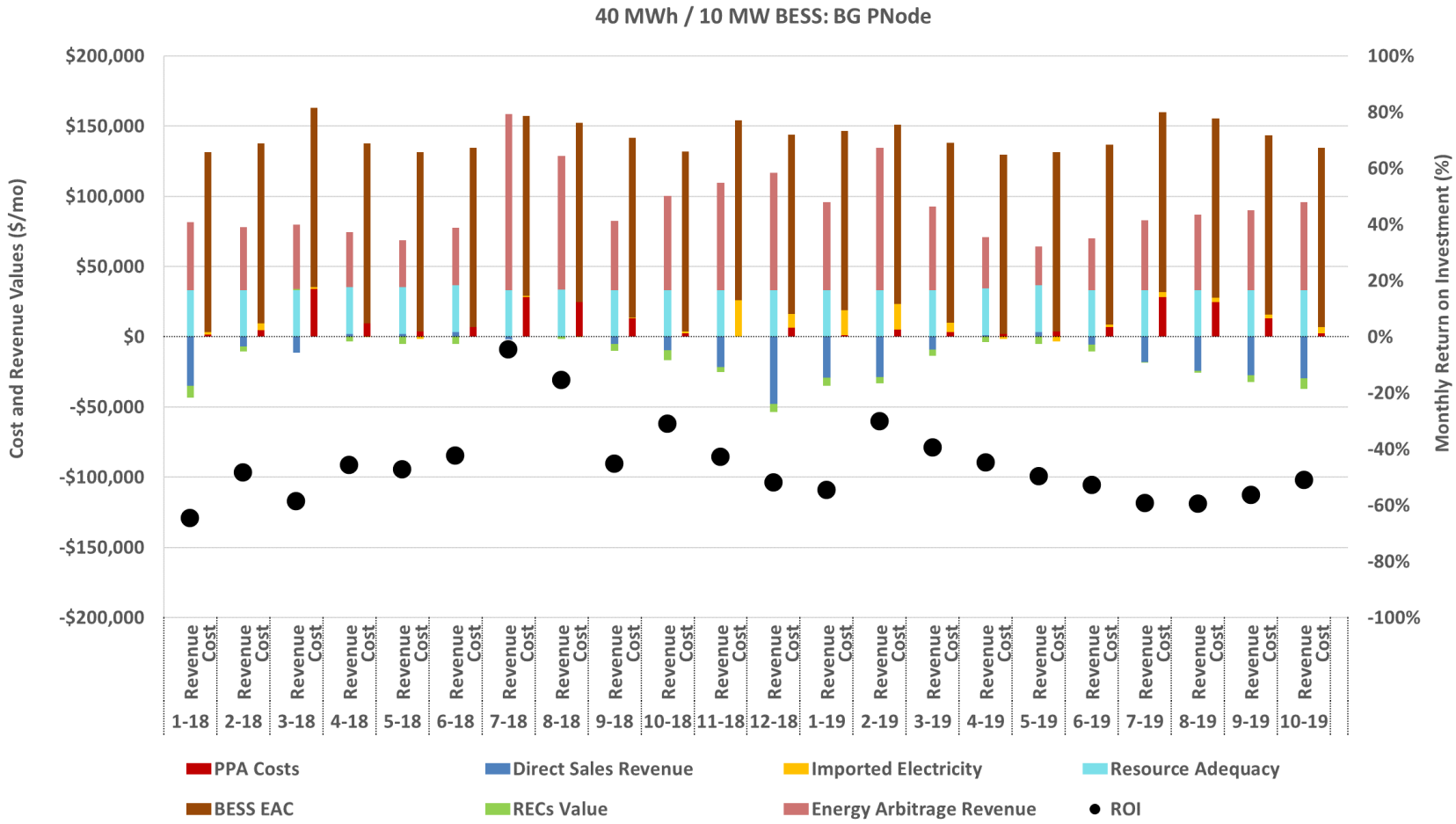
40 MWh / 10 MW BESS: BG PNode
Cost and Revenue Values ($/mo)
Monthly Return on Investment (%)
$200,000
$150,000
$100,000
$50,000
$0
-$50,000
-$100,000
-$150,000
-$200,000
100%
80%
60%
40%
20%
0%
-20%
-40%
-60%
-80%
-100%
Revenue
Cost
1-18
2-18
3-18
4-18
5-18
6-18
7-18
8-18
9-18
10-18
11-18
12-18
1-19
2-19
3-19
4-19
5-19
6-19
7-19
8-19
9-19
10-19
PPA Costs
Direct Sales Revenue
Imported Electricity
Resource Adequacy
BESS EAC
RECs Value
Energy Arbitrage Revenue
ROI

b)

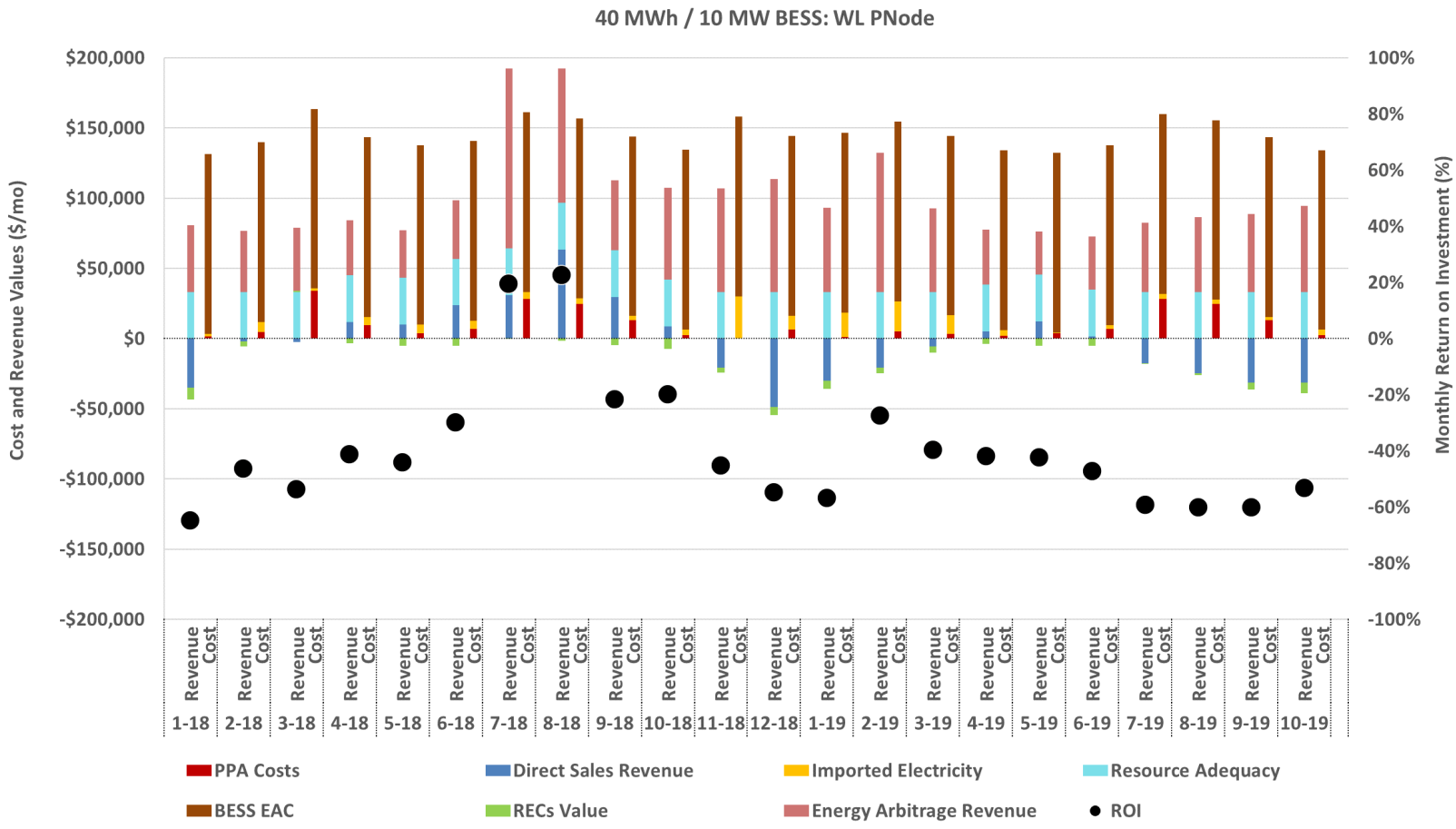
40 MWh / 10 MW BESS: WL PNode
Cost and Revenue Values ($/mo)
Monthly Return on Investment (%)
$200,000
$150,000
$100,000
$50,000
$0
-$50,000
-$100,000
-$150,000
-$200,000
100%
80%
60%
40%
20%
0%
-20%
-40%
-60%
-80%
-100%
Revenue
Cost
1-18
2-18
3-18
4-18
5-18
6-18
7-18
8-18
9-18
10-18
11-18
12-18
1-19
2-19
3-19
4-19
5-19
6-19
7-19
8-19
9-19
10-19
PPA Costs
Direct Sales Revenue
Imported Electricity
Resource Adequacy
BESS EAC
RECs Value
Energy Arbitrage Revenue
ROI

c)

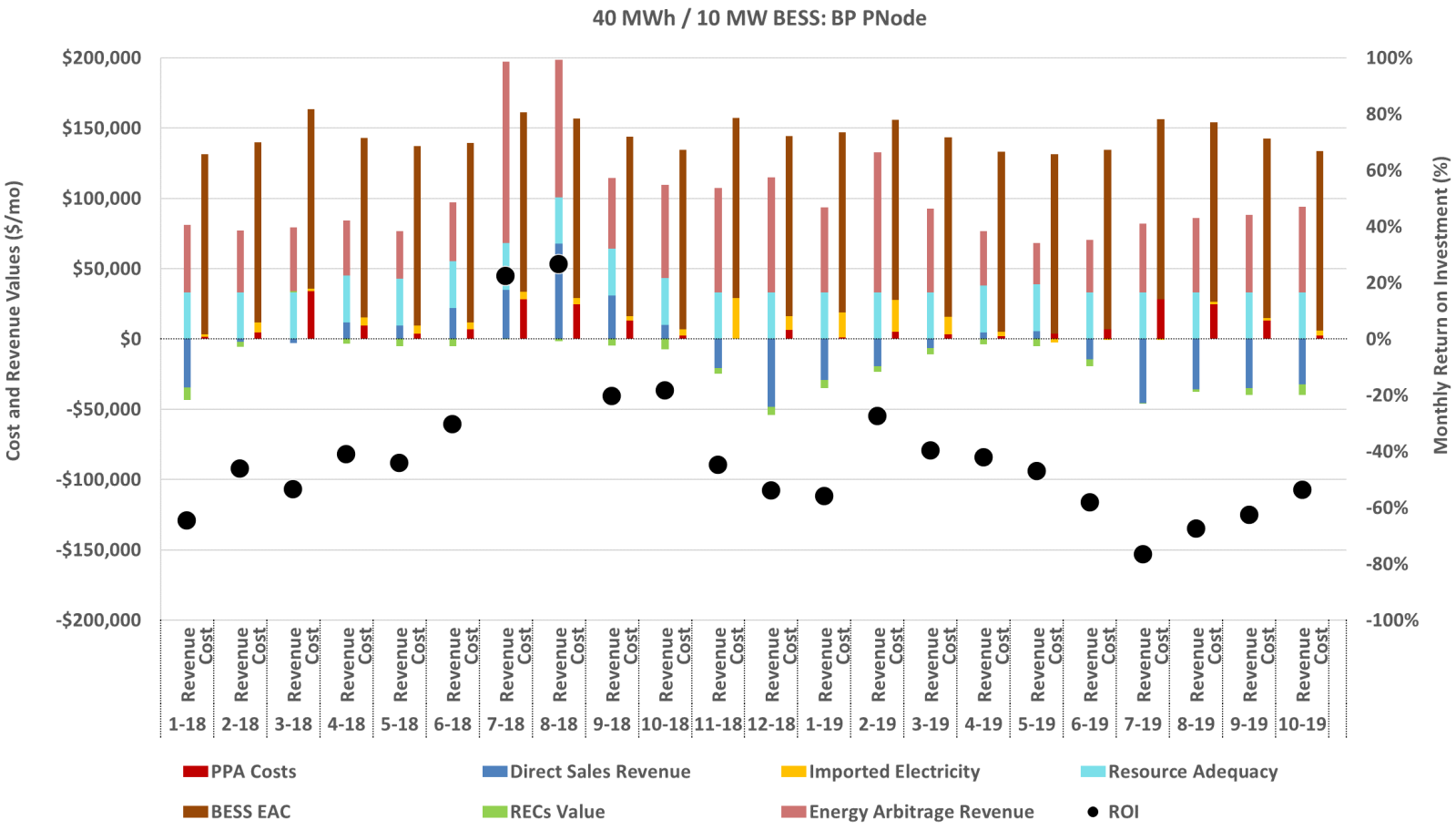

Figure 9 – Monthly costs and revenue from implementing 40 MWh, 10 MW BESS at Burford Giffen assuming a) BG price node b) WL price node and c) BP price node.

In general, smaller BESS sizes have the less negative ROI because they have the smallest associated capital cost. However, the smaller the BESS system, the less valid the assumption that the energy storage system relieves the transmission line congestion becomes. As a sensitivity analysis the capital cost of the prior BESS cases is varied to investigate how decreasing battery costs in the future could affect the ROI. Figure 10 displays the change for system capital cost as low as 150 $/kWh. At 150 and 175 $/kWh the ROI crosses over into positive territory when using the BP and WL CAISO price node data, respectively.

a)

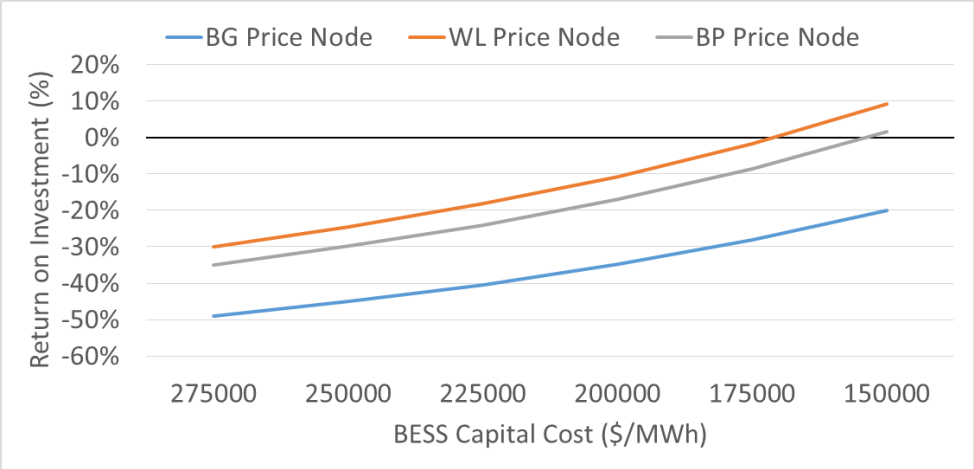

b)

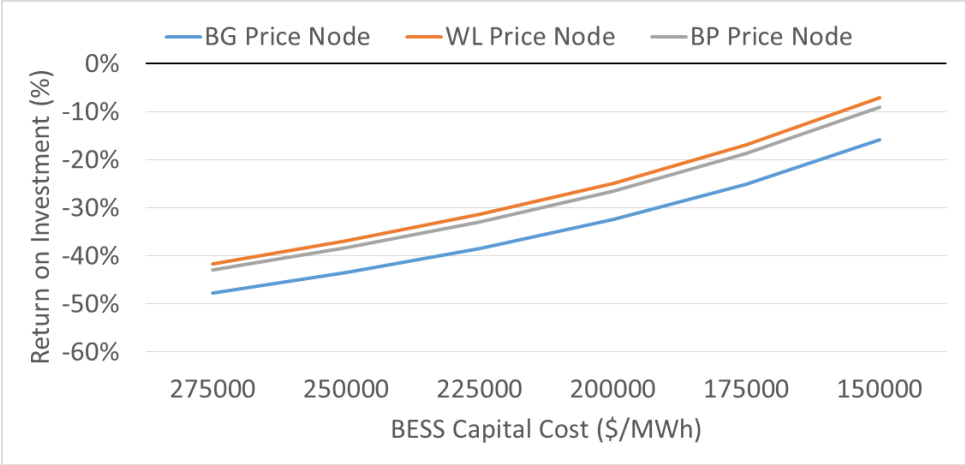

Figure 10 - ROI for at Burford Giffen assuming difference price nodes and capital cost values for a BESS sized to be a) 20 MWh / 5 MW and b) 40 MWh / 10 MW.

Although a 12 MW maximum export for Burford Giffen in the entire considered timeframe is assumed, it is important to note that PG&E's permanent curtailment for the site (and presumably other local sites) was not implemented until 2019. This fact is reflected in the staggering differences in historical LMP and consequently energy arbitrage returns for the BESS scenarios. This is also seen in how there is some difference between the BG and WL price nodes in 2018 but the values converge in 2019 in Figure 9. The same pattern persists in the P2G2P and

LCFS results to follow. Local congestion is thought to exist in 2018 and has severely been mitigated in 2019 which explains the difference of ROI ranges.

Though this seems to imply the BESS ROI seen in Figure 7 and Figure 9 will remain largely negative when congestion is relieved (as seen in the 2019 values), solar resources will likely continue to be deployed throughout the state faster than transmission and distribution (T&D) system upgrades will be executed. In addition, these T&D system upgrades come with associated costs (which are usually spread out over all ratepayers) that can be avoided with energy storage and the savings of avoided T&D upgrades can through existing programs and policies in many jurisdictions be given to the owners of energy storage systems to improve ROI (either through capital cost buy down, or access to special tariffs). With many uncertainties regarding how other market participants may act and how future policies may evolve, long cycling periods of local congestion and non-congestion will be a reasonable future system state.

3.2.2 Power-to-Gas-to-Power (P2G2P)

The P2G2P scenario has EAC columns for the fuel cell, electrolyzer, and physical storage system separately. The other costs and revenues remain the same as from the BESS scenario. The P2G2P scenario utilizes an 8 MW electrolyzer, 2 MW fuel cell, and 500 MWh energy storage system. The most distinguishable aspect of the P2G2P scenarios is the operation. Rather than attempting to purchase low midday prices and selling within the same day, the advantage of low self-discharge and cheap energy capacity to achieve long-duration storage is considered. This is accomplished by setting a price threshold for sending electricity to the electrolyzer when the hourly price is under 20 $/MWh and producing electricity with the fuel cell when the price is above 40 $/MWh. Sensitivity for these thresholds is evaluated in a latter case. As done in the BESS

analysis, all the three price nodes are considered. Figure 11 illustrates how the P2G2P system fairs over the previous 22 months resulting in an ROI of -96%, -88%, -90% when using BG, WL, and BP price nodes, respectively.

a)

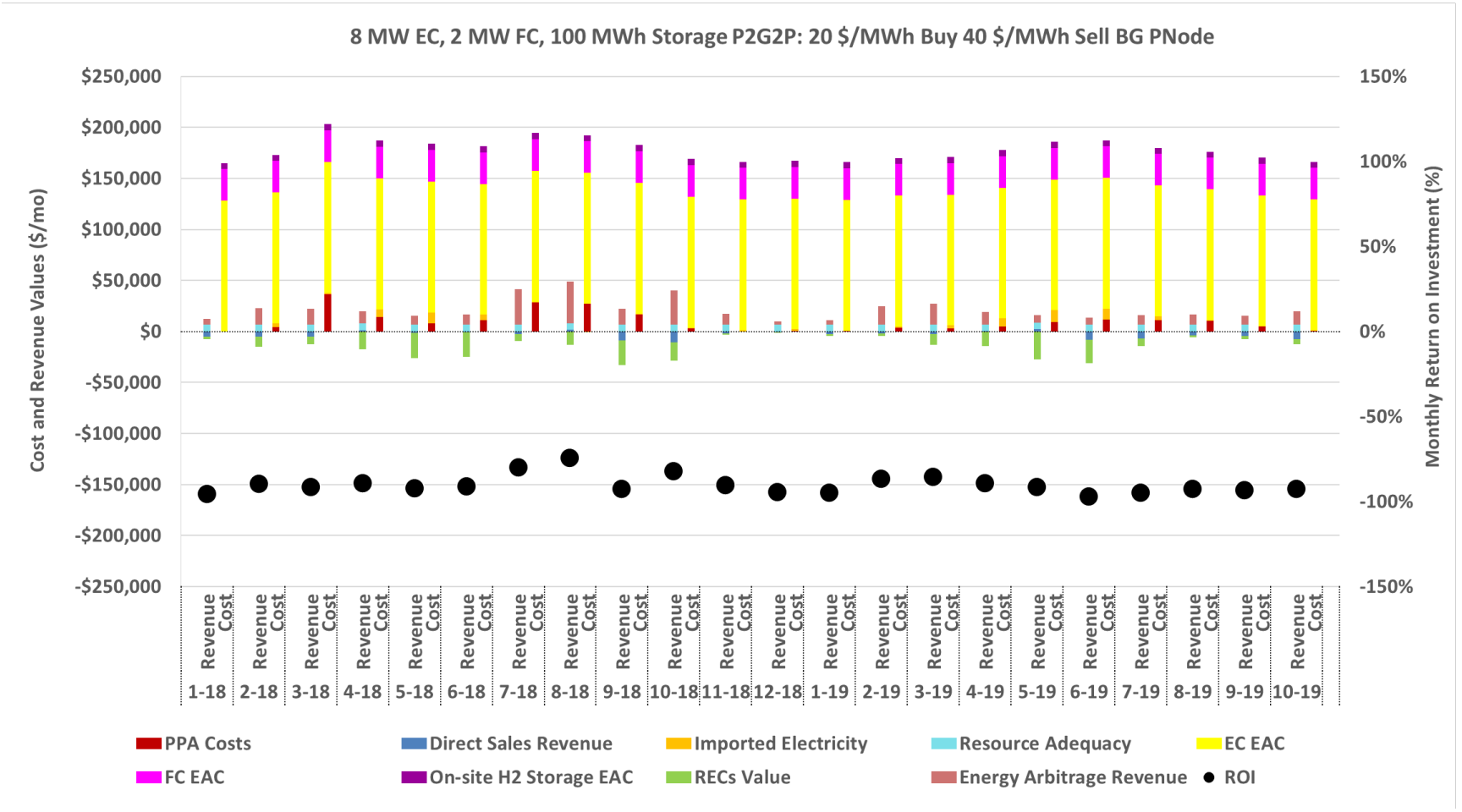
8 MW EC, 2 MW FC, 100 MWh Storage P2G2P: 20 $/MWh Buy 40 $/MWh Sell BG PNode
Cost and Revenue Values ($/mo)
Monthly Return on Investment (%)
$250,000
$200,000
$150,000
$100,000
$50,000
$0
-$50,000
-$100,000
-$150,000
-$200,000
-$250,000
150%
100%
50%
0%
-50%
-100%
-150%
Revenue
Cost
1-18
2-18
3-18
4-18
5-18
6-18
7-18
8-18
9-18
10-18
11-18
12-18
1-19
2-19
3-19
4-19
5-19
6-19
7-19
8-19
9-19
10-19
PPA Costs
Direct Sales Revenue
Imported Electricity
Resource Adequacy
EC EAC
FC EAC
On-site H2 Storage EAC
RECs Value
Energy Arbitrage Revenue
ROI

b)

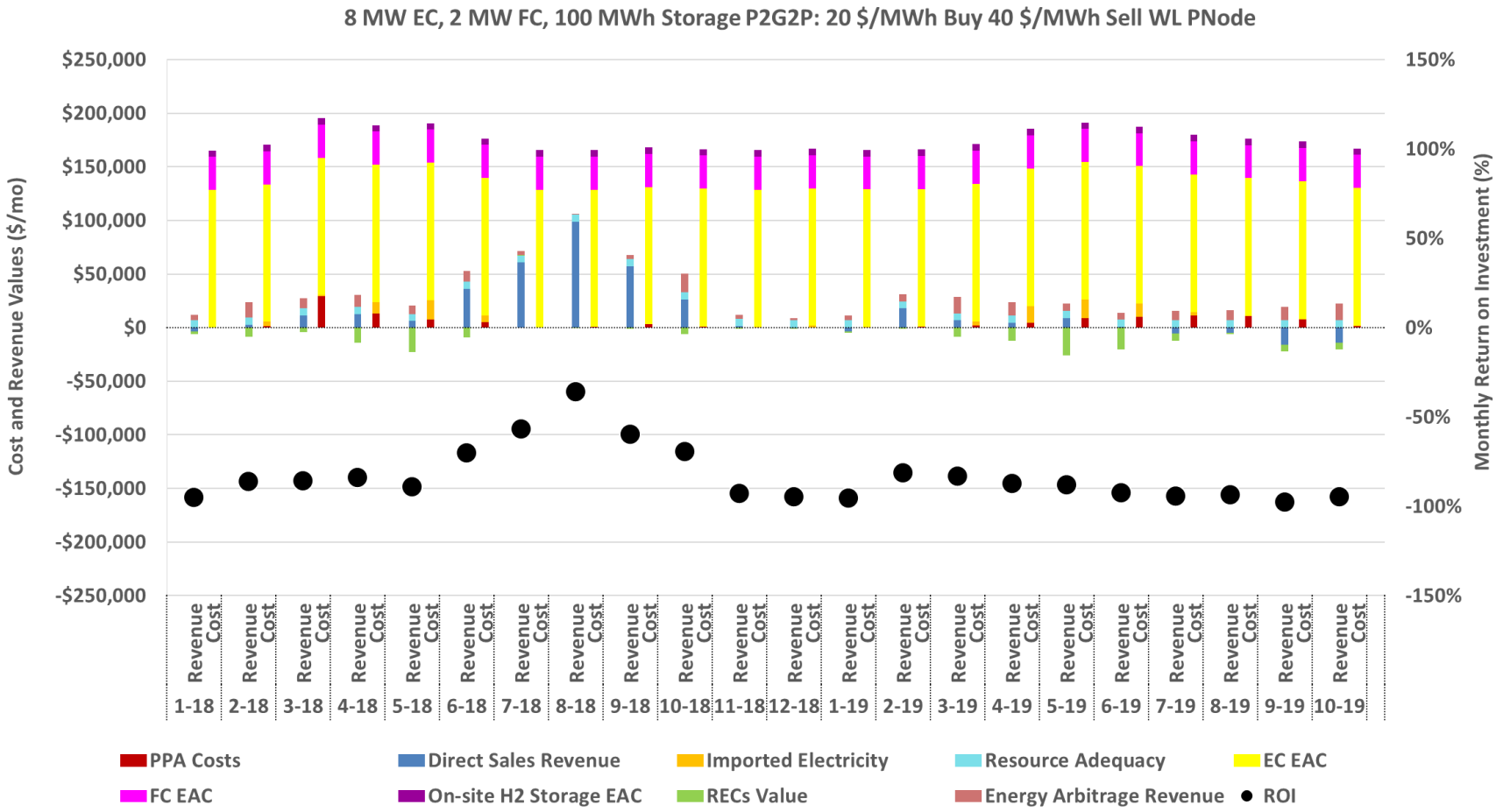
8 MW EC, 2 MW FC, 100 MWh Storage P2G2P: 20 $/MWh Buy 40 $/MWh Sell WL PNode
Cost and Revenue Values ($/mo)
Monthly Return on Investment (%)
$250,000
$200,000
$150,000
$100,000
$50,000
$0
-$50,000
-$100,000
-$150,000
-$200,000
-$250,000
150%
100%
50%
0%
-50%
-100%
-150%
Revenue
Cost
1-18
2-18
3-18
4-18
5-18
6-18
7-18
8-18
9-18
10-18
11-18
12-18
1-19
2-19
3-19
4-19
5-19
6-19
7-19
8-19
9-19
10-19
PPA Costs
Direct Sales Revenue
Imported Electricity
Resource Adequacy
EC EAC
FC EAC
On-site H2 Storage EAC
RECs Value
Energy Arbitrage Revenue
ROI

c)

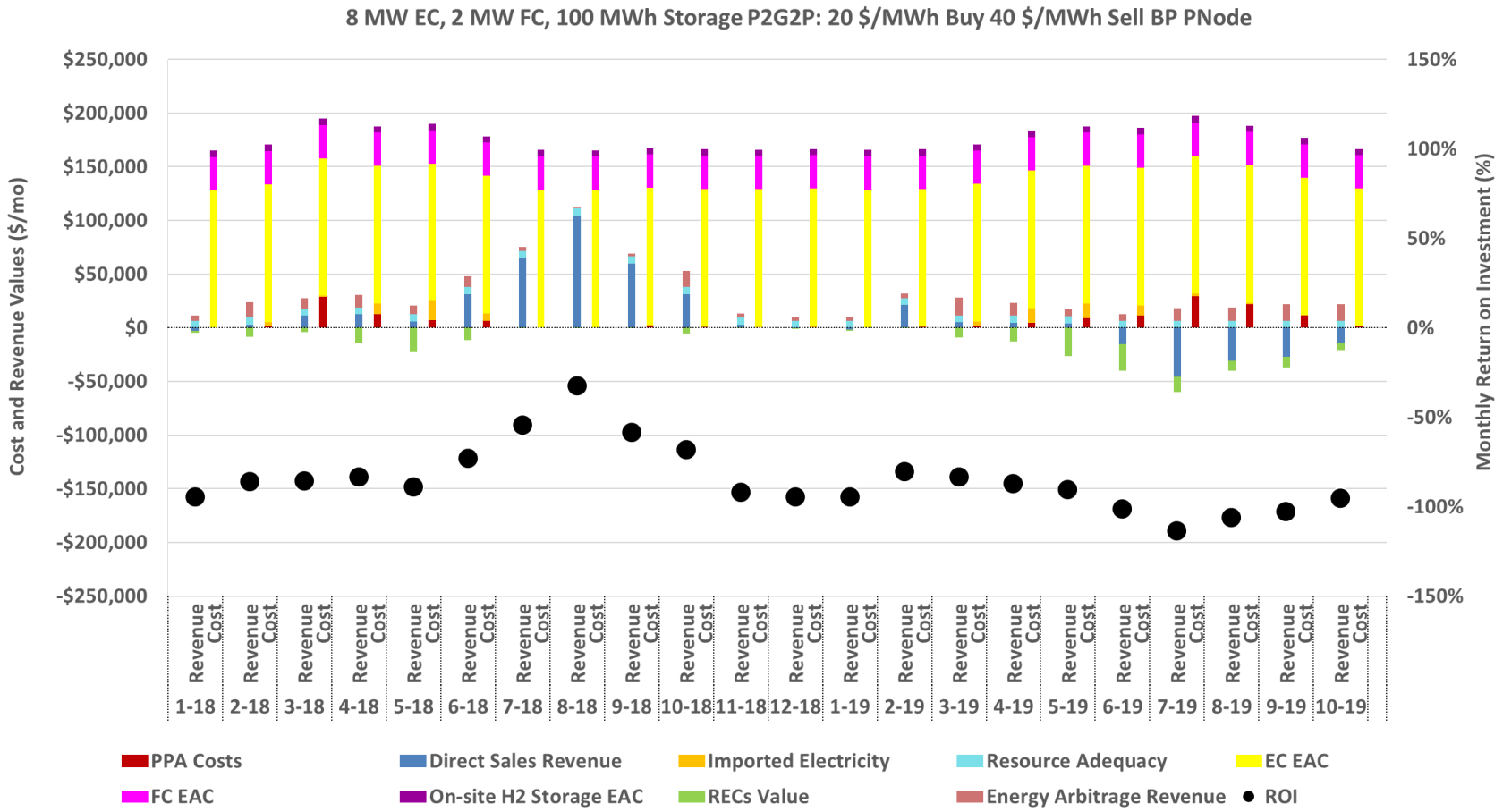

Figure 11 - Monthly costs and revenue from implementing 2 MW fuel cell, 8 MW electrolyzer with 20 and 40 $/MWh price thresholds at Burford Giffen assuming a) BG price node b) WL price node and c) BP price node.

The largest revenue is seen in the 2018 summer months due to increases in direct sales of electricity that was previously curtailed. Though the P2G2P system produces power even in the winter months, the 40 $/MWh price floor is slightly more frequent in the spring and summer months.

We consider a separate case in which the electrolyzer price threshold is lowered to 0 $/MWh and the fuel cell price threshold is increased to 50 $/MWh as an attempt increase the margins of energy arbitrage. Though this slightly increases the energy arbitrage revenue by lower charging cost for the storage system, the total volume of energy sales decreases resulting in a similar net revenue amount as previously. In general, the lower throughput corresponding to a shrink of the wholesale energy sales columns seen in Figure 12. This results in an ROI of -95%, -84%, -87% when using BG, WL, and BP price nodes, respectively.

a)

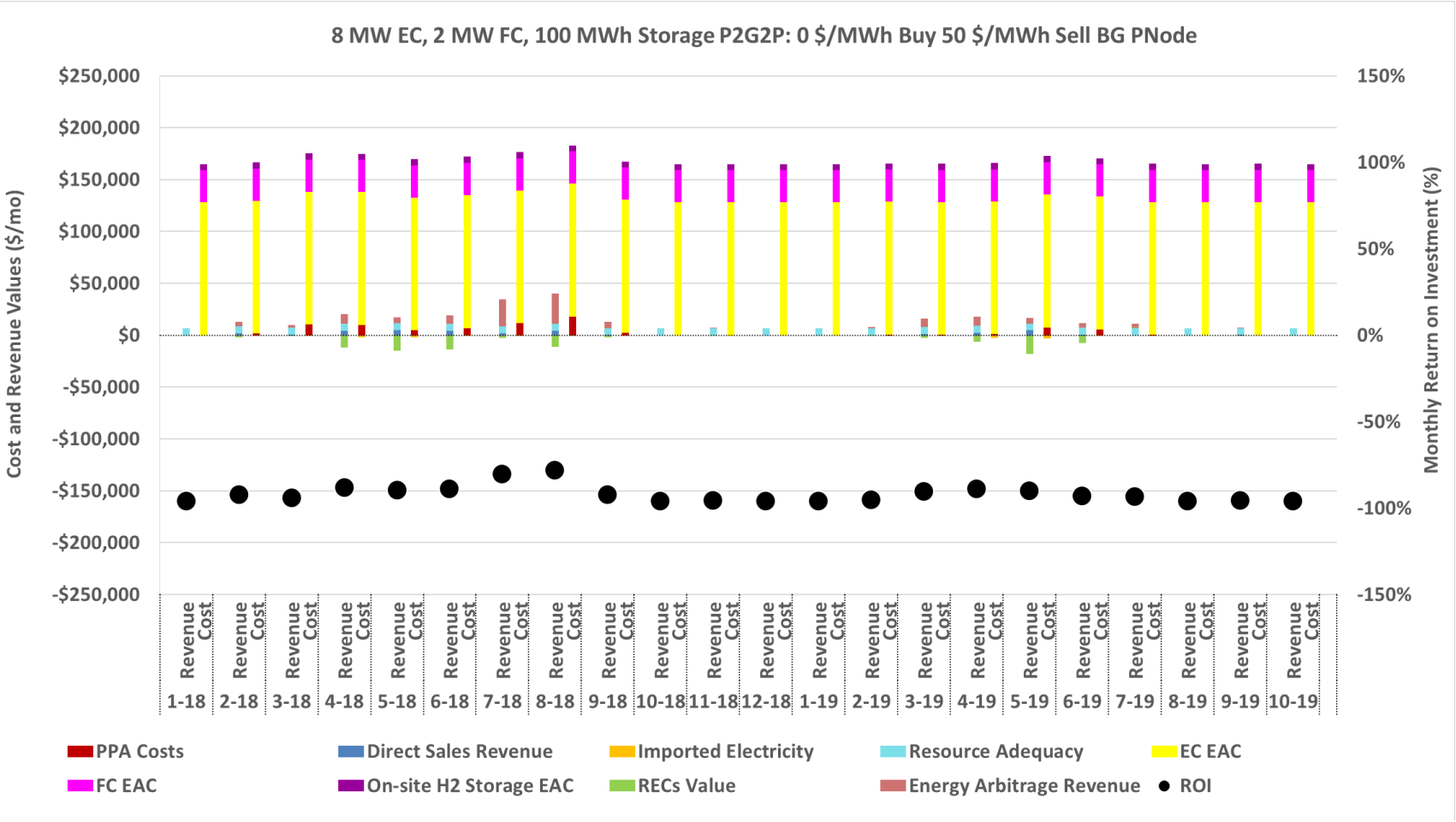
8 MW EC, 2 MW FC, 100 MWh Storage P2G2P: 0 $/MWh Buy 50 $/MWh Sell BG PNode
Cost and Revenue Values ($/mo)
Monthly Return on Investment (%)
$250,000
$200,000
$150,000
$100,000
$50,000
$0
-$50,000
-$100,000
-$150,000
-$200,000
-$250,000
150%
100%
50%
0%
-50%
-100%
-150%
Revenue
Cost
1-18
2-18
3-18
4-18
5-18
6-18
7-18
8-18
9-18
10-18
11-18
12-18
1-19
2-19
3-19
4-19
5-19
6-19
7-19
8-19
9-19
10-19
PPA Costs
Direct Sales Revenue
Imported Electricity
Resource Adequacy
EC EAC
FC EAC
On-site H2 Storage EAC
RECs Value
Energy Arbitrage Revenue
ROI

b)

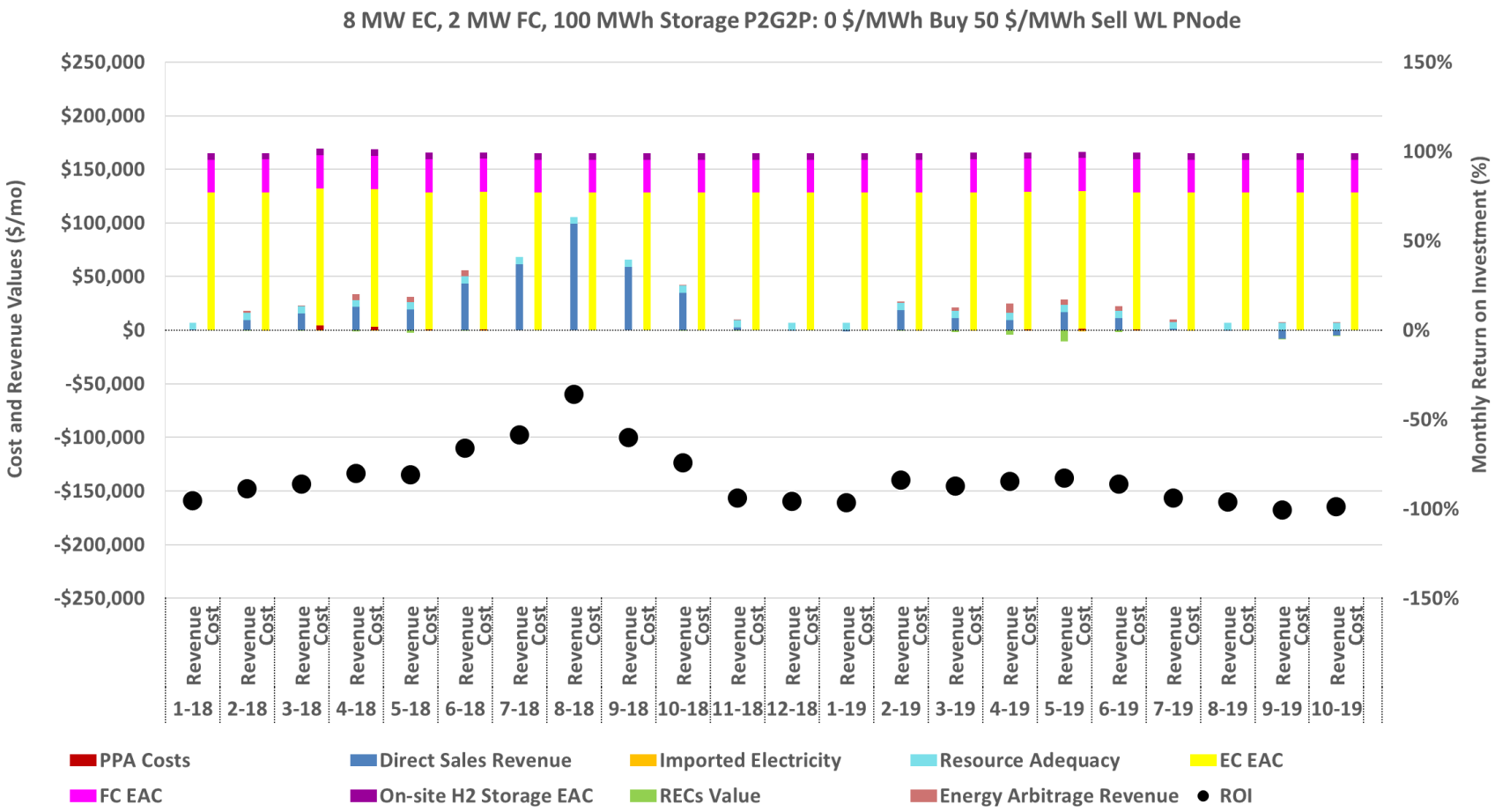
8 MW EC, 2 MW FC, 100 MWh Storage P2G2P: 0 $/MWh Buy 50 $/MWh Sell WL PNode
Cost and Revenue Values ($/mo)
Monthly Return on Investment (%)
$250,000
$200,000
$150,000
$100,000
$50,000
$0
-$50,000
-$100,000
-$150,000
-$200,000
-$250,000
150%
100%
50%
0%
-50%
-100%
-150%
Revenue
Cost
1-18
2-18
3-18
4-18
5-18
6-18
7-18
8-18
9-18
10-18
11-18
12-18
1-19
2-19
3-19
4-19
5-19
6-19
7-19
8-19
9-19
10-19
PPA Costs
Direct Sales Revenue
Imported Electricity
Resource Adequacy
EC EAC
FC EAC
On-site H2 Storage EAC
RECs Value
Energy Arbitrage Revenue
ROI

c)

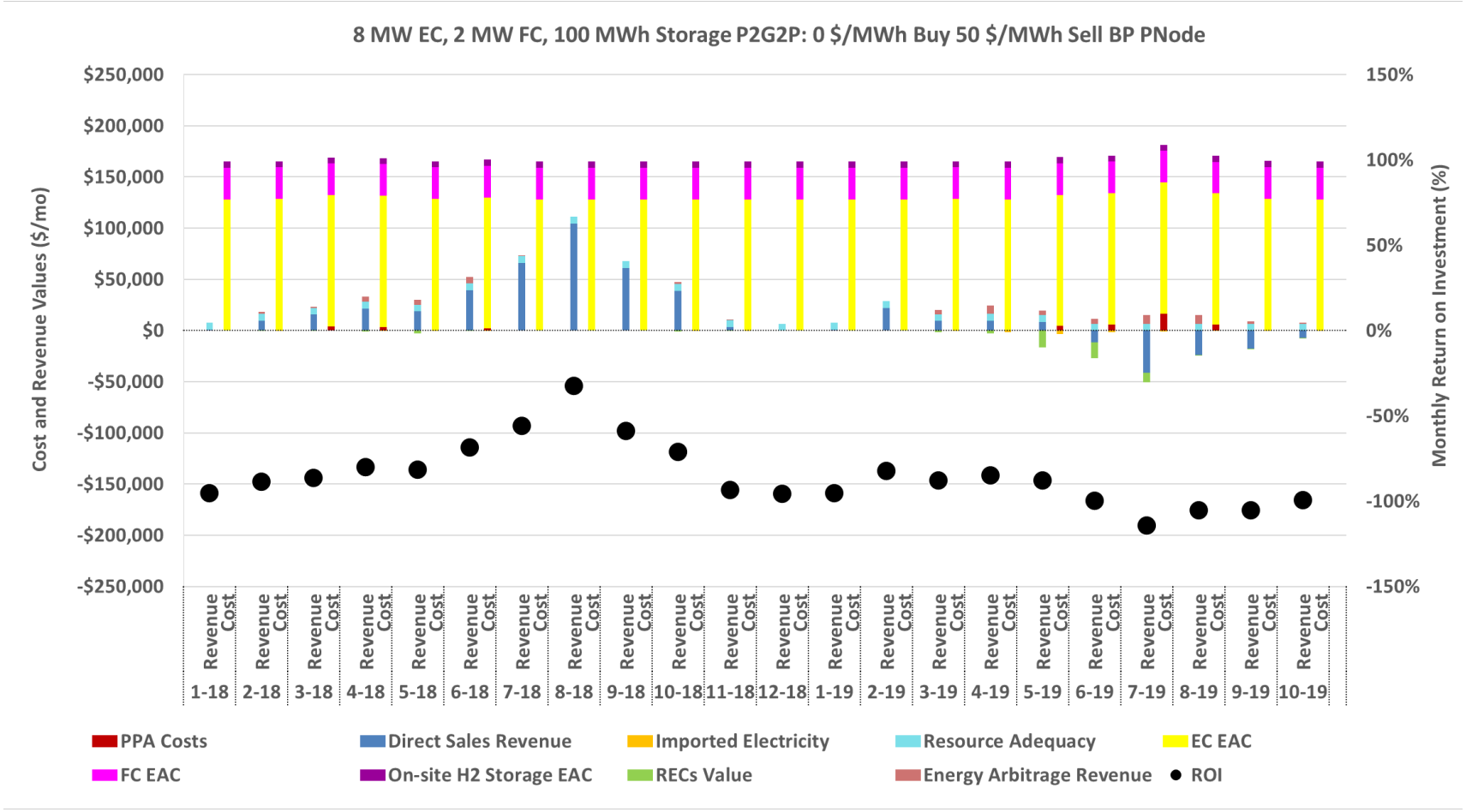

Figure 12 - Monthly costs and revenue from implementing 2 MW fuel cell, 8 MW electrolyzer with 0 and 50 $/MWh price thresholds at Burford Giffen assuming a) BG price node b) WL price node and c) BP price node.

These more selective price thresholds pose a threat to the base assumption that the storage system relieves the transmission line congestion. In addition to ensuring the electrolyzer must be large enough to relieve congestion, it must also be operating at high enough power amounts to do so. Notice there are hardly any costs associated with imported electricity, so it is difficult to suggest that congestion is relieved unlike in the 20 and 40 $/MWh price threshold case. More selective price thresholds also result in lower utilization from the components while capital costs remain the same. The activity of hydrogen storage from the beginning of 2018 to April 2019 for the two prior discussed cases is shown in Figure 13. Note that the storage amount assumed is quickly filled in the Spring and quickly emptied in the Fall and how the selective price threshold case fluctuates much less.

a)

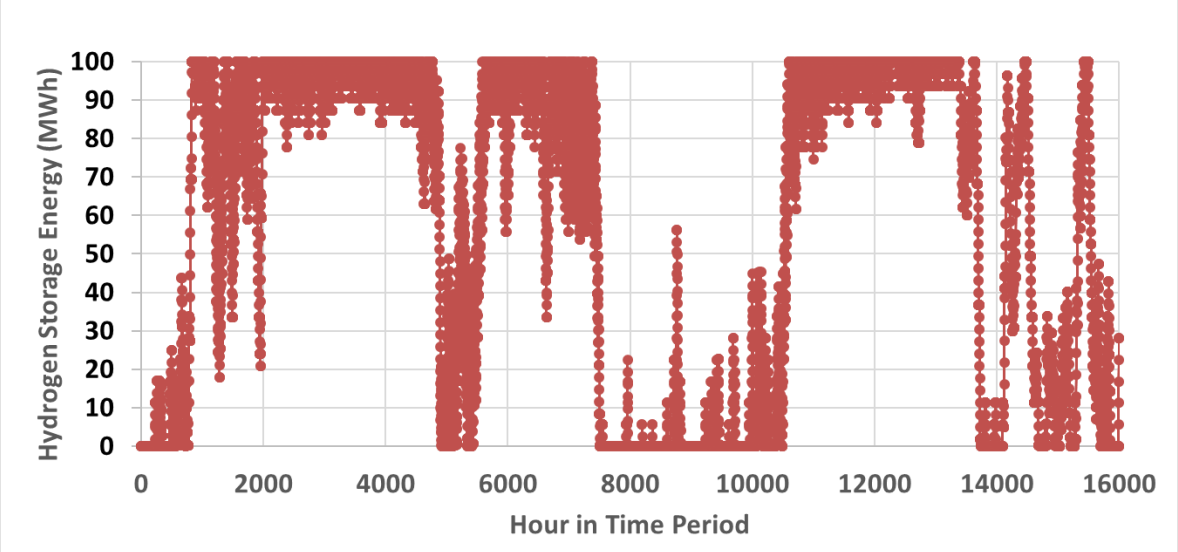

b)

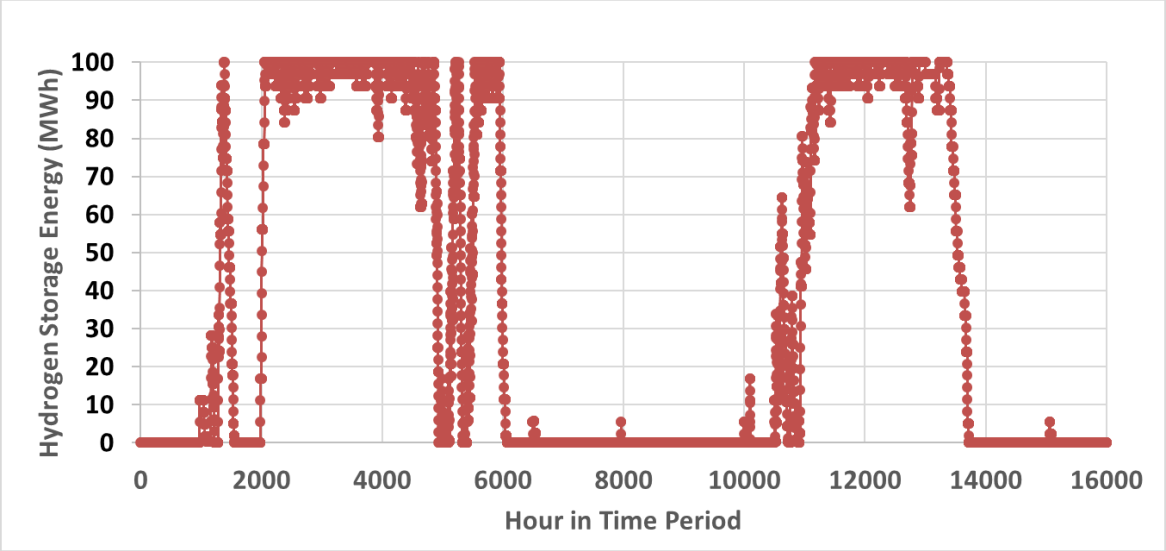

Figure 13 – Storage level with 2 MW fuel cell, 5 MW electrolyzer, and 100 MWh storage capacity at Burford Giffen in scenario with a) 20 and 40 $/MWh price thresholds and b) 0 and 50 $/MWh thresholds.

Several electrolyzer and fuel cell capital cost numbers are evaluated to investigate the necessary capital cost reduction to achieve profitability using the 20 and 40 $/MWh price thresholds. The results are summarized visually in Figure 14.

a)

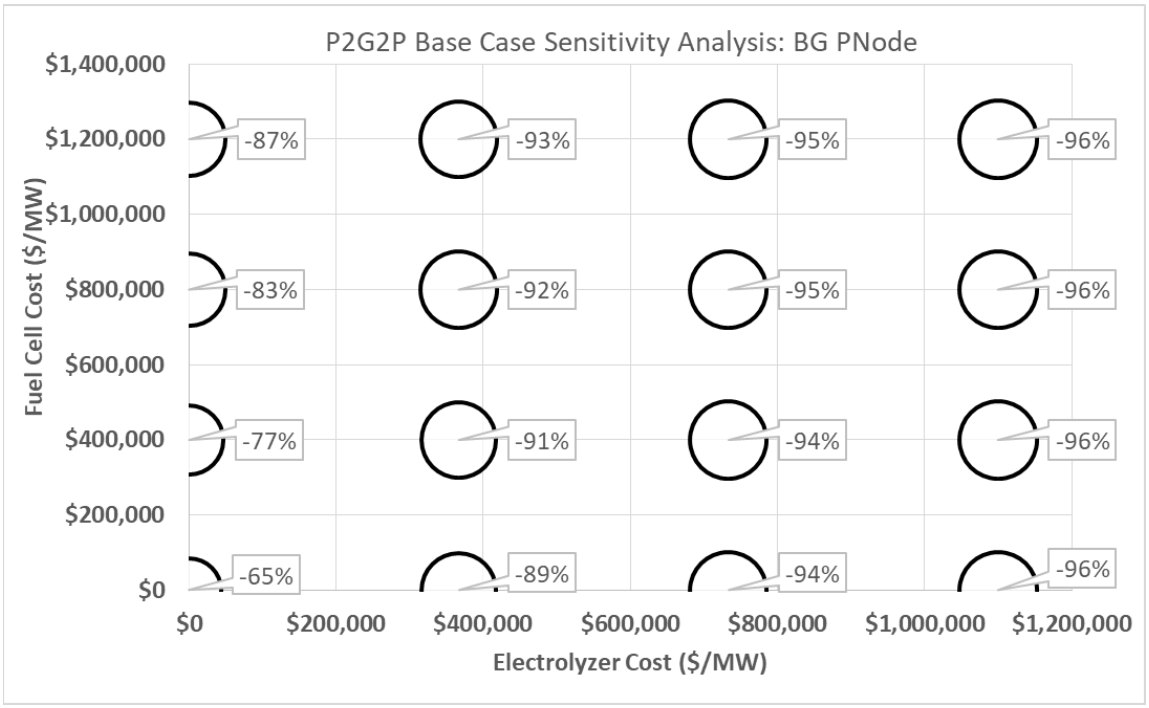
P2G2P Base Case Sensitivity Analysis: BG PNode
Fuel Cell Cost ($/MW)
$1,400,000
$1,200,000
$1,000,000
$800,000
$600,000
$400,000
$200,000
$0
-87%
-93%
-95%
-96%
-83%
-92%
-95%
-96%
-77%
-91%
-94%
-96%
-65%
-89%
-94%
-96%
$0
$200,000
$400,000
$600,000
$800,000
$1,000,000
$1,200,000
Electrolyzer Cost ($/MW)

b)

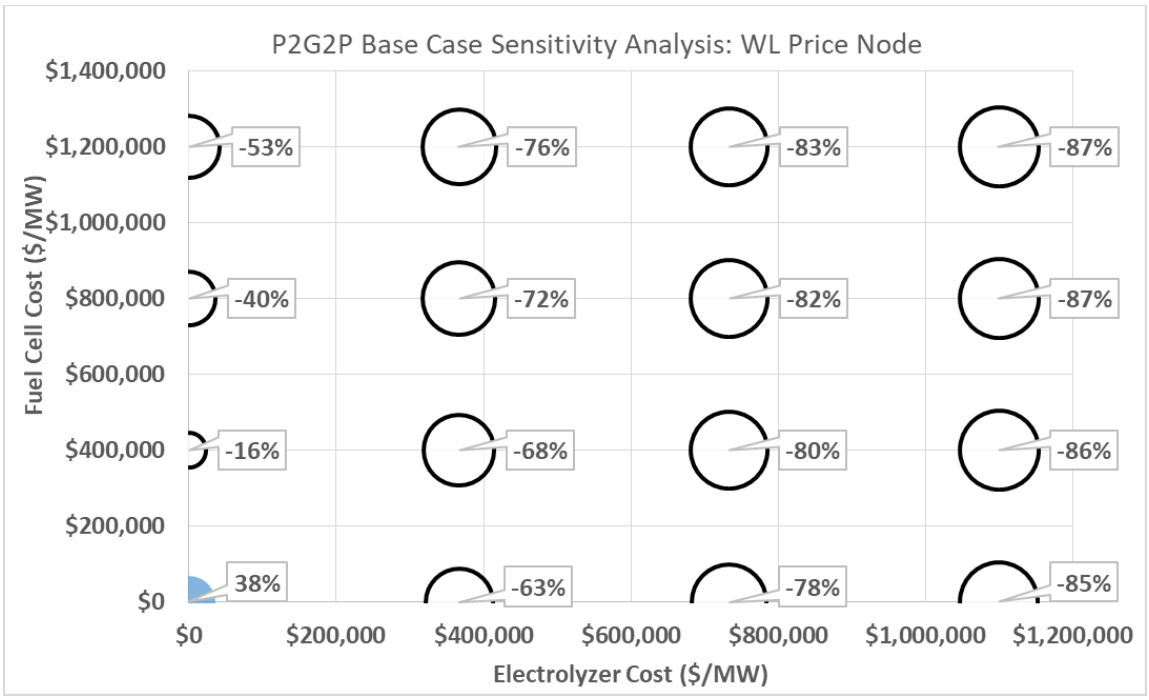
P2G2P Base Case Sensitivity Analysis: WL Price Node
Fuel Cell Cost ($/MW)
$1,400,000
$1,200,000
$1,000,000
$800,000
$600,000
$400,000
$200,000
$0
-53%
-76%
-83%
-87%
-40%
-72%
-82%
-87%
-16%
-68%
-80%
-86%
38%
-63%
-78%
-85%
$0
$200,000
$400,000
$600,000
$800,000
$1,000,000
$1,200,000
Electrolyzer Cost ($/MW)

c)

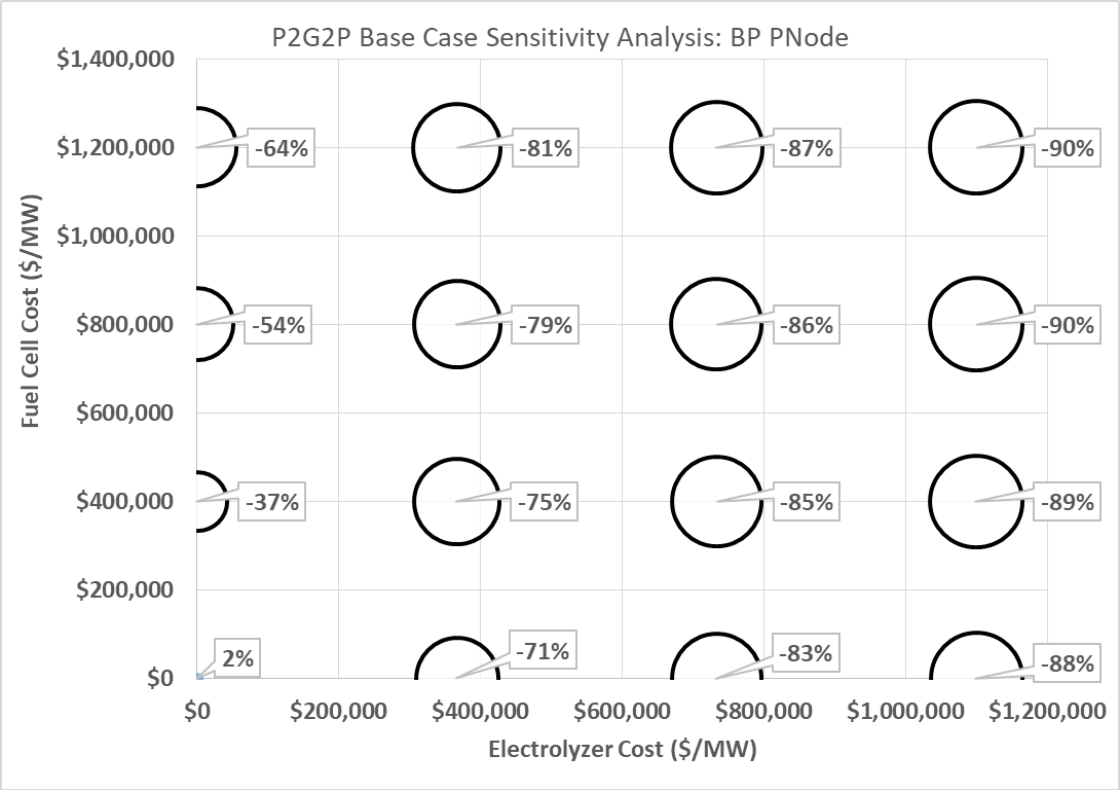

Figure 14 – ROI for P2G2P base case operation with lower capital cost values assuming a) BG price node b) WL price node and c) BP price node.

Even if the large cost of the fuel cell and electrolyzer are free, the PPA cost that the UCOP would have to pay the developers is almost always sold to the grid at lower wholesale prices. The cost recovered when selling electricity to the grid is exacerbated by the roundtrip efficiency of P2G2P as well. A revision of the base case monthly costs and revenues when the electrolyzer and fuel cell costs are zero is presented below in Figure 15. These graphs correspond to the greatest ROI points in Figure 14 where the electrolyzer and fuel cell capital cost is zero.

a)

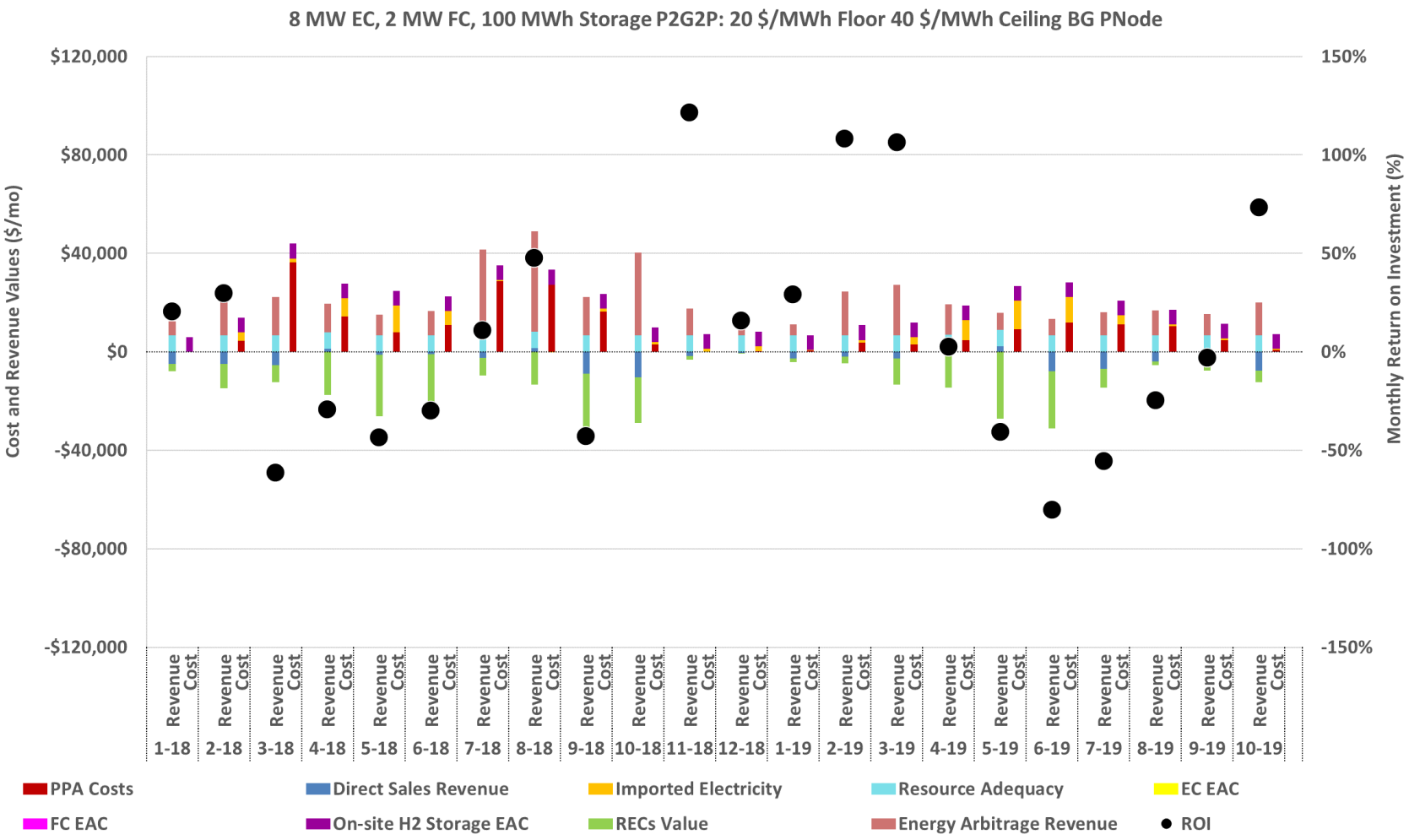
8 MW EC, 2 MW FC, 100 MWh Storage P2G2P: 20 $/MWh Floor 40 $/MWh Ceiling BG PNode
Cost and Revenue Values ($/mo)
Monthly Return on Investment (%)
$120,000
$80,000
$40,000
$0
-$40,000
-$80,000
-$120,000
150%
100%
50%
0%
-50%
-100%
-150%
Revenue
Cost
1-18
2-18
3-18
4-18
5-18
6-18
7-18
8-18
9-18
10-18
11-18
12-18
1-19
2-19
3-19
4-19
5-19
6-19
7-19
8-19
9-19
10-19
PPA Costs
Direct Sales Revenue
Imported Electricity
Resource Adequacy
EC EAC
FC EAC
On-site H2 Storage EAC
RECs Value
Energy Arbitrage Revenue
ROI

b)

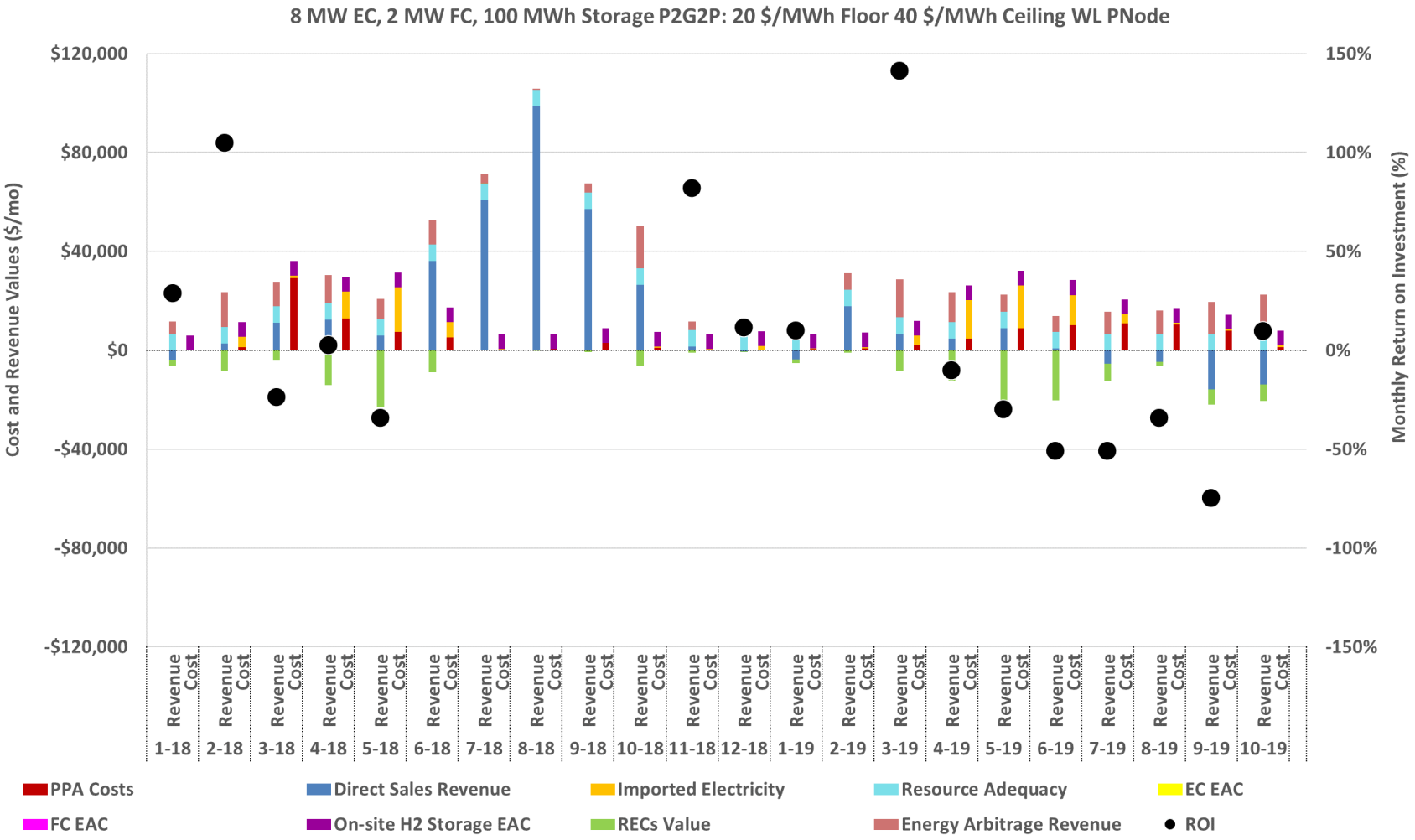
8 MW EC, 2 MW FC, 100 MWh Storage P2G2P: 20 $/MWh Floor 40 $/MWh Ceiling WL PNode
Cost and Revenue Values ($/mo)
Monthly Return on Investment (%)
$120,000
$80,000
$40,000
$0
-$40,000
-$80,000
-$120,000
150%
100%
50%
0%
-50%
-100%
-150%
Revenue
Cost
1-18
2-18
3-18
4-18
5-18
6-18
7-18
8-18
9-18
10-18
11-18
12-18
1-19
2-19
3-19
4-19
5-19
6-19
7-19
8-19
9-19
10-19
PPA Costs
Direct Sales Revenue
Imported Electricity
Resource Adequacy
EC EAC
FC EAC
On-site H2 Storage EAC
RECs Value
Energy Arbitrage Revenue
ROI

c)

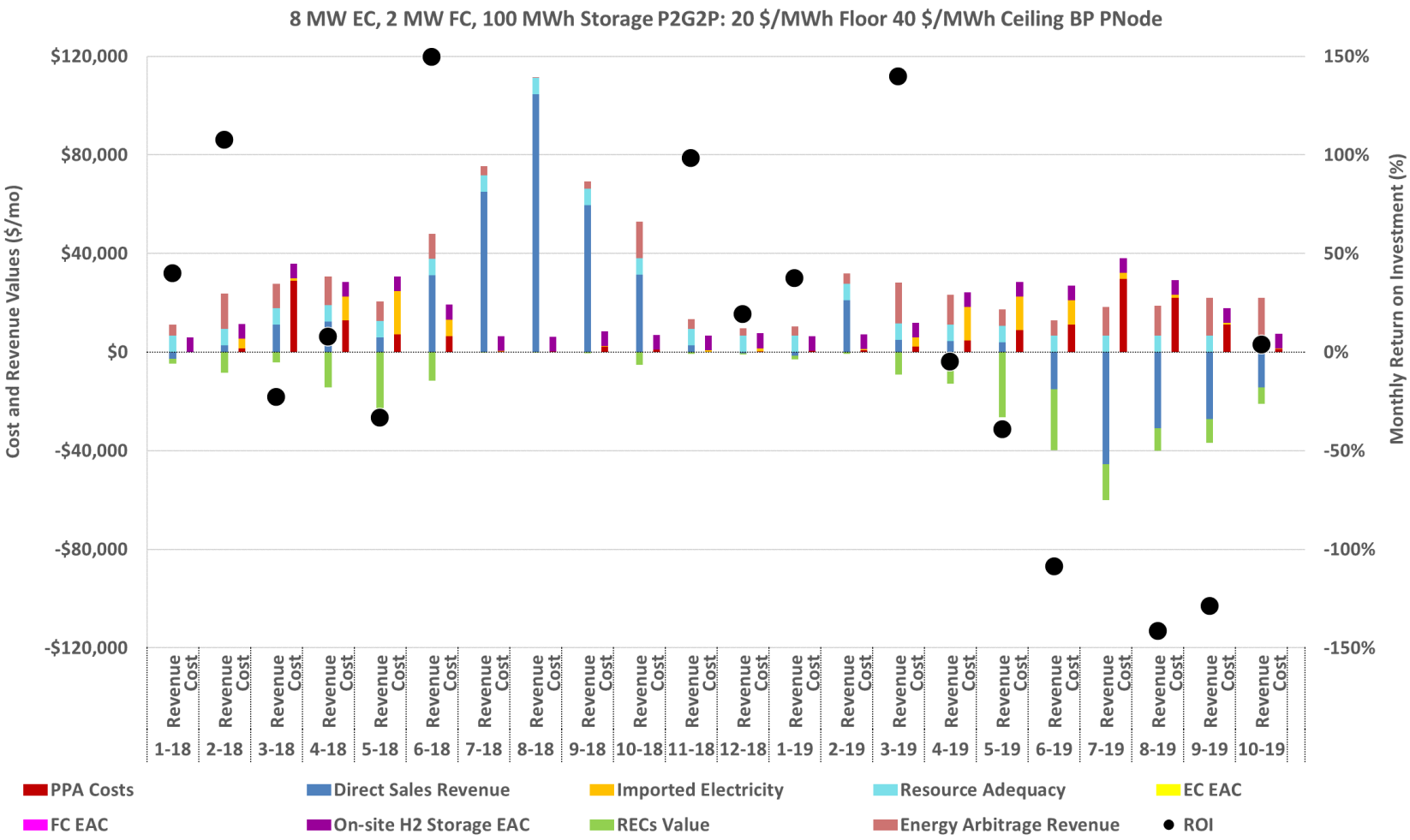

Figure 15 – P2G2P base case results when electrolyzer and fuel cell capital cost are zero assuming a) BG price node b) WL price node and c) BP price node.

Note that the results from seen in Figure 15 above are still in reference to the BAU case. Much of the wholesale energy sales can still be attributed to direct sales as discussed previously in the BESS and P2G2P base cases. Some months have a ROI much higher than 150% only because the new total costs are relatively small in comparison to the revenue.

Though the ROI is negative even at substantially low capital cost prices, the P2G2P operation of the system based on LMP allows it to shift energy from one season to another. Note that zero income is being provided to the P2G2P system for this seasonal energy storage capability. If operating based on prices thresholds, this type of system will undoubtedly provide major seasonal shifting value to the grid that currently is not rewarded. Note that for the prior P2G2P analysis, energy capacity was limited to a comparable amount as in the BESS case. Increasing the energy storage capacity only slightly worsens the resulting ROI due to the increased cost and lowered utilization. This could be offset if an additional revenue stream for seasonal shifting is considered. With the same equipment size and operation characteristics as the P2G2P base case, thousands of MWh can be moved to another season at Burford Giffen regardless of the price node as shown in Figure 16.

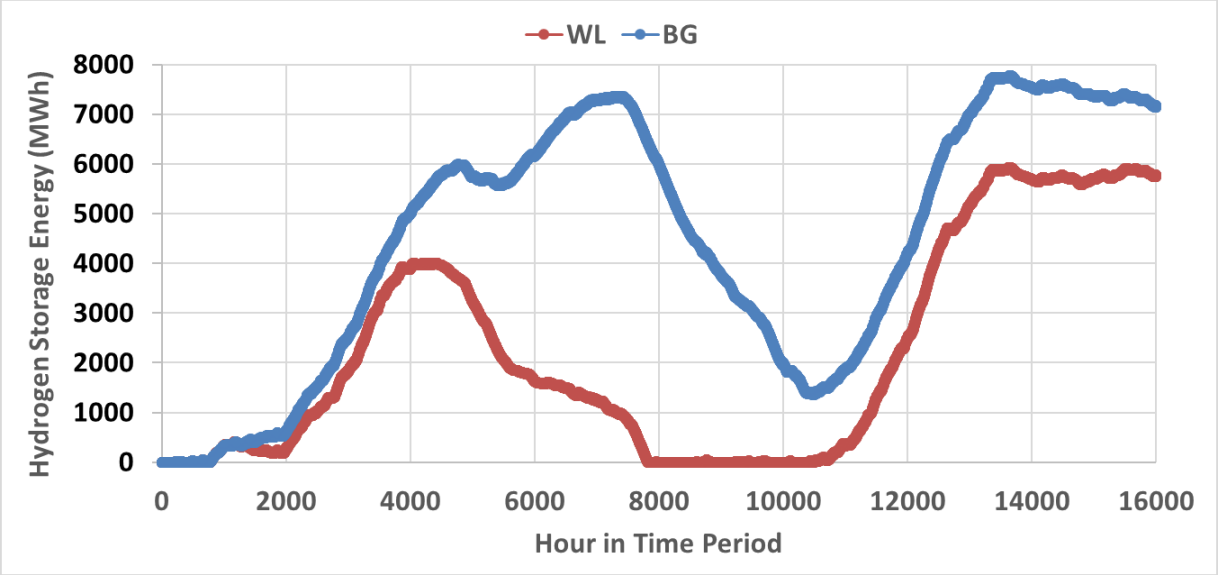

Figure 16 - Hydrogen storage levels from implementing 2 MW fuel cell, 8 MW electrolyzer without storage capacity constraint and utilizing 20 and 40 $/MWh price thresholds.

3.2.3 Low Carbon Fuel Standard (LCFS)

When using the WL price node, there are fewer low-price hours during peak solar generation as there is very little congestion. As compared to the other more historically congested price nodes, the opportunity is lesser and makes using the WL values a conservative estimate and generalizable for solar generation sites that are deployed in areas with sufficient electric transmission capacity. This is an increasingly valid assumption when considering larger electrolyzer sizes.

Using many of the operational assumptions in the P2G2P base case for a base LCFS case. The monthly cost and revenue breakdown for an 8 MW electrolyzer, 20 $/MWh price electrolyzer threshold, and LCFS credit price of 190 $/MTCO2e are presented in Figure 17. This results in an ROI of -75%, -88%, -76%, -82% when hydrogen is directly transported to a fueling station 30 miles away a) by truck at 20 $/MWh price ceiling b) by pipeline at 20 $/MWh price ceiling c) by truck at

40 $/MWh price ceiling and d) by pipeline at 40 $/MWh price ceiling, respectively, seen in Figure 17.

a)

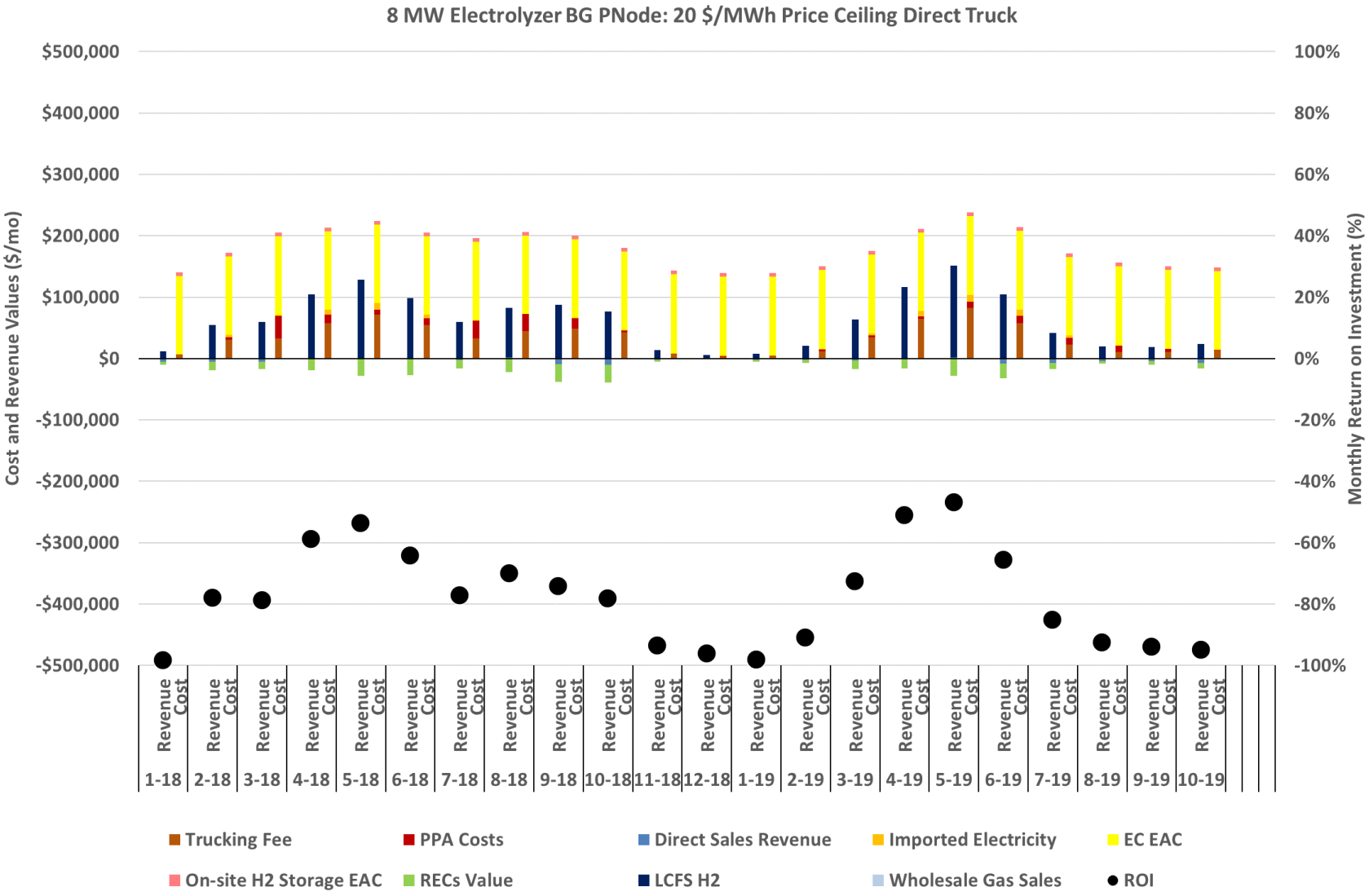
8 MW Electrolyzer BG PNode: 20 $/MWh Price Ceiling Direct Truck
Cost and Revenue Values ($/mo)
Monthly Return on Investment (%)
$500,000
$400,000
$300,000
$200,000
$100,000
$0
-$100,000
-$200,000
-$300,000
-$400,000
-$500,000
100%
80%
60%
40%
20%
0%
-20%
-40%
-60%
-80%
-100%
Revenue
Cost
1-18
2-18
3-18
4-18
5-18
6-18
7-18
8-18
9-18
10-18
11-18
12-18
1-19
2-19
3-19
4-19
5-19
6-19
7-19
8-19
9-19
10-19
Trucking Fee
PPA Costs
Direct Sales Revenue
Imported Electricity
EC EAC
On-site H2 Storage EAC
RECs Value
LCFS H2
Wholesale Gas Sales
ROI

b)

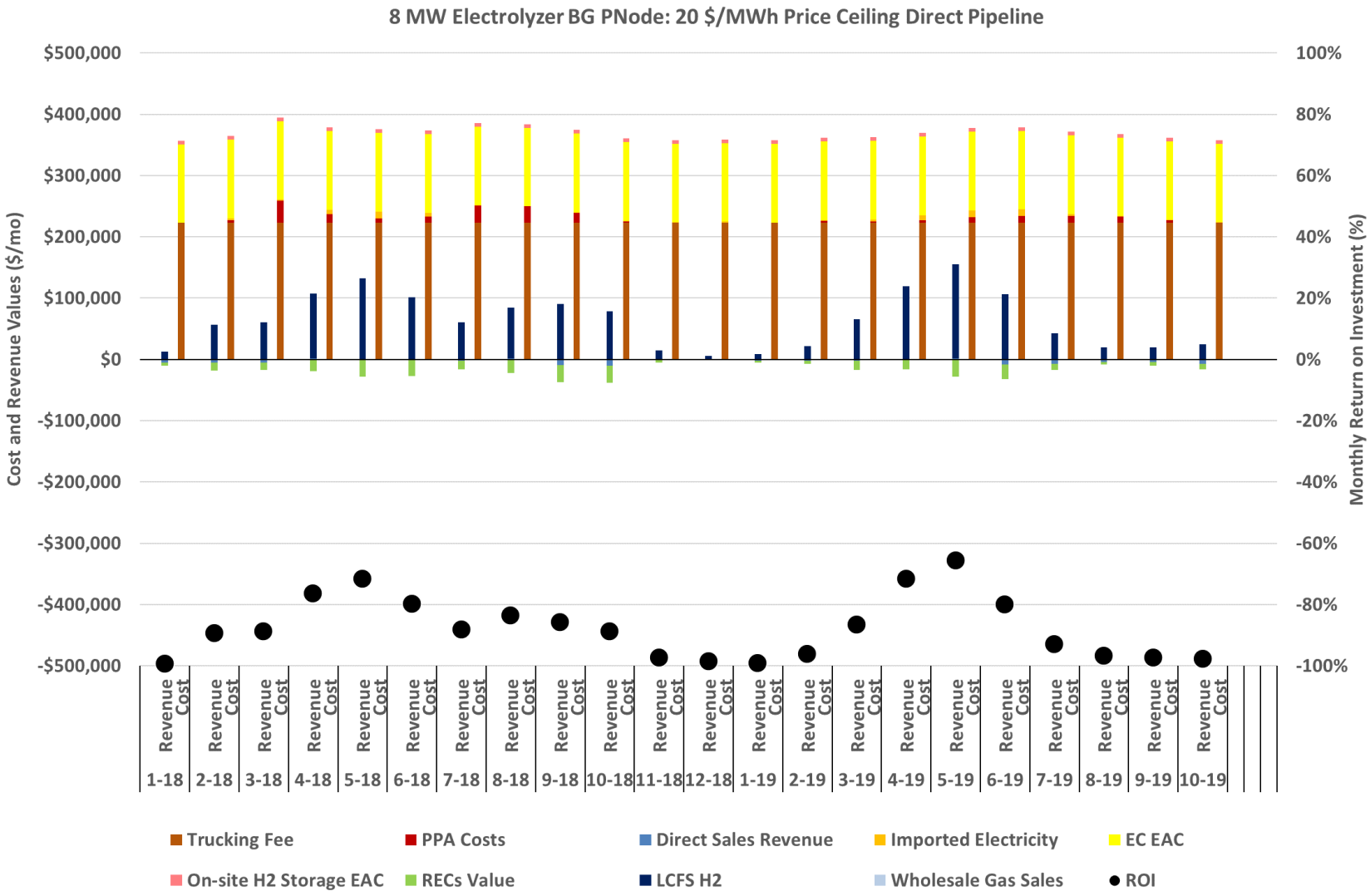
8 MW Electrolyzer BG PNode: 20 $/MWh Price Ceiling Direct Pipeline
Cost and Revenue Values ($/mo)
Monthly Return on Investment (%)
$500,000
$400,000
$300,000
$200,000
$100,000
$0
-$100,000
-$200,000
-$300,000
-$400,000
-$500,000
100%
80%
60%
40%
20%
0%
-20%
-40%
-60%
-80%
-100%
Revenue Cost
1-18 2-18 3-18 4-18 5-18 6-18 7-18 8-18 9-18 10-18 11-18 12-18 1-19 2-19 3-19 4-19 5-19 6-19 7-19 8-19 9-19 10-19
Trucking Fee
PPA Costs
Direct Sales Revenue
Imported Electricity
EC EAC
On-site H2 Storage EAC
RECs Value
LCFS H2
Wholesale Gas Sales
ROI

c)

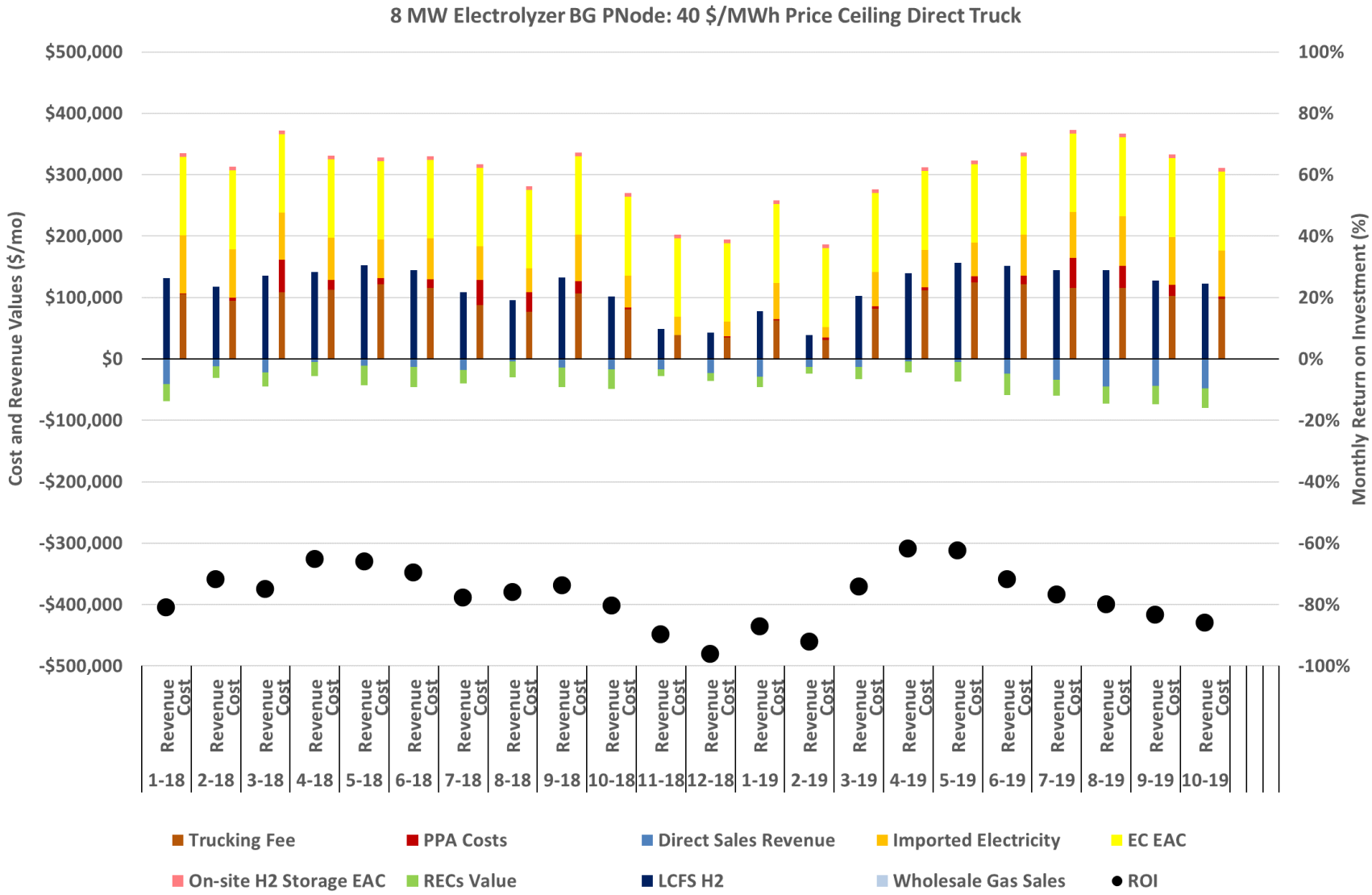
8 MW Electrolyzer BG PNode: 40 $/MWh Price Ceiling Direct Truck
Cost and Revenue Values ($/mo)
Monthly Return on Investment (%)
$500,000
$400,000
$300,000
$200,000
$100,000
$0
-$100,000
-$200,000
-$300,000
-$400,000
-$500,000
100%
80%
60%
40%
20%
0%
-20%
-40%
-60%
-80%
-100%
Revenue
Cost
1-18
2-18
3-18
4-18
5-18
6-18
7-18
8-18
9-18
10-18
11-18
12-18
1-19
2-19
3-19
4-19
5-19
6-19
7-19
8-19
9-19
10-19
Trucking Fee
PPA Costs
Direct Sales Revenue
Imported Electricity
EC EAC
On-site H2 Storage EAC
RECs Value
LCFS H2
Wholesale Gas Sales
ROI

d)

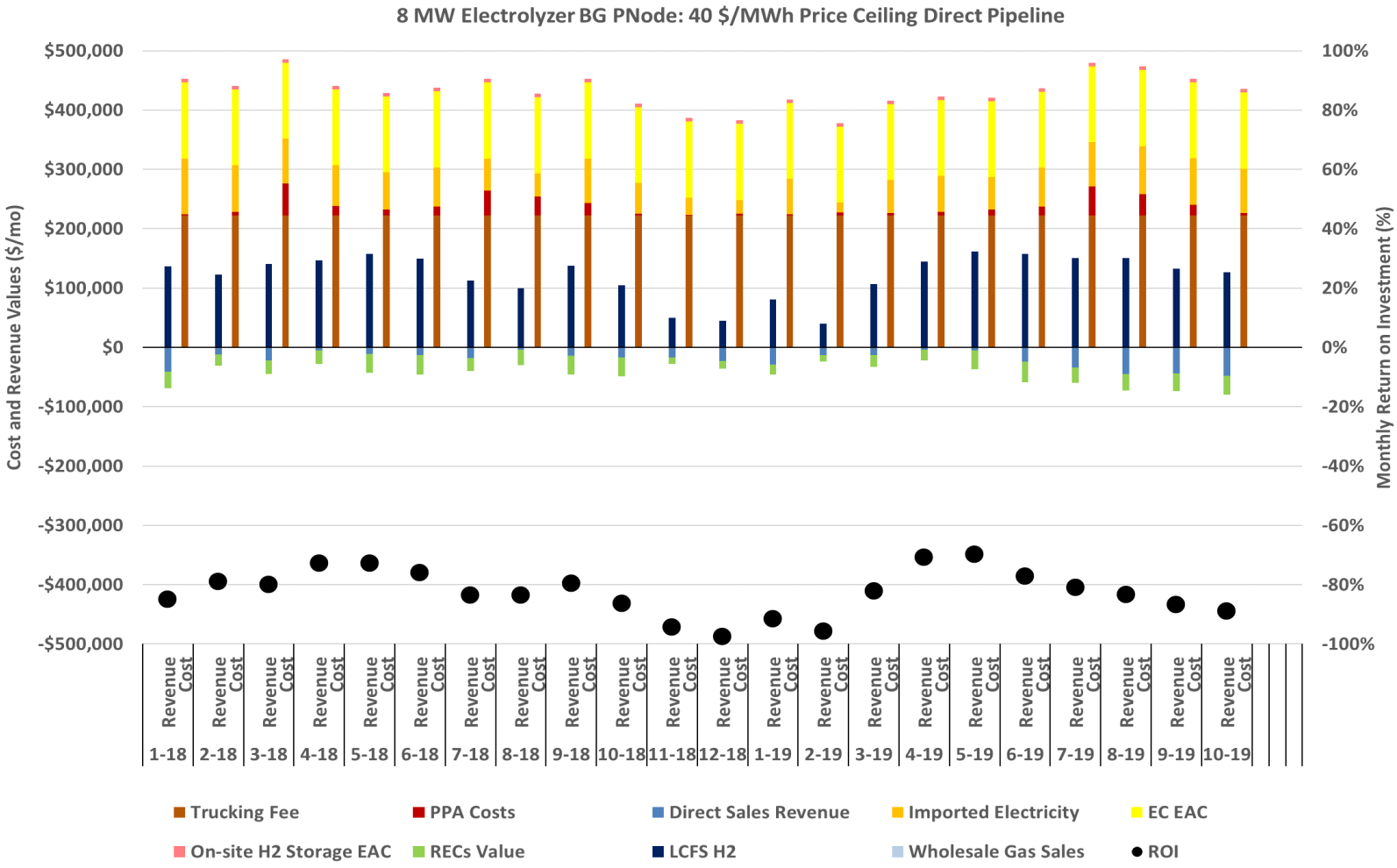

Figure 17 – Monthly cost and revenue breakdown for direct transport of hydrogen from Burford Giffen to a fueling station transported 30 miles away a) by truck at 20 $/MWh price ceiling b) by pipeline at 20 $/MWh price ceiling c) by truck at 40 $/MWh price ceiling and d) by pipeline at 40 $/MWh price ceiling.

The truck direct cases have less negative ROI as some of the pipeline capacity is not being utilized. The truck cases maintain a similar ROI across the board as the marginal cost and revenue for additional hydrogen production is already on a per kilogram basis, whereas the pipeline capital cost is a fixed amount which should aim to maximize its capacity factor. For this reason, the pipeline case improves slightly when increasing the price ceiling from 20 $/MWh to 40 $/MWh, but still not enough to surpass the truck scenarios. Similar to the energy arbitrage cases, there is slightly more low-cost electricity available in the spring and summer months.

3.3 Additional Pathways and Future Scenarios

Due to the duration curve of each of the price nodes, as presented previously in Figure 6, increasing the electrolyzer price ceiling from 0 $/MWh to 10 $/MWh results in a much smaller increase in electrolyzer activity than increasing the price ceiling from 30 $/MWh to 40 $/MWh. Note that a linear increase in price ceiling does not translate into a linear increase in capacity factor. The relation between these two manifests as an s-curve behavior as shown in Figure 18.

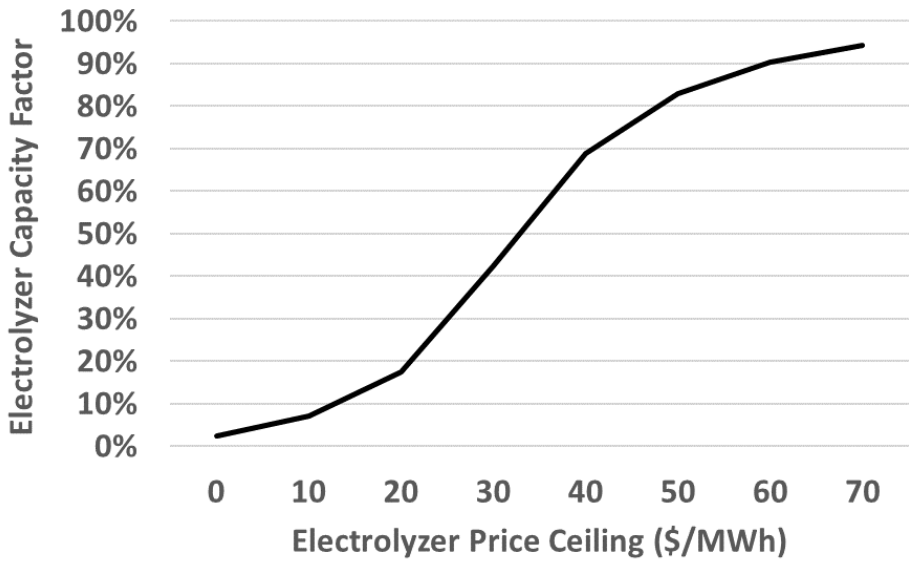

Figure 18 – Electrolyzer capacity factor can be controlled by considering the hourly wholesale electricity prices, consequently affecting feedstock carbon intensity, potential LCFS credit revenue, and ultimately return on investment of the project.

When the hourly price node is lower than the electrolyzer price ceiling, solar produced on-site is sent to the electrolyzer before the remainder of the capacity is filled with imported electricity. Hourly prices are at the lowest midday coincidentally with peak system wide and local solar production. Any grid electricity imported at low prices typically also have a low CI. The hourly price node value increases outside of peak solar hours as non-solar generators take over more of the load and corresponds with higher hourly grid CI. This results in a higher average CI for electrolysis if the system were operated more hours of each day seen in Figure 19. Operating at 100% capacity factor implies operating regardless of the hourly price node value.

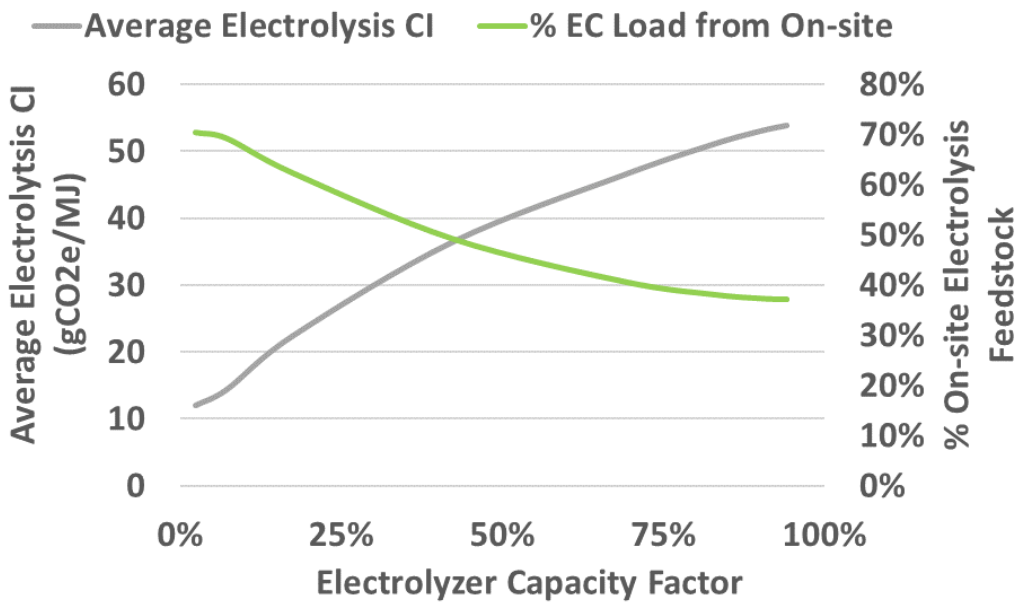

Figure 19 – Improving electrolyzer utilization requires importing hourly dependent grid electricity. Average feedstock electricity carbon intensity increases due to imports outside of peak solar generation.

Figure 20 is a collection of graphs presenting how three primary measures change when operating an electrolyzer at varying price ceilings (and thus capacity factors). Other than the addition of LCFS pathways, the assumptions remain the same as in the previous LCFS base case. These three measures are: 1) total pathway CI which includes production, transport, and end-use conditioning, 2) the amount of LCFS credit value relative to the amount from the predominant HYF pathway, and 3) the overall project ROI which considers all cost and revenue streams as done in previous analyses.

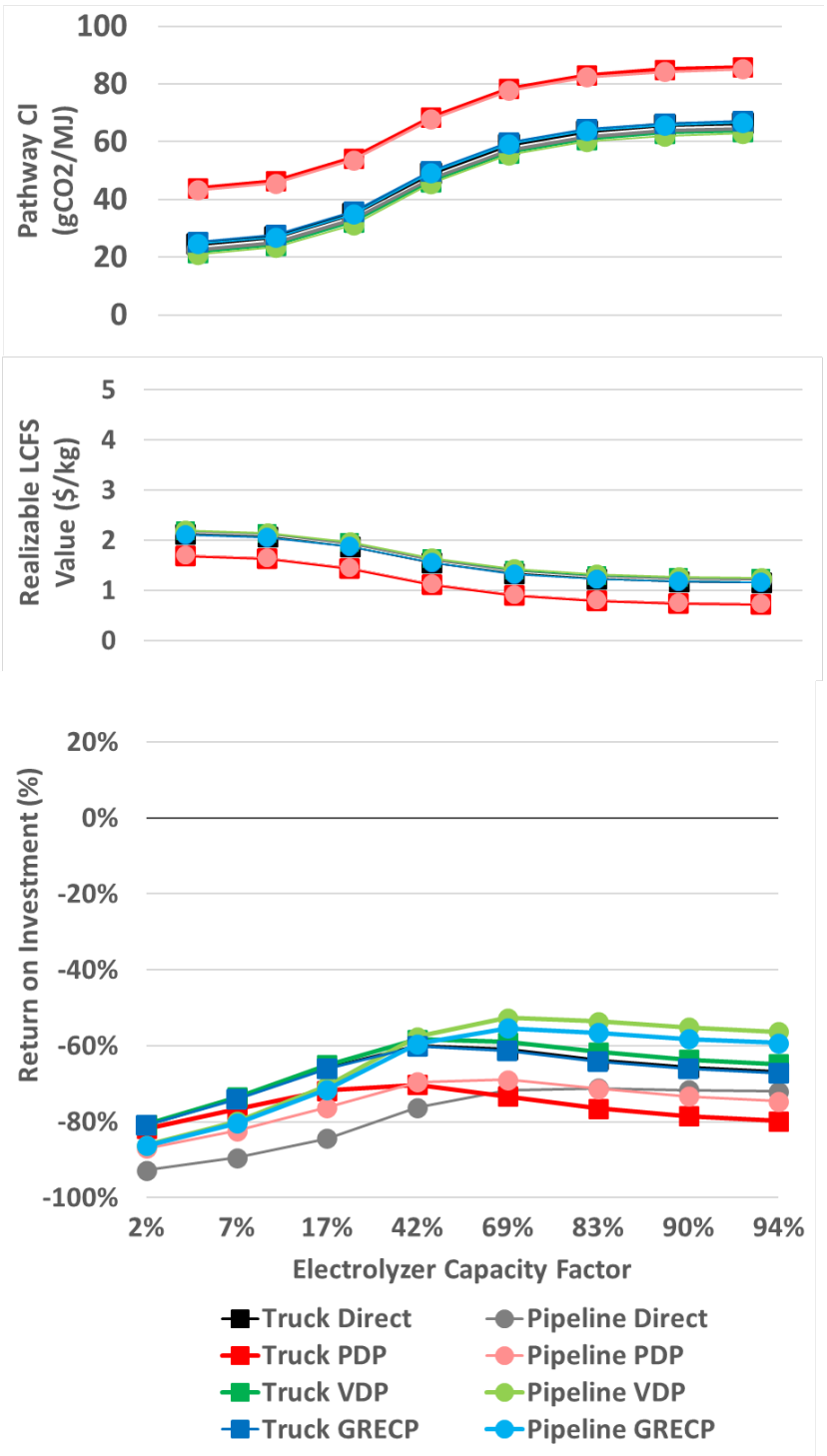

Figure 20 – Base case total pathway carbon intensity, the resulting LCFS credit revenue per kilogram hydrogen, and overall project return on investment.

The total pathway CI curve is a similar shape as the s-curve seen for electrolysis only, as each pathway has a relatively fixed CI for downstream processes. The LCFS curves are inversely

related with the CI curves, so that the higher CI pathways yield the lowest LCFS revenue. The difference between the PDP, the lowest CI pathway, and the VDP, the highest CI pathway, is roughly 22 gCO2e per MJ of hydrogen fuel. The CI difference between trucking and piping hydrogen away from the solar farm is minor. This difference is 2.7 gCO2e/MJ for the direct pathways, 0.74 gCO2e/MJ for the PDP, VDP, and GRECP. These differences effectively arise from the assumed diesel truck's delivery of hydrogen from Burford Giffen to the fueling station directly or the closer compressor station. Transport mode away from production comes to play when considering the cost of each pathway. At low-capacity factors, trucking the hydrogen from production is more cost effective. At about 42% capacity factor, the pipeline reaches parity with the trucking scenario for their respective pathway. ROI is nonmonotonic with electricity capacity factor. Though the electrolyzer and pipeline capacity factor increases and offsets their capital costs, the marginal revenue from LCFS diminishes as the average electrolysis CI decreases.

Across all the pathways, the highest ROI remains largely negative. Three factors are adjusted to investigate potential future market changes that would considerably shift this result. As done previously, the EC capital cost is reduced from the 1100 $/kW base case to a 200 $/kW. Another scenario considers increasing the LCFS credit price from the 190 $/MTCO2e base case to 300 $/MTCO2e. The third factor is the hourly grid electricity CI. A future of greater renewable deployment will involve more solar, wind, and battery capacity resulting in lower generation CI across the board is assumed. To simulate this, a case in which the hourly CI values are reduced to 25% of current values is assumed. Two more scenarios are presented in which each of these factors are set to a medium-level (650 $/kW electrolyzer capital cost, 250 $/MTCO2e LCFS credit price, and 50% of CI hourly values) and high values (200 $/kW electrolyzer capital cost, 300

$/MTCO2e LCFS credit price, and 25% of CI hourly values). An 8 MW and 20 MW electrolyzer case is presented for each of these five future scenarios, summarized in Figure 21.

a) 200 $/kW Electrolyzer

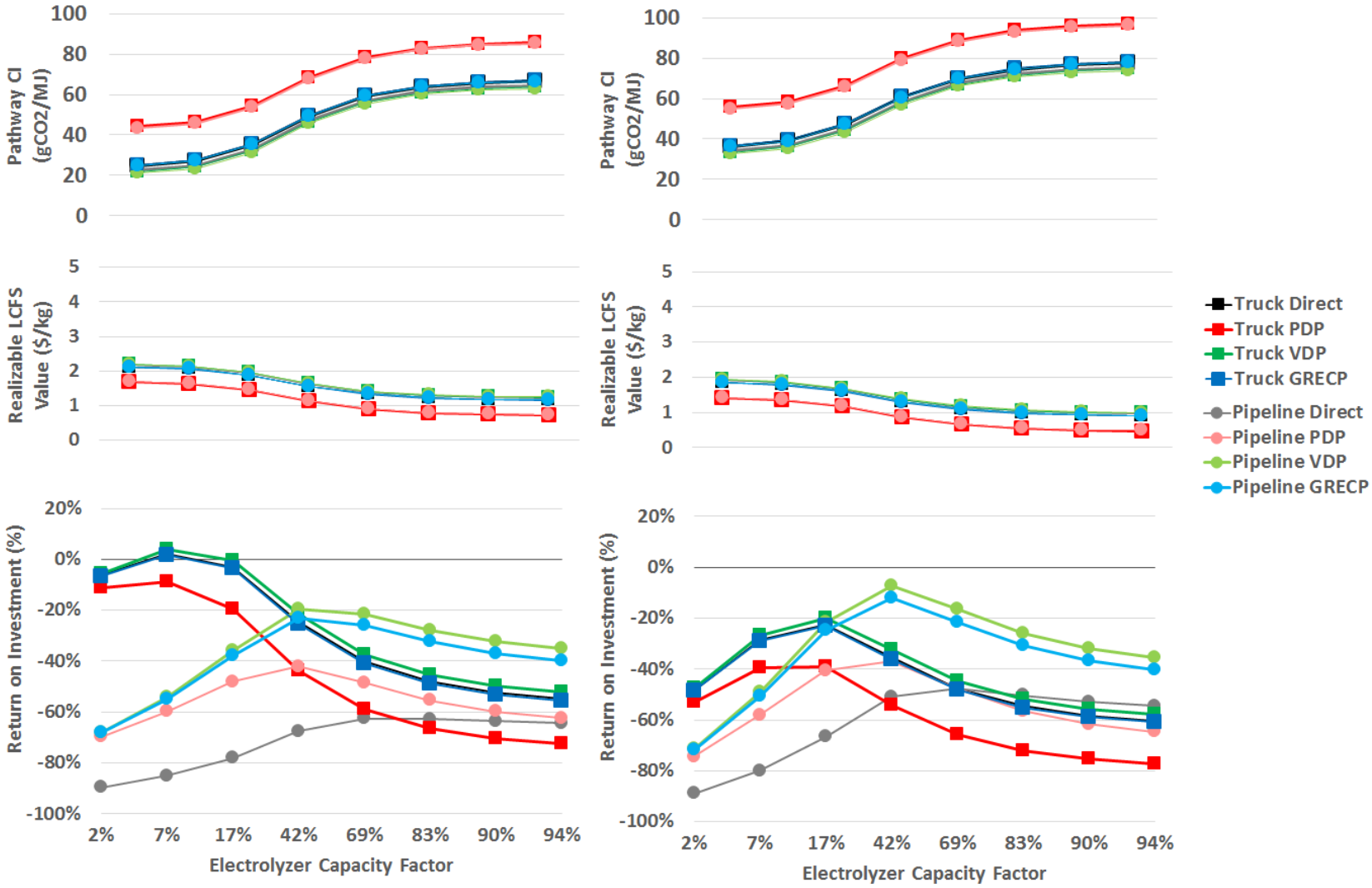

b) 300 $/MTCO2e LCFS Credit Price

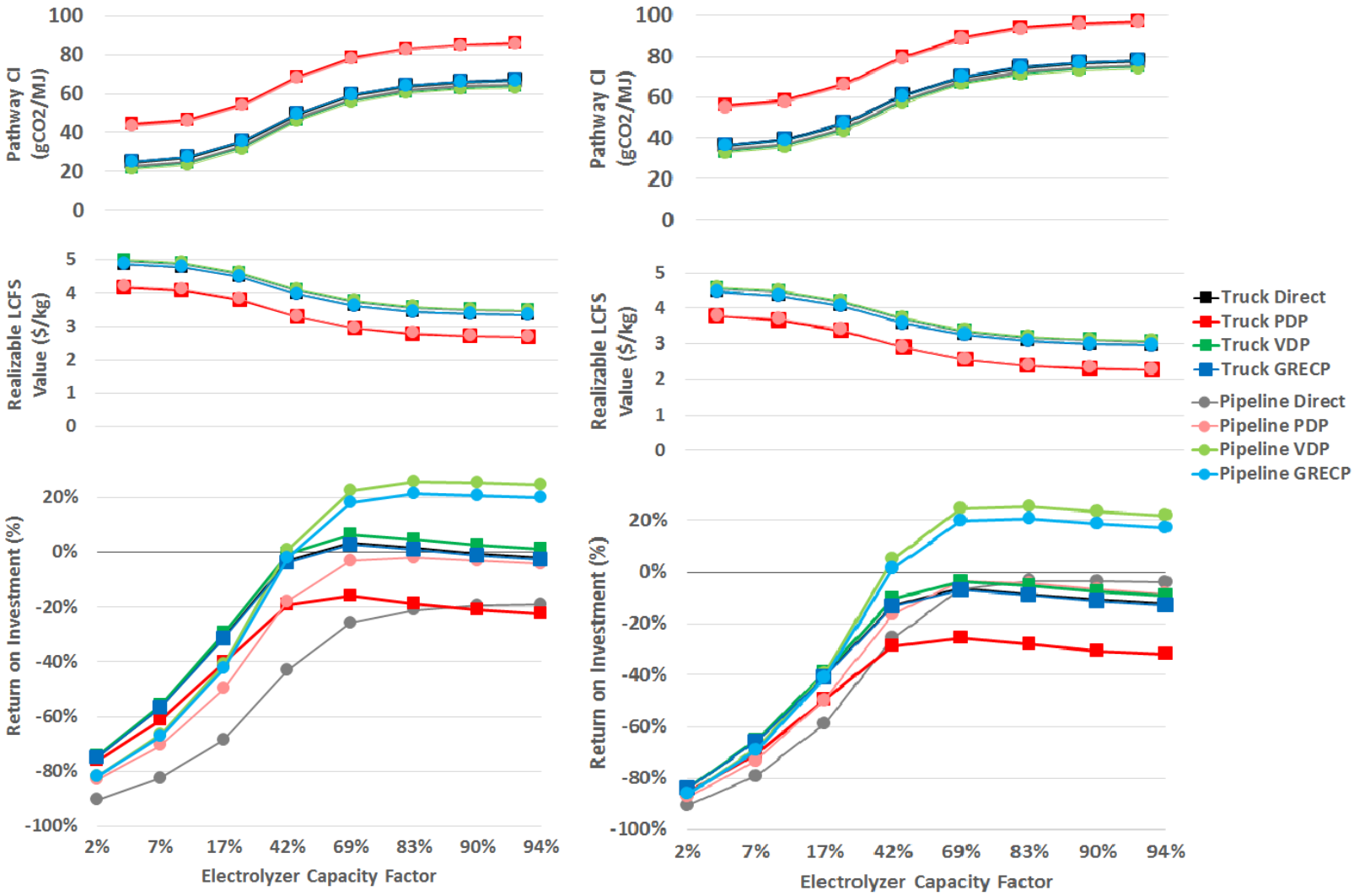

c) 25% Hourly Grid CI

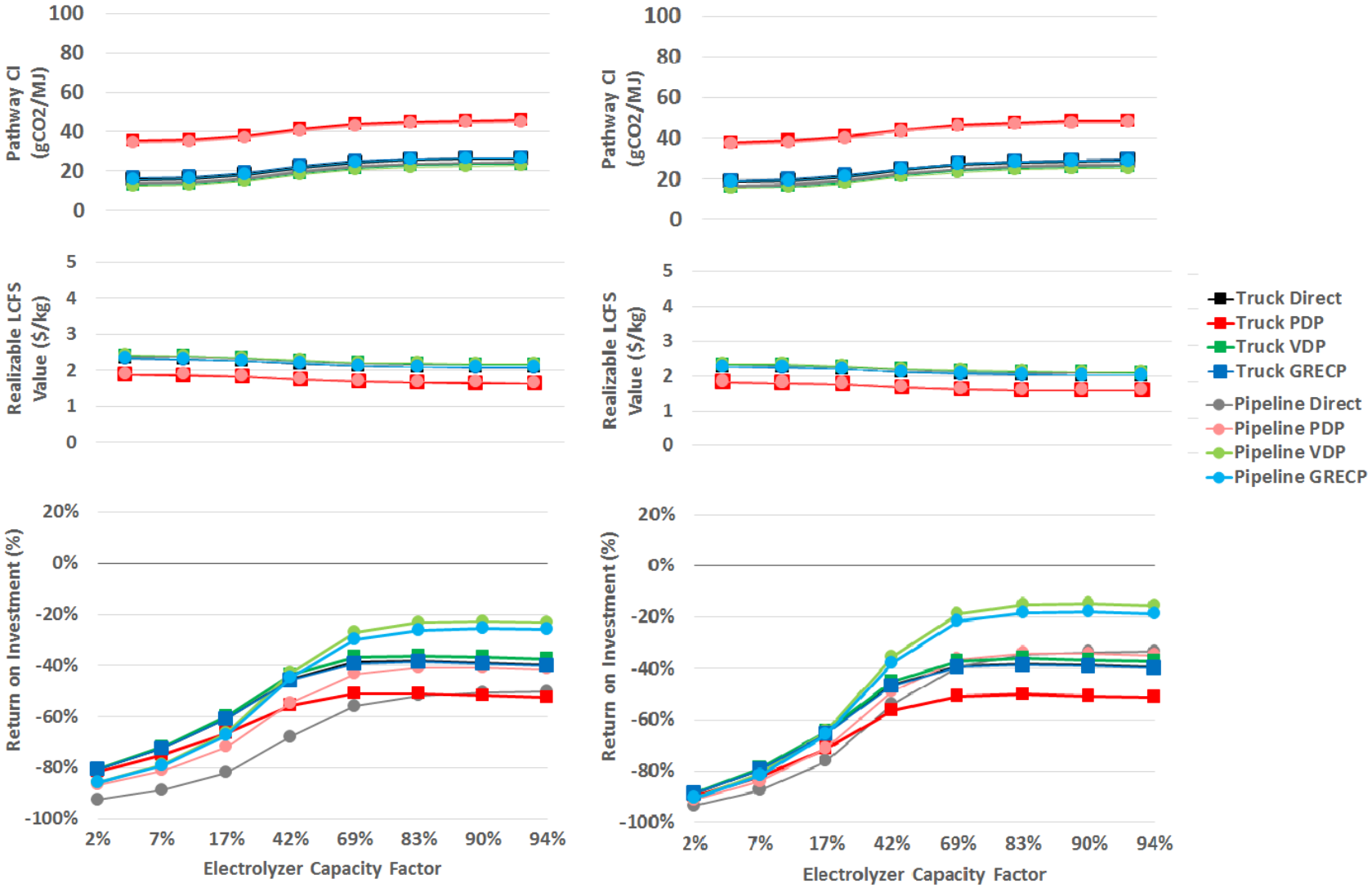

d) 650 $/kW Electrolyzer, 250 $/MTCO2e LCFS Credit Price, 50% Hourly Grid CI

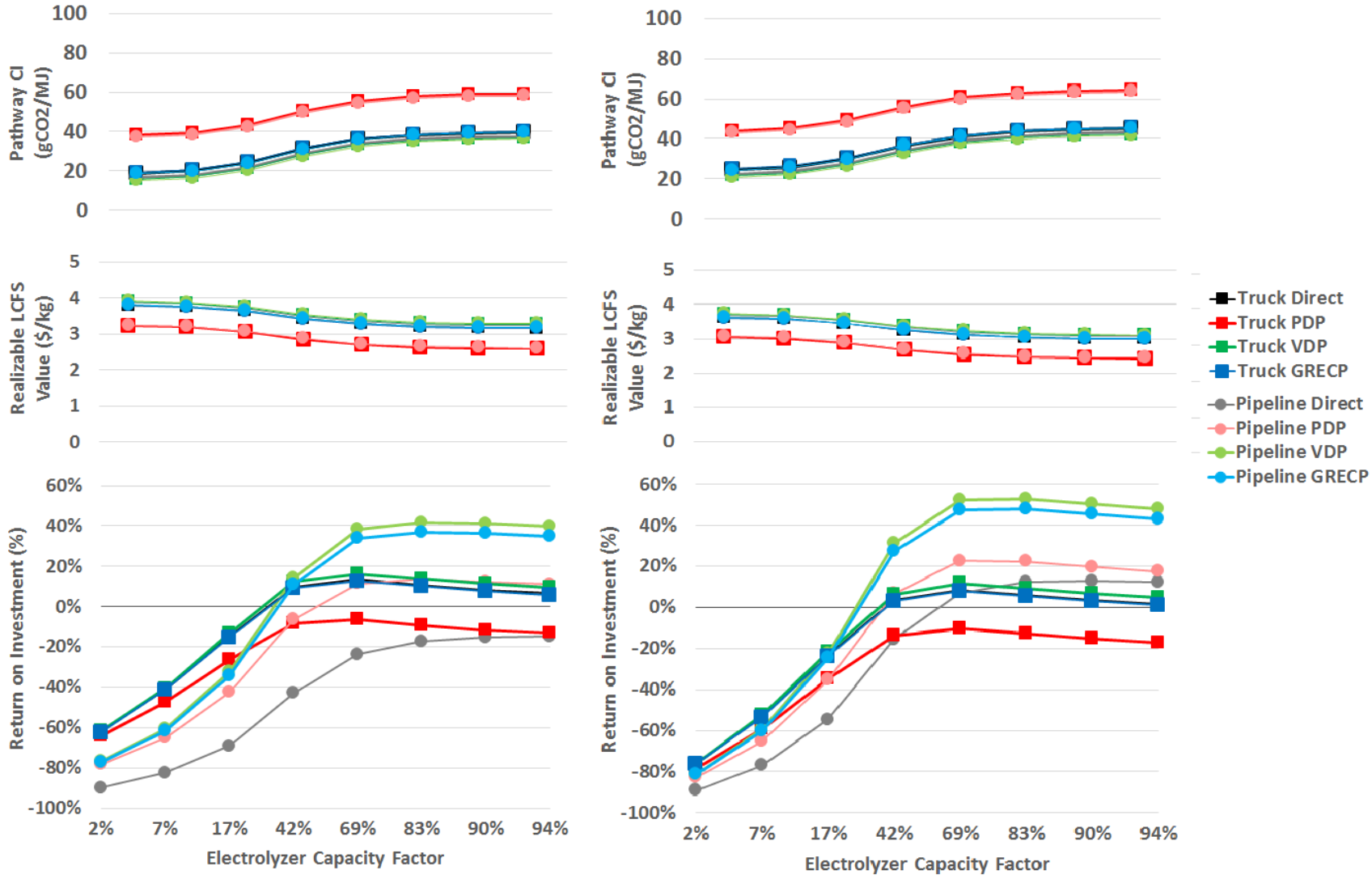

e) 200 $/kW Electrolyzer, 300 $/MTCO2e LCFS Credit Price, 25% Hourly Grid CI

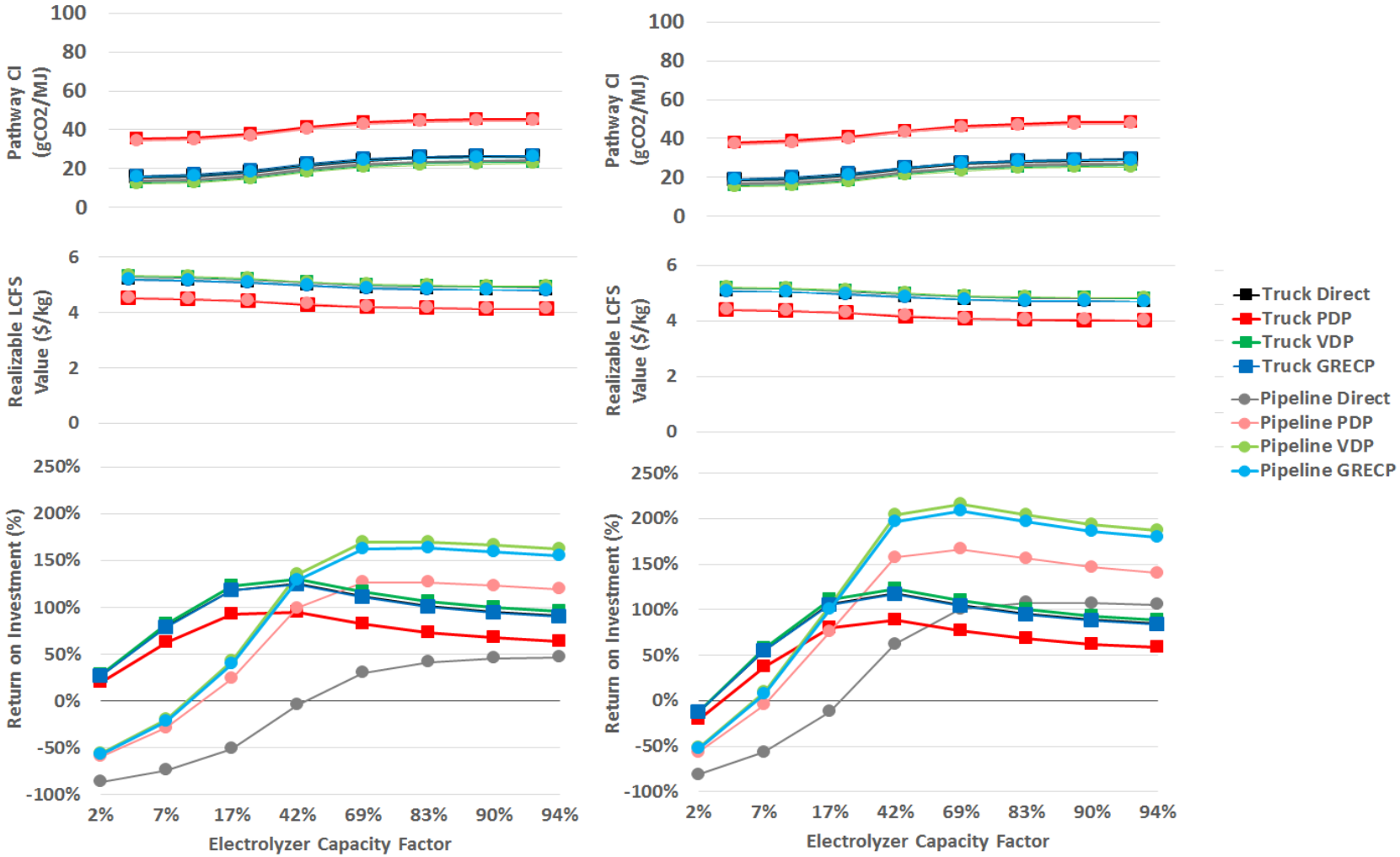

Figure 21 – Project return on investment sensitivity based on three primary factors: electrolyzer capital cost, LCFS credit price, and hourly grid electricity carbon intensity. An 8 MW case (left) and 20 MW case for each is presented (right).

The a) 200 $/kW electrolyzer case still results in negative ROI at nearly all price ceiling values. At a price ceiling value of 10 $/MWh or 7% capacity factor, the ROI for the trucking pathways is near-zero because the amount of hydrogen produced from otherwise curtailed and low priced electricity offsets the electrolyzer EAC. As the price ceiling increases, the increasing cost of the feedstock electricity begins to outpace the revenue from the LCFS credits. The pipeline cases improve at higher capacity factors as the asset is utilized, but the marginal revenue from LCFS credits decreases quicker corresponding with the increase in pathway CI and increasing imported electricity price.

The b) 300 $/MTCO2e LCFS credit price scenario sufficiently rewards higher capacity factors when highly utilizing the pipeline and electrolyzer. The downward trend from the increasing average electrolysis CI is counterbalanced by this slightly higher LCFS price. This proves to be a favorable scenario as there is a large range of electrolyzer capacity factors in which the ROI sits well in the positive region whilst presenting a stronger case for transmission congestion relief. The capacity factors corresponding to a 30 to 70 $/MWhr price ceiling result in an ROI range of 17% to 26% for the pipeline VDP and GRECP scenarios. When a 20 MW electrolyzer is modeled, the throughput is further increased, and all pipeline cases improve slightly while all truck scenarios decrease slightly. The shared 8-inch pipeline achieves higher utilization so even the higher CI pipeline direct and pipeline PDP cases approach, but do not pass the breakeven ROI point.

The c) 25% hourly grid CI fails to achieve positive ROI. It is found that though the average electrolysis CI decreases compared to the base case, the 190 $/MTCO2e insufficiently offsets the electrolyzer and transport costs that hold back the base case. An interesting point is that at higher capacity factors, a reduction in the hourly grid CI only serves to flatten the ROI curve rather than

elevate it. When considering this case and the LCFS case, the ROI is more sensitive to an improvement of 58% for the LCFS credit price than a 75% reduction in grid electricity CI.

The d) medium level factors scenario illustrates characteristics of all three previous single-factor scenarios. In the 20 MW scenario, all pathways but the truck PDP scenario (and pipeline direct if 8 MW electrolyzer) cross into the positive ROI region. Across the board, the combination of these factors presents a more profitable scenario than any single extreme level factor. Here, the winning pathways in the b) 300 $/MTCO2e LCFS still remain largely ahead of all the other series, though the rest of the pathways now float in the positive region at 40% capacity factor and higher.

The e) high level factors scenario is the most optimistic as it combines the already extreme levels of each factor all into one scenario. The peak 216% ROI results from a roughly 70% capacity factor 20 MW electrolyzer utilizing the pipeline VDP. In this scenario, all considered pathways have a means to cross into the positive ROI region and a larger electrolyzer only proves to be more profitable. In all these scenarios, a smaller electrolyzer will have a larger region of low capacity factor which favors trucking hydrogen whereas larger electrolyzers will have a larger capacity factor range which reaps major benefits when paired with sufficient capacity pipelines. As seen from transitioning from 8 MW to the 20 MW case, even larger scale of economies could presumably be achieved with larger solar PV, electrolyzer, and pipeline capacities. Note that these results still are relative to the BAU case, but the higher rated electrolyzer provides some evidence that in certain market conditions a standalone electrolyzer may also be profitable.

3.4 Discussion: Wholesale Sector Limitations

At current market conditions there seems to be no profitable case for energy storage at the Burford Giffen site regardless of whether the price nodes are congested or not. A lithium-ion battery energy storage system (BESS) seems to be the least worse approach with the highest potential in the summer months when solar generation is high and historically curtailed due to the local transmission line congestion, so that the high roundtrip efficiency system can move energy to latter hours in the same day. However, outside of this time the BESS falls short of recovering its cost via energy arbitrage in non-congested conditions. It is seen that for the BESS scenario, significant reductions in capital cost or a massive change in the hourly price dynamics are required to facilitate massive deployment.

In the P2G2P cases, the stretch toward profitability requires not only significant component cost reductions, but also changes in system wide LMP. The California electric grid has evolved significantly in the previous decade and additional renewable installations may continue to decrease the midday LMP values and increase the evening values. The potential to seasonally shift energy even at the 20 MW Burford Giffen site is enormous as illustrated in Figure 16. A P2G2P system at Burford Giffen could become economical if it were compensated for seasonal shifting or observed a massive change in hourly price dynamics. On the other hand, if not compensated for seasonal shifting and if hourly price dynamics do not change much then the P2G2P scenario remains economically unattractive even with large reductions of P2G2P capital costs.

The current market condition LCFS scenario which utilizes the direct delivery of hydrogen to a fueling site (the case that has similar carbon intensity (CI) to the existing co-located renewables pathway) does not have frequent enough hourly prices to justify producing hydrogen. Like previous scenarios, there is value to be gained from the hours in which curtailment does occur

but using only on-site solar PV electricity results in low electrolyzer utilization and capital expenditures that are too large. Increasing electrolyzer capacity factor requires importing electricity which also increases the average electricity CI for hydrogen production. At current LCFS prices and hourly grid CI, this proves to only worsen the ROI as the imported electricity diminishes the marginal realizable value from the LCFS system. The sensitivity analysis finds that some moderate changes to market conditions could result in a combination of factors that present regions operating profitably.

The greatest uncertainty is how the system wide LMP will change when additional renewable generation projects spawn throughout the state to meet future renewable goals. Considering how the BESS case would have been profitable in the 2018 summer months before curtailment was enforced, it seems likely that this local congestion issue will begin to arise throughout the system at the Burford Giffen site and at other locations throughout the utility grid network. It is very probable that in the future, tariffs will be established to reward shifting energy both on the daily as well as on the seasonal timeframes to relieve congestion and to assist with other system needs. This would be the alternative to upgrading transmission and distribution system infrastructure that are mostly overloaded from peak solar generation and otherwise have low utilization factors the remainder of the time. Allowing congestion to occur will stunt renewable generation deployment if developers cannot dispatch the entirety of the designed power plant capacity either because the LMP is negative or otherwise curtailed by instructions from transmission system operators.

Promoting renewable generation deployment to meet renewable state goals has historically been of ease due to plummeting PV solar prices. However, moving forward the current

electric grid capacity is challenged in places such as Burford Giffen and as a result, considerations of T&D system upgrades, or widespread use of energy storage systems are becoming more prevalent. Transmission deferral is typically provided for distributed energy resources or energy efficiency programs that can delay or eliminate substation and/or T&D line upgrades. For example, one can look to Consolidated Edison's Brooklyn-Queens Neighborhood Program in New York and how public and private agencies provided roughly 100 million dollars to avoid a billion-dollar substation upgrade. A future shift to allowing generators to actively defer transmission upgrades would help lower the barrier for interconnection and facilitate further renewable deployment. When considering the 19.6 to 23.4 $/kW of transmission capacity deferral for California IOUs [189], this could prove to be an additional revenue stream worth roughly 14% of the base case pipeline VDP annual revenue. This would promote the deployment of PV solar with BESS and/or P2G energy storage systems.

This would not only support the decarbonization of the transportation sector but would also likely allow for the lower hours of electric production to increase the electric grid RPS. In addition, a network of direct pipelines to hydrogen fueling stations may prove to be an asset to the natural gas infrastructure and could grow its renewable content and storage capacity significantly. The simultaneous achievement of these sectors by implementing a PV-P2G system is illustrated in Figure 22.

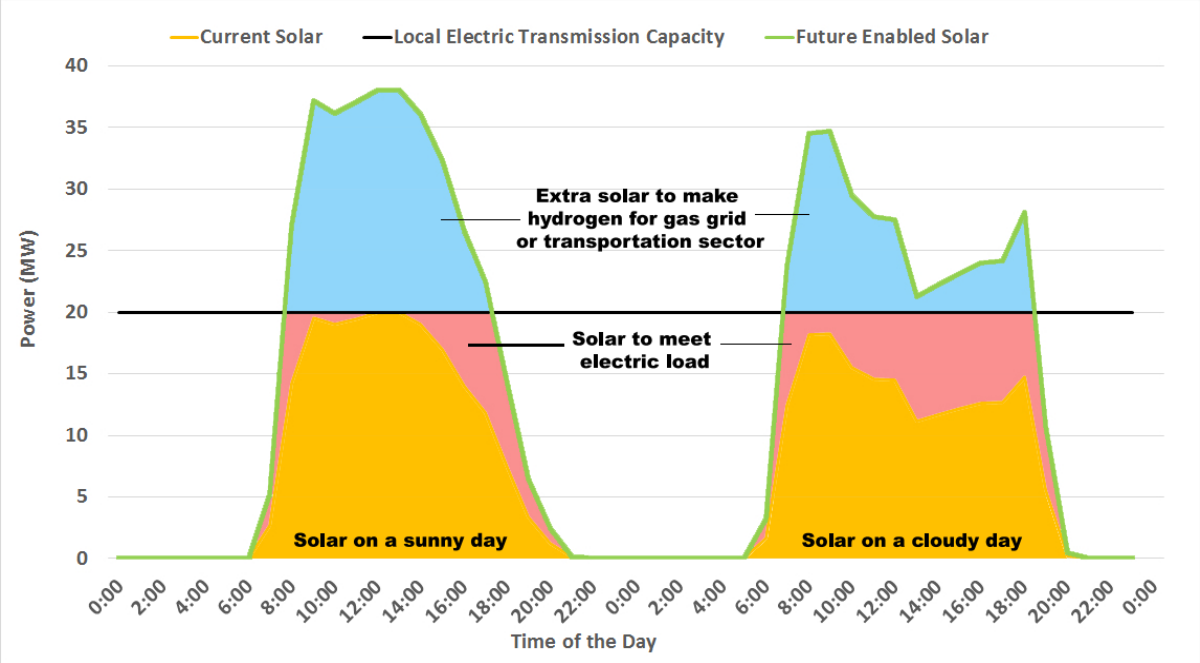

Figure 22 – Illustration of how increasing solar capacity could provide more renewable electricity, renewable gas, and zero emission transportation fuel without upgrading transmission lines.

3.5 Chapter Summary and Conclusions

Major conclusions from the current analyses associated with energy storage use at the Burford Giffen solar site of the University of California are enumerated as follows:

1) The increase in better wholesale prices represented by the California Independent System Operator (CAISO) WESTLNDS (WL) price node for both direct sales and energy from storage is contingent upon the energy storage system adequately relieving the transmission line congestion required.
2) The integrated energy storage systems have a greater ROI in the setting of a solar farm facing permanent curtailment because there is value in relieving the local transmission line to enable regular direct sales in addition to the energy arbitrage and resource adequacy revenue streams inherent with energy storage operations.
3) BESS ROI is only potentially positive in summer and fall months when congestion exists. During the time at which permanent curtailment was historically implemented, the prices were no longer massively negative resulting in a negative overall annual ROI.
4) In the P2G2P scenarios, the current LMP prices provide few opportunities to buy at a low enough price and sell at a high enough price to be profitable. Even when fuel cell and electrolyzer costs are zero, P2G2P scenarios does not yield reliable positive ROI as the PPA costs for the UCOP, decrease in value from RECs, and storage costs are larger than the wholesale electricity prices received by the fuel cell exported electricity. The system must face much more local and system-wide congestion resulting in lower charge prices; or current load following generators must retire to yield higher ramp time prices in the

evening. In addition, revenue from the presumably necessary future seasonal shifting of renewable energy would have to be valued and paid for to favor this P2G2P scenario.

5) The direct delivery of electrolytic hydrogen to fueling stations and injecting hydrogen into the natural gas system, as represented by the indirect pathways, provide significant relative benefit compared to existing hydrogen production pathways from natural gas via SMR. Despite this, no considered pathway is profitable under current market conditions.
6) In a sensitivity analysis, a combination of improved factors presents several scenarios in which most of the considered pathways become profitable. These factors include a reduction in electrolyzer capital cost, an increase in LCFS credit price, and a decrease in hourly grid electricity carbon intensity.

4 Retail Perspective Case Study: University of California, Irvine

This chapter serves to understand the role energy storage could fulfill in a distributed setting, the selection of a representative urban or post-secondary education setting, this step serves to:

1) Investigate the feasibility and cost for utilizing power-to-gas technologies for on campus power generation needs and backup power.
2) Consider the applicability for daily and seasonal storage in this setting.
3) Understand the limitations and context of decarbonization through distributed resources in this setting.

4.1 Approach

University of California, Irvine (UCI) is selected as a representative campus with a gas turbine combined cycle (GT-CC) power plant capable of meeting most of the load. As a departing load campus, electricity is rarely purchased and imported from the local utility, Southern California Edison (SCE). This report provides an analysis of implementing previously identified high-levels of distributed generation with behind-the-meter energy storage for UCI in a detailed manner.

The following details the approach to obtaining the solar generation profile, electrical load profile, and how existing generation resources for applicable campuses are dispatched. Sizing and integration of energy storage components are included in the model. Figure 23 is a visualization of logic the model uses to dispatch generation and storage resources. The existing natural gas turbine power plant attempts to meet load or accommodate additional PV generation by

operating at lower loads. Excess power may be sent to storage and residual loads are met by power from storage. Each component is a zero-dimensional model with average efficiencies ensuring the amount of electricity from generation resources or storage after any inefficiencies is equal to demand at all hourly simulated time steps.

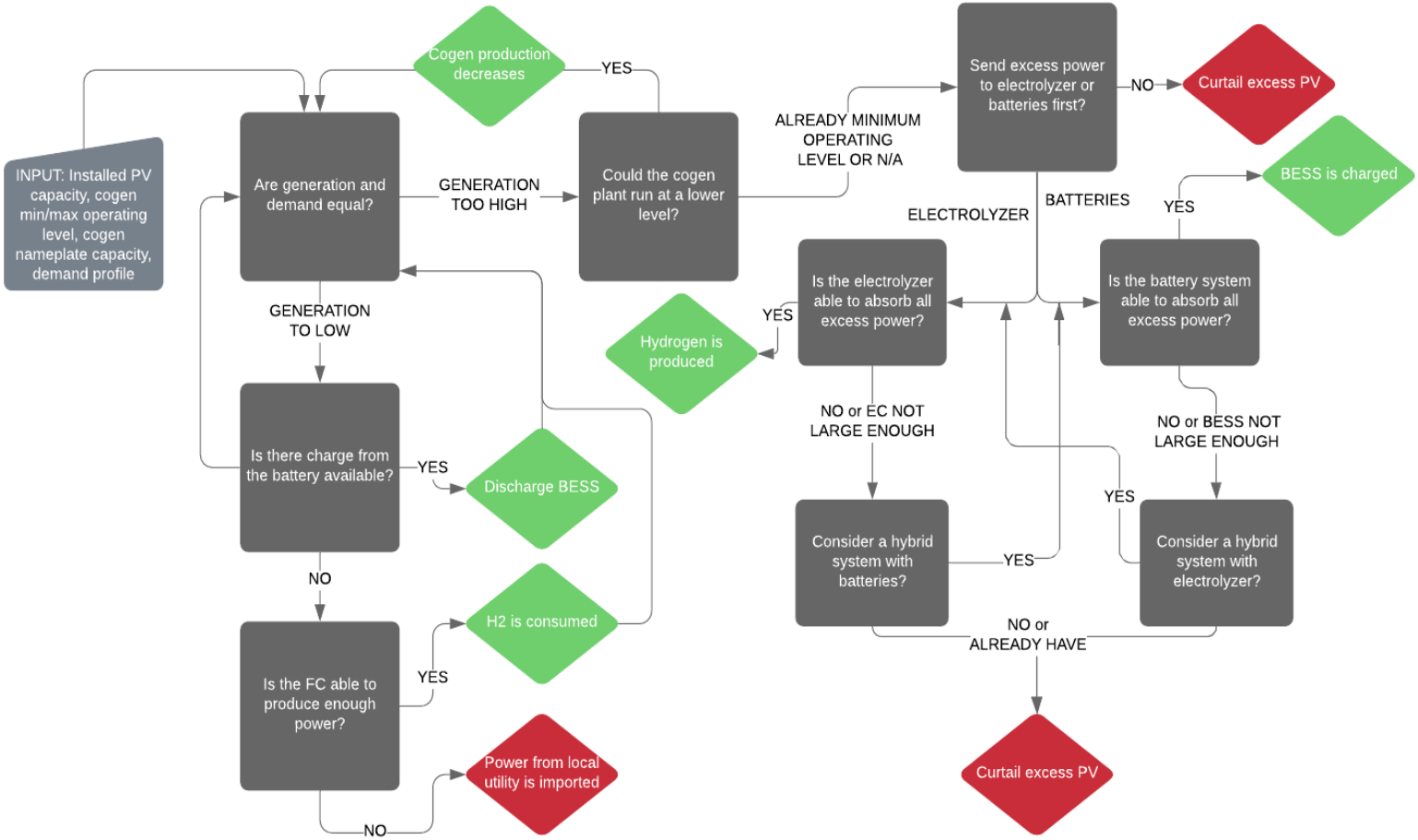

Figure 23 – Visualization of the logic-based heuristics of implementing storage on each campus.

4.1.1 Hourly Profile Inputs

PV generation hourly dynamics are derived by utilizing National Renewable Energy Laboratory's (NREL) typical meteorological year (TMY) data which is derived from the National Solar Radiation Data Base archives. TMY datasets report representative irradiance levels per area that are scaled to match the 2017 total annual production from solar provided by the UCOP for UCI to model current installations. These 2017 levels of installed capacity and production act as the reference case compared to the simulated integrated energy storage pathways that employ the maximum PV potential previously identified. The Santa Ana John Wayne AP TMY weather station dataset was used for UCI. 2018 Historical metered electrical demand data has been provided for UCI. The profile is then scaled to known 2017 annual electrical production and consumption provided by the UCOP.

4.1.2 Gas-Turbine Combined-Cycle (GT-CC) Plant

Gas turbines typically have a minimum operating level before efficiency drops significantly and emission levels are no longer compliant, also known as minimum emissions-compliant load. This is typically somewhere around 70% of gas turbine nameplate capacity. UCI's GT-CC is a 1-1 configuration, so the gas turbine operating at its minimum load results in a plant minimum operating load of around 50% of nameplate capacity. It is assumed that CHP operations are dependent on electrical loads and heating loads are met secondarily.

Figure 24 illustrates an example dispatched resources to meet the hourly load dynamics. The yellow bars represent the solar that comes online and the grey bars that cover much of the evening load represent the GT-CC electricity production. Note that due to cogeneration minimum operating constraints, sometimes when solar PV generation peaks, there is excess electricity going

to storage or being curtailed. The green and lighter red represent the discharge of energy from storage. When all generation resources are insufficient for meeting load, electricity must be imported from the grid, represented by purple. A week is provided to illustrate the daily shifting of the battery energy storage system (BESS) and the fuel cell handling longer timescale energy shifting. Though some natural gas is used for independent heating (e.g., duct burners and boilers) rather than cogeneration, it is assumed that most of the natural gas consumption amongst campuses is utilized for cogeneration dictated by electrical demands.

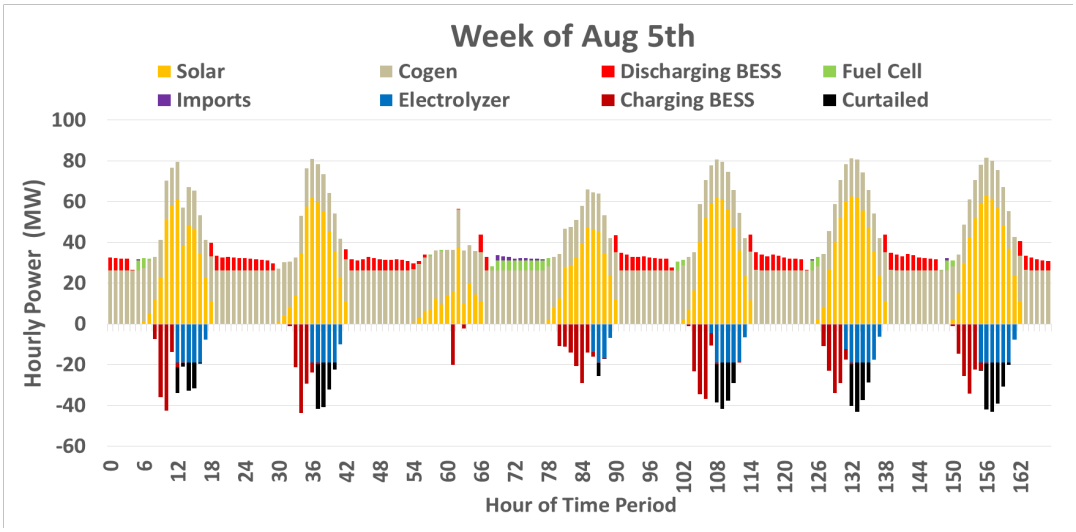

Figure 24 – Sample of energy dispatch to meet campus electrical load.

Imported electricity and on-site electricity generated would have to be 100% renewable or enough renewable energy certificates (REC) equal to the non-renewable electricity generation would need to be owned to make the claim of reaching the 2025 electricity goal. Even then, the 2025 carbon neutrality goal may still not be obtained because since the combustion of imported natural gas for heating demands nor the transportation fleet emissions for these campuses are not accounted for. Some suggest the procurement of carbon offsets from other renewable projects, which are essentially the gas-equivalent of electricity RECs. The integrity of making such

claims is subject to public criticism and is a considerable discussion point that reoccurs in this report. A cost of 8 $/MMBtu (premium cost of environmental attributes from contracted landfill gas) is considered for renewable biogas delivered for electricity production via the GT-CC plant and the gas turbine system is assumed to be a fully depreciated asset.

4.1.3 Backup Generation and Ancillary Services

Backup power generation for reliability is a major value proposition especially considering recent extreme weather events causing public safety power shutoffs. While it may be challenging for a BESS to be at a sufficient charge to backup power for long, a fuel cell system has access to major energy storage capacity used in energy arbitrage scenarios. An additional cost is incurred in the BESS scenarios when replacing old backup generators is considered. Fuel cell systems, on the other hand, can double as zero-emission backup generators without significantly affecting the operational lifespan. The diesel cost of ownership assumes a capital cost of 1200 $/kW and a lifespan of 30 years. This capital cost number includes the operation and maintenance costs which is expected to be roughly a third of the total cost of ownership when normalized by its power rating [190].

California Independent System Operator's (CAISO) proxy demand response allows electrolyzers to participate in grid ancillary services that fuel cells and batteries had access to prior. Eichman and Flores-Espino [191] evaluated the potential revenue when electrolyzers can participate in the ancillary service market. The same method is used in this report with updated 2019 market values.

4.1.4 Energy Storage Component Capacity Factors and Sizes

GT-CC operations are modeled to be online year-round without downtimes for maintenance and prioritized over energy from storage to meet loads. Energy from storage is only dispatched when the GT-CC is inadequate for meeting total electric load. Cogeneration production is turned down without violating minimum operating constraints before any solar is curtailed. Any excess power not being used for the load is sent to storage if the BESS and hydrogen storage is not full, else it is curtailed.

The fuel cell, electrolyzer, and BESS capacities are sized so that a moderate capacity factor, roughly the average of the extreme high and low values, is achieved. The capacity factors are defined as each component's average operational power level normalized by its capacity. As the electrolyzers only use on-site solar PV generated electricity, their capacity factor in this work is limited by the PV production. An extreme high-capacity factor typically results in a high level of curtailment resulting in a low utilization of solar PV production. On the other hand, an extreme low-capacity factor typically results in a high energy storage costs that are not utilized to its potential. The moderate capacity factor case is the average of these two extremes and consequently assumed to be representative of a practical case regarding storage implementation.

The BESS system operates similarly in all considered scenarios—attempting to fully charge and discharge once a day and often does so due to the limitations of joint power and energy capacity. The P2G components' operation spans a large capacity factor range. In addition to PEM technology's low operating temperatures, the lifespan is modeled based solely on operation hours rather than calendar time to reasonably consolidate the capital recovery cost from the range of capacity factors. A 10-year lifespan is assumed for the BESS system, 30 years for the hydrogen storage component, and a 15,000-operation-hours for both the fuel cell and electrolyzer. The

alkaline electrolyzer system is modeled with at 800 $/kW capital cost [192] and the PEM fuel cell system is modeled with a 1,200 $/kW capital cost. The BESS capital cost is modeled at 300 $/kWh.

Increasing the renewable contents of the fuel used in the on-site power plant can be achieved by increasing the renewable attributes on imported gas on an accounting basis but may provide greater integrity to the claim when the renewable natural gas is produced onsite. This motivates the consideration of using the abundant distributed solar generation to produce 100% renewable electrolytic hydrogen to be injected into the fuel mixture for the central plant. The limitation to how much hydrogen can be produced depends on 1) the amount of distributed PV and 2) the size of the electrolyzer. The fixed maximum distributed PV capacity and the dependence on electrolyzer size is summarized and contextualized relative to the campus load in Figure 25.

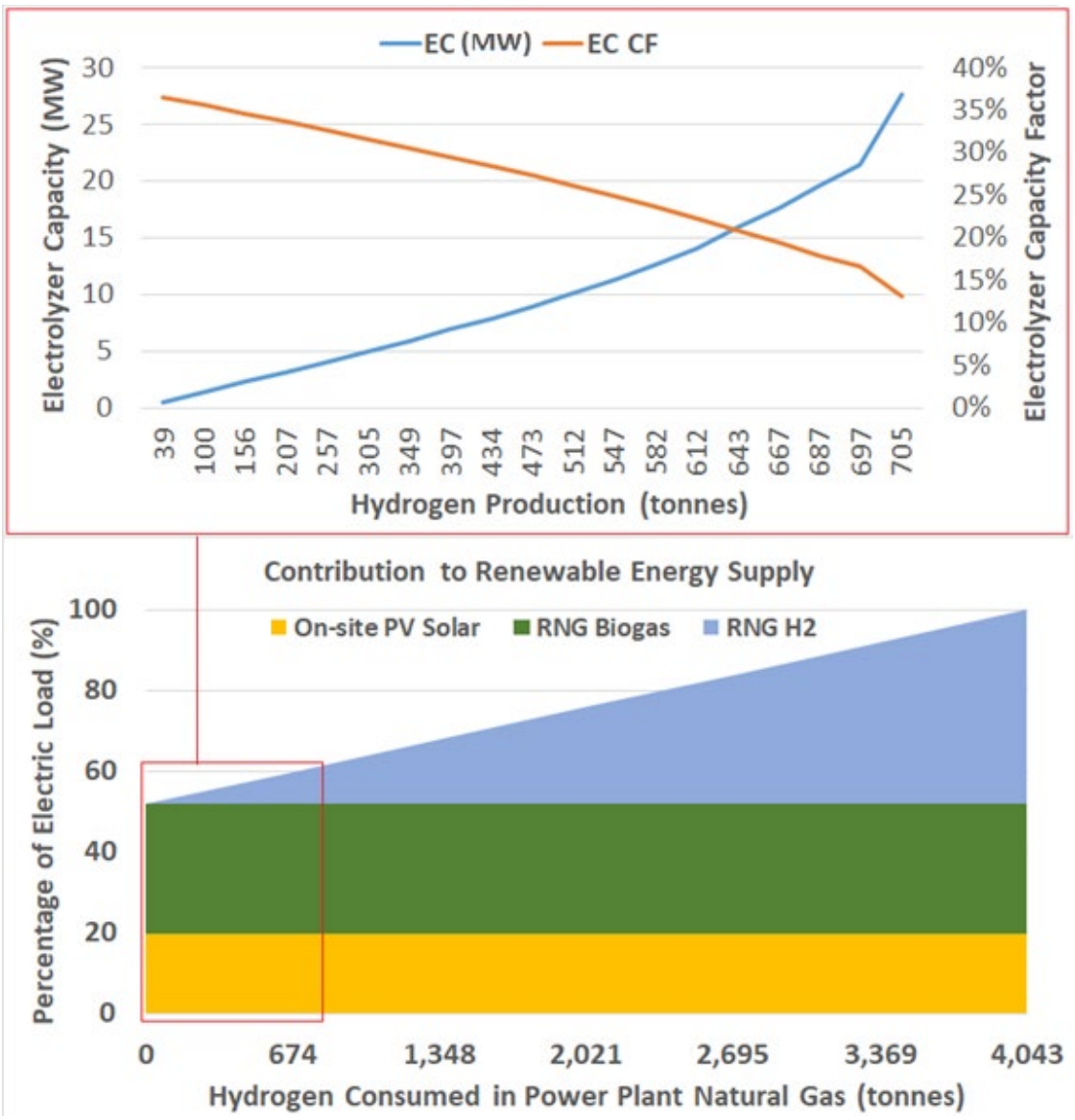

Figure 25 – Electrolytic hydrogen production potential range relative to the UCI campus load. More hydrogen must be produced or imported beyond 700 tonnes.

In the above scenario, procuring renewable biogas for 40% of the cogeneration fuel stream leaves the balance as non-renewable natural gas. By implementing a 27 MW electrolyzer, about an additional 10% of the cogeneration fuel stream and consequently produced electricity is renewable. Even at high levels of distributed PV meeting 20% of the electric load, additional renewable gas must be procured to justify the zero-carbon emission of the existing power plant.

A potential method of increasing the renewable content of the power plant production would be to import greater amounts of renewable electricity (using RECs) but an efficiency penalty would arise from using electricity to drive power-to-gas (P2G) to simply re-electrify via a gas turbine. It would be more cost-effective to directly use the imported renewable electricity for heating, cooling, or electric loads. The gas equivalent of using RECs would be to procure greater amounts of biogas as already planned, electrolytic hydrogen (e.g., through centralized resources like Burford Giffen), or other carbon neutral/negative gases. Unless campuses like UCI have the technical feasibility for new distributed generation, a strong dependence on importing resources seems to be the most reasonable approach. Policy and methods must be established to promote procurement of centralized resources that would promote grid health as techno-economic viable pathways for Burford Giffen were found to be challenging to implement.

4.2 Energy Storage System Integration

Despite this, it is also known that low utilization assets result in high costs. From this point onward, the integration of energy storage to explore the contribution to renewable energy supply and the associated costs is undertaken. Three energy storage integration pathways are established: sending excess solar PV electricity to 1) BESS for daily energy shifting, 2) to an electrolyzer to produce hydrogen for injection in the central plant gas turbines (P2G-GT), and 3) to an electrolyzer to produce hydrogen to be electrified by a fuel cell system (P2G-FC). Each energy storage pathway considers 5 capacity levels to span a range in which the cost to emission reduction can be evaluated. The set of five electrolyzer sizes are the same in both P2G strategies. A set of radar charts is presented in Figure 26 for a quick comparison of metrics: amount of PV electricity curtailed and the percentages of how much each resource meets the load.

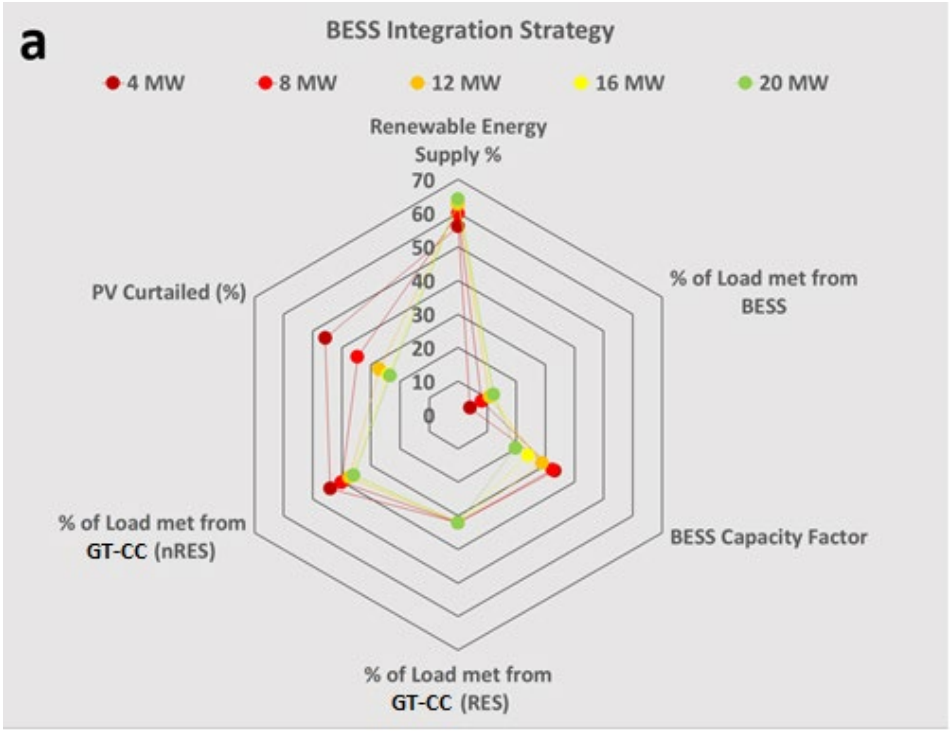
a
BESS Integration Strategy
4 MW
8 MW
12 MW
16 MW
20 MW
Renewable Energy Supply %
70
60
50
40
30
20
10
0
% of Load met from BESS
BESS Capacity Factor
% of Load met from GT-CC (RES)
% of Load met from GT-CC (nRES)
PV Curtailed (%)

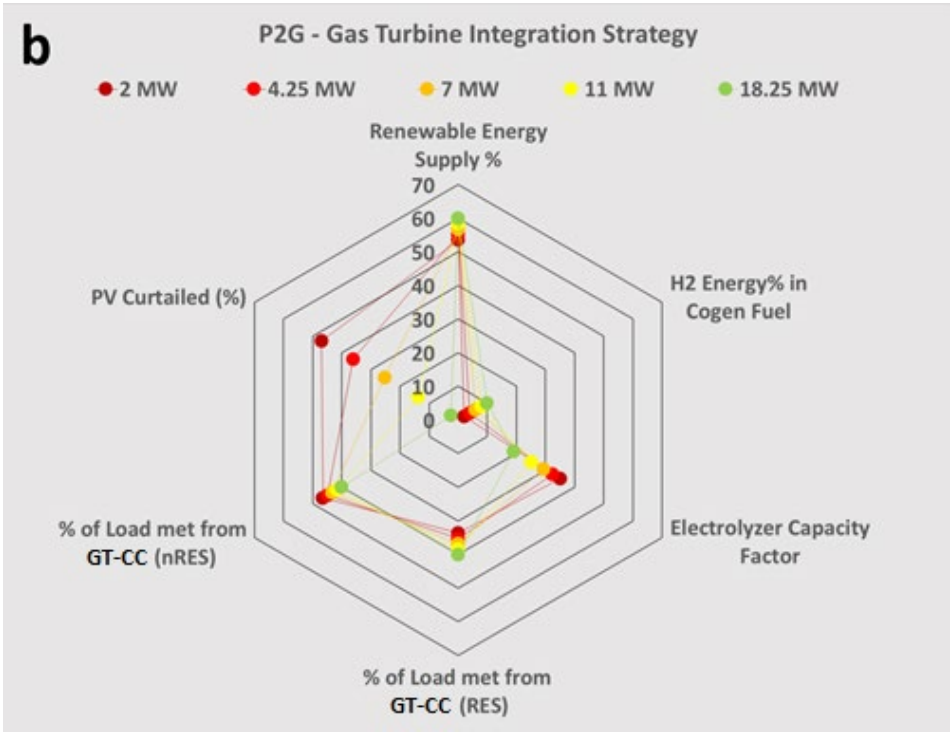
b
P2G - Gas Turbine Integration Strategy
2 MW
4.25 MW
7 MW
11 MW
18.25 MW
Renewable Energy Supply %
70
60
50
40
30
20
10
0
H2 Energy% in Cogen Fuel
Electrolyzer Capacity Factor
% of Load met from GT-CC (RES)
% of Load met from GT-CC (nRES)
PV Curtailed (%)

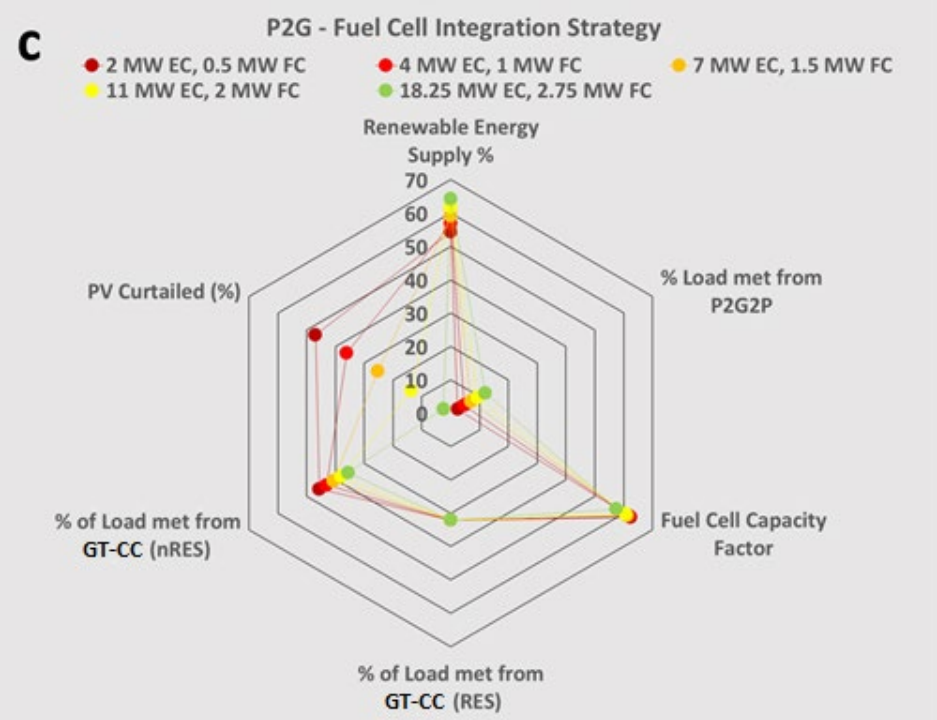

Figure 26 – Overview of energy dispatch metrics for varying capacities of a) battery energy storage, b) power-to-gas to be injected, and c) power-to-gas to be used in fuel cell. The 40% renewable portion of biogas is included in the cogeneration.

Due to the nature of procuring resources, it is unlikely that the amount of procured biogas is consistently equal to 40% of the fuel used for cogeneration due to changes in operation. For this analysis, the fixed amount of procured biogas is 40% established at the time before energy storage operation and after the solar PV is dispatch is known. Note that considering the 40% procurement in the instance after energy storage dispatch is known would decrease the total percentage of load being met by the biogas portion, whereas considered the instance before the high level of distributed PV installed would increase it whilst implementing the gamut of distributed solutions.

Of the metrics provided for each integration strategy, several trends remain the same: 1) PV curtailment goes down as battery or electrolyzer size increases to capture excess energy. Energy shifted to later in the day or further timeframes means the GT-CC ultimately meets less of the load. Here, the renewable portion of the cogeneration only increases slightly in the P2G-GT

case from the increase of renewable hydrogen in the fuel mixture. The five capacities of electrolyzers correspond to hydrogen being 2, 4, 6, 8, and 10% energy of the cogeneration. Capacity factor behaves as expected, with increasing capacities resulting in lower capacity factors. The maximum level of campus electric load being met by renewables is roughly 60% for the injection strategy and 64% for the other two. An electrolyzer sized at 25 MW would further decrease the capacity factor to 14.5% but only increase the annual hydrogen production by 4% due to increasingly less hours of excess on-site solar. In the P2G cases, the 18.25 MW electrolyzer results in 2.5% PV curtailment, but for the BESS scenario, the larger capacities do not achieve as low PV curtailment because the system reaches full state-of-charge.

The amounts of energy storage vary for the P2G-GT strategy as the gas turbine maximum hydrogen blend constraint results in a necessary buffer storage as the hydrogen production does not match the consumption used to produce power. As previously described, a smaller fuel cell capacity allows for higher capacity factor economic dispatch. Because the storage component is decoupled, the total system cost is lower when increasing storage capacity instead of power capacity. Doing this results in fuel cell operation in almost all hours outside of solar production. It is for this reason, despite the lower roundtrip efficiency, the P2G-FC pathway can meet 12% of the electric load just as the high capacity BESS case does. The hydrogen storage levels vary throughout the year-- dependent on seasonal campus dynamics and is discussed later in the generalized UC campus results. On the other hand, the BESS state of charge varies on an hourly basis--predictably low after alleviating meeting peak evening loads and high during solar generation. This dynamic provides the basis for whether enough energy is stored on campus in the event of an emergency. The contribution to load from each resource is summarized below in Figure 27.

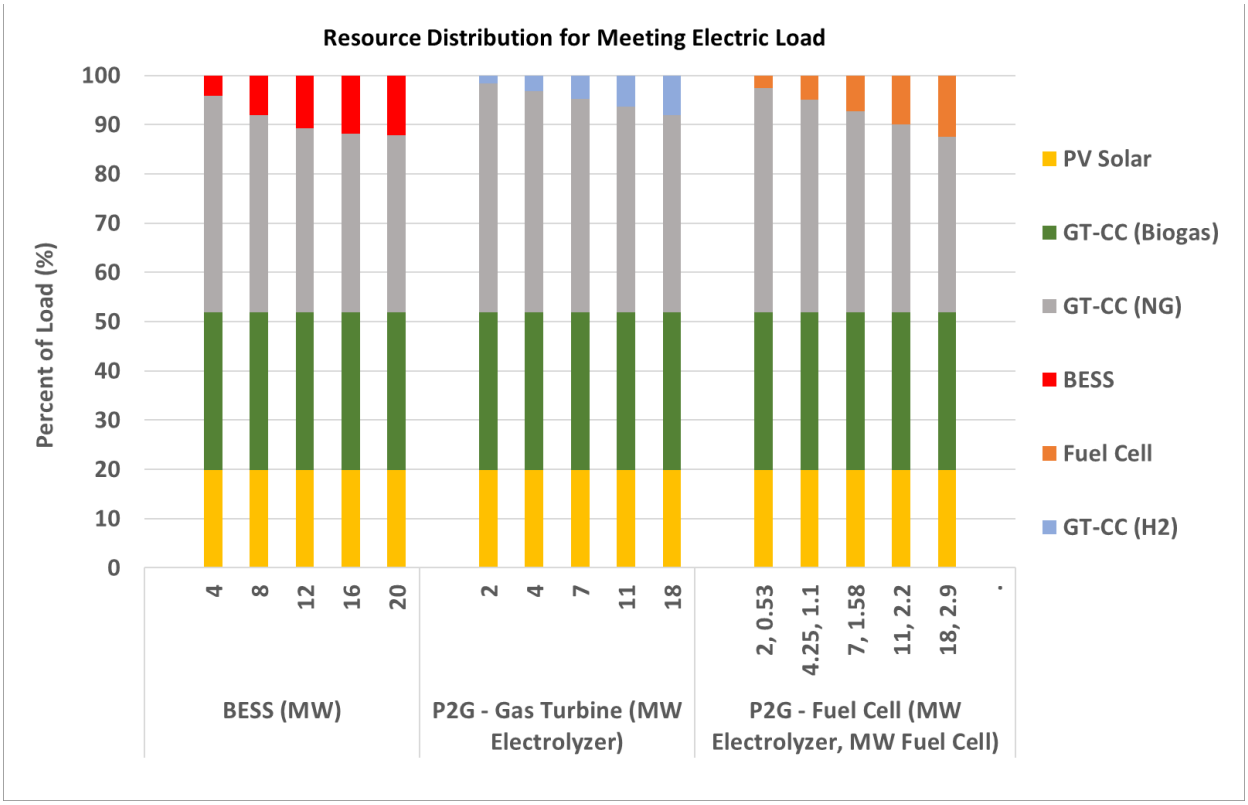

Figure 27 – Contribution to UCI's electric load for each energy storage strategy.

For UCI, the amount of solar is simply 20% due to dynamics and the minimum operating constraint of the GT-CC. A significant portion of the renewable energy supply percentage (RES%) is the procured biogas. With no energy storage, PV solar curtailment is 58%. If almost all the excess PV is stored, it seems only a maximum increase of 13% RES is possible due to dynamics and energy losses for all three strategies. The cost breakdown for these strategies is presented in Figure 28 before discussing the levelized cost of electricity and additional revenue streams. A 5% discount rate is assumed for the UCI case study cost calculations. The 5 MW fleet of backup generators requirement is observed here. The PV and biogas costs are the same throughout all scenarios. Previous demonstrations at the central plant have found that the largest cost of injecting hydrogen into the cogeneration fuel mix is the electrolyzer stack itself and the piping, metering, and regulators are relatively lower costs.

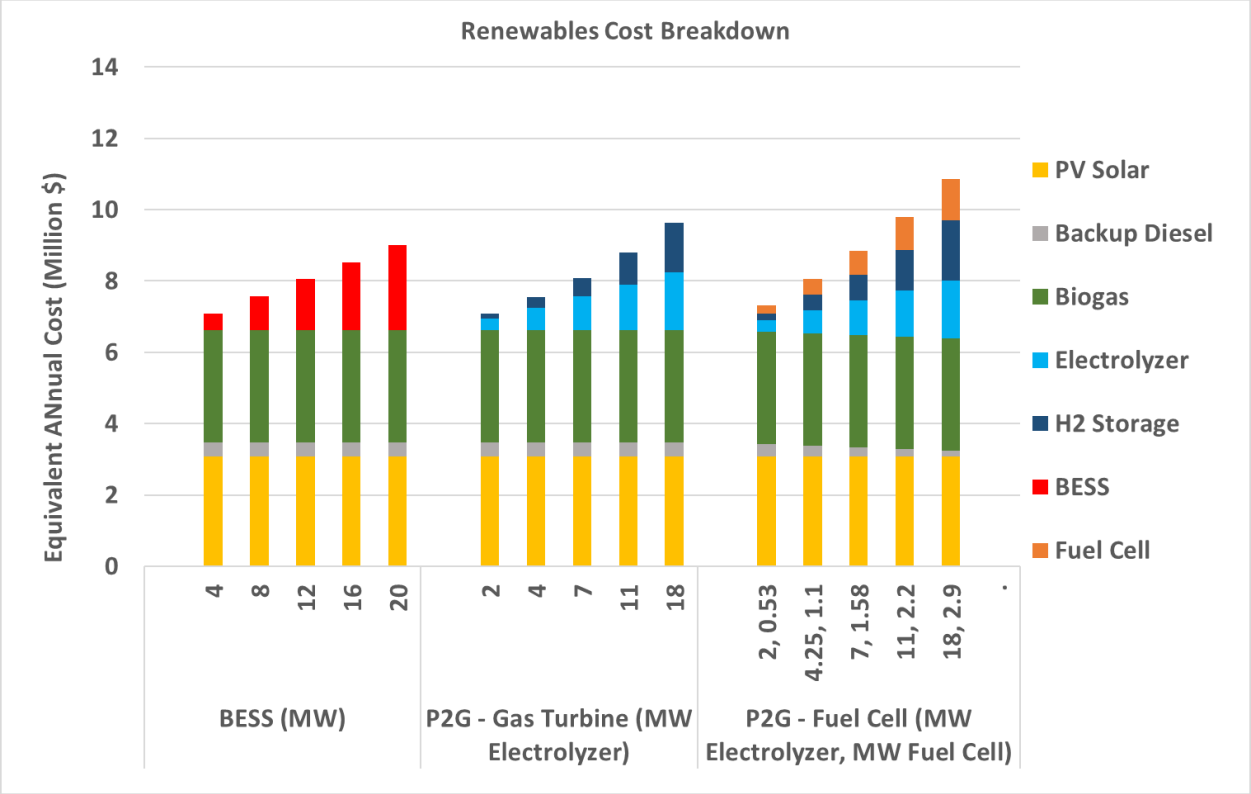

Figure 28 – Annualized cost of ownership for each energy storage strategy.

4.3 Duality of Energy Arbitrage and Standby Operation: Partial Fleet (5 MW)

One notable niche that fuel cell systems have been able to claim is their prevalence in backup systems. Plug Power is a leader in fuel cell systems acting as backup generators as an alternative to diesel gensets. If one considers that the fuel cell used for energy shifting could also double as a backup generator (operation is a marginal amount of hours per year and consequently inconsequential to the stack replacement), then the BESS case effectively has a slightly higher additional cost associated with replacing diesel generators relative to the P2G cases. An internal inventory of the campus's backup generators suggests the total fleet capacity is roughly 15 MW, however a third of the capacity was commissioned before 2000. A 5 MW of backup capacity replacement is assumed, corresponding to the older units in UCI's fleet that need to be replaced

in the near-term. If this capacity replacement is inevitable, then roughly half of the capacity quota is fulfilled by the fuel cell capacity from the energy arbitrage scenario, resulting in a slight discount in overall costs in the P2G-FC scenarios.

The potential revenue from participating in ancillary services markets as evaluated in Eichman and Flores-Espino [191] is calculated with 2019 average market values. Revenue from these streams primarily depends upon power capacity bid into the market. In addition, electrolyzers participate in proxy demand response. This suggests that electrolyzers (or charging the BESS) must have bid to import grid electricity ahead of time and be flexible enough to lower demand to artificially provide demand response if called upon. In addition, providing grid services that require exporting power will reduce the amount of energy used to meet load. As such, the potential revenue from ancillary services and effects on previous results are largely dependent year to year. Historic volumes and prices of the ancillary service products can be found in annual CAISO reports [193]. The annualized cost of replacing the 5 MW of backup generation capacity and potential revenue from ancillary services are added to the renewable LCOE seen in Figure 29 to compare strategies.

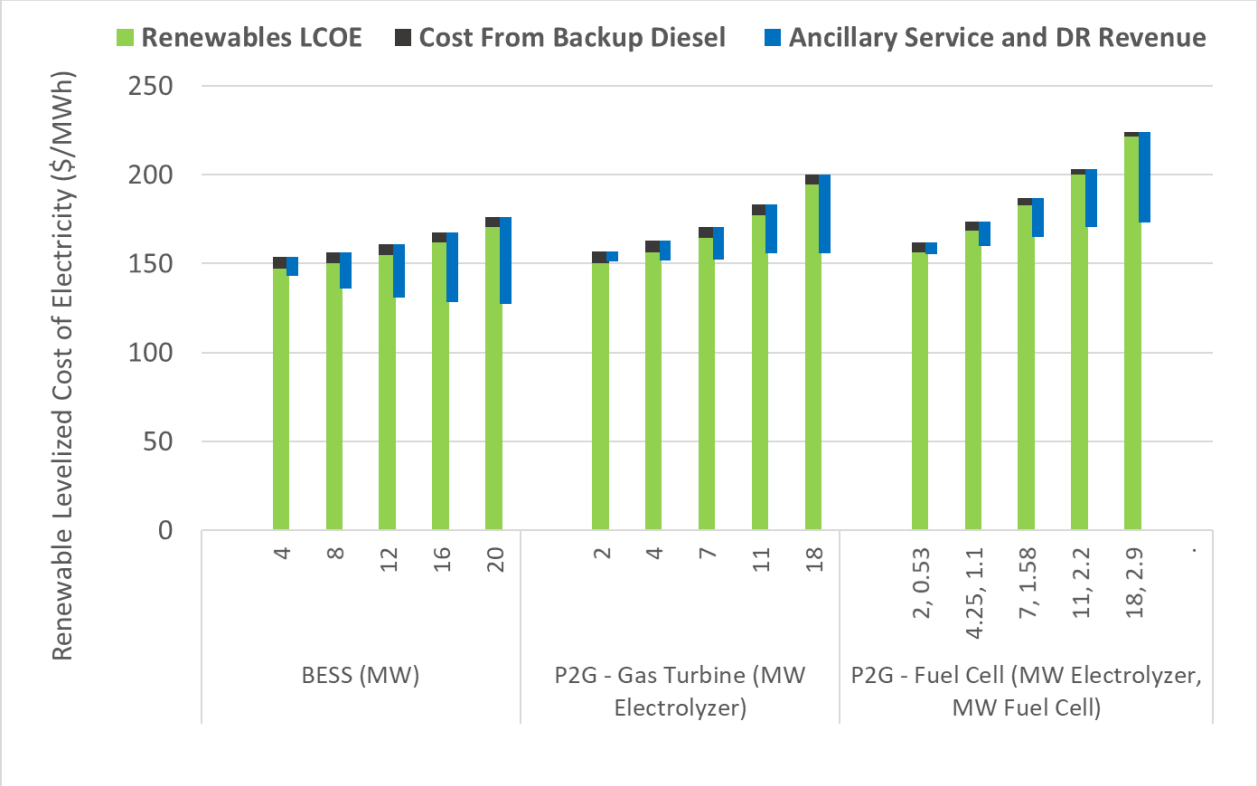

Figure 29 – Levelized cost of renewable electricity including costs and benefits of backup generation and ancillary service participation.

Based on a 2016 UCI electric service provider electricity bill, the direct access rate is estimated as 65 $/MWh. In addition to this, the investor-owned utility delivery costs and surcharges bring this up to 90 $/MWh. The resulting effective LCOE for the highest considered capacities for the BESS, P2G-GT and P2G-FC are 127, 156, and 173 $/MWh, respectively. The slightly larger energy storage and cost of the fuel cell makes the injection strategy seem more cost effective. The BESS strategy typically has lower costs for comparable RES%.

The amount of necessary storage then needed for these energy arbitrage scenarios is of interest when compared to the amounts needed for typical backup generation. SCE's reliability reports are consulted to find the system average interruption index (SAIDI). This is an average amount of time which does not capture the extreme outage scenarios that have posed major

challenges in extreme weather conditions in 2019 and 2020. The average of 3 to 4 hours of backup generation per year is a conservative duration considering some customers can go days until power is restored. The last four years SAIDI (without excluding major event days) for the districts and cities that UCI and UCSB are located are presented in Figure 30

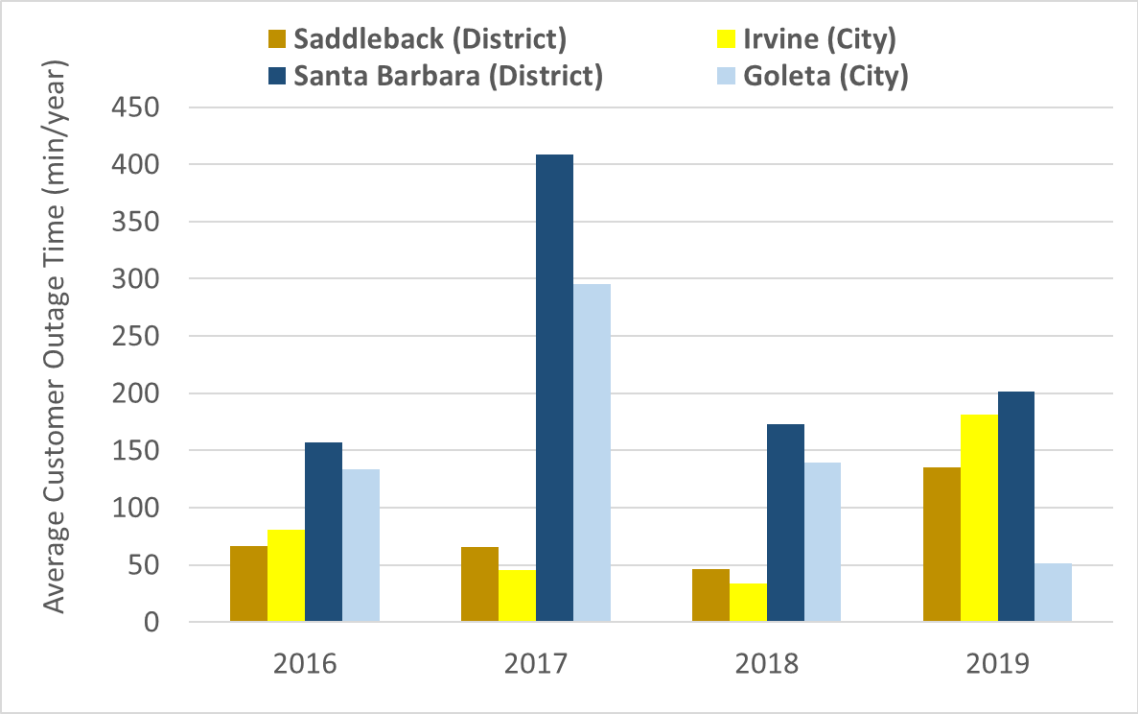

Figure 30 –Previous years outage time including major event days for UCI and UCSB areas.

Because the BESS cycles daily, it cannot reliably be at a state-of-charge to act as a backup generator without foresight, availability of solar, and adequate time to charge. The amount of energy storage needed for the energy arbitrage scenario is massive relative to the amounts needed for reliability. While there also is not a guarantee that the state of charge for the fuel cell is sufficient, there is far greater capacity to buffer the need. This allows the utilization of hydrogen energy storage for both energy arbitrage and backup reliability. Private communication with Plug Power representative, Darin Painter, suggests the storage needed for extended hours of operation is the cost component which makes owning backup fuel cell generators more costly than backup

diesel generators because hydrogen gas is more difficult to store than liquid diesel fuel. On a power basis, the annualized cost of owning fuel cells and diesels is comparable. Also, if long duration zero emissions backup power is required then hydrogen and fuel cell technology is cheaper than the alternative battery technology. Both battery backup power systems and hydrogen and fuel cell backup power systems qualify for federal tax incentives that can sometimes make them the economically preferred option. Unfortunately, tax incentives are not applicable if the host is tax-exempt. The storage capacity magnitudes needed for the energy arbitrage and reliability scenarios are presented in Figure 31.

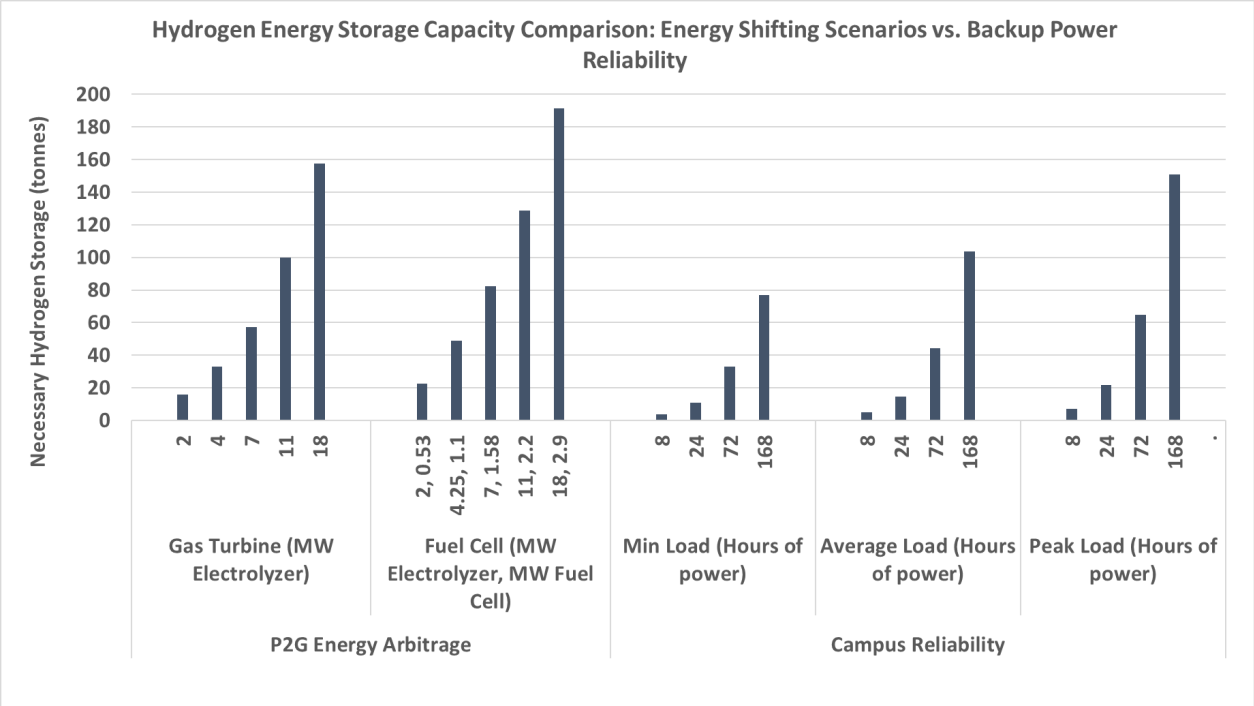

Figure 31 – Comparison of energy storage capacity in energy arbitrage strategies versus reliability storage capacity.

On an annual net basis, a 2 MW electrolyzer produces enough hydrogen for at least a day of continuous power. The minimum, average, and peak load are presented to bound the actual amount of hydrogen needed for the fuel cell system fleet. In the event of an emergency, the

campus is likely sensitive to reducing loads where possible and as a result can be assumed to be operating below the presented average load. On the other hand, having excess storage energy may provide the opportunity for the campus to export power. However, the value of this service is not quantified in this work and may be of interest for future work. The largest electrolyzer and storage size can meet three days of the average campus load if the storage is 28% and 23% full for the P2G-GT and P2G-FC strategies, respectively. The physical feasibility of hosting this amount of energy storage capacity at UCI is then considered. The current solution for fuel cell backup generators is typically low-pressure gas cylinders as it circumvents the costs associated with liquefying or compressing and storing hydrogen. The footprint of the existing central plant area is used as a relative unit of measure. The footprint considered is roughly 9500 square meters shown in Figure 32.

Figure 32 – Overhead view of UCI's central plant area, the highlighted area being roughly 9500 square meters.

Storage in 165 Bar cylinder storage modules, 700 Bar cylinder storage modules, and a central tank of liquid hydrogen at atmospheric pressure is considered. Storage at 165 Bar is the current low-pressure solution and 700 Bar is the typical light duty vehicle transportation fuel tank pressure. The cylinder storage modules are assumed not to be stacked vertically and their footprint is taken from Plug Power's product catalog [194]. Even at 700 Bar, the higher capacity electrolyzer scenarios require a storage footprint exceeding the central plant. Of the considered options, the liquid storage capacity requires the least amount of space but would require additional conditioning of the electrolytic hydrogen. A centralized tank is proposed and prototyped by Kawasaki for transoceanic shipping of hydrogen. The cost and efficiency analysis for the 700 bar and liquid forms are not considered in this work but suggests that larger distributed storage

tanks may be in demand to make these types of applications viable. Rather than aggregating several smaller gas cylinders, large central gaseous storage tanks may be a viable solution. Otherwise, tariffs will need to be developed so that aggregated communities or large customers can utilize the existing gas grid as a storage asset to promote sustainable development. The storage capacity footprints in the established scenarios are presented in Figure 33.

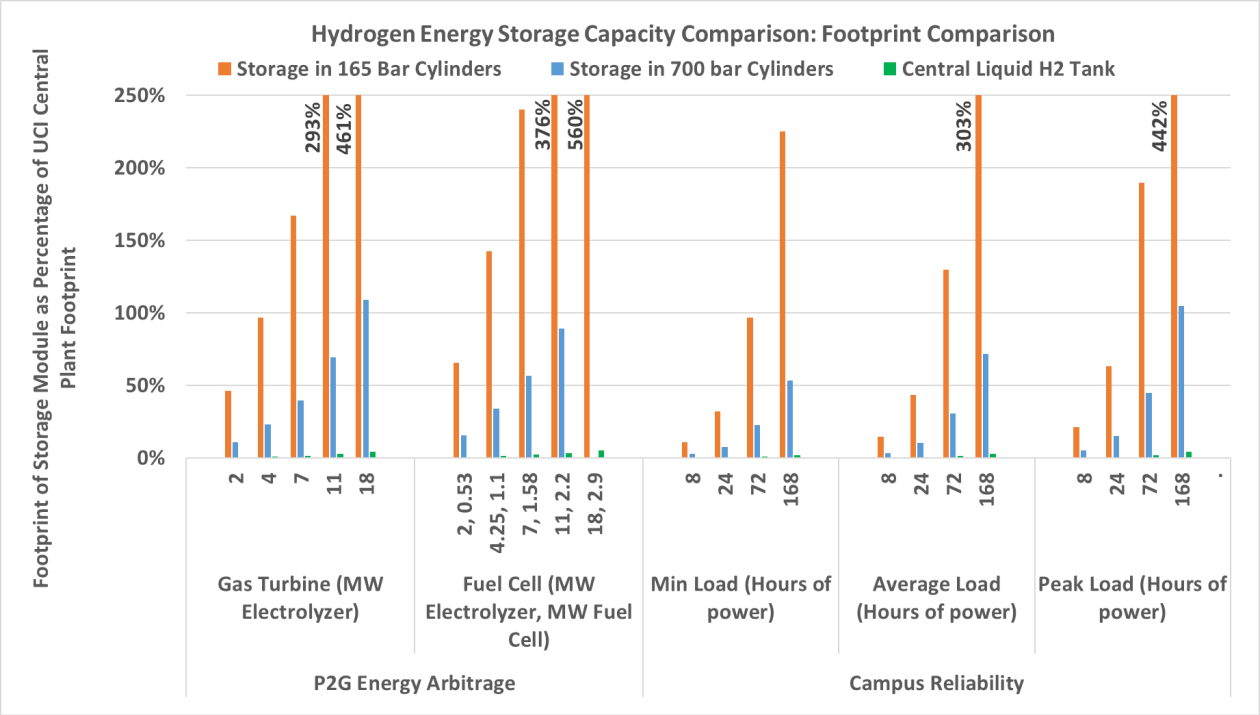

Figure 33 – Comparison of the footprint of storing high pressure gaseous and liquid hydrogen compared to UCI's central plant footprint.

4.4 Zero-Emission Backup Generation Only Full Fleet (17 MW)

Two additional factors can be considered to provide further insight: 1) what if the backup fuel cell generators are distributed among campus buildings with critical loads and 2) what is the cost and environmental impact of zero-emission backup generators if evaluated completely independent of campus energy arbitrage needs? To address the prior question, the mechanical portion of non-assignable square footage of buildings which already have generators installed is

used as the unit of measure in lieu of the central plant's footprint. The sum of the mechanical areas totals roughly 257,000 square feet or 27 times that of the previously assumed central plant footprint. This result makes the storage of hydrogen seem more feasible if enough of the existing mechanical area can be re-allocated for fuel storage but does not account for any fire code restrictions, location of distributed resources and loads.

The list of generators is separated into four groups based on their commissioning date. Those installed between 1965 and 1989 are designated as group one, 1990-1999 are designated as group two, 2000-2009 are designated as group three, and those after 2010 are designated as group four—with the most recent one listed being in 2016. The combined capacity of the two oldest groups amounts to 5.5 MW, which provided the basis for replacement capacity in the preceding analysis.

Multiple studies in the past have studied the health impacts impact of diesel backup generators. Among them, the United States Environmental Defense Fund [195] and California Air Resources Board (CARB) [196] have produced reports that suggest there is a risk to humans even as far away as 400 meters during operation. The CARB study [196] models a 500 hp diesel backup generator with a particulate matter emission factor of 0.1 g/bhp and finds that at around 50 meters, the maximum concentration of particulate matter results in an additional 3.5 per million people risk of cancer. The concentration of particulate matter looks almost normally distributed, where even beyond the concentration peak there is significant risk (e.g., at 100 meters the risk is slightly above 2 per million people.

For context, the UCI fleet is almost 50 times the capacity of this 500 hp engine modeled in the CARB study with many documented to having particulate matter emission factors double (and

sometimes defaulted to 10 times when specifications are unknown). The total effect on students and staff on campus is challenging to model without modeling dwelling time and air quality dispersion, but it can be assumed that there is significant cancer-inducing diesel particulate matter anywhere from 10 to 200 meters from the source--and even further for larger or more active generators [195]. from the source. To illustrate the potential risk zone each of the generators on campus are shown by their commission date with 100-meter radii in Figure 34.

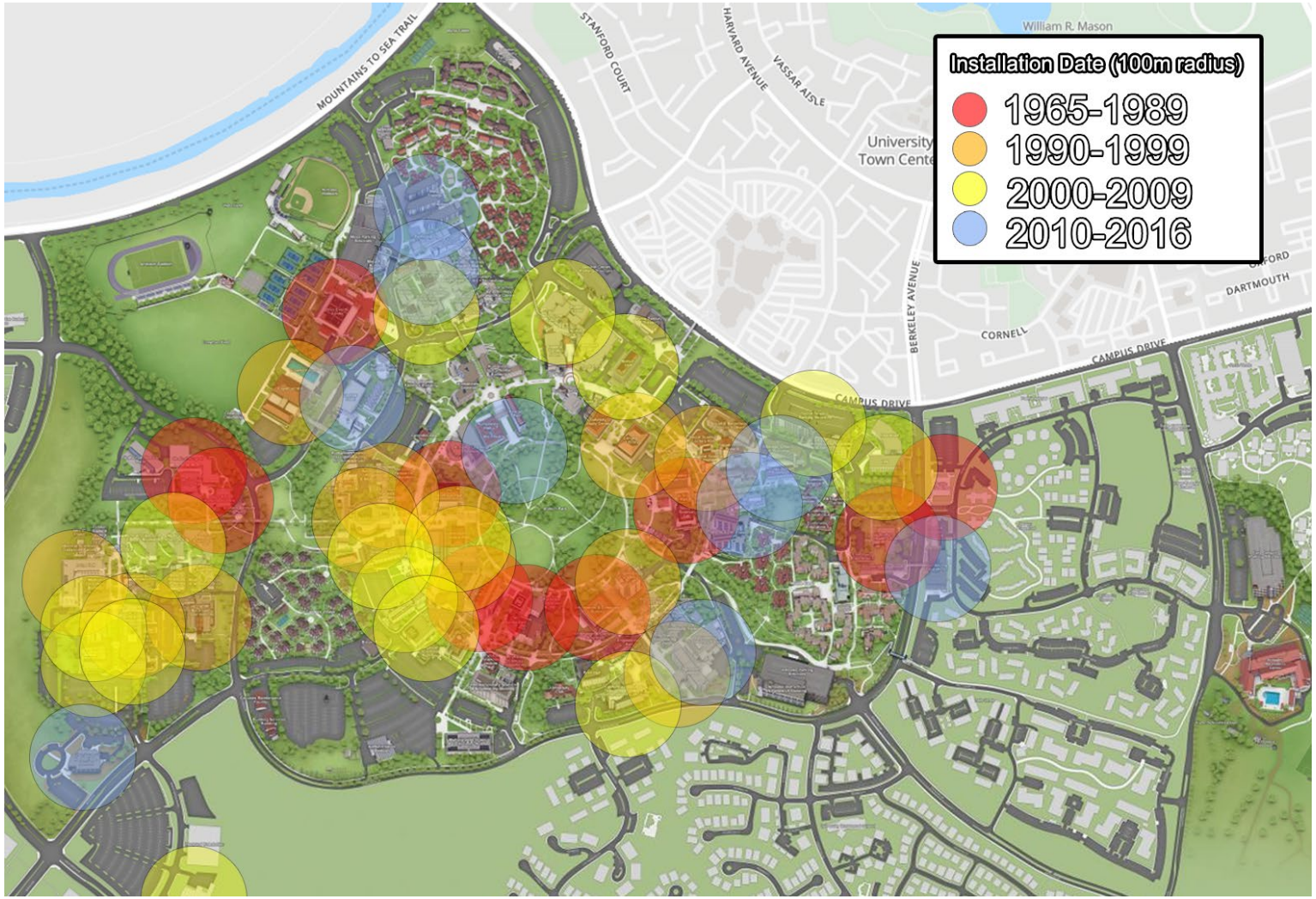

Figure 34 – Illustration of 100-meter risk radius for each UCI backup diesel generator by commission year. Other studies have significant risk of cancer even beyond 200 meters from the source.

Several residential buildings fall into the risk areas, but there seems to be very few core campus buildings that escape all exposure. This is an inevitable challenge as the most critical loads (e.g., time and temperature-sensitive experiments) are in research facilities at core campus and require reliable power in the event of an emergency. This is at the cost of potential health risk to researchers and students on the campus alike. To estimate the emissions from campus backup generators, the emission specifications for each generator model are used when available and South Coast Air Quality Management District's stationary diesel engine emission factors otherwise. Diesel generators require 20 test hours yearly to ensure performance when, whereas those with more critical loads may have as much as 50 test hours yearly. The historical operation of the fleet for each year from 2013 to 2016 is used to estimate historical fleet emissions. The total emissions from the fleet of UCI diesel backup generators and therefore possible emission reduction from zero-emission fuel cell and battery-based generators are reported in Figure 35.

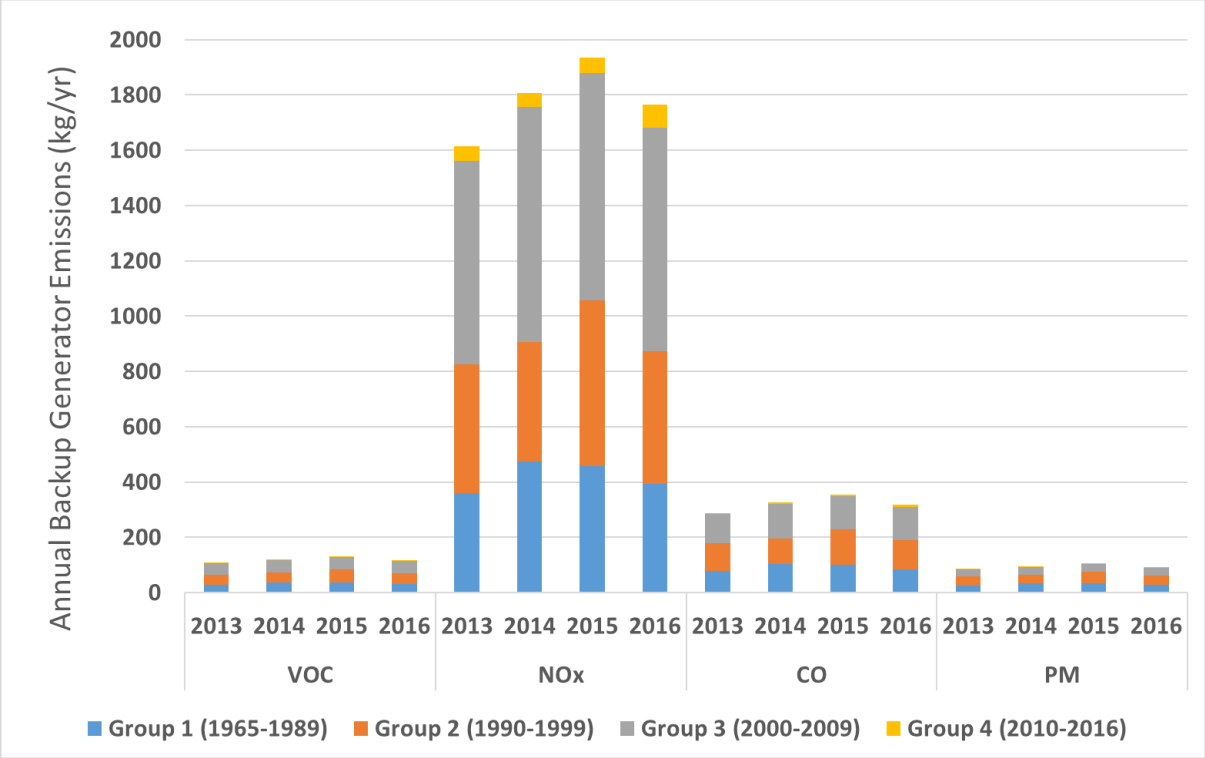

Figure 35 – Historical annual emissions from UCI's diesel backup generator fleet by commissioned year.

The power capacity of group three is the largest group at roughly 9 MW of the 17 MW fleet. They seemingly contribute the most emissions because of this as seen in Figure 35. The historical pollutant emissions are normalized by the groups' power capacity to quantify the potential reduction in emissions by replacing generators based on their age. The average annual historical emissions from the diesel backup generator fleet normalized by power capacity from 2013 to 2016 are summarized in Figure 36 below.

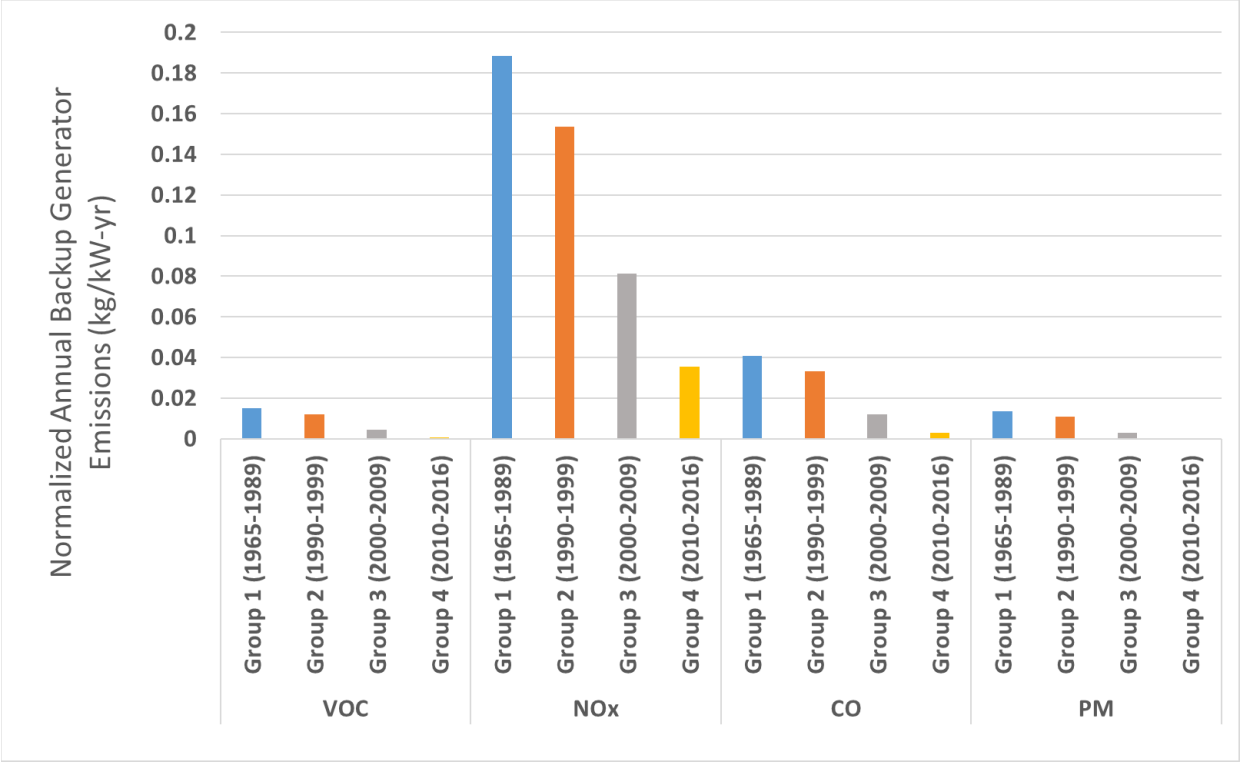

Figure 36 – Average annual historical emissions normalized by power generation capacity from 2013 to 2016.

While zero-emission backup generators are indisputably better for the environment, there can be cost challenges due to the technologies. If long durations of operation are required for a diesel generator, the marginal cost for additional tanks of liquid fuel is negligible relative to the annualized capital, installation, operation, and maintenance costs. Natural gas backup generators (two of which make up less than 100 kW of the fleet and not considered in this analysis) have the advantage of being fueled by the gas grid rather than limited to an on-site tank.

On the other hand, for a PEM fuel cell backup generator the commonplace storage of hydrogen in on-site gaseous low-pressure steel cylinders can become expensive if many cylinders are required without relying on trucked fuel deliveries amidst an emergency. An NREL report [197] suggests that run times as long as a week can avoid some hydrogen storage capacity costs if a

smaller capacity storage module can be refilled, but this feasibility and cost effects of this idea is not explored.

Even more challenging for the BESS is the inherent coupling of power and energy storage capacity. Due to the coupled nature of the two attributes, increasing the duration the system can run would result in a greater power capacity than if the system were sized to meet power requirements. This similarly rapidly increases costs when extended continuous runtime is required. Figure 37 illustrates the range of annualized cost of ownership for replacing the entire 17 MW backup generation fleet with zero-emission generators for various run times. Note that existing diesel generations in the fleet have tanks capable of running at capacity for an average of 17 hours.

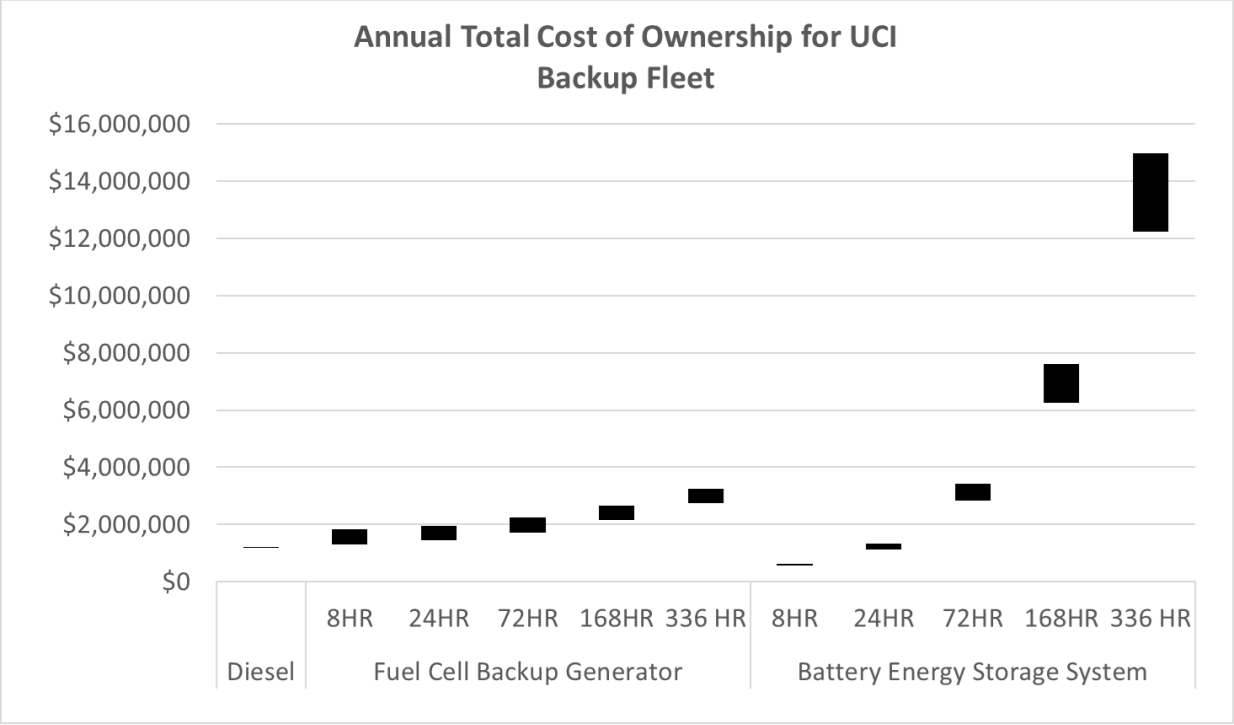

Figure 37 – Range of total annual cost for 17 MW UCI backup generator fleet for different fuel capacity for continuous reliability. Additional diesel fuel capacity costs are assumed to be negligible.

The lower and upper bound for the fuel cell scenarios are established by assuming a fuel cell capital cost of 800 $/kW and 1200 $/kW [198], respectively. These numbers are representative of commercial solutions available today as well as the expected cost reductions in the short-term due with the increase of volume [199]. A variable O&M cost of 16 $/MWh [200], fuel cost of 3.0 $/kgH2, system efficiency of 60%, and 8 $/kWh hydrogen storage capacity cost [201]. A scale factor of 0.7 is used for larger quantities of storage with 4 hours being the reference case. Similarly, a conservative and optimistic estimate of 350 $/kWh and 250 $/kWh, respectively, are assumed for the BESS [202]. A fixed O&M cost of 10 $/kW-yr, variable O&M cost of 30 $/MWh, electricity charging cost of 100 $/MWh, power to energy capacity ratio of 4 and roundtrip efficiency of 85% is assumed [203]. The diesel replacement $/kW capital cost is estimated by fitting a logarithmic

curve based on Generac Industrial Power's Total Cost of Ownership calculator [204] for a diesel replacement of same size for each of the UCI backup generators seen in Figure 38 – Fitting a curve to estimate cost of diesel backup generation system cost capital costs based on power capacity.– fitting a curve to estimate cost of diesel backup generation system cost capital costs based on power capacity. A fixed O&M cost of 10 $/kW-yr, variable O&M cost of 10 $/MWh, and a fuel cost of 2.5 $/gal [205]. The installation costs for diesel and fuel cell system are modeled as equal to their capital cost whereas for the for the BESS it is 60% of the capital cost [197]. A 5% discount rate over a 20-year project payback period is assumed for all scenarios.

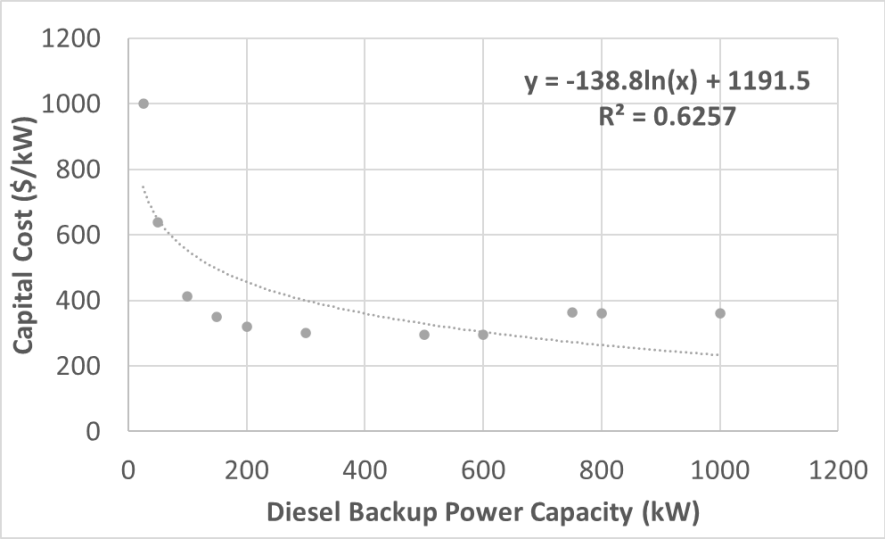

Figure 38 – Fitting a curve to estimate cost of diesel backup generation system cost capital costs based on power capacity.

Further, a sensitivity analysis for how various variables can independently affect the results previously presented in Figure 39. Due to relatively low-capacity factors compared to energy arbitrage scenarios, the changes to fuel costs and system power generation efficiencies yield the smallest changes. Because extended operation of various times is of interest, it seems consistent that the marginal cost of energy storage capacity has the greatest effect. This would be the cost

to store additional hydrogen on-site as well as the possibility for various battery chemistries that would enable higher energy capacity to power ratios.

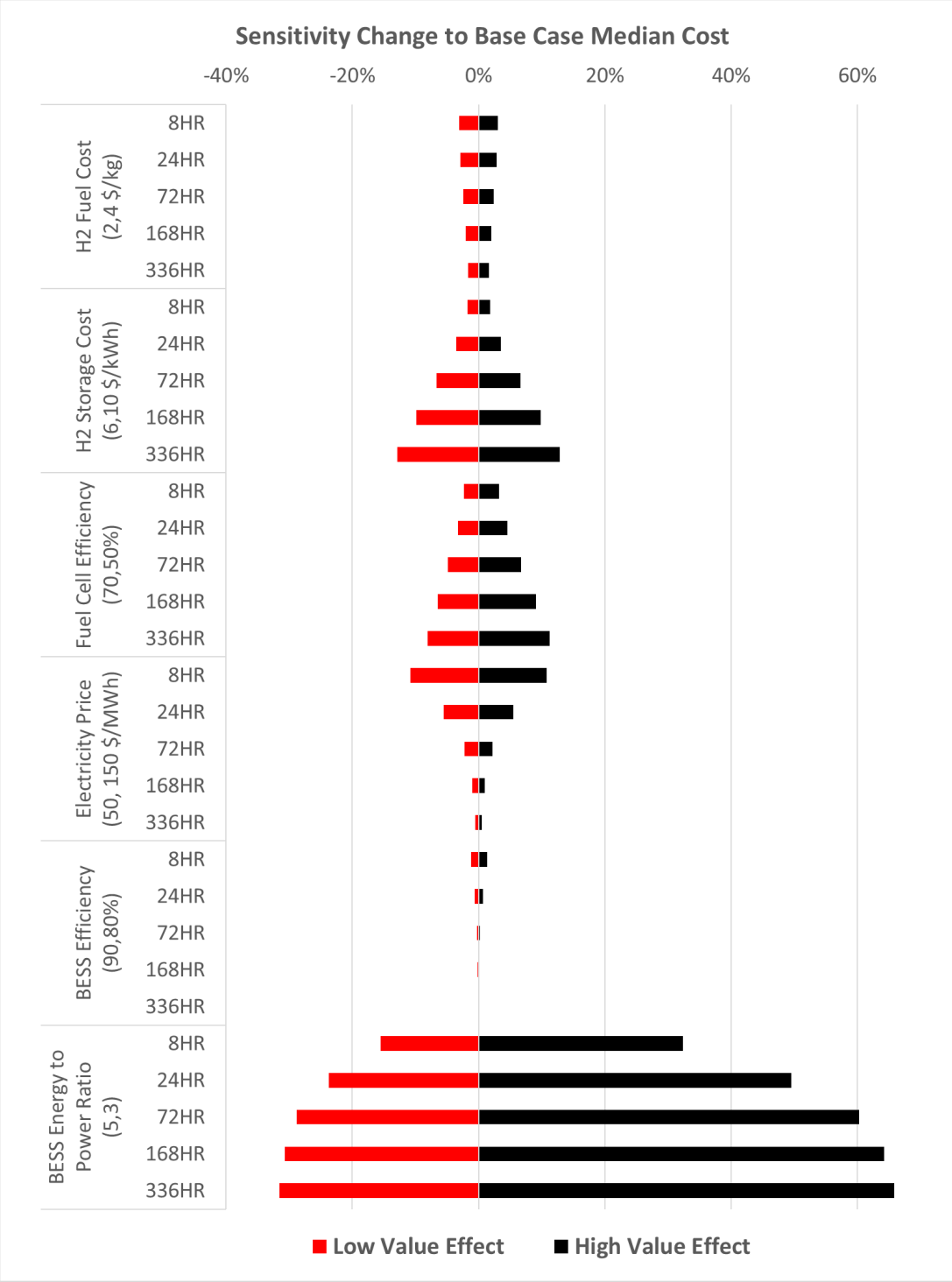

Figure 39 – Single factor sensitivity analysis effect on median annualized cost of ownership for replacing the UCI backup generator fleet.

In review, diesel generators are the clear economic choice, especially for longer and longer continuous run times due to the relatively high marginal cost of hydrogen fuel storage or battery-

based energy capacity. However, with increasing desire to move toward zero-carbon and reducing hazardous air pollutants diesel may be out of the question. When evaluating between PEM fuel cell backup generators running on hydrogen and batteries with similar specifications to massively popular lithium-ion based battery systems, the battery systems seem to be the better choice for continuous run times of a day or less. Beyond this, the ranges between the two technologies are much more comparable and ultimately becomes much more comparable for run times up to 168 hours. One caveat for this comparison, however, is that hydrogen fuel cylinders have more transport flexibility and have the potential to be refilled or replaced amid an emergency. Increased storage capacity for both technologies imply greater footprints but seem feasible relative existing mechanical areas designated to ensure the operation of each campus building. Transitioning to the next subsection, the CO2 emission factor is used to estimate the potential reduction in carbon emissions associated with the fleet of backup generators, as done above with the pollutant emissions. These estimates are presented in Figure 40.

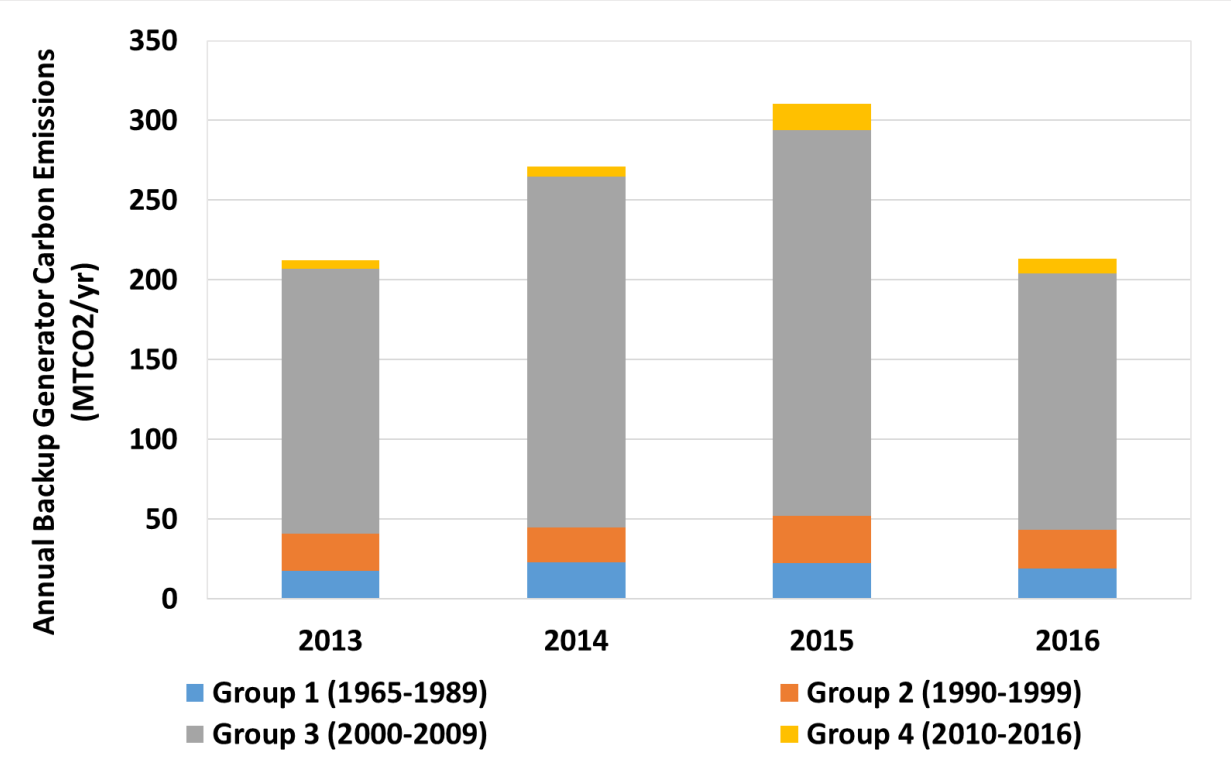

Figure 40 – Estimated carbon emissions from UCI backup fleet historical operation.

4.5 Discussion: Pathway to Carbon Neutrality

The carbon emission reduction from renewable sources is estimated from the EPA emission factor of 0.4 kg-CO2e per kWh electricity produced from natural gas combined-cycle plants. The carbon reduction from the different strategies is summarized in Figure 41. The reductions presented do not include the portion from solar PV installations which is essentially enabled by energy storage. The emissions reduction is proportional to the amount of load that is met by energy from storage effectively displacing cogeneration generation.

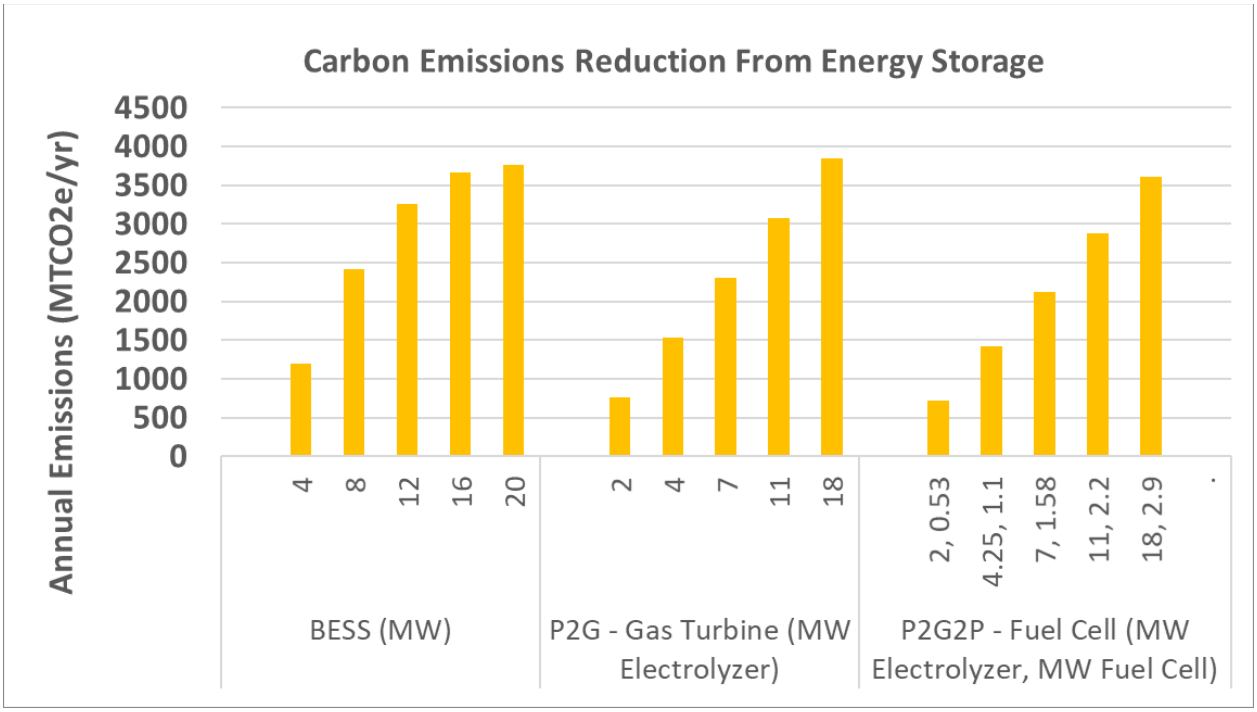

Figure 41 – Comparison of carbon emissions reduction from using stored energy to displace cogeneration electricity production.

At the selected capacities, the BESS strategy begins to marginally decrease at the higher capacities. This is due to the limitation of the BESS shifting energy daily and quickly reaching full state-of-charge while some solar is still curtailed. To increase the carbon emission with a BESS, renewable imported electricity would have to be imported outside of typical solar generation hours. This may be potentially possible with RECs coming from wind generators, assuming RECs in the future are time dependent rather than simply being on an accounting basis. The reduction in the P2G cases increases linearly with the amount of available hydrogen. Likewise, greater amounts of renewable electrolytic hydrogen would be needed to further increase reductions. However, since all the considered scenarios already fully utilize the distributed generation potential, additional resources seem necessary.

To further contextualize the reduction magnitude seen above, the climate action plan (CAP) for UCI established in 2016 is referred to [206]. In the CAP, the business as usual (BAU) scenario forecasts the load and resulting emissions reduction needed for subsequent years. The solutions to reducing these emissions are made by reducing the load usage by developing more energy efficient buildings, as well as retroactively making existing loads more efficient, installing on-site PV to meet load, procuring biogas for the power plant usage, switching the bus fleet from diesel to electric and fuel cell buses, and offsetting the remainder with RECs (to justify renewable electricity imports) and carbon offsets (to justify zero on-site emissions). The projected load and reduction strategy are presented in Figure 42. The 2025 emission reduction breakdown is used as the numeric details are available from the CAP. Note that post-energy efficiency electric load in 2025 is roughly 10% lower than in 2017.

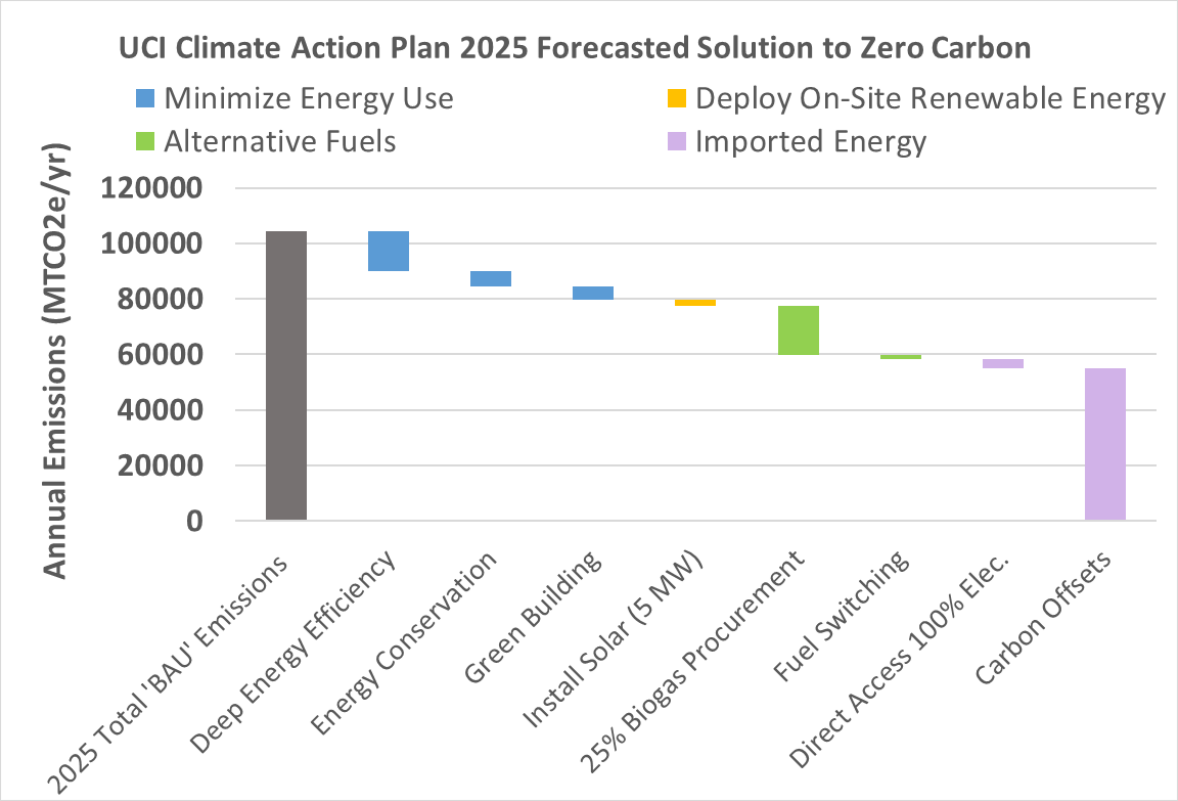

Figure 42 – UCI climate action plan 2025 load and emission reduction strategy to reach carbon neutrality.

Recent electricity consumption numbers can be used to check progress relative to the CAP. A notable difference is that the 2017 historical load (the total used for this analysis) is far lower than that in that predicted in the CAP. Assuming 100% of the load is met by natural gas combined-cycle plant, the total forecasted emission in 2017 would be about 80,000 MTCO2e (after energy efficiency measures) and correspond to an electric annual load of 190 GWh. However, historical 2017 data suggest that the load was much lower at 115 GWh. The reduction from the energy minimization measures is kept constant and added onto other emission reduction strategies, including those evaluated in this analysis in detail to establish what could be considered an update on the forecasted load and compared.

As a comparison, this study assumes installing 32 MW of distributed solar generation, which, opting to not have energy storage results in a third of the renewable electricity being curtailed. The carbon emissions resulting from this are consistent by being about four times the emission reduction found in the CAP from installing 5 MW of solar. The modeled energy storage reduction assumes 4000 as an optimistic scenario from the prior Figure 41. The reduction from using biogas for a fraction of natural gas consumption is much lower in this work's 40% scenario compared to the CAP 25% due because the total forecasted load in the CAP is significantly higher. This is due to the higher load previously forecasted in CAP whereas the load historically was much smaller in 2017. Fuel switching is assumed to remain the same amount of reduction and the remainder is offset.

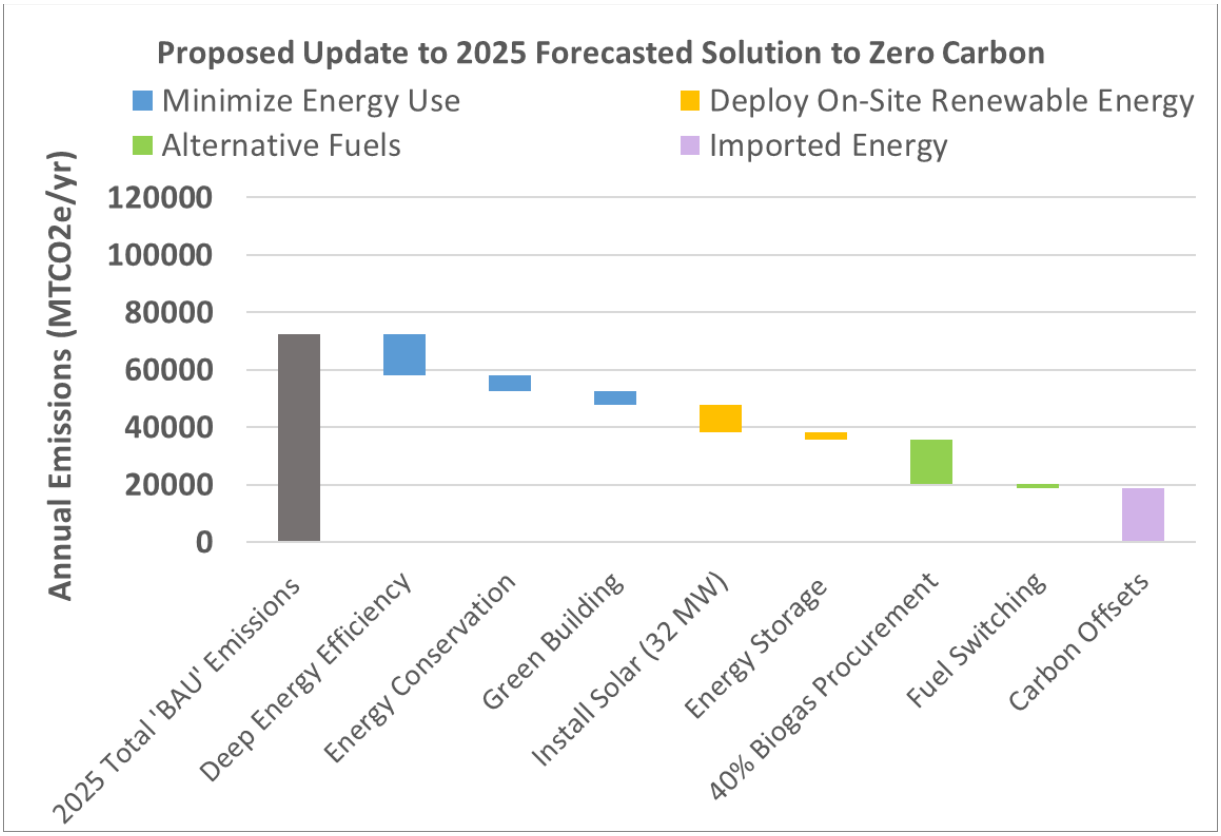

Figure 43 – Comparing the reduction in carbon emissions from different strategies.

A previous 2014 study which considers the deep energy efficiency potential to reduce UC campus emissions [207] is believed to be captured as one of the factors in the UCI CAP. While some of the evaluated projects may have already been actualized by the time of writing this report, there is much uncertainty regarding what projects are still being pursued and how the avoided costs compare to the price of capacity additions considered in this report. In addition, the criteria set out in the report considered the highest impact load reductions and may have significant additional reduction potential if sufficient opportunities exist around campus. This type of analysis is recommended for future work but based on the 2014 study, roughly a doubling of the reduction from deep energy efficiency is needed to eliminate the need for carbon offsets seen in Figure 43.

With newer information, the trajectory toward carbon neutrality looks better than previously predicted in the CAP. However, even with the optimistic use of distributed energy resources, the campus still relies on importing renewable attributes: biogas as a renewable fuel, carbon offsets for the non-renewable portion of cogeneration, and RECs for any imported electricity—all of which on an accounting basis. In this case study for UCI, the apparent answer seems to be to procure greater and greater amounts of centralized resources at off-campus sites. However, previous analyses for managing challenges associated with centralized PV plants (i.e., Buford Giffen) encountering grid constraints and poor wholesale price economics poses the question whether there is a better sustainable strategy to carbon neutrality at the utility-scale level. BESS systems are becoming increasingly commonplace at the utility-scale and demonstrations of novel P2G projects seem like the next logical step to explore additional pathways.

4.5.1 Retail Sector Limitations

This work focuses on a university campus as an exemplary community and evaluates the capability to transition to completely decarbonize and depollute electricity usage. Net-metering incentives for distributed solar PV in California (for systems less than 1 MW installed capacity) have spurred many distributed PV installations. But net metering incentives are not typically applicable to larger loads or microgrids. Thus, larger load users or campuses need to manage supply and demand within the campus infrastructure, which may benefit from the installation and operation of energy storage systems.

The cost of importing energy and claiming renewable attributes through market instruments (e.g., RECs) is currently cheaper than self-generation plus storage and is currently

treated legally as having an equal reduction in emissions. The trading of RECs, however, especially in disparate geographic regions, does not account for energy arbitrage, T&D infrastructure, or storage assets that would otherwise be required to directly handle renewable power and demand dynamics to physically firm renewable resources. Such approaches are not sustainable nor extensible for the continual deployment of renewables, so that the claim of 100% renewable electricity provision through RECs may be called into question in the coming decades. Even smaller distributed PV systems may lose their net-metering privileges, which will require on-site energy storage capacity to address the current challenges and obstacles associated with deploying much more solar PV in any particular jurisdiction.

Decarbonizing more economic sectors will eventually require massive and local deployment of storage systems and T&D investments to complement renewable generation. This is being reflected in current proceedings for net metering reform to account for this, implying upward pressure on direct-access PPAs. Extensibility in the current case is significantly supported by the local renewable-fueled GT-CC. If the GT-CC were shut down in this setting, the geospatial potential of PV would increase from directly meeting load from 20% to 37% and the necessary BESS capacity decreases from 15% to meeting approximately 7% of load, with over 55% of the remaining load would be met by grid electricity. All of this utility demand occurs at night, thus requiring the highly solar renewable utility grid network to meet all of this demand with storage resources. This would alleviate the cost investment locally but would require re-evaluation for grid upgrades to meet nighttime demand only.

Moving forward, society would benefit from a better understanding of the balance between distributed and centralized (utility-scale) resources. Some policies in place, such as net

metering, have allowed the initial deployment of PV systems, but further deployment faces many challenges due to significant overgeneration or T&D congestion. The considered campus comprises of a mix of occupancy, in addition to having an existing gas power plant. It is found in this work that there simply is not enough PV potential to meet the entire electric load—completely independent of the techno-economic challenges from low-capacity factor energy systems.

Prices are typically cheaper in centralized settings from economies of scale, implementing long-duration storage does not seem to be viable without new policy. Historically, ancillary service clearing prices have increased on average in the past few years but more opportunity for revenue needs to become available for distributed energy storage systems to become economically competitive with procuring power in bulk from centralized resources. Long-duration, or seasonal storage, in conjunction with being able to provide backup power could be one such service to motivate increasing distributed resource capacity. By mandating long duration storage in distributed and retail settings, the grid can deploy greater amounts of renewable power and with more energy storage capacity, the transmission constraints can be overcome through more local resources to support high renewable power use in the context of climate change (e.g., achieve high reliability in the events of extreme weather or public safety power shutoffs).

Future policy will have to be conscious of how the new system costs will be shifted toward developers, investor-owned utilities, or the end consumers. The current analyses show that additional economic incentives (e.g., more valuable ancillary services, or incentives for energy storage) are required to promote distributed energy storage systems and bolster grid reliability. This is especially true with the potential decarbonization of the gas grid that must compete with

electric energy storage, transmission, and distribution assets in their roles supporting the evolving and highly renewable electric grid.

4.6 Chapter Summary and Conclusions

Major conclusions thus far from the current analyses associated with energy storage on UCI are enumerated as follows:

1) Installing the maximum amount of solar PV potential (geospatially limited) results in directly meeting 20% of the electric load. 58% of PV electric production is curtailed in this case unless energy storage is implemented. Large amounts of curtailment occur due to overgeneration exacerbated by the minimum operating constraint of the existing GT-CC. Despite this, the GT-CC is necessary as it meets a major portion of load and removing it requires additional renewable energy storage investments and results in procuring more imports via PPA to meet over 50% of remaining load, burdening the electric grid and disabling the vehicle for renewable gas usage.
2) The P2G-FC and BESS strategies result in similarly high 64% RES despite having different roundtrip efficiencies. This is because the BESS participates in daily shifting of energy whereas the smaller capacity fuel cell can operate consistently throughout the night, shifting a greater amount of energy. The P2G-GT strategy produces the same amount of hydrogen as in the P2G-FC strategy, but only reaches 60% RES due to the lower reconversion efficiency of a gas turbine compared to a fuel cell. Roughly half of the RES% arises from biogas procurement from off-campus, suggesting very limited ability to reach complete decarbonization with on-site assets.

3) The LCOE for a high degree of energy storage capacity at UCI is 0.16 $/kWh, 0.19 $/kWh, and 0.20 $/kWh for the BESS, P2G-GT, P2G-FC strategies, respectively. If factoring in the cost of ownership for replacing backup generators and potential market ancillary costs, these levelized costs can be as low as 0.12 $/kWh, 0.15 $/kWh, and 0.16 $/kWh. These costs are still higher than the current direct access purchase of power, providing no economic incentive to invest in on-site assets other than for reliability, decarbonization, and depolluting reasons.
4) Gaseous hydrogen storage requires potentially massive amounts of space. Utilization of the gas grid or having gas storage used for energy arbitrage and backup power seems to be the most probable and cost-effective solution to storing electrolytic. The potential of having backup energy storage in a distributed setting is a considerable potential benefit to the grid.
5) Novel policy needs to be in place to promote distributed energy storage and act as a better integrity vehicle for carbon neutrality rather than procuring off-campus resources. Even then, on-site distributed renewable resources are geospatially limited in meeting community loads in all urban settings. As a result, policies should be developed to standardize a mix of distributed energy resources and centralized solutions to balance incentivizing deployment of distributed energy resources and the premium costs associated with these assets that allows high renewable use and delivers reliability and efficiency benefits.

5 Transportation Perspective Case Study: Freight Industry

This chapter largely originates from a collaborative effort between Clinton Thai, Luca Mastropasqua, Alejandra Hormaza Mejia, Alireza Saeedmanesh, Emily Dailey, Robert Flores, Jeff Reed, Michael MacKinnon, Kevin S. Gill, Steven J. Davis and Jack Brouwer This chapter largely describes the methodology and results of estimating total hydrogen demand for the freight sector as a key input for Chapter 7. The authors' contributions are that: C.T. conceived the idea and oversaw methodology. L.M. carried out the cost analysis (not in this dissertation). C.T., A.H.M., A.S. carried out the formal analysis for fuel demand. R.F. led project administration. C.T., L.M., E.D. were responsible for visualization under the guidance of S.J.D., and J.B. C.T., L.M., A.H.M., A.S., E.D., J.R., developed the original draft. R.F., S.J.D., J.B., reviewed the draft. C.T. finalized the manuscript. Other authors provided critical data for the analyses.

5.1 Motivation

Freight transportation by heavy-duty trucks, rail, and transoceanic ships is a crucial component of the modern global economy. In recent years, the global freight industry moved more than 90 trillion ton-km of goods [208] with an estimated value of nearly $29 trillion in 2021 [209]. The International Trade Forum (ITF) projects the mass of global freight transport to increase by 3.6% per year to 350 trillion ton-km in 2050 [210]. In turn, greenhouse gas (GHG) emissions related to freight transport represented 2.9% of fossil fuels and industry emissions, or 1.1 Gt CO_2, in 2018 [211], having grown by 1.5% per year between 2012 and 2018 [211]. Total GHG emissions from marine shipping are projected to increase another 50% by 2050 [211], and emissions from

heavy-duty trucking and freight rail are projected to grown by 1.6% to 2.8% per year through 2050 [210]. Moreover, criteria pollutant emissions from freight operations are major contributors to degraded and dangerous air quality in many regions [212]–[214].

Whereas emissions from light-duty passenger vehicles may be feasibly eliminated by electrifying vehicles [215]–[217], the energy density of lithium-ion batteries make it challenging to use them to electrify transportation of heavy payloads over long distances [218]–[223]. Thus, proposed strategies for decarbonizing freight operations generally rely upon the availability of low- or zero-carbon fuels that can supply the energy and power density required by modern freight transportation, often as part of alternative hybrid powertrains that also include electric batteries [224]–[226]. Among the alternative fuels that have been studied are liquefied natural gas (LNG [227], [228]), compressed natural gas (CNG [229]), hydrocarbons (gaseous or liquid) or ammonia synthesized from renewable primary energy [230], [231], and advanced biofuels [232]. Liquid biofuels are often regarded as a preferred alternative fuel [233], [234] as they are close to a "drop-in" fuel in heavy-duty trucking [235], [236]. However, such liquid fuels are currently either limited in supply or expensive [234], [237], [238]. Lower cost options, such as LNG and CNG, do not substantially reduce CO_2 emissions and are not renewable [228], [239]. Moreover, none of these alternative fuels eliminate air pollution when converted by combustion-based engines.

Another fuel and heavy-duty powertrain option that can eliminate CO_2 is renewable hydrogen (H_2) when used in fuel cell-based power systems [231]. Recent studies have shown that fuel cell designs could feasibly power at least 90% of medium- and heavy-duty truck routes in the U.S. [240] as well as a range of marine vessels [241], and that hybrid locomotive designs (e.g., pairing a solid oxide fuel cell with a gas turbine) could power trains over the most demanding

routes in California [242]. Other work has demonstrated that hydrogen can be produced cost-effectively from renewable biogas and biomass feedstocks [243], [244], although such biomass feedstocks are limited [245] and often in demand for other uses [246] (e.g., for food). On the other hand, many regions have renewable energy sources sufficient to produce vast quantities of renewable hydrogen production by water electrolysis. Although electrolytic hydrogen is expensive (between $5 and $11 per kg H_2 [247]) relative to fossil methane-derived hydrogen (~$1.50/kg H_2 [243], [248]), electrolyzer system improvements and optimization, economies of scale, and falling costs of solar and wind electricity have decreased the cost of electrolytic hydrogen substantially in recent years (by 10% to 50% from 1995 to 2018 [249]), with substantial further reductions expected in the coming years [250].

As with any of the technological options for decarbonizing heavy-duty transportation, development of a renewable hydrogen-based freight transportation system would entail substantial new infrastructure for transmission, storage, and distribution. For example, use of hydrogen at large scales might require new hydrogen pipelines, or the transformation of existing natural gas infrastructure for renewable hydrogen use (as opposed to the more conventional trucking of compressed or cryogenic liquid) [251]–[254]. Decades of experience in the U.S. and Europe show that pipeline transport of hydrogen is feasible [255]–[258], and there are roughly 3200 kilometers of hydrogen pipelines [259] in use today, transporting ~500 billion cubic meters per year [260], More recently, research has demonstrated the potential to use the existing natural gas pipeline network to store and deliver renewable hydrogen [261]–[263] , finding that such a conversion may be economically viable [264] despite known challenges of pipeline degradation and gas leakage[265]. In addition, the use of the gas system to store electrolytic hydrogen for

seasonal electricity generation via fuel cells will be increasingly possible and perhaps necessary as the gas and electricity systems transform [266].

5.2 Vehicles

Here, a detailed assessment of the resource requirements to repower the entire California freight sector with hydrogen. California is a major economy in the U.S. with both a particularly important freight sector (e.g., the two largest U.S. ports in San Pedro and Oakland, the second-most rail carloads of any state [267], and the second-most freight transported by truck of any state in terms of both tons and value [268]) as well as a legacy of strict regulation of air pollution and ambitious mandates to eliminate statewide CO_2 emissions by 2050 [269], [270].

A baseline scenario that assumes all freight vehicles with duty cycles amenable to electrification (here defined as routes less than 300 miles or payloads less than 15 tons) will be electrified by conventional batteries [220], [271]. Pathways to meet all remaining freight transportation demand are evaluated, including for transoceanic ships, freight rail, and heavy-duty trucks used for long-distance (greater than 300 miles) freight, are electrified using renewable, electrolytic hydrogen and fuel cell powertrains. Hydrogen demand for trips originating in California and reaching their primary destination (i.e., excluding return trips) is developed based on travel surveys and datasets from 2017 and 2018 scaled to 2050 levels based on projected [272], [273] current and future vehicle performance characteristics of ships [274]–[276], trains [260], [277], and heavy-duty trucks [260], [277]. Future hydrogen powertrains [241], [242], [278], [279] performances are used to convert distances traveled into fuel demands.

Given large uncertainties in future freight demand, scenarios including a “Base-Growth” scenario where trade demand increases as expected, and a “High-Growth” scenario where trade

demand growth is doubled is developed. Total hydrogen demand for these two scenarios is further augmented by considering the speed at which ships traverse the ocean. As fuel price decreases, ships are operated at higher speed [280], [281]. To capture this difference a "low-speed" and "high-speed" ship speed scenarios are developed for the two trade growth cases. Total hydrogen demand for these four scenarios is then converted into solar and wind power plant capacities using resource potential maps [282]–[284] (maps are 4x4 km and 1x1 km for solar and off-shore wind resources, respectively), land-use layers [285] (30 x 30 m resolution), and accounting for energy losses and use associated with production, liquefaction or gaseous compression, and delivery of the fuel [250], [286]–[288]. Excluding already existing onshore wind power plants, available land suitable for new onshore wind development (e.g., wind power class of 3 or higher) is limited to areas of the Sierra Nevada and San Bernadino Mountain ranges and the Sonoran and Mojave Deserts [289]. Because these available areas are only able to meet 5 to 10% of the projected energy demand for freight, they are excluded from the current analysis.

5.2.1 Ships

The air emissions inventory released by the Port of Los Angeles in 2017 [290] is used for estimating energy demand. By assuming a 2-stroke diesel engine with 50% [291]conversion efficiency, the visitation and operation statistics are used to predict total energy demand [292]. This energy demand is converted to hydrogen demand by assuming fuel cell system efficiency of 65% [293]. The HHV of hydrogen is used for heating loads whereas the LHV is used for electric loads. Maneuvering instances are assumed to be half an hour. Time for hoteling while anchored or at berth are provided in the inventory.

To calculate main propulsion load required to move a ship between ports, a random sampling of forty ships appearing in Port of Los Angeles port calls from the Maersk fleet is selected with known shipping routes and time at sea [274]. Using a sampling of ships, a regression is made relating voyage distance to twenty-foot equivalent rating, seen in Figure 44 below. This regression is used to predict distance by all other vessels docking and departing from California ports. Pairing this information with ship powerplant size and efficiency allowed for total energy demand to be predicted.

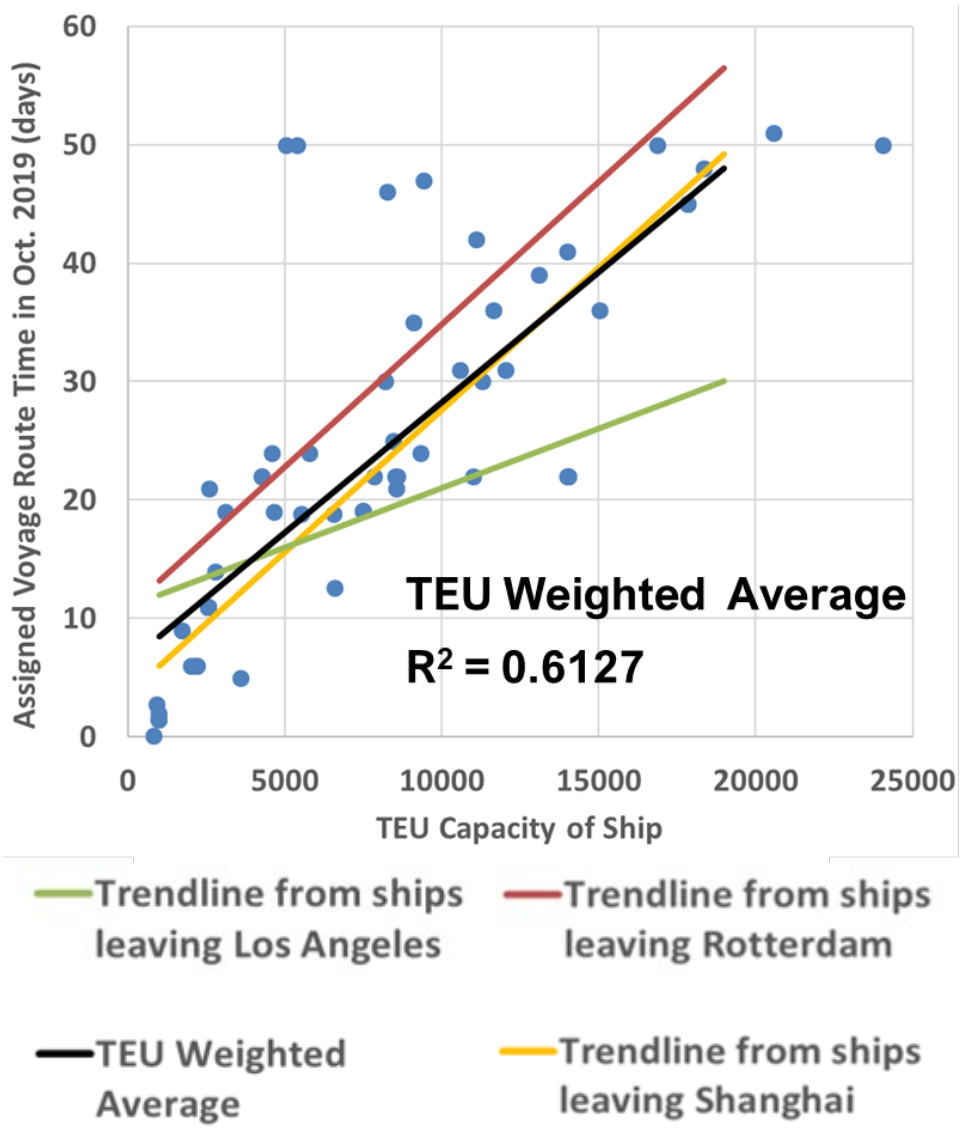

Figure 44 – Sampling of cargo ships leaving the globally largest ports to relate carrying capacity with voyage times.

Total hydrogen demand for ships departing from California is calculated by considering the energy demand per 2017 TEU throughput for the Port of Los Angeles and extrapolated using statewide TEU throughput [294]. Since this analysis considers a futuristic scenario, annual trade growth is assumed to increase by 3.4% annually through 2050 [273]. Vessel size is also assumed to increase by 2.2% per year [295], up to an additional 9,500 TEU, to accommodate increased

trade, decreasing energy requirements per TEU. Additionally, a 17% fuel economy per transmitted good improvement is expected [296].

5.2.2 Ground Freight

The Freight Analysis Framework (FAF) is a platform that incorporates data from the Commodity Flow Survey (CFS) plus an extra category involving imports to create a comprehensive database of freight movements among different states in the US by all modes of transportation [297]. In this study, the FAF data is assumed to be representative of domestic region level freights in state of California (intrastate) as well as state level freights from/to California (interstate). This data allowed for total freight mass and ton-miles for trucks traveling through California to be predicted. Using this information, the average trip for intra and interstate truck trips is calculated, allowing for total vehicle miles travels to be calculated when considering total truck fleet size. Since prior studies have considered the partial electrification of the heavy-duty truck fleet, it is assumed that only the remainder would be converted from diesel to hydrogen. Hydrogen demand is predicted using efficiency-conversion. Note that inter and intrastate travel are predicted by assuming the ratio of inter and intrastate VMT still applies to the subset of trucks that are converted to hydrogen. This is critical since interstate travel requires refueling outside of California, necessitating the development of hydrogen infrastructure that expands beyond California.

The FAF also captures the cross section of rail industry trade characteristics [297]. Using FAF's 2017 commodity flow statistics and 2045 projections, average annual growth of goods shipped via rail and the percentage of ton-miles attributed to within the state versus out of state were both calculated. The intrastate ton-mile for rail is given by the sum of the intrastate ton-mile

total and the segment of out-of-state trips that are still within state boundaries. The same average distance from port to state boundary in the trucking scenario is also used here. It is assumed that only half of out of state travel fuel demand would be met using California hydrogen. Using this travel data and diesel and fuel cell-based engine efficiencies, total hydrogen demand is calculated.

5.3 Siting of Renewable Resources

5.3.1 Solar Siting

Solar potential direct normal irradiance maps were used to predict primary energy availability [298]. Assuming a 1% annual improvement on 1-D tracking solar PV panel performance [299] from 19.1% in 2017 [300], installed panel efficiency reaches 26.5% in 2050. The adoption rate of newer technologies is not readily available, so this 1% improvement is a conservative assumption given recent improvements. Offshore wind turbines operate with a power coefficient of 47%; Average electrolyzer and liquefaction efficiency of 74% [234] and 68% respectively were assumed to remain constant [301]. Alkaline electrolyzer learning rate of 18%, based upon predictions elaborated in the literature [302]

Solar sites were selected so that they are within five miles of existing electric and gas transmission infrastructure. Solar is limited to these areas due to an assumption that new electrical and gas infrastructure development would occur in parallel to already existing electrical and gas transmission corridors. Bulk hydrogen delivery occurs via pipeline [253]

The overall objective of the renewable power production siting analysis is to minimize the levelized cost of electricity by selecting sites with the greatest renewable resource potential while minimizing travel distance to existing natural gas infrastructure. Selection of solar and wind resources used different methods. For selection of solar – electrolysis facilities, the ArcGIS

location-allocation tool under the network analysis extension is used to select optimal solar farm sites such that hydrogen production per unit of land area is maximized. Data on solar direct normal irradiation [298] is processed to yield a geospatial grid of irradiance data across 4 km by 4 km grid points. This data is further processed by applying both solar and electrolyzer conversion efficiencies to provide a kg H_2 per day yield. From this 4 km solar data shapefile, two constraints were added to limit land use to feasible locations. First, select National Land Cover Database categories were chosen so that only land suitable for development is included. This included barren land, herbaceous grassland, hay pastures considered suitable for grazing, and developed open space [303]. Second, land use is limited to allow for electrolyzer development to occur within one mile of current natural gas pipelines, and to limit solar farm development to occur within 5 miles of an electrolyzer to limit the development of large solar – electrolyzer circuits. Sites were then selected based on allocating the most amount of hydrogen production to a chosen electrolyzer site. The selected electrolyzer sites were accompanied by a corresponding solar farm used to power the electrolyzer.

5.3.2 Offshore Wind

To select the location of the offshore wind farm, a spatial analysis of the total offshore wind resource energy potential in California is first conducted. ArcGIS is used to estimate the total ocean area available for the development of offshore wind farms on the coast of California. The total area is classified using a wind power class (WPC) dataset [304]. Only areas with a WPC greater than or equal to three were considered. This analysis did not include environmental or military exclusions. The Weibull probability distribution function is used to statistically analyze a range of average annual velocities given by the wind power class datasets. Rayleigh statistics were used to

express the wind speed probability distribution to capture the transient characteristics of wind velocities [305]. It is assumed that the foundation technology for floating wind turbines will be further developed by 2050 to allow installation and deployment of 25MW floating turbines in depths up to 1000 m. In this study, the total net offshore energy potential for 2050 is estimated to be between 5,780,000 and 7,780,000 GWh/yr. The location of the offshore wind farm is selected based on resource availability and proximity to the shore. Thus, based on the spatially resolved WPC data, a potential site for an offshore wind farm is selected near Humboldt, Mendocino, and Sonoma counties with WPC 6 and 7. Lastly, the total area of this wind farm site is selected so that enough hydrogen could be produced to meet the entirety of California's freight transportation demand. The proposed offshore wind scenario does not present the optimal deployment, but instead shows a scenario developed to maximize offshore wind output. Additional work is required to refine the design if offshore wind is to be implemented to produce renewable hydrogen.

Table 1 - Summary of annual average renewable resource potential equivalents and assumed hydrogen potential.

Annual solar direct normal irradiance (DNI) [kWh/m2/day]	H2 equivalent from annual solar DNI [kg/m2/year]	Offshore average wind speed range [m/s]	Annual H2 equivalent from wind speeds [kg/m2/year]
3.9-6.1	8.0-12.4	6.4-7.0	1.5-2.0
6.1-6.8	12.4-13.7	7.0-7.5	2.0-2.5
6.8-7.4	13.7-15.1	7.5-8.0	2.5-3.0
7.4-8.0	15.1-16.3	8.0-8.8	3.0-3.9
8.0-8.8	16.3-18.0	8.8-12.0	3.9-9.5

In developing a view of a future freight sector fueled by renewable electrolytic hydrogen, a key consideration is whether electrolyzers should be close to load or close to solar and wind

resources. In the former case, bulk energy transport must use electric transmission, and, in the latter, long-distance pipelines are needed. The present analysis assumes that pipelines are the dominant mode based on a high-level analysis of comparative cost [68], which makes several points reiterated here. First, the conversion losses of electrolyzers reduce the necessary energy transport if the energy is moved as hydrogen. Second, pipeline systems offer the collateral benefit of access to bulk geological storage which allows diurnal and up to seasonal storage opportunities. Third, the potential of repurposing existing natural gas infrastructure has the potential to enable lower costs than assumed here. For the economic analysis in this study, the LCOE endogenous to this study and presented below is used to power compressors and capital costs of transmission infrastructure is calculated as done in Thai [68]. By considering an average efficiency of 74% [234], 68% [60], 97% [41], and 95% [42] for producing, liquefying, transmitting, and storing hydrogen, respectively, the total pathway efficiency is roughly 46%.

5.4 Results

Figure 45 shows total annual hydrogen demand, renewable power plant capacity, and land area required for the four scenarios spanning economic growth and ship travel speed. These results indicate that, under base economic growth, between 9 and 10 million tons (Mt) of hydrogen per year is needed in 2050 to decarbonize all California heavy-duty transportation that cannot be electrified via battery electric drivetrain systems. Hydrogen demand grows to between 16.4 to 19.9 Mt under the high economic growth upper case. Ship hydrogen demand is between 2.4 Mt and 3.7 Mt for the base case depending upon fuel price, and 6.3 and 9.9 Mt for the high growth case. Ship demand makes up between 23% and 32% of total hydrogen demand in the low-cost base and high growth cases, respectively. Heavy-duty truck demand makes up 47% and 34%

of total demand in the low-cost base and high growth cases, respectively. Within heavy-duty truck demand, 44% of all hydrogen is used to meet interstate travel. Rail demand is 17% and 16% for low-cost base and high growth cases, respectively. Approximately 30% of all hydrogen for rail transportation is used to power interstate freight transport.

Figure 45 also provides projected land and sea area, and renewable power plant capacity required to meet the annual hydrogen demand under solar and offshore wind resource scenarios. These results are based on siting and sizing of renewable powerplants required to meet all hydrogen production, conditioning, and transportation energy demands, assuming that the applicable renewable resource is used to meet all energy needs to produce, condition (i.e., compress or liquefy), and deliver the required hydrogen.

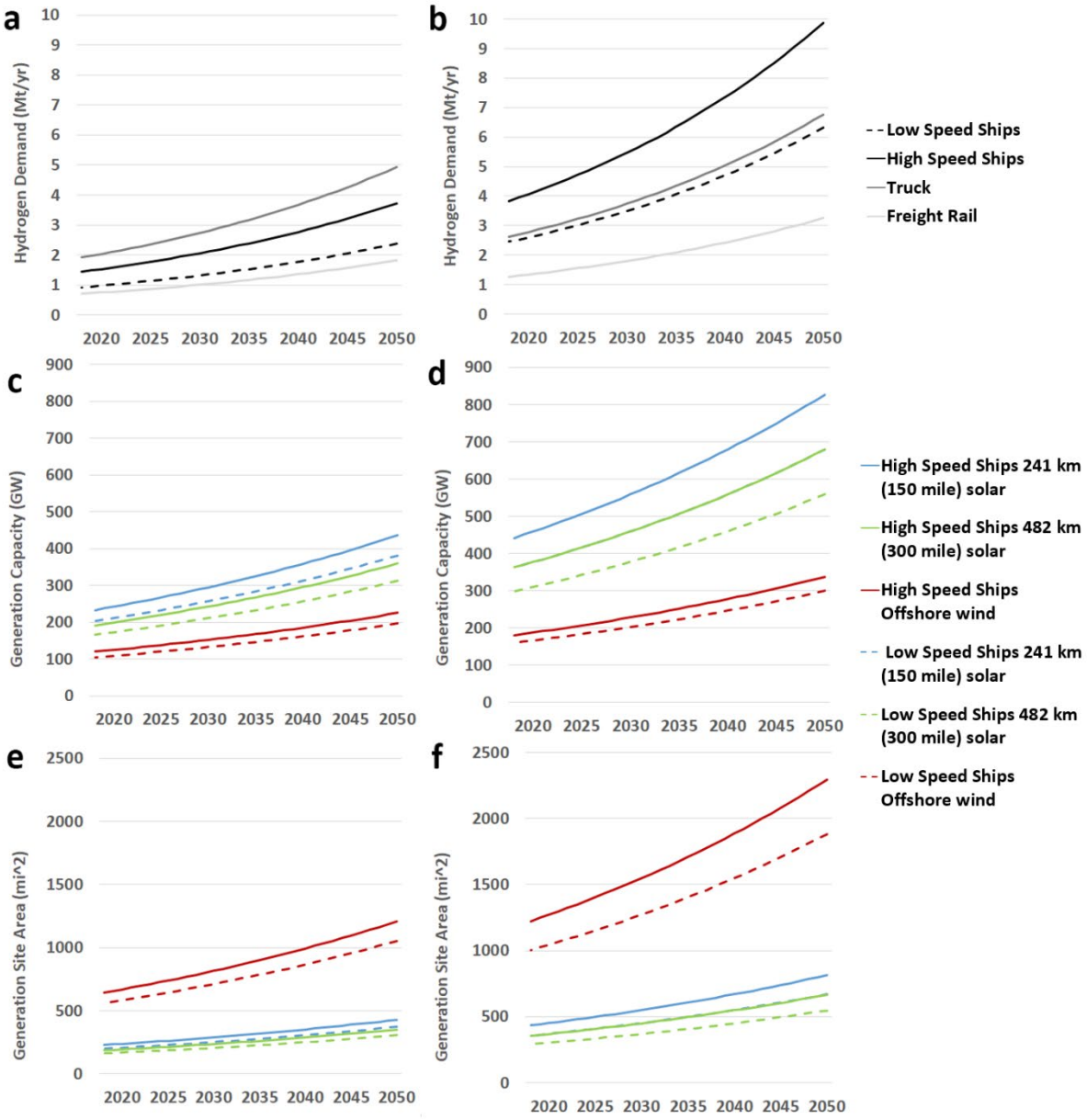

Figure 45 - Summary of annual hydrogen demand for the base growth case (a), high growth Case, renewable generation land use and capacity (b), renewable generation capacity for the base growth case (c), high growth case (d), and the renewable generation site area for the base growth case (e), high growth case (f).

Example results from the siting and sizing design are shown in Figure 46. Potential solar power plants are shown in Figure 46, subplot a) and b), and offshore wind power plants in subplot c). These results show siting and sizing of renewable power plants to produce sufficient hydrogen for the most demanding "high growth, high-speed ship" scenario. Solar resources were sited such

that capacity is minimized while being developed within five miles of existing gas pipeline infrastructure. This infrastructure is shown as blue lines in Figure 46. Siting results for the "high growth" scenario are similar to "base growth" in that siting occurs in and around the regions where solar potential is highest. Results are only shown for high-speed ship travel, but do not significantly change graphically under the low-speed scenario. The low-speed scenario requires more ships to meet the same demand as the high-speed scenario. However, these life cycle emissions are not accounted for in this work.

The two solar scenarios shown in Figure 46a and Figure 46b are selected to show the difference that solar siting, and, consequently, quality of solar resource, has on hydrogen production. These two scenarios show the different power plant capacities required for different regions in California. The first scenario constrains the construction of any new solar power plant to at least 241 km (150 miles) from the Los Angeles and San Francisco metropolitan areas, while the second scenario allows for development only within 241 km of these metropolitan areas. For both solar scenarios, multiple solar PV farms are selected with a range of sizes between 285 and 384 km^2, with an annual equivalent hydrogen production of between 4.9-6.2 Mt hydrogen per site per year. In the 241 km or less case, seven sites are required, totaling 2,112 km^2 of generation site area. Additional generalizations from Figure 46, subplots a) and b), can be made in relation to the effects of shifting solar production towards regions with lower solar potential. If solar power plants are developed to meet energy needs other than hydrogen production for heavy-duty transportation, the maps indicate extensive areas in and around the Mojave Desert with excellent solar resources. However additional supporting infrastructure to transmit electricity from the generation site to an electrolyzer near a pipeline, or to develop new hydrogen pipelines distant

from current pipelines, will increase cost. Additionally, shifting solar power plant development towards areas with lower insolation will also increase the required plant size due to reduced energy output. Locations and approximate area of these solar installations are also shown in Figure 46 subplot a). The inset boxes provide enlarged views of the areas of highest hydrogen production.

In the offshore wind hydrogen production scenario, a representative wind farm is designed in Northern California as a site that could produce enough hydrogen to meet the entirety of California's freight transportation demand. Figure 46c shows both spatially resolved wind resources and the location of the offshore wind farm. The offshore wind farm outlined here can produce between 19 and 32 Mt H_2 per year and requires 5939 km^2 of ocean area. The maximum distance from the shore is about 27.4 km, and onshore electrolyzer sites feed pipelines to deliver hydrogen for rail and truck demand for the San Pedro ports. Because ships make up 34% (25% in the low-speed scenario) of the demand, it is assumed they are able to fuel at the point of production, resulting in a reduction of necessary transmission capacity compared to the solar cases. However, this reduction in transmission capacity is offset by an increased transmission distance to fulfill the San Pedro port demand and a predicted higher levelized cost of wind electricity compared to the solar case, as demonstrated in the following paragraph. The total length of pipelines in the wind scenario is 15,200 km.

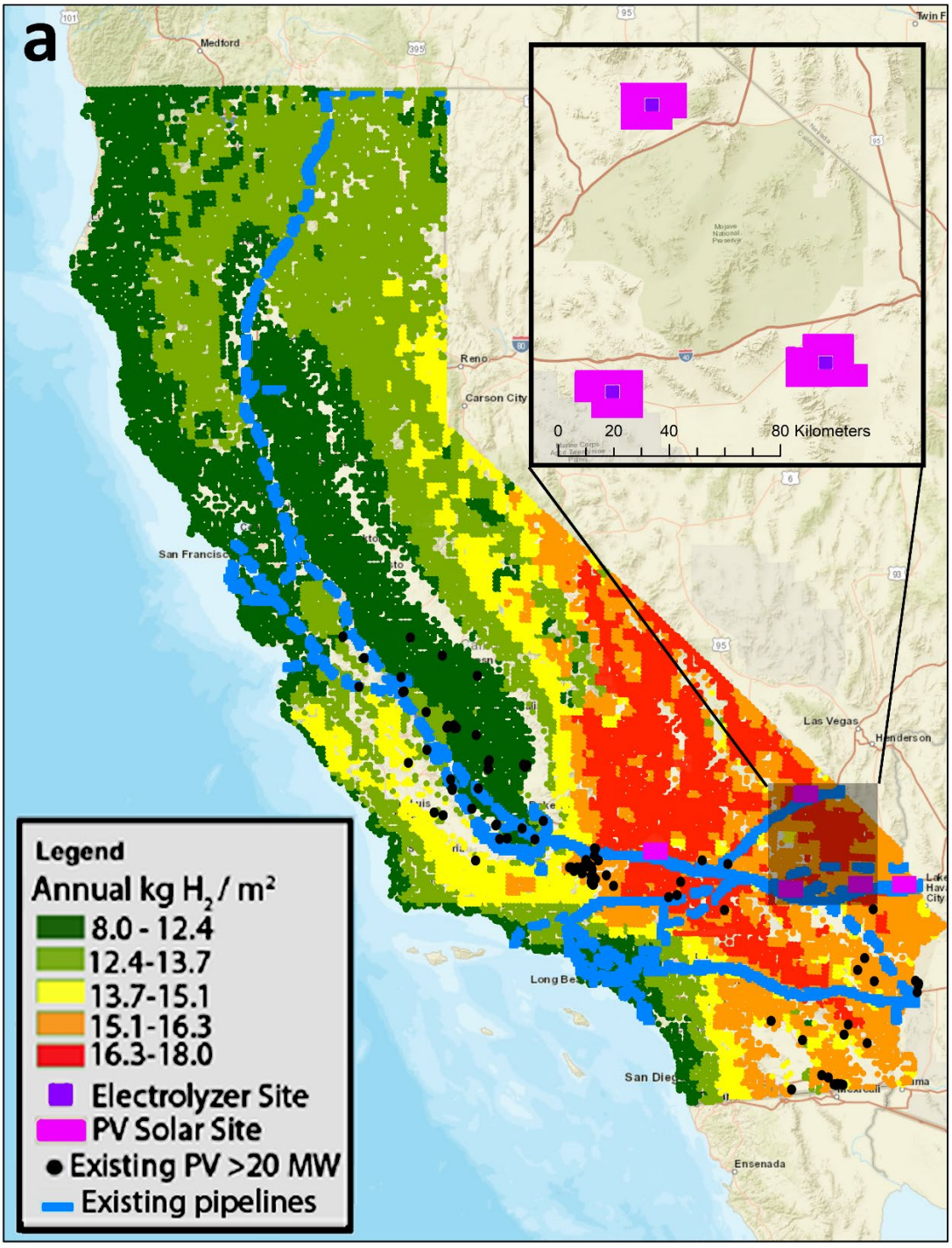
a
Medford
Reno
Carson City
San Francisco
Las Vegas
Henderson
Long Be
San Dieg
Ensenada
0 20 40 80 Kilometers
Legend
Annual kg H2 / m²
8.0 - 12.4
12.4-13.7
13.7-15.1
15.1-16.3
16.3-18.0
Electrolyzer Site
PV Solar Site
Existing PV >20 MW
Existing pipelines

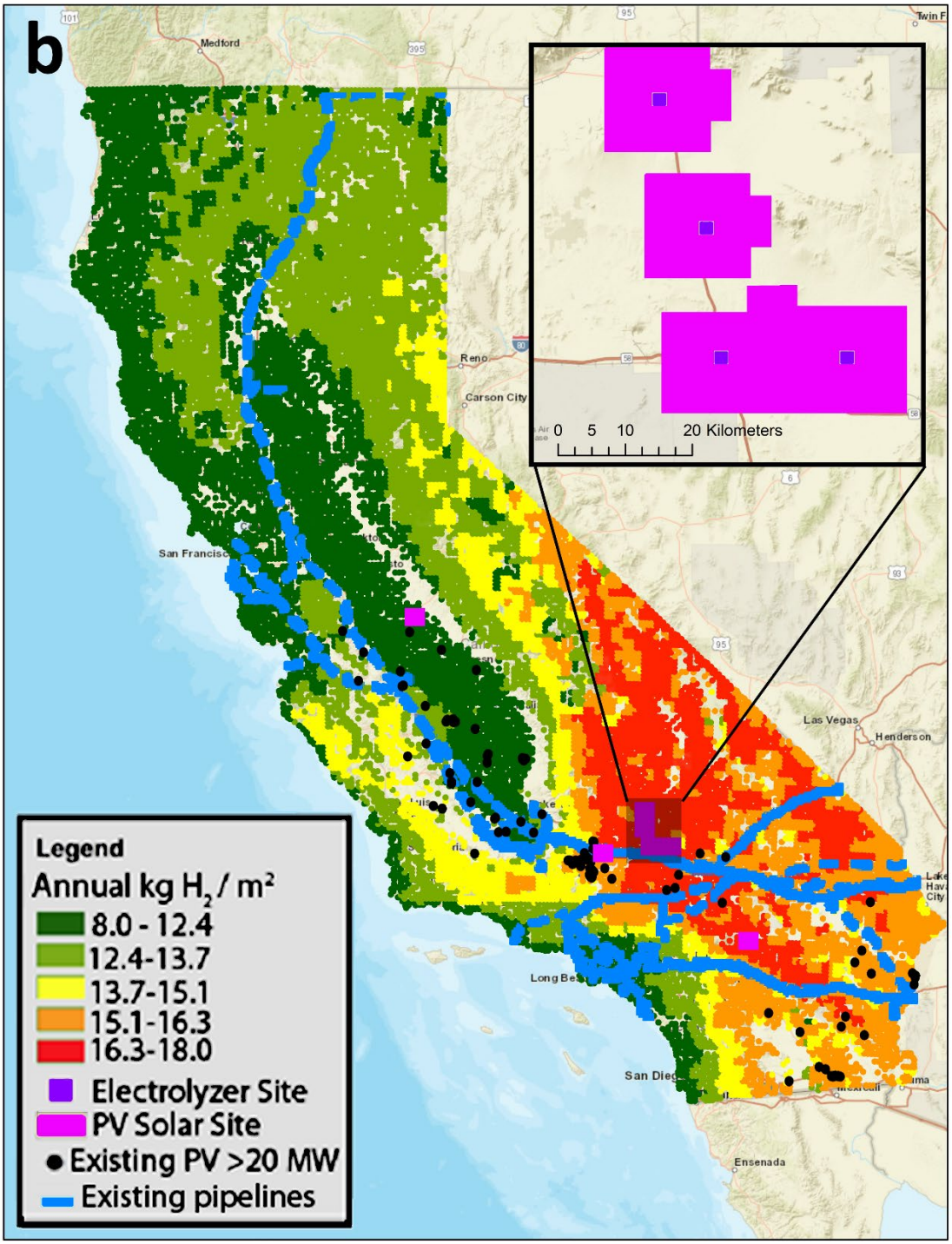
b
Medford
Reno
Carson City
San Francisco
Las Vegas
Henderson
Long Beach
San Diego
Ensenada
0 5 10 20 Kilometers
Legend
Annual kg H2 / m2
8.0 - 12.4
12.4-13.7
13.7-15.1
15.1-16.3
16.3-18.0
Electrolyzer Site
PV Solar Site
Existing PV >20 MW
Existing pipelines

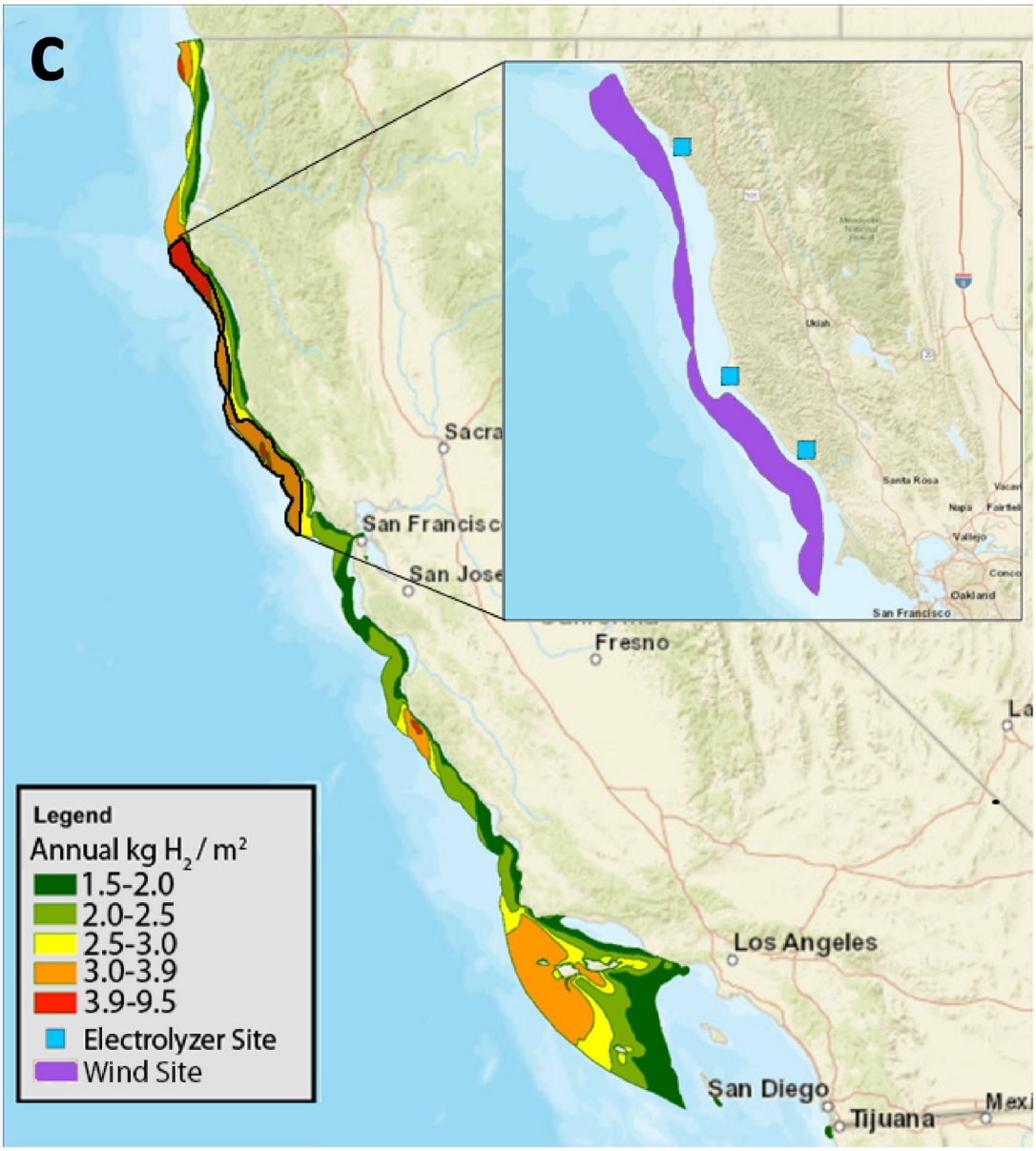

Figure 46 - Selected electrolyzer sites to meet the 20 million ton port demand with technical potential background gradient for 150 mile solar-dominant scenario (a) and 300 mile solar-dominant scenario (b) and offshore wind dominant scenario (c).

To resolve the differences between hydrogen demand dynamics and those associated with producing, delivering, and administering renewable hydrogen to the disparate freight applications, hydrogen storage infrastructure is required. By 2050, the average daily fueling volume for the high growth case results in roughly 55 kt H_2 per day. If one considers the capacity of an existing commercial liquid hydrogen storage tank (20m in diameter), which is 335 tons (1.25 million gallons at -235°C), roughly 164 tanks are needed to store the per diem demand for all three transportation modes. Although this is a relatively large number, the relatively small area of existing liquid fuel storage tanks at the Port of Long Beach alone is sufficient to accommodate more than 120 of the necessary hydrogen tanks (see Figure 47). This work does not resolve storage requirements for the proposed system. However, a transition towards renewable hydrogen to power heavy-duty transportation could use and supplant current fuel storage equipment and facilities located in and around the port, potentially providing sufficient buffer to manage and match freight demand and renewable production and delivery dynamics.

Figure 47 - Example of existing liquid fuel storage area filled with commercially available liquid hydrogen storage tanks.

5.5 Chapter Summary and Conclusions

Several important caveats and limitations apply to these findings. Development of new and emerging hydrogen fuel cell-based powertrains is necessary to fully electrify all heavy-duty modes of transportation addressed in this work. Regardless, there are no fundamental technical barriers to such development. This analysis is focused on California, which—although it is a major and trade-intensive economy—cannot implement a full-scale transition of international and interstate

trade to hydrogen without other jurisdictions. Similar hydrogen production and fueling infrastructure will need to be deployed at vehicle destinations outside of California. Lastly, this assessment here does not capture all the benefits of a transition to hydrogen for freight transport, such as improvements to regional air quality. Communities nearby California's transportation routes and hubs (such as major ports) suffer degraded air quality as a result of the emissions from on-road and off-road diesel equipment including heavy-duty diesel trucks, cargo and materials handling equipment, ships, and rail [306]. Although not quantified here, reductions in air pollution related to the analyzed transition to hydrogen-powered freight may therefore be quite substantial. Indeed, a prior study found that the health benefits of converting three-quarters of heavy-duty trucks, ocean-going vessels, and harbor craft auxiliary engines to hydrogen at the San Pedro ports and throughout the densely populated southern California region were as great as *$7 million per day* during modeled air quality episodes [307]. The complete conversion to hydrogen-based freight systems might thus be expected to achieve even larger benefits to air quality and human health [307].

Regardless of these caveats, this analysis demonstrates that the large-scale conversion of long-distance and heavy-duty freight systems to hydrogen is achievable. Whether or not such a transition can occur over the next 30 years is largely a matter of policy. Given the net-zero emissions goals of California and a growing number of other states and countries, it is vital to identify options such as renewable hydrogen for decarbonizing and depolluting freight transportation services that are difficult or impossible to electrify with conventional batteries and without depending upon limited and sensitive bioenergy resources.

6 Distributed Electrolyzers Case Study: California

6.1 Motivation

Several studies evaluate the capacity potential and effects from distributed electrolyzers. Reed et al. [176] considers feasible sites via proximity to gas pipelines and electric pipelines but uses population density layers to avoid siting electrolyzers in metropolitan areas. However, while this previous study is generous in siting distributed electrolyzers, Rose and Neumann [120] site electrolyzers only at existing gas stations and evaluate the impact on the electric grid. In this work, electrolyzers are sited by considering parcel-level data to capture eligibility based on industrial designated land-use. Siting electrolyzers in a distributed setting can have the benefit of injecting closer to the load and circumventing any associated risks on critical infrastructure (i.e., transmission pipelines). Additionally, differences in handling identifying electrolyzer sites injecting into high-pressure distribution as opposed to transmission are identified and discussed in this work. While there is no universal agreement for the definition of transmission vs high-pressure distribution gas pipelines, this work generally refers to high-pressure distribution as being up to 200 psig, whereas anything higher is categorized as transmission.

6.2 Approach

6.2.1 Data Sources

Candidate distributed electrolyzers locations are scoped by considering proximity to electric infrastructure, gas pipelines, and land-use data. The electric line dataset is maintained by California Governor's Office of Emergency Services Public Data Hub [308]. It is a comprehensive data set containing subtransmission electric lines in California ranging from 33 kV to 500 kV. Gas

pipeline data is obtained by digitalizing screenshots of Southern California Gas Company's (SCG) and SDG&E online interactive transmission and high-pressure distribution map, defined as greater than 60 psig. PG&E transmission and high-pressure distribution pipelines are provided. Land-use data sets are a little more challenging to obtain as there is no central database. Six counties in Southern California are represented by Southern California Association of Governments dataset [309]. The remainder are available online or by request per metropolitan planning organizations (MPO). Generally, these datasets are provided "as-is" without guarantee for accuracy. Omitted counties are primarily smaller by population or excluded due high gradient terrain [310]. The counties included within this study make up 88% of the California population [311]. The data provided by the MPOs, and their corresponding jurisdictions, are provided in Table 2.

Table 2 – Metropolitan planning organization land-use data available

County	Metropolitan Planning Organization
Alameda, Contra Costa, Napa, San Francisco, San Mateo, Santa Clara, Solano, Sonoma	Metropolitan Transportation Commission
Butte	Butte County Association of Governments
Fresno	Fresno Council of Governments
Imperial, Los Angeles, Orange, Riverside, San Bernardino, Ventura	Southern California Association of Governments
Kern	Kern Council of Governments
Kings	Kings County Association of Governments
Madera	Madera County Transportation Commission
Mariposa	Merced County Association of Governments
Merced	Merced County Association of Governments
Monterey	Association of Monterey Bay Governments
Sacramento	Sacramento Area Council of Governments
San Diego	San Diego Association of Governments
San Joaquin	San Joaquin Council of Governments
San Luis Obispo	San Luis Obispo Council of Governments
Santa Barbara	Santa Barbara County Association of Governments
Shasta	Shasta County Regional Transportation Planning Agency
Stanislaus	Stanislaus Council of Governments
Tulare	Tulare County Association of Governments

6.2.2 Data Processing

A 0.1-mi buffer polygon on both sides (i.e., 0.2-mi wide) is created around electric lines and high-pressure distribution pipelines. This buffer represents the maximum length for which an eligible industrial-designated parcel would build a connection to either utility. Though this distance is subject to be on a per project basis due to associated costs, 0.1-mile represents the adjacent most parcels to major utility pathways. Increasing this distance would increase the eligibility of contiguous parcels and would require coordination to avoid violating pipeline injection constraints. For transmission pipelines, the buffer polygon is 0.5-mi (i.e., 1-mi wide), which

primarily acts as a proxy for indicating upstream flow of high-pressure distribution lines. Compressor stations appear on digitalized maps as high-pressure distribution pipelines and appear as points along transmission pipelines. This results in them often being selected as an electrolyzer site but are removed to focus on distributed electrolyzer systems injecting into high-pressure distribution pipelines. This is achieved in the model by dictating a minimum pipeline length of 0.005 mi prior to creating buffer polygons and is done to maintain the logic of utilities injecting hydrogen without risking degradation on critical backbone transmission pipelines.

The intersection of utility buffers with any portion of the industrially zoned parcels identifies those parcels as eligible. To consolidate differences in planning agencies' industrial subcategorizations, no distinction is made beyond industrial use in the selection of sites. However, agricultural-oriented subcategorizations are considered later for electrolyzer systems injecting into the transmission pipelines. A sample visual depiction of these buffer polygons and industrial-zoned parcels for Orange County is provided below seen in Figure 48.

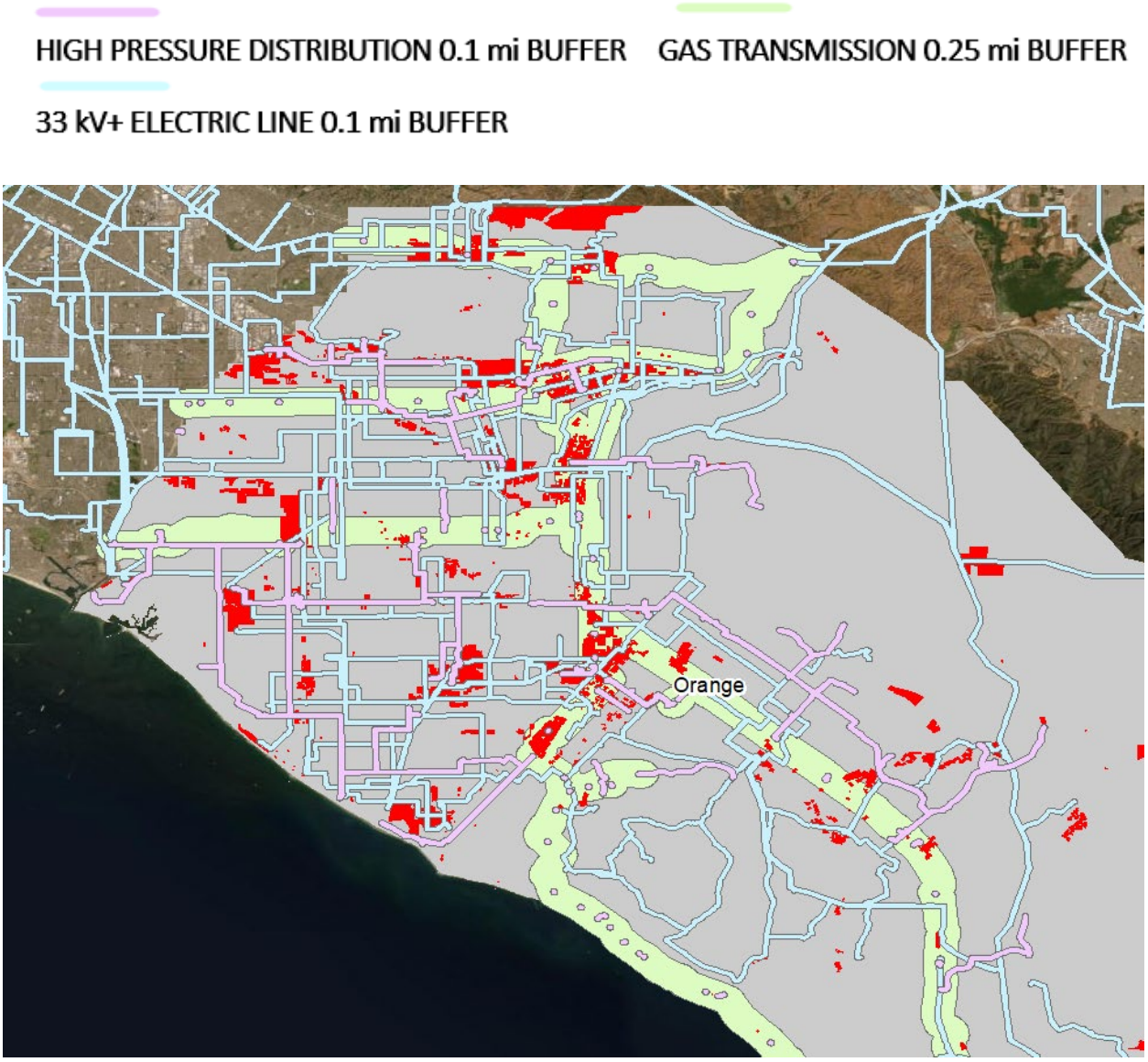

Figure 48 – Electric line (blue), high-pressure gas distribution (blue), transmission gas pipeline (pink) buffer polygons, and industrial zoned areas (red) in Orange County, California.

Selected parcels are then combined into selected areas if contiguous. Selected areas that are not contiguous but would inject into the high-pressure distribution line within 0.25 mi of each other are systematically removed by only considering the largest selected area to account for redundant systems potentially violating pipeline hydrogen mixing constraints. Using a representative high-pressure pipeline average flow of 6-25 mmscfd, provided by gas system

operators, and a 20% volume hydrogen injection limit, the corresponding electrolyzer size is estimated to be roughly 10-45 MW. Using existing commercial electrolyzer systems, an estimation of 34 MW/acre is assumed. A minimum area of 0.05 acres is used corresponding with a 2 MW electrolyzer system and any area greater than 1.3 acre is capped at a maximum of 45 MW due to hydrogen blend limits.

6.2.3 Development Potential

While many sites are identified as eligible with respect to proximity to utilities and properly zoned, the development of electrolyzer systems at these sites will vary on a case-by-case basis. Many factors, such as the cooperation and opportunity cost of existing landowners can impact the likelihood of development. To garner some insight of the development potential of the eligible areas are, three sets of ten sites are sampled to investigate the developability of the selected sites. Sites are categorized as low, medium, and high, corresponding to an arbitrary 20%, 50%, and 80% chance, respectively, of being able to host an electrolyzer system. High development sites are characteristically large undeveloped parcels, typically used for agriculture as seen in Figure 49a. Medium development sites have a mixture of undeveloped and developed areas (see Figure 49b), characteristically used for raw material industrial purposes. Finally, low development sites are generally well-developed areas and are typically relatively new office spaces (see Figure 49c).

a)

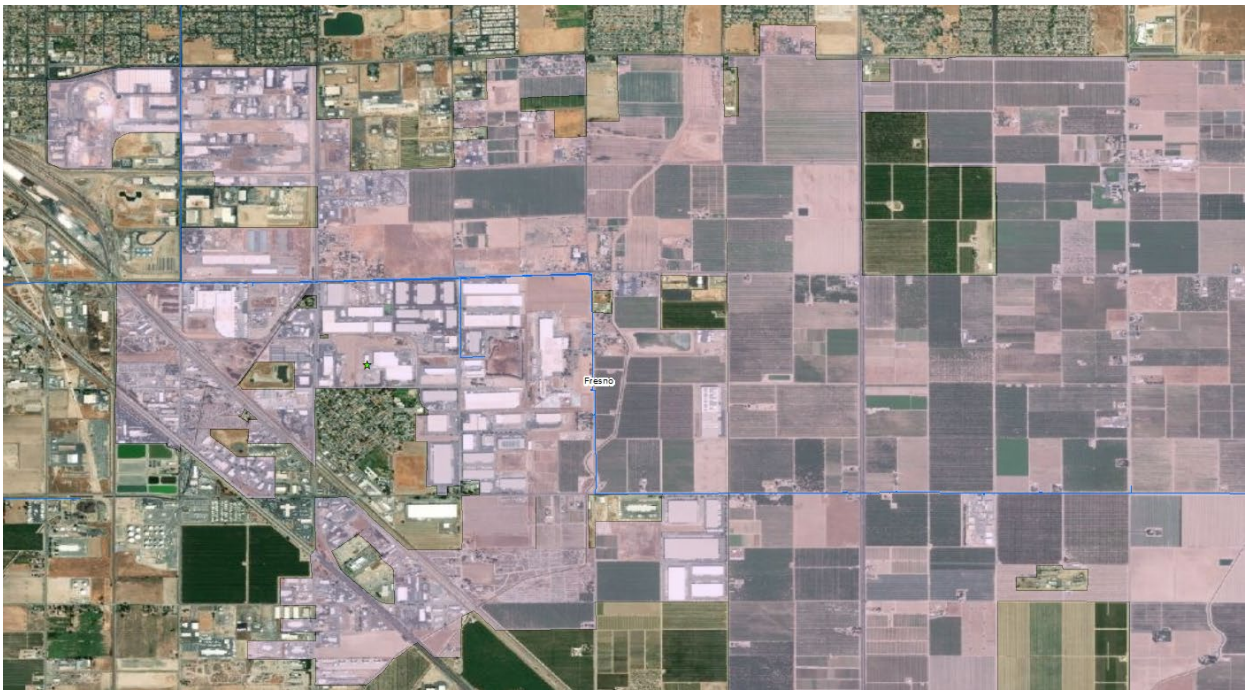

b)

c)

Figure 49 – Snapshots of eligible areas for electrolyzer system representative of a) high development potential, b) medium development potential, and c) low development potential.

6.2.4 Transmission Electrolyzers

Any site that is capable of injecting hydrogen into the high-pressure distribution system would likely also be able to inject into the transmission system. However, if the goal is to maximize the amount of hydrogen blending on the system, it would be logical to inject much more upstream of the load and supplement injection with the spread out distributed electrolyzer systems. This also allows for the opportunity for electrolyzers to be purposefully co-located with large PV power plants. To identify transmission electrolyzer sites, the approach remains the same as in the high-pressure distribution with some slight adaptations. The proximity to high-pressure distribution pipelines is relaxed and instead of using industrially-zoned land parcels, a set of specifically large undeveloped areas is considered consisting of: 1) previously identified agricultural-use parcels, 2) previously omitted areas due to lower populations but now included by evaluating zip codes with similar population densities with that of agricultural-use parcels [311], and 3) areas of critical

environmental concern (ACEC) as designated by the Bureau of Land Management (BLM). The ACEC dataset is included as it is federally owned land and would not have been captured by the datasets provided by the MPOs. With enough planning and care, the development of renewable energy projects may be possible in these ACEC. These sets of large areas overlayed with the electric transmission grid and PG&E transmission pipelines can be seen in Figure 50 below.

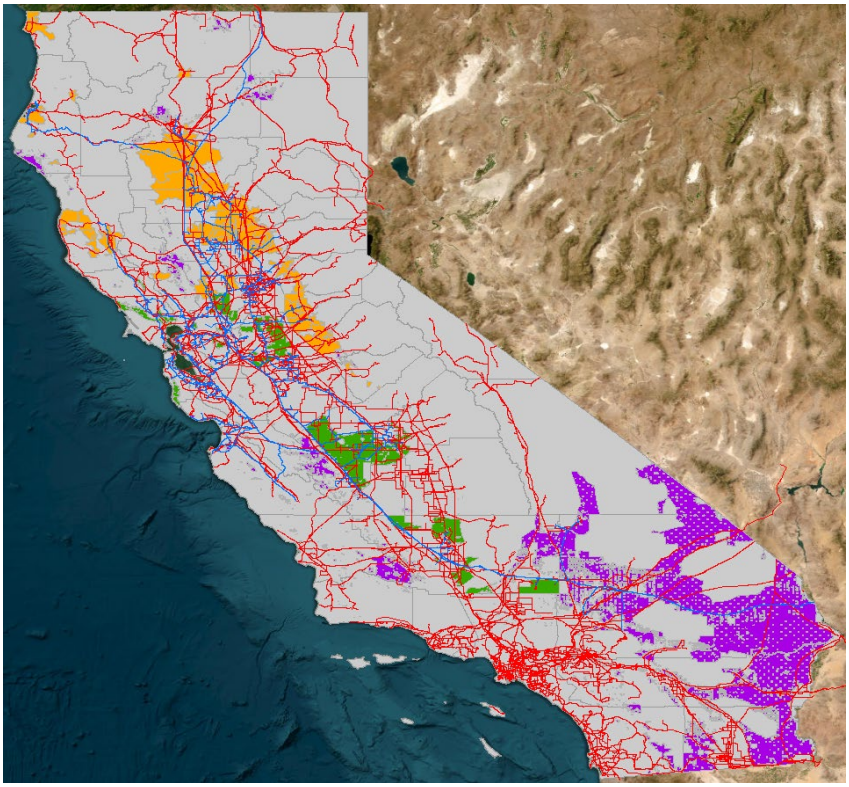

Figure 50 – Electric transmission grid (red), PG&E transmission pipeline (blue) overlayed with federal-owned land (purple), agricultural-use land (green), and similar population density areas (orange).

Using a representative transmission pipeline average flow of 25-250 mmscfd, provided by gas system operators, and 20% volume hydrogen injection limit, the corresponding electrolyzer size is estimated to be roughly 45-450 MW. With the inclusion of co-locating solar PV, the land requirements would be much higher than that previously considered for high-pressure distribution electrolyzers. According to an NREL report [312], [313], the overwhelming dominant

fixed-axis and one-axis tracking PV power plants larger than 20 MW average out to using 3.7 and 3.3 acres/GWh/yr, respectively. Assuming new solar power plants are one-axis tracking, co-located with electrolyzer with a 1:1 capacity ratio, the largest individual solar project would be 450 MW requiring 3900 acres of land, or roughly 16 km^2. As such, the large set of undeveloped land area is discretized into 4x4 km squares.

This approach generates many input parcels for screening relative to the high-pressure distribution set, with the distribution pipeline proximity constraint lifted and the land set being much more abundant in size. The total amount of solar and electrolyzer capacity sited to inject into the transmission pipelines is dependent upon the natural gas throughput imported from out-of-state. Historical annual totals and projections for the state can be found in the collaborative state gas report [314]. Imported natural gas comes from the Rocky Mountains region and Canada, both entering the state from the north. The remainder enters the state in the Southeastern region of California from the other American Southwestern states. Using the figures available in the state gas report [314] and the PG&E 970 Bcf/yr throughput, it can be estimated roughly two-thirds of gas is imported to the PG&E service territory from the north and the remainder from the southeast. Assuming an average solar capacity factor of 30% in the southern half of the state and 25% in the northern half of the state the resulting corresponding amounts of electrolyzer capacity to saturate the blending limit of hydrogen on the PG&E transmission system results in roughly 6.4 GW and 2.3 GW for the imports from the north and southeast delivery points, respectively.

After eligible parcels are identified, via proximity to utilities, sites further screened by prioritizing solar resources until hydrogen blending limits are satisfied. Other major gas operators with service territories in the southern half of the state also import from the American Southwest

and would likely have similar results obtained for the southern sites injecting into the PG&E system. However, sites prioritizing solar resource availability in the northern half of the state actively works against the constraint of maximizing hydrogen injection on the gas grid and is a challenge unique to the PG&E system. To resolve this challenge, electrolyzers are sited periodically prior to major branching in the transmission system and prior to metropolitan load centers. Only sites injecting in the PG&E transmission system are considered to investigate the nuance of this challenge. Sites identified in this work represent a general trend and the development of such sites to accommodate electrolyzer systems require additional due diligence on a site-by-site basis.

6.3 Results

6.3.1 High-Pressure Distribution Electrolyzers

The total number of high-pressure distribution electrolyzer sites found is 190 (seen in Figure 51a), 143 (seen in Figure 51b), and 14 (seen in Figure 51c) for the PG&E, SCG, and SDGE systems, respectively.

a)

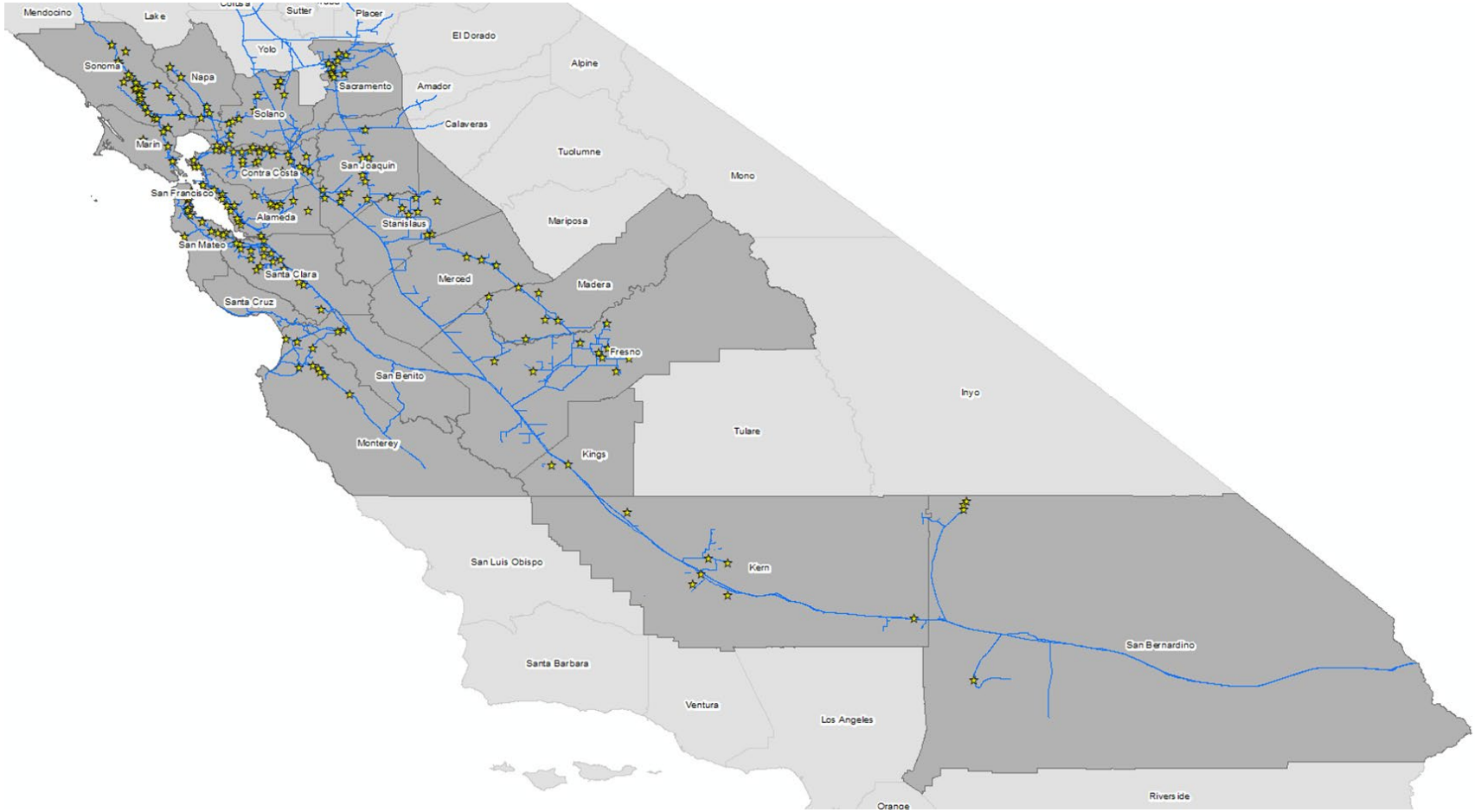
Mendocino
Lake
Sutter
Placer
El Dorado
Yolo
Sonoma
Napa
Sacramento
Amador
Alpine
Solano
Calaveras
Marin
Tuolumne
Contra Costa
San Joaquin
Mono
San Francisco
Alameda
Stanislaus
Mariposa
San Mateo
Santa Clara
Merced
Madera
Santa Cruz
Fresno
San Benito
Inyo
Tulare
Monterey
Kings
San Luis Obispo
Kern
San Bernardino
Santa Barbara
Ventura
Los Angeles
Orange
Riverside

b)

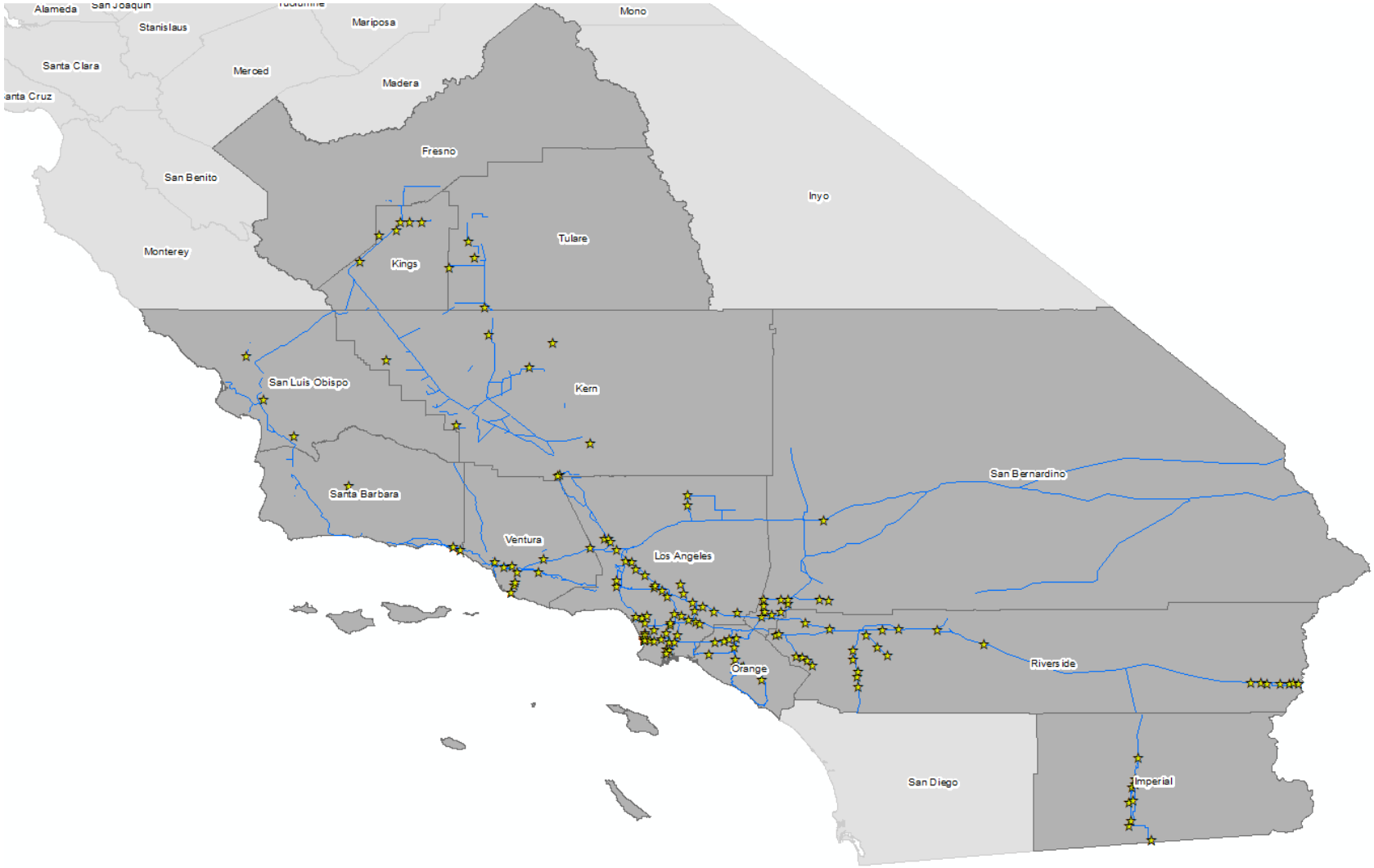
Alameda
San Joaquin
Stanislaus
Mariposa
Mono
Santa Clara
Merced
Madera
Santa Cruz
Fresno
San Benito
Inyo
Monterey
Tulare
Kings
San Luis Obispo
Kern
San Bernardino
Santa Barbara
Ventura
Los Angeles
Orange
Riverside
San Diego
Imperial

c)

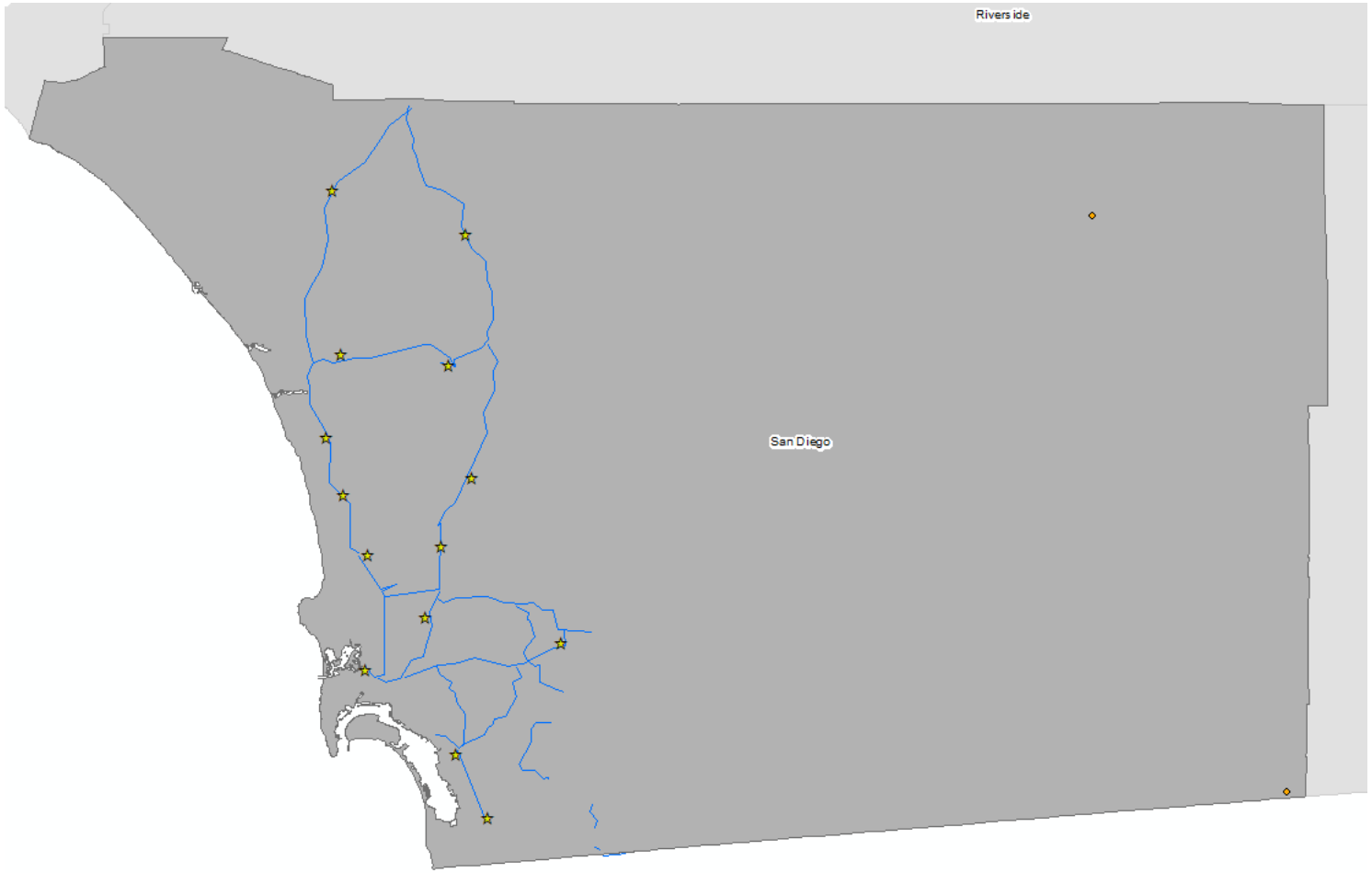

Figure 51 – Eligible high-pressure distribution injection electrolyzer sites for the a) PG&E system, b) SCG system, and c) SDG&E system.

Assuming, the electrolyzer sites are not co-located with PV power plant, either transmission or new large rooftop PV systems are necessary. Figure 52 displays the relation between the 347 sites' size and their distance to the nearest solar power plant greater than 10 MW. Due to the large range in parcel sizes, attributed to agricultural-use, the area axis is provided on a logarithmic scale. 12%, 23%, and 44% of the sites are within 5 miles, 10 miles, and 20 miles, respectively of a 10 MW or greater solar power plant. The closer the sites, the greater the indication that these electrolyzer sites are in regions of high solar insolation and may be prime locations to co-locate additional solar capacity if rooftop or land PV developments are available.

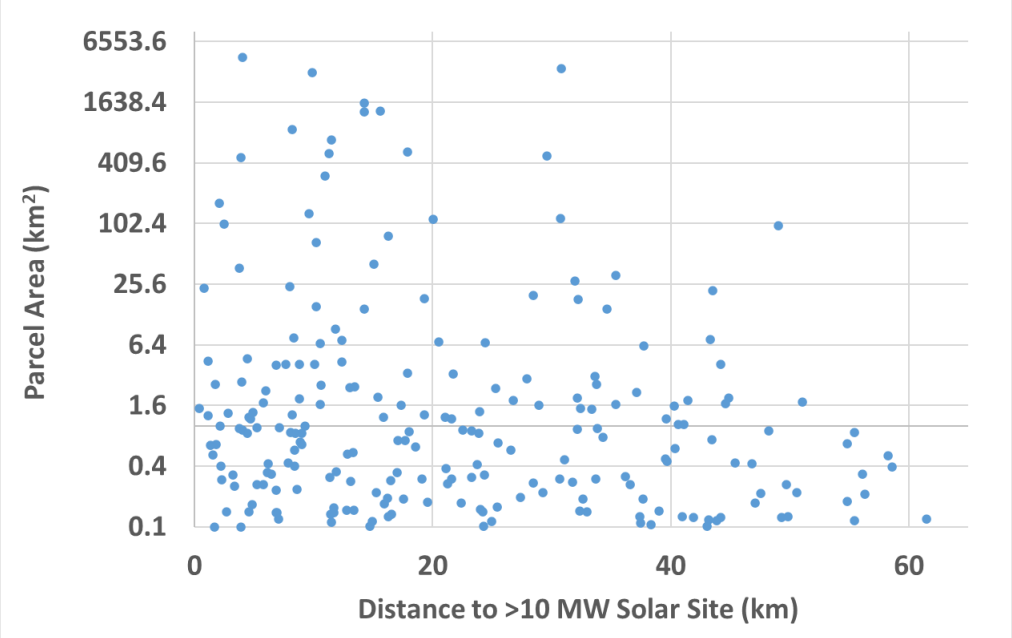

Figure 52 – Selected areas parcel sizes versus their distance to the closest PV solar power plant greater than 10 MW.

Across the 347 sites, an estimated 3.1 GW of electrolyzer capacity is available. While development will occur on a case-by-case basis, an estimate on the probability of development is conducted by randomly sampling sets of ten sites. The distribution between low, medium, and high development potential and consequently the weighted-average probability of development

is provided in Table 3. The percentages of resulting sites for agricultural use, which typically have high development potential, are 25%, 22%, and 0%, for PG&E, SCG, and SD&GE, respectively.

Table 3 – Sample development potential

	Low (20%)	Medium (50%)	High (80%)	Average
Set 1	2	3	5	59%
Set 2	2	1	7	65%
Set 3	3	3	4	53%

Assuming the weighted-average development probability leans toward the medium to high potential, the 3.1 GW of electrolyzer capacity may be closer 1.6 to 2.0 GW when accounting for potential land development constraints. Regarding the 190 PG&E sites, private communication with PG&E has revealed that the number of transmission to high-pressure distribution points is roughly 2000. This suggests that even in the most optimal case, only 10% of high-pressure distribution pipelines would achieve their hydrogen blend limits via distributed electrolyzers. This percentage would be even lower assuming development constraints and solidifies the requirement of injecting at the transmission level to increase the renewable contents of the gas grid via hydrogen injection.

6.3.2 Transmission Electrolyzers

By hydrogen production and injection volume, one-third is in the southern half of the state cluttered in the highest solar resource area. The remaining two-thirds would also be sited in roughly the same area if there were not any additional constraints to capture the injection of hydrogen into the gas grid. This poses a challenge as an arbitrary line of latitude must be drawn to force promoting hydrogen injection upstream. In fact, the solar potential is inversely related to the distance from the delivery point in the north from out-of-state. However, the further north electrolyzers are sited, one of two developments would need to occur: 1) lower solar PV-capacity

power plants must be sited in the northern half of the state, co-located with these electrolyzer sites or 2) additional transmission capacity would need to be built to transmit lower cost renewable electricity. Ultimately, despite the lower capacity factor in the northern half of the state relative to in the southern half of the state, other states in the country have economically deployed PV systems with even lower capacity factors.

This is not as significant of a challenge for the PG&E system injecting into the gas transmission pipeline importing from the southeast, as majority of their system load is still downstream of the selected sites. Figure 53 illustrates the eligible sites as red squares and the selected sites to satisfy the injecting blend limits as star icons.

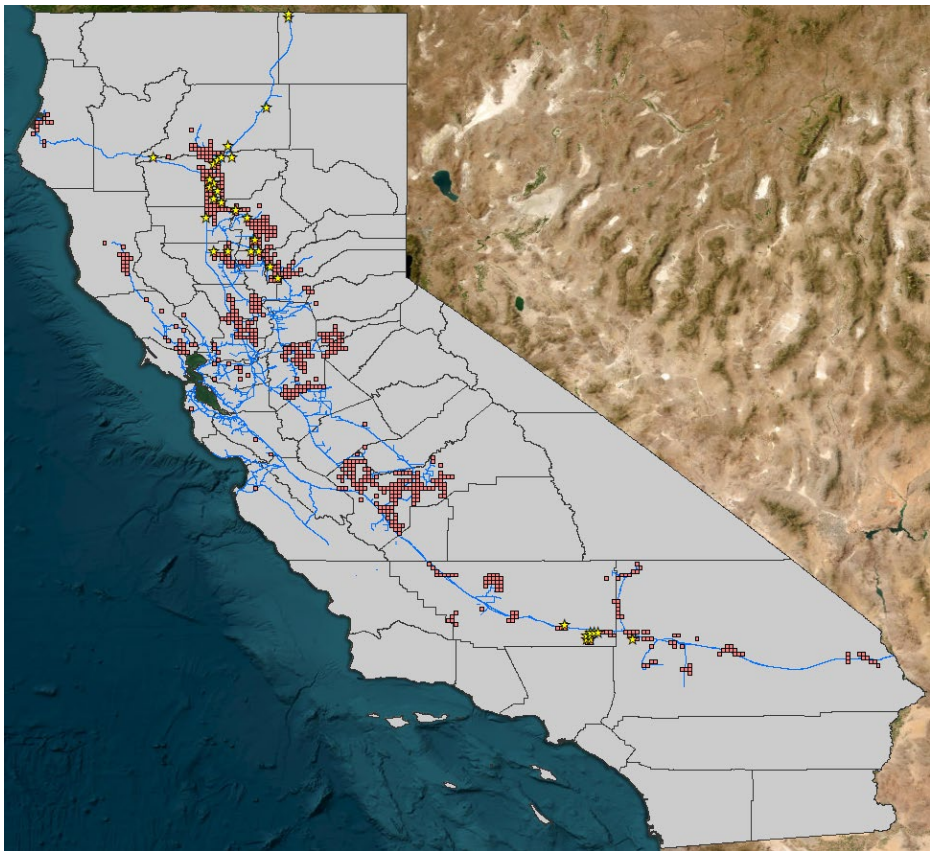

Figure 53 – Eligible transmission injection electrolyzer sites (red squares) and selected sites to maximize hydrogen injection on the transmission system (stars).

While 33 kV is the minimum voltage level required for both high-pressure distribution and transmission electrolyzer sites, the larger electrolyzers injecting into the transmission system would certainly require much higher electric transmission capacity if the co-located solar PV power plants were used for the dual purpose of hydrogen injection and general power production and usage for the state. If the site is used exclusively for the purpose of hydrogen production with co-located solar (e.g., the north sites for maximizing gas system hydrogen content), then the supporting electric transmission capacity is only supplementary. Table 4 tabulates the voltage level of the closest transmission line to the identified transmission electrolyzer site, which in part provided eligibility for the site. Most of the selected transmission electrolyzer sites are on the

lower levels of the transmission voltage level range, requiring larger fractions of their transmission capacity to bring electricity to the electrolyzer system. Further investigation is required to determine whether increasing transmission capacity or co-locating solar PV power plants would be the most cost-effective on a case-by-case basis.

Table 4 – Electrolyzer transmission injection site electric transmission voltage level from nearby infrastructure.

Voltage Level (kV)	Transmission Sites	Distributed Sites
33	0	1
60	15	57
115	11	105
230	5	24
500	3	3

6.4 Chapter Summary and Conclusions

Electrolyzers injecting into the high-pressure distribution gas system to avoid risking degradation or other hydrogen integration issues is limited to roughly 2 GW capacity based on proximity to utilities and land-usage designations. In addition, this would likely leave many high-pressure distribution lines with untapped potential to injection as well. The development of distributed electrolyzers would likely depend upon the development possibility of distributed PV sites as only areas with undeveloped land or currently used for agricultural purposes may be able to supplement up to a 45 MW electrolyzer. Further, while many locations are identified, the actual development of electrolyzers injecting into the high-pressure distribution pipelines would depend on the actual typical gas flow rather the representative values used in this work. Electrolyzers injecting into the transmission gas system remains the most favorable toward maximizing hydrogen injection as available undeveloped land area is a much less constraining. Large area

availability enables the co-location of electrolyzers and PV, regardless of suboptimal solar capacity factors. Co-located PV and electrolyzers would require limited local electric transmission capacity as all the electricity for hydrogen production may be procured on-site. This is one possible strategy to approach the 20% volume hydrogen blend limit on the gas system, supplemented by downstream electrolyzers injecting on the high-pressure distribution mains.

7 State Perspective Case Study: California Independent System Operator

7.1 Approach

7.1.1 Optimization model

Energy Exemplar's PLEXOS production model built in the Microsoft .NET framework with SCIP as the solver is used to resolve the unit commitment economic dispatch problem. The scope of this work is a multi-nodal annual simulation representing California's power grid in 2050. The spatial resolution is established by furthering the discretization established in a California Independent System Operator (CAISO) 2020 [315] study modeling year 2026 and 2030 which evaluates the reliability of a low carbon emission resource plan portfolio. The existing list of generators, including scheduled retirements, up to 2030 act as a starting point for estimating 2050 capacities. The high electrification scenario in the 2021 SB Joint Agency Report is referred to estimate the necessary amount of capacity additions up to 2045. Then, renewable capacity unique to this work is added to accommodate meeting renewable hydrogen demand via electrolysis. The electric load modeled is a 2035 hourly portfolio projection [316] scaled to meet a 2050 annual projection total of 449 TWh [317]. Two scenarios deploy 21 GW of offshore wind capacity. Each of those two scenarios are then split by representing a low and high level of hydrogen demand each to evaluate the synergistic effects of co-optimizing power generation from varying renewable hydrogen fuel production. In short, a year-long hourly optimized dispatch problem is solved for four different scenarios under the presupposed generation portfolios.

7.1.2 Energy system integration strategy

Due to the magnitude of the formulation, one tradeoff taken is inputting system characteristics that are fixed (e.g., transmission line loading limits, gas generator heat rates) to focus on fuel commitment dynamics throughout the year as opposed to identifying optimal rollout of new system capacity. Gas nodes are co-located with electric nodes, connected by hydrogen pipelines modeled without capacity constraints to allow the flow of hydrogen to a central gas storage inventory. This is done under the assumption that gas transmission is sufficient in throughput capacity and the physical buffering of gas allows greater leniency in times of hydrogen gas demand and supply mismatch. It is likely that any gas transmission constraints would be less constraining compared to the electric transmission system constraints due to inherent storage available in the linepack, making gas transmission the most cost-effective bulk energy transmission approach. However, the fluid dynamics of pipeline transport and development feasibility are outside the scope of this work but are recommended for future high renewable penetration analyses.

The economic dispatch problem aims to minimize total system cost. Renewable generators (i.e., solar, wind, geothermal, some hydropower) must commit or otherwise be curtailed if load is sufficiently met and storage systems are fully loaded. Several gas turbine generators are also designated as must commit for reliability reasons. These are converted to hydrogen gas turbines to facilitate carbon neutrality and their operation creates a variable hydrogen demand. The three major storage assets are 1) BESS 2) electrolyzers and 3) PHES facilities. Establishing a penalty price on curtailment incentivizes excess electricity going toward storage rather than being curtailed. This promotes both daily energy shifting and seasonal energy storage. While there are major challenges in pinpointing an optimal distribution of renewable generation and storage

technologies with a far outlook, this study provides a representative snapshot of an annual dispatch if one were to accept the 1) 2045 generator capacity established in the high electrification scenario of the California Energy Commission (CEC) [317] as a "close-enough" to an optimal portfolio and 2) the deployments (i.e., solar, offshore wind, fuel cells, and electrolyzers) to accommodate massive amounts of fixed cross-sectoral hydrogen demand as well as its variable usage in power generation are operating in an economically-viable manner.

Total system load reported in the results section of this paper will include electrical loading of storage systems in addition to the 449 TWh of retail electric load. The fixed non-power generation annual hydrogen demand for reference is 49 TWh and 165 TWh for the L-scenarios and H-scenarios, respectively. The low and high hourly hydrogen demand is static, split evenly throughout the year, and corresponds to the low and high 2050 annual projection in Reed et al. [289], comprising usage mostly for the transportation sector, but also including heating applications, and other industrial uses.

7.1.3 Spatial discretization

Spatial nodes and transmission system are laid out CAISO 2020 [315] as in but the SCE service territory is further broken down into five nodes guided by CAISO 2019 [318] nominally: 1) CISC-Metro representing the metropolitan area of SCE, 2) CISC-East representing the eastern area of SCE, 3) CISC-EoL representing the area east of Lugo, 4) CISC-NoL representing the area north of Lugo and, 5) CISC-TabCC representing the Tehachapi and Big Creek area as depicted in Figure 54 below.

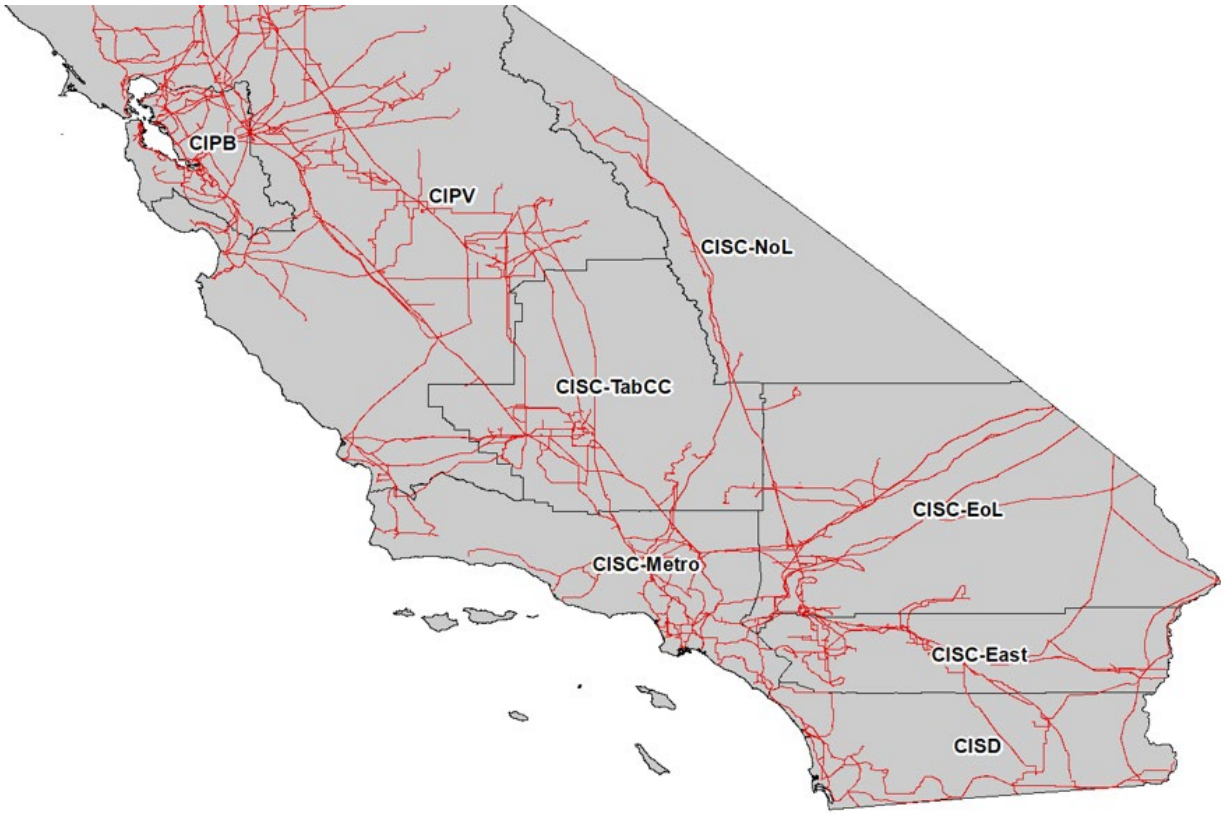

Figure 54 - Spatial discretization for the California electric grid model. Nodes are formed by grouping counties overlayed with 115 kV and higher existing transmission electric lines.

Transmission line capacities also follow the CAISO study and transmission line capacities resulting from the CISC region breakup are established by evaluating existing corridors circuits [308]. The loading limits used in this work are summarized in Table 5. CISC and CISD are used nominally in this work to roughly represent the SCE and SDG&E investor-owned utility (IOU) service territories, respectively, and both CIPV and CIPB comprise the PG&E service territory. The nodes are established on a county basis resulting in some simplification in spatial nodes' bordering areas and should not be interpreted as necessarily associated to an IOU.

Table 5 – Electric transmission line flow capacities

From Node	To Node	Maximum Flow (MW)	Minimum Flow (MW)
CIPB	CIPV	3500	-3500
CIPV	CISC-TabCC	4000	-3000
CISC-Metro	CISD	4100	-2500
CISC-East	CISC	2000	-2000
CISC-EoL	CISC	5000	-5000
CISC-Metro	CISC	14500	-14500
CISC-NoL	CISC	1500	-1500
CISC-TabCC	CISC	6000	-6000
External	CISC	13500	-12500
External	CISD	4200	-3800
External	CIPV	7800	-6600

Imports and exports are defined as electricity exchange between regions in the model. By this definition the total amount of imported electricity is equal to the total amount of exported electricity as the external node, representing OOS, is included.

7.1.4 Generator Costs

The total cost of generation consists of three factors that establish the merit order of dispatch: fuel costs, emissions costs, and supplementary generation costs. Three of the most prominent fuels with explicit costs in this work are natural gas, biogas, and hydrogen gas. Natural gas fuel prices in the future are quite uncertain, however, higher natural gas prices would imply greater dependence on renewable power generation and fuels. As such, the decision to use frozen natural gas prices as used in the CAISO 2020 [315] simulation would implicate a more conservative adoption of renewable resources to meet the scenario demands. The utilized natural gas prices have regional and monthly differences but generally range from a minimum price of 3.3 $/MMBtu to a maximum price of 5.5 $/MMBtu. Note that this range falls into the median of EIA Henry Hub price estimations in 2050 [319], so that the expected cost would be higher to deliver the produced

natural gas to California. Biogas is modeled by feedstock with prices ranging from 3-7 $/MMBtu based upon a Duke study evaluating the supply cost curve in the United States [79]. The cost of hydrogen is 33 $/MMBtu established by conducting a cashflow analysis as done by Lazard [320] but with a 25% electrolyzer capacity factor (CF). This CF, which can significantly affect hydrogen price, is established through iterative simulations that indicate this value is typical of an electrolyzer operating solely for green hydrogen production with dominantly solar electricity as feedstock.

The cost of carbon modeled is 250 $/MTCO2e [321]. Carbon emission rates are tied to the fuel, with natural gas being 117 kg of CO2 per MMBtu of fuel consumption [322]. Similarly, for biogas this number is 50 kg/MMBtu [322] and zero for hydrogen, as all hydrogen production is electrolytic in the current analyses.

Supplementary generation costs effectively encapsulate all other costs including annualized costs from the capital expenditures and typical VO&M costs. For the most part, these costs can be broken down by fuel technology type. Natural gas, biomass, and nuclear power plants are assumed to be fully depreciated and are taken from [323] minus fuel costs. The lower range of wind from the same source, 26 $/MWh, is taken to represent the development of high renewable potential sites as well as out-of-state excess wind imports. A new gas turbine combined-cycle plant capital cost is used to represent new hydrogen gas turbine combined-cycle plant capital cost at 24 $/MWh. Hydropower and geothermal costs come from IRENA's historical evaluated costs [324]. Behind the meter PV (BTMPV) costs are taken from NREL's annual technology baseline [325]. BESS costs are taken by removing the cost associated with PV from the PV paired with batteries in Lazard's evaluation in the cost of storing energy [326].

Fuel cell generators are modeled with a supplementary generation cost necessary to offset capital costs from a system with a 10% CF operation, 42 $/MWh. This is calculated assuming a stack life of 40,000 hours, 1,200 $/kW initial installation cost and a 425 $/kW stack replacement cost. The dispatch within the scenarios is then reviewed and the capacity heuristically increased until the CF decreases to roughly 10%. A CF higher than 10% suggests that this level of revenue would be sufficient to justify economically deploying fuel cell system capacity at this cost and operation. This is to balance the necessary power generation needed to meet nighttime loads without overbuilding fuel cell capacity with low CF that may be deemed economically unviable. Despite this, the fuel cost associated with generating electricity with fuel cells comprises a majority of the cost and slight differences in these supplementary generation costs are inconsequential to the dispatch behavior between scenarios. Future work is recommended to investigate sensitivities to this CF which directly impacts 1) the fuel cell capacity deployed, 2) consequently the additional primary renewable electricity generation and electrolyzer system capacity required to balance the hydrogen gas consumption, and 3) the resulting reduction in carbon emissions due to reduced dependence upon natural gas fueled power plants.

Utility-scale solar and offshore wind primarily deployed in addition to the 2045 CEC [317] portfolio are treated slightly differently. Due to the multi-GW scale capacities considered, the cost of interconnection also needs to be considered to fairly compare the two. The generation portion for utility-scale solar is 30 $/MWh [323] and 63 $/MWh for offshore wind [327]. However, offshore wind would likely need additional cost of interconnection which is thought to range from 14-41 $/MWh [327] or an average of 28 $/MWh, which is used in this study. The equivalent for

low CF spur-lines delivering new build solar is modeled at 5 $/MWh [328]. The sources for these costs are summarized in Table 6 below.

Table 6 – Supplementary generation cost. Supplementary generation cost in addition to fuel costs and emissions costs make up total generation cost for each technology type.

Generator Type	Supplementary Generation Cost ($/MWh)	Source
BESS	85	[326]
Biomass	10	[323]
BTMPV	40	[325]
Geothermal	50	[324]
Hydrogen FC	42	[153]
Hydrogen GT	45	[323]
Hydropower	10	[324]
NG GT	10	[323]
Nuclear	29	[323]
Offshore wind	91	[327]
Utility-scale solar	35	[323]
Onshore wind	26	[323]

7.1.5 Generator Capacities

The CEC Report [317] anticipates 55 GW of BESS capacity additions in the 2045 core and high flexibility scenarios which results in a total of roughly 57 GW. The total BESS capacity modeled in this work is also 57 GW with the difference from the capacity modeled in CAISO 2020 [315] distributed along with solar, electrolyzer, and fuel cell capacity, geospatially sited based upon existing capacity-weighted CEC solar power plants above 10 MW found to be: East 24%, EoL 20%, Metro 16%, NoL 0%, and TabCC 40%. These total capacities are summarized below in Table 7.

Table 7 – Installed system capacity. Utility-scale solar, offshore wind, and electrolyzer system capacity for hydrogen production vary by scenario.

	L-S	L-W	H-S	H-W
	Installed Capacity (MW)			
Electrolyzer	80,000	55,500	146,500	114,700
Fuel Cell	26,000	6,000	23,500	6,000
Solar	150,620	95,500	212,610	163,490
Wind	14,770	35,940	14,770	35,940
BESS	57,440	57,440	57,440	57,440
Biomass	50	50	50	50
BTM Solar	34,250	34,250	34,250	34,250
Geothermal	1,850	1,850	1,850	1,850
Hydrogen GT	8,430	8,430	8,430	8,430
Hydropower	11,070	11,070	11,070	11,070
Natural Gas GT	28,820	28,820	28,820	28,820
Nuclear	4,210	4,210	4,210	4,210

7.1.6 Carbon and Pollutant Accounting

The difference between the cost of fuel and the amount of carbon emissions associated with the fuel displaced by renewable hydrogen amongst the H-scenarios and L-scenarios is estimated, allowing the four scenarios' total cost and emissions to be compared on the same basis. Hydrogen demand in the L-scenarios primarily meets FCEV LDV demand, thus displacing primarily gasoline per Reed et al. [55]. However, the hydrogen demand in the H-scenarios displaces a mixture of gasoline, diesel, and natural gas used for fuel cell LDVs, MDVs, HDVs, and industrial applications. Additionally, BTS 2030 emission factors [329] are used to estimate pollutant emissions factors. The offset market for NOx, CO, and particulate matter in California is not as mature as the offset market for CO2 resulting in low trade volume and high price volatility. Despite this, 2,500 $/tonne, 25,000 $/tonne, and 15,000 $/tonne are used for CO, NOx, and PM2.5,

respectively, as representative values based upon market data averages from 2017 to 2018 [330]. These values are expected to be conservative as the price in 2050 could increase as allowances change in the future akin to the CO2 market.

7.1.7 Other Considerations

Wind and solar generation profiles per node are modeled using a fraction of CAISO aggregate totals. Reserve demands are used as done in CAISO 2020 [315] with non-spinning and spinning requirements being 3% of load per region. Thermal power plants are modeled with previously CAISO established outage rates, maintenance rates, outage times, time to repair, startup costs, and associated fuel offtake amounts at start. Fixed heat rates are established across the fleet by categorizing generators as peaker plants, baseline generators, or an intermediary to reduce solution convergence time. Some out-of-state resources are designated must-take dedicated import, which resources share a maximum import capacity with any additional purchases. The maximum import limit at any given hour is 7.8, 13.5, and 4.2 GW for the PG&E, SCE, and SDG&E areas, respectively.

7.2 Results

7.2.1 Scenarios overview

Four scenarios are nominally referred to in this study as the L-S, L-W, H-S, and H-W scenarios with the first letter denoting the level of fixed hydrogen demand input (L=low, H=high) and the latter denoting the installation of offshore wind capacity (S=no offshore wind, W=21 GW offshore wind).

Solar makes up 60%, 46%, 67%, and 58% of total generation for the L-S, L-W, H-S, and H-W scenarios, respectively. The relatively low cost of solar generation is evident from the optimal dispatch generation and cost results presented in Figure 55 (comparing total solar (a) generation and (b) cost). On the other hand, the cost of energy storage is evident as well as BESS which makes up 11%, 9%, 9%, 7% of total generation but account for 26%, 23%, 24%, and 21% of the total cost for the L-S, L-W, H-S, and H-W scenarios, respectively. Similarly, hydrogen-fueled generators make up 5%, 3%, 4%, and 2% of total electric generation, but account for 20%, 11%, 16%, and 9% of total system cost for the L-S, L-W, H-S, and H-W scenarios, respectively.

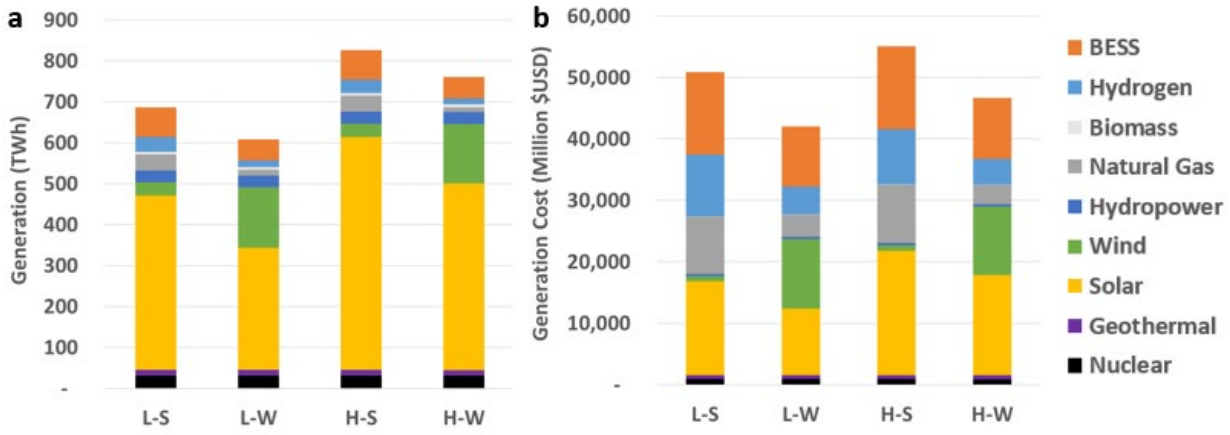

Figure 55 - Total scenario generation and cost. a) Annual generation and b) generation cost by scenario and fuel type.

meeting the same electric and hydrogen demand, the wind scenarios are more cost-efficient with both equivalent wind scenarios costing 17% and 15% less in the low and high hydrogen demand scenarios, respectively.

7.2.2 Carbon emissions

The L-S and H-S scenarios result in an annual CO2 emission total of 31 and 32 MMT, respectively. The L-W and H-W scenarios result in 12 and 10 MMT CO2 emissions, respectively.

The high hydrogen demand scenarios have less carbon emissions than their low hydrogen demand counterparts because there is greater solar capacity deployed—reducing the need for flexible generators in the off-peak solar generation hours. Figure 56 provides a direct comparison between scenarios by accounting for the cost of purchasing emissions offsets for any fossil fuel use that remains in the scenario and the incumbent fuel costs themselves, which are avoided with increased usage of hydrogen as a renewable fuel in both the power and transportation sectors.

The carbon reduction achieved by using hydrogen outside the power generation sector is 26.6 MMTCO2e. The cost of carbon is key for comparing the low-high pairs as the cost of carbon and pollutants from displaced fuel use outside of power generation makes up 12 and 14% of the total cost for the L-S and L-W scenarios, respectively. at a carbon price of roughly 38 $/MTCO2e, the incurred costs of producing and conditioning more renewable hydrogen fuel for transportation usage are equivalent to the cost of the fossil fuels being displaced and their associated environmental premium costs.

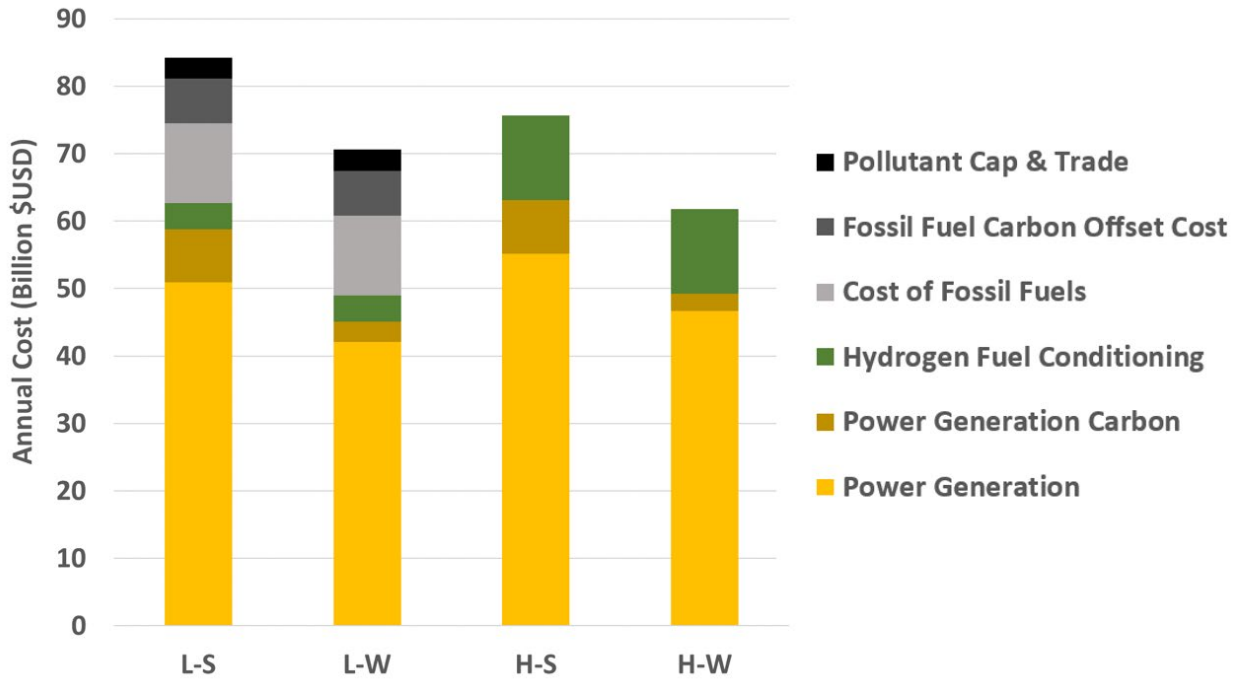

Figure 56 - Comparison of total scenario costs. Electricity generation costs, hydrogen transport and fuel conditioning costs, fossil fuels costs and associated pollutant cap and trade value are considered.

While the low-high pair for wind has a 14% carbon reduction from power generation, the H-S scenario has 2% higher carbon emissions from power generation than its L-demand counterpart. This is only explained by the slight differences in fuel cell capacity deployed. The L-S scenario has 26 GW of fuel cell systems operating at an 11.3% capacity factor (CF) whereas the H-S scenario has 23.5 GW operating at a 10.6% CF. More electricity from fuel cell generators results in a lower dependence on natural gas fueled generators. The two wind scenarios both have 6 GW of fuel cell capacity installed with a 10.0% CF in L-W and an 8.0% CF in H-W.

Fuel cells operate with more capacity at a higher CF in the L-demand scenarios than the H-demand scenarios because the higher capacity of solar installed in the H-demand scenarios provides more electricity to load in characteristically low solar production hours (i.e., mornings, evenings, and winter months). In other words, deploying more fuel cell capacity creates a virtuous

feedback loop where the opportunity to dispatch between deployed fuel cell systems shrinks, but also the additional solar capacity deployed to balance hydrogen production also slightly reduces the need for fuel cells to dispatch in winter months. In short, major carbon emission reductions outside of the power generation sector can be achieved with electrolytic hydrogen while also synergistically reducing the need for flexible generators, most notably during times of low solar production. While this phenomenon may slow the actual deployment of fuel cell capacity resulting in a slight increase in carbon emissions in the power generation sector, the reduction from hydrogen use in the transportation sector and the net overall carbon emissions reductions are an order of magnitude higher.

7.2.3 Generator dispatch

Dispatching natural gas generators with the carbon premium still occurs primarily due to the lower fuel price. This could change if the price of hydrogen, which makes up majority of the hydrogen gas turbine levelized cost, shrinks, or the cost of natural gas fuel is higher. The cost of hydrogen is dependent upon the electrolyzer CF and the cost of feedstock electricity. A reduction in capex and electrolyzer stack replacement of 50% is found to reduce the LCOH from 4.42 $/kg to 3.69 $/kg whereas doubling the CF with offshore wind would increase the price from 4.42 $/kg to 6.04 $/kg. While more offshore wind capacity can be installed to increase the CF of the electrolyzer, the average cost of feedstock electricity would increase. In this case, the complementary dynamics of offshore wind and solar would not necessarily decrease the price and promote more hydrogen fueled power generation, though if another source of cheap renewable electricity is available when solar is not this would further decrease the hydrogen cost. If the CF could double at the same solar price perhaps by similarly priced renewable imports from out-of-

state (OOS) dispatch, the LCOH reduction would be the same as the 50% reduced capex case. By far, the most sensitive single factor to the LCOH is the price of feedstock electricity, where if the LCOE is reduced to 15 $/MWh from 35 $/MWh, the resulting LCOH would be 2.75 $/kg.

Due to the nighttime generation of offshore wind, less hydrogen is used for power generation in the evenings throughout the year with BESS being nearly sufficient in the wind scenarios. The annual total power generation from BESS is 72 and 73 TWh for the L-S and H-S scenarios, whereas it is lower in the L-W and H-W scenarios at 52 and 53 TWh, respectively. The annual hydrogen-fueled power generation in the L-S and H-S scenarios is 36 and 33 TWh, respectively, whereas for the L-W and H-W scenarios this number is 15 and 14 TWh, respectively. Seasonal differences can be seen as BESS operates providing roughly the same amount of power every month in the solar scenarios and provides slightly more in the winter and autumn in the wind scenarios. Power generation using hydrogen is skewed toward the autumn and winter months for all four scenarios but more evidently so in the solar scenarios (see Figure 57).

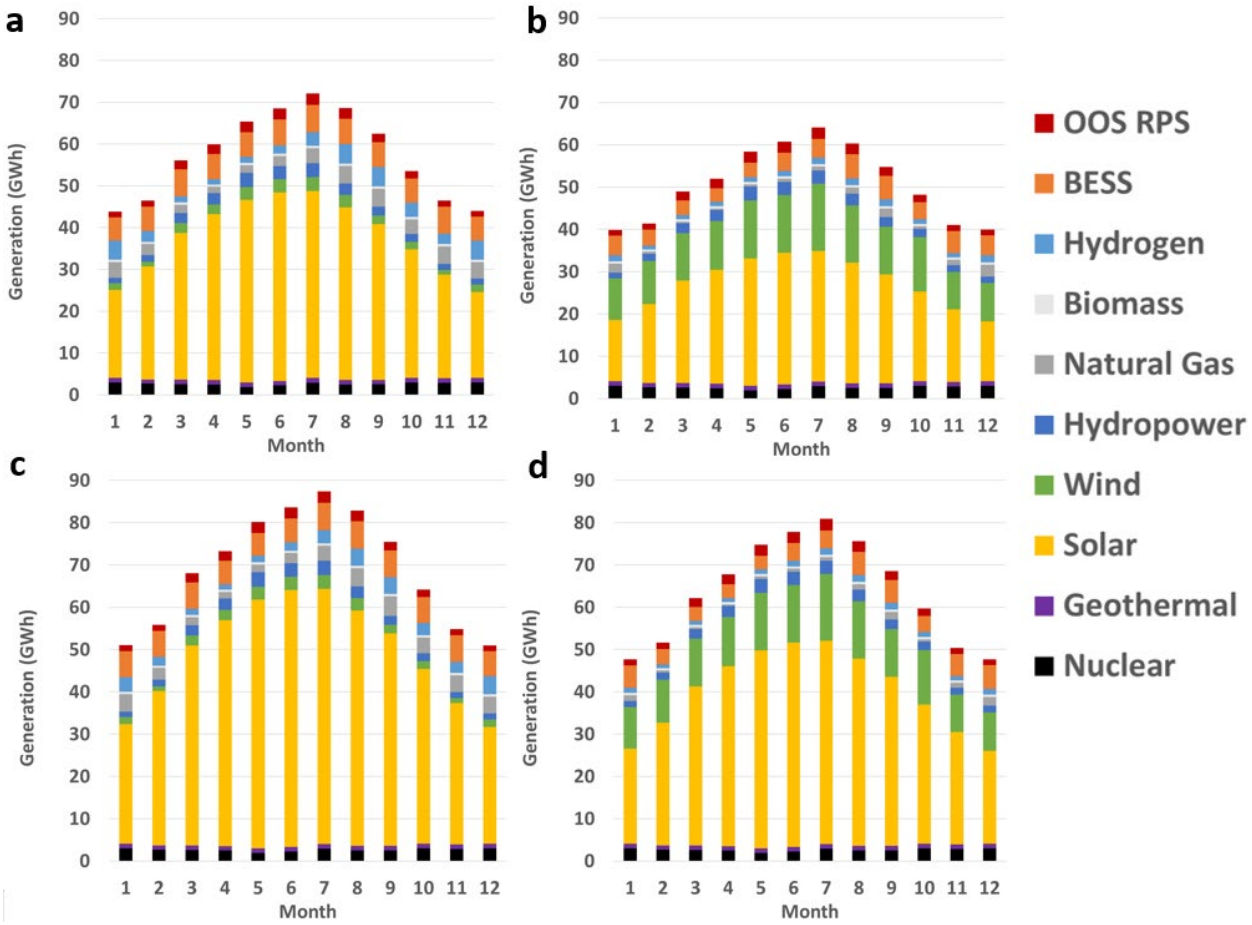

Figure 57 – Monthly electricity generation by fuel type for a) L-S scenario, b) L-W scenario, c) H-S scenario, and d) H-W scenario.

The LCOE between solar cases and between wind cases does not significantly change, thus Figure 58 presents a subplot for each pair; however, with the deployment of offshore wind it is clear that the levelized cost is much more even from month to month. Without offshore wind capacity, the solar scenarios are more reliant on flexible generators. Similarly, the magnitude of solar generation is significant and is reflected by the relatively lower costs in the Southern California Edison (SCE) region, as this is where most solar and battery capacity is located.

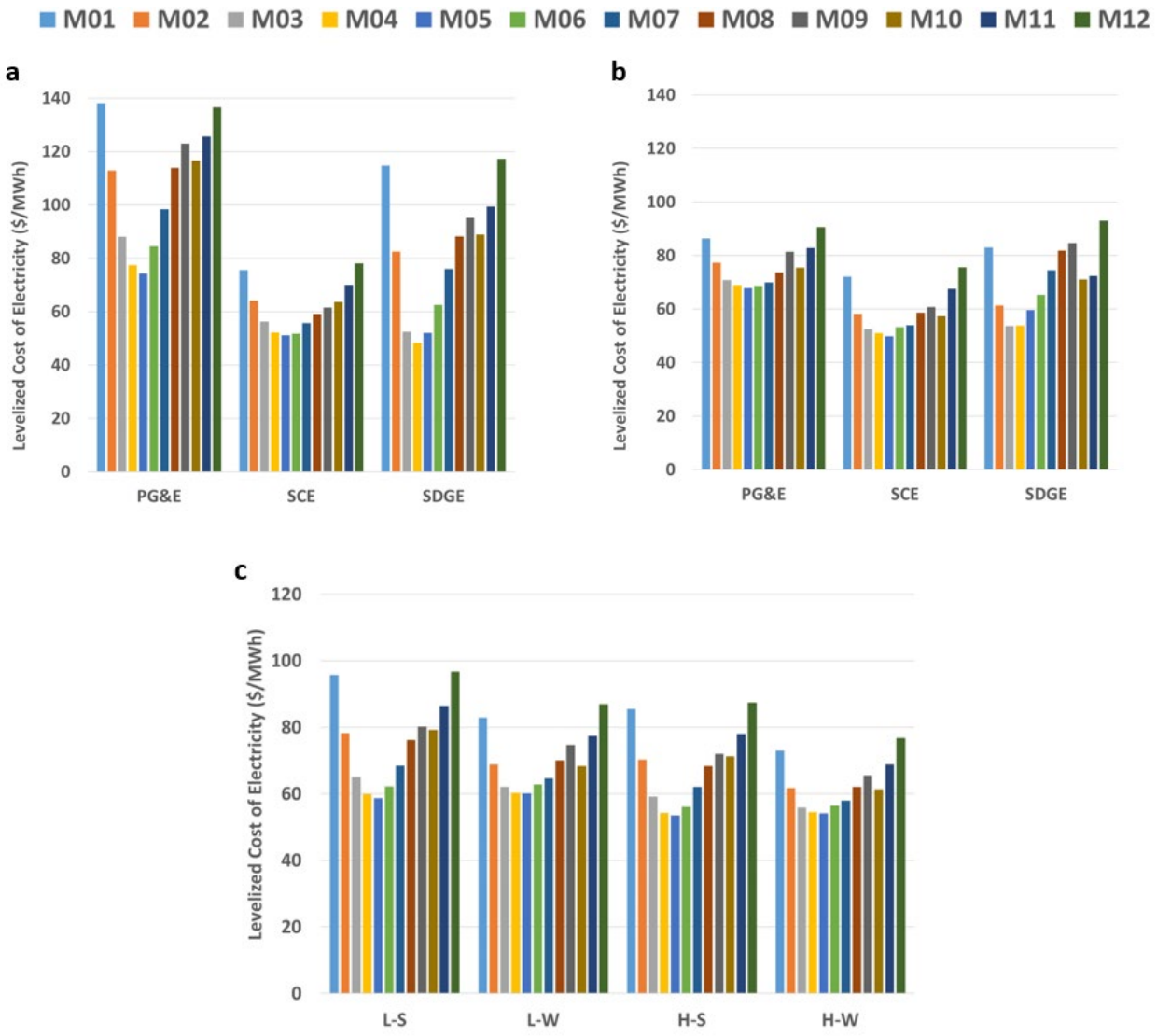

Figure 58 - Levelized cost of electricity. a) Solar scenarios by region and month b) wind scenarios by region and month and c) all scenarios by scenario and month.

In the solar scenarios, natural gas power plants meet 5% of the total annual load, whereas this figure drops to 2% for both wind scenarios. Hydrogen used in both gas turbines and fuel cell systems meets 5% and 4% of the total annual load for the L-S and H-S scenarios, respectively, whereas this figure is 3% and 2% for the L-W and H-W scenarios, respectively. BESS meet 11% and 9% of the total annual load in the L-S and H-S scenarios, respectively, as opposed to 9% and 7% of load in L-W and H-W scenarios, respectively. In part, because of the higher utilization of BESS in

solar scenarios, the overall levelized cost across the board is higher than in the corresponding months in the wind scenarios. These percentages of load are lower than other studies as other studies do not include the cross-sectoral transportation demand leading to large loads associated with electrolytic hydrogen production. The annual capacity factor of generators by fuel type can be found in Table 8. The electricity used for electrolysis compared to total load is 28%, 21%, 41%, and 39% for L-S, L-W, H-S, and H-W, respectively.

Table 8 – Capacity factor of generators by fuel type.

	L-S	L-W	H-S	H-W
Nuclear	85%	85%	85%	85%
Geothermal	80%	80%	80%	80%
Solar	25%	25%	26%	25%
Wind	21%	45%	21%	45%
Hydropower	28%	28%	29%	29%
Natural Gas	15%	5%	15%	5%
Biomass	85%	83%	85%	83%
Hydrogen (GT)	50%	48%	50%	49%
Hydrogen (FC)	11%	10%	11%	8%
BESS	14%	10%	14%	10%

Unless offshore wind costs are more expensive than expected the ability to directly meet load without storage is ultimately more cost-effective than shifting energy daily in a solar-dominant portfolio. The average cost of generation by power generation type does not significantly vary across scenarios. The natural gas turbines average levelized cost spans from 242 to 258 $/MWh with the solar scenarios on the lower end and the wind scenarios on the higher end attributable to the start-up costs and lower total production. The most efficient natural gas power plants are dispatched until the cost of carbon is too constraining resulting in the dispatch

of hydrogen power plants, first toward the limited capacity fuel cell systems, then toward the hydrogen gas turbine power plants due to high fuel costs.

7.2.4 Energy storage dispatch

In all cases, hydrogen energy storage is adopted to significantly contribute to seasonal energy storage for the electric sector, with hydrogen storage system dynamics for all four scenarios presented in Figure 59. The resulting required hydrogen storage capacities for the L-S, L-W, H-S, and H-W scenarios are 123, 72, 149, and 115 TBtu, respectively. For reference, the working natural gas storage capacity from depleted oil and gas fields in California in 2021 is 339 TBtu [331], although the volumetric energy density of natural gas is three times that of hydrogen. The total storage capacity necessary in wind scenarios is lower due to two factors: 1) the seasonality of hydrogen usage for power generation, but also 2) the dependence on solar availability for hydrogen production. During the winter months, hydrogen consumption in the solar scenarios is higher than in the wind scenarios due to the larger seasonal dependence of solar compared to wind. The sum of the six months of the year in which hydrogen is utilized the most for power generation amounts to 28 TWh and 24 TWh of the 36 TWh and 38 TWh annual amounts, or 77% and 73% of the yearly amount, in the L-S and H-S scenarios, respectively. This figure is 11 TWh and 10 TWh, or 71% and 70% of the yearly amount, in the L-W and H-W scenarios, respectively. On the production side, the sum of the best six months of the year in which hydrogen is produced the most uses 174 TWh and 316 TWh of electricity, or 69% and 66% of the annual amount used for hydrogen production, in the L-S and H-S scenarios, respectively. This figure is 117 TWh and 270 TWh, or 72% and 67% of the annual amount used for hydrogen production, in the L-W and H-W scenarios, respectively.

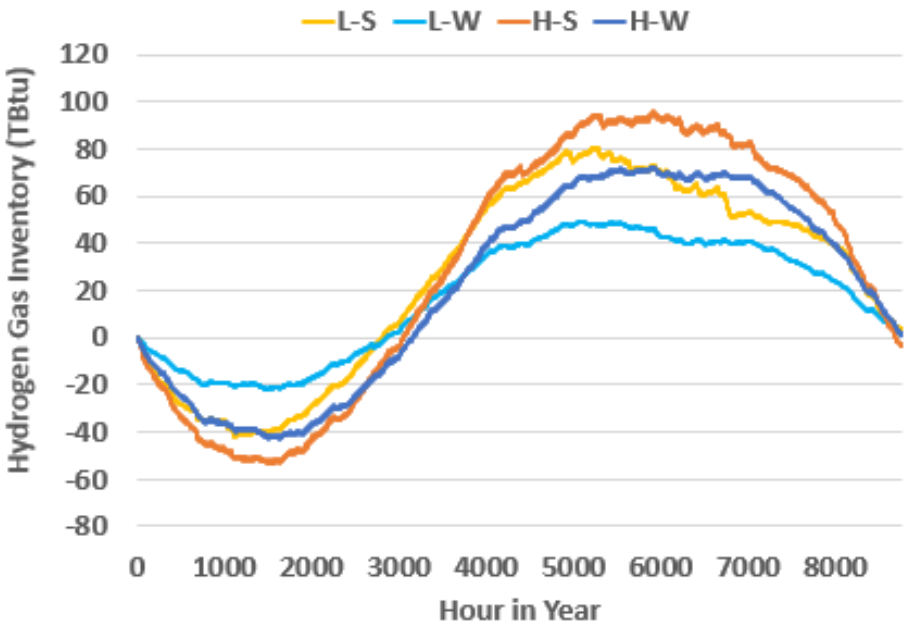

Figure 59 - Annual hydrogen gas inventory. Storage amount throughout the simulated year with an arbitrary starting volume and unconstrained storage limits.

The differences between electrolyzer capacity factors are within a couple percentage points for all months and scenarios as shown in Figure 60. The annual electrolyzer CF for L-S and L-W scenarios are both 25%, whereas, for the H-S and H-W scenarios, these numbers are 24% and 27%, respectively. Even when more wind is adopted, excess generation primarily occurs during the hours of solar power generation. Note that the electrolyzer CF between the solar and wind cases is similar because additional solar capacity is deployed proportionally to complement additional electrolyzer capacity. The primary difference between the solar and wind scenarios is the hydrogen demand necessary for power generation, as the solar cases require more hydrogen for fuel to meet nighttime loads. Much more wind capacity than considered here would be required to have wind power surplus during late night toward morning hours. Even then, the higher LCOE of offshore wind may be undesirable as it may be unfavorable relative to much cheaper solar electricity. For this reason, the majority of electrolyzer projects would likely operate

close to a solar power plant's CF, although necessarily lower due to the solar power plant meeting electric load outside of peak hydrogen production hours. Hydrogen production varies in each month throughout the year and total annual hydrogen production varies amongst the scenarios considered (Figure 60). However, the trend of hydrogen production is generally similar across the scenarios: most of the hydrogen production occurs in the spring and early summer months when solar resource availability is high and coinciding with the relatively lower retail electric load. Later in the summer, while the solar resource remains highly available, electricity demands increase due to air conditioning loads.

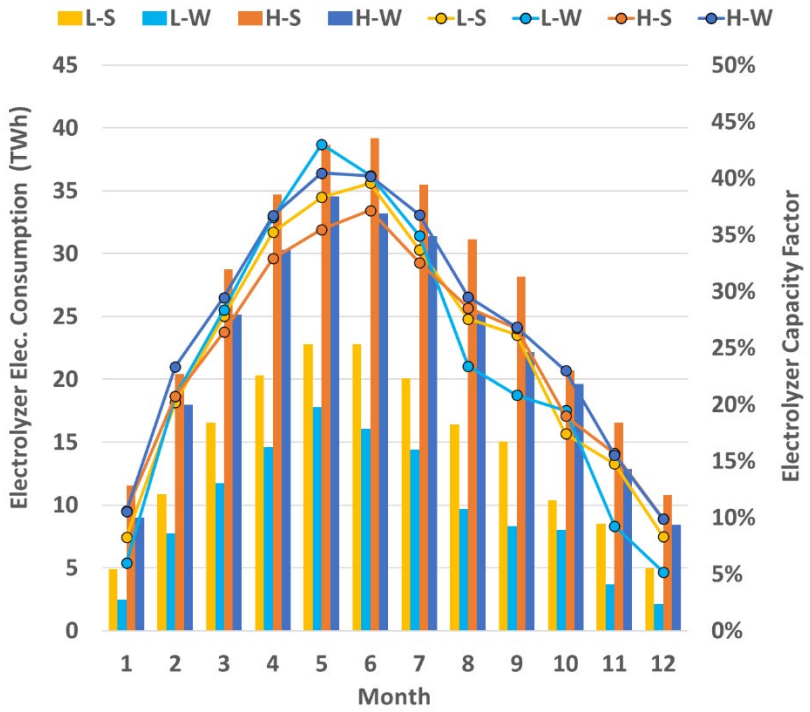

Figure 60 - Electrolyzer power consumption and capacity factor. Combined bar and point graph representing monthly electrolyzer electricity consumption and capacity factor, respectively, for the four scenarios.

Curtailment of renewable sources is less than 1% for all scenarios. The overall capacity of electrolyzers is higher than BESS, which is why across all scenarios more electricity goes toward

electrolyzer systems than toward BESS. The amount of electricity going to BESS is 92, 70, 93, and 71 TWh for the L-S, L-W, H-S, and H-W scenarios, respectively. The amount of storage load going to electrolyzer systems is 174, 117, 316, and 270 TWh for the L-S, L-W, H-S, and H-W scenarios, respectively. Figure 61 illustrates the large magnitude of solar and loading of electrolyzer systems and BESS in the first week of a Summer and Winter month for the H-demand scenarios.

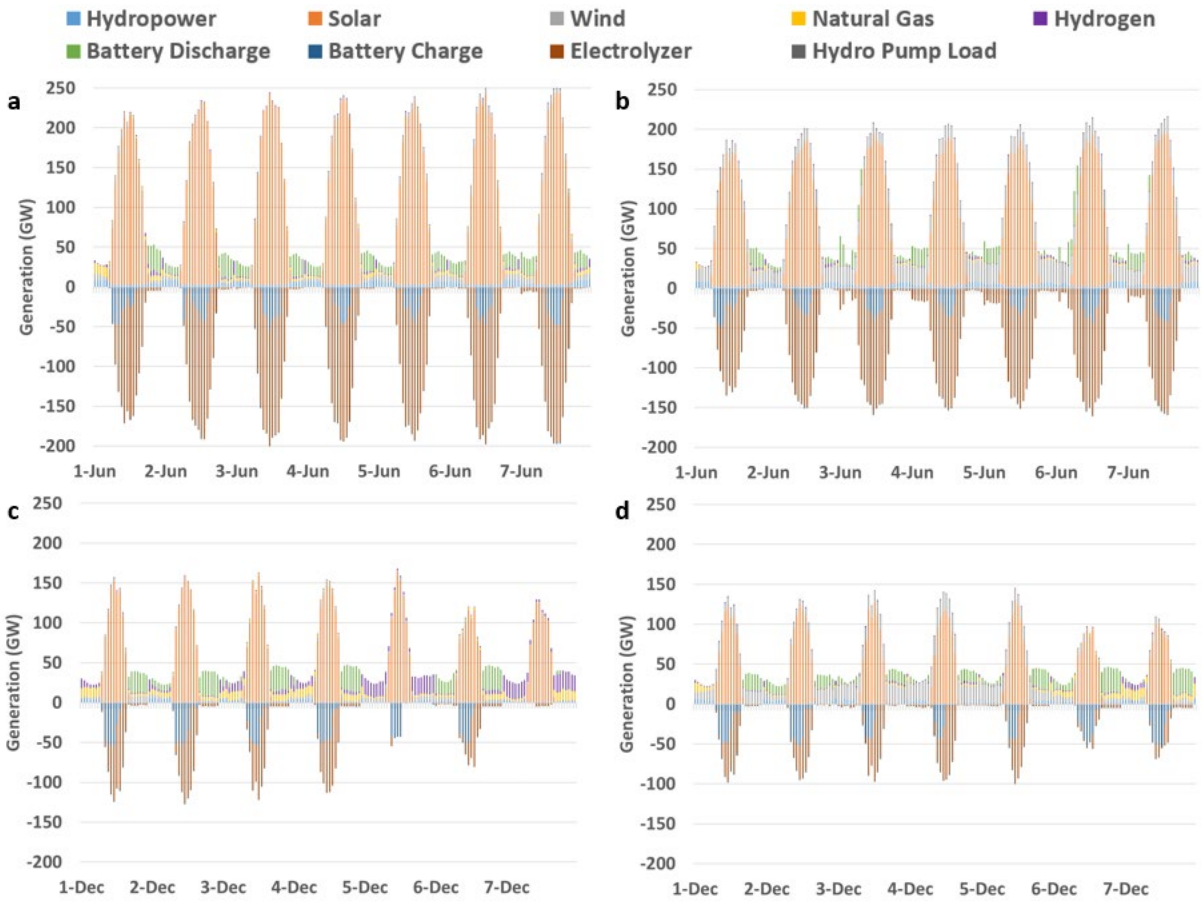

Figure 61 - Weekly power generation seasonal snapshots. The first week in a) June H-S scenario, b) June H-W scenario, c) December H-S scenario and d) December H-W scenario.

In terms of storage system loading, by region, SCE service territory generally meets most of the load for both types of storage as this is where most of the utility-scale solar is located. This balance is only shifted in the wind scenarios as all of the offshore wind and complementary electrolyzer systems are sited in the Pacific Gas and Electric (PG&E) service territory nodes. Figure

62 portrays the seasonal loading of the storage systems. The amount of electricity sent to SCE and San Diego Gas and Electric (SDG&E) BESS are operation is relatively static throughout the year, whereas the PG&E BESS in the wind scenarios have increased seasonal system loading coinciding with increased generation from offshore wind. While this represents a slight seasonal shift in BESS dispatch, all scenarios show that hydrogen energy storage is the primary resource selected for seasonal storage in the electric sector.

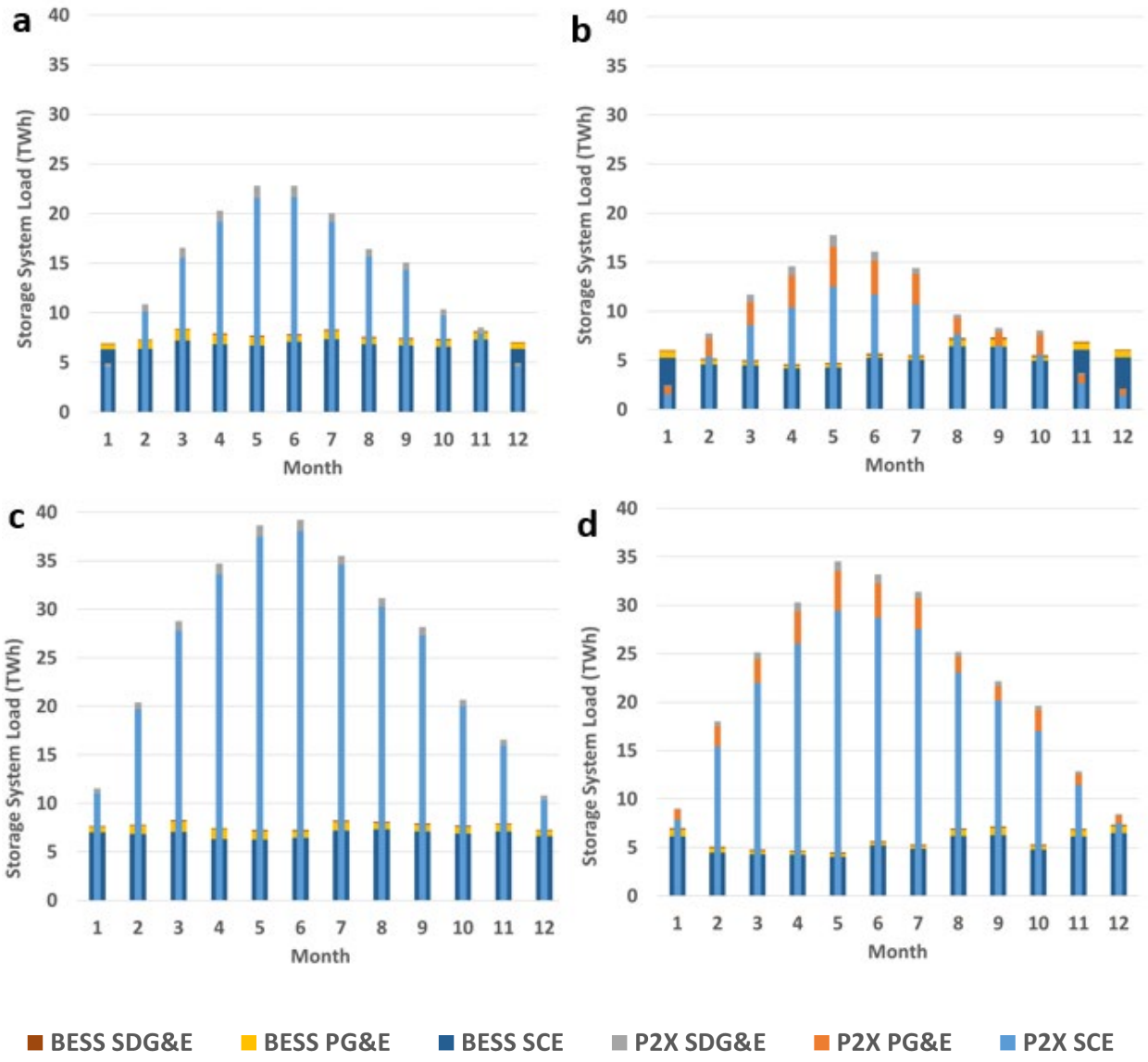

Figure 62 - Monthly regional BESS and electrolyzer system electricity usage. a) L-S scenario, b) L-W scenario, c) H-S scenario, and d) H-W scenario.

Peak hydrogen production occurs in May and June for all scenarios coinciding with the lowest months of electricity going toward BESS by a slight margin in the solar areas. While this might be counterintuitive, as one might expect the increase in solar generation to also result in an increased utilization of BESS, this is primarily due to multiple factors: 1) relatively lower need for BESS to meet night loads 2) relatively low retail electric load in the day coinciding with 3) increased

solar generation. This seasonal mismatch of supply and demand is the same reason driving high solar curtailment in the spring and early summer months of the present-day California grid.

7.2.5 Regional analysis

Regarding electricity exchange via electric transmission and considering transmission constraints, 46% of imports are purchased from OOS in solar cases and 43% in the wind scenarios. The total amount of exports to OOS is only 3% and 2% in the L-S and H-S scenarios, respectively. This number is 1% in both wind scenarios. The balance of these percentages is electricity exchange between regions as summarized in Table 9.

Table 9 – Electricity exchange for each IOU regions by scenario.

Scenario	Region	Import (TWh)	Export (TWh)
L-S	PG&E	105	30
	SCE	34	31
	SDG&E	19	5
L-W	PG&E	56	36
	SCE	60	10
	SDG&E	22	10
H-S	PG&E	105	30
	SCE	34	30
	SDG&E	19	5
H-W	PG&E	57	35
	SCE	57	11
	SDG&E	22	9

With the majority of the solar sited in the SCE nodes, PG&E relies heavily on imports but less so in the wind scenarios where offshore wind can meet a large portion of load. However, in the solar scenarios a significant portion of solar is sited in SCE territory and exporting out of the region is limited by transmission line capacity. The line connecting SCE territory and PG&E territory as well as the line connecting PG&E valley region to PG&E bay region are fully loaded in more than

60% of the hours throughout the year in the solar scenarios, occurring mostly during solar generation timeframes. These two lines are similarly loaded as there is no direct connection between SCE territory and PG&E bay area with the latter being a major load center. The number of congested hours drops to roughly a third of all annual hours in wind scenarios (see Figure 63).

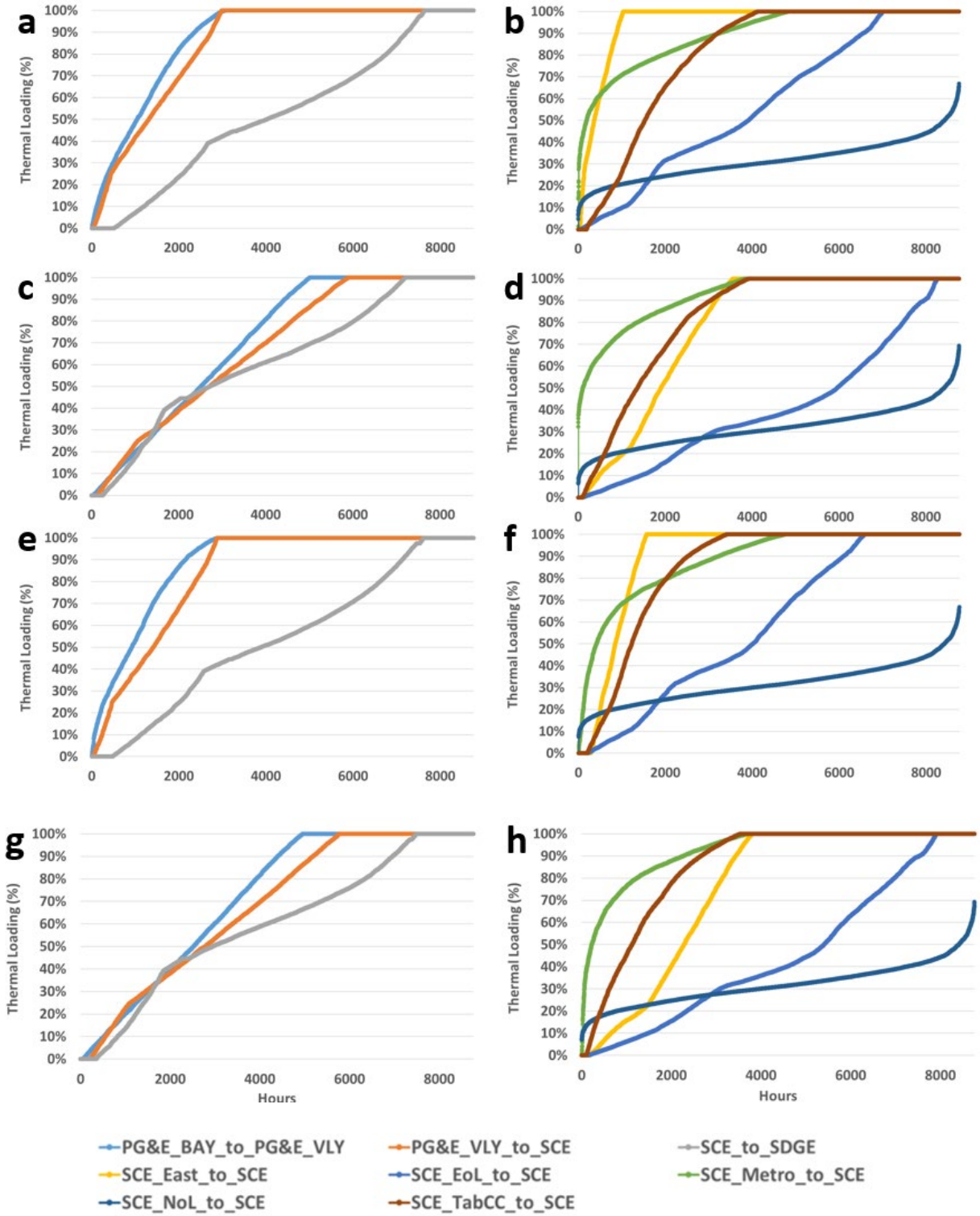

Figure 63 – Thermal loading duration curve for transmission lines a) between L-S scenario IOU regions b) within L-S scenario SCE region c) between L-W scenario IOU regions d) within L-W scenario SCE region e) between H-S scenario IOU regions f) within H-S scenario SCE region g) between H-W scenario IOU regions h) within H-W scenario SCE region

The loading duration curves of the transmission lines between SCE territory nodes do not change too significantly between scenarios. Only the line connecting the eastern area to the remainder of the SCE territory is congested in the summer months during peak solar generation as the node with the highest share of solar generation capacity. All the other SCE nodes generally are not congested due to the amount of energy storage available to act as a sink for excess generation. More interestingly is that congestion occurs the most in the evening when the BESS that are co-located at the PV plants must dispatch to meet local loads and transmit electricity to meet the major evening load of the metropolitan area within SCE territory. This also occurs to a lesser degree on the line connecting the PG&E valley node with the PG&E bay area node, most prominently seen in the evening hours from February to June in the solar scenarios. Tables presenting the average remaining capacity of each line by month and hour to quickly identify these trends are available in the Appendix: Remaining Line Capacity.

7.3 Discussion

If the development of offshore wind capacity is possible, it would generally result in better system performance in terms of required transmission capacity, cost, and emissions up to the point where nighttime until dawn loads are mostly met. Because LCOH is sensitive to the cost of feedstock electricity, low-cost solar still seems to be the best source for electrolytic hydrogen production, effectively providing a ceiling for electrolyzer CF. Any solar capacity deployed that is not already mostly meeting electric loads or charging BESS for evening dispatch would not be deployed at all if not for the purpose of renewable fuel production. The investigated amount of renewable hydrogen fuel demands considered resulted in significant loading of electrolyzer systems amounting to 21% to 41% of total electric load in the scenarios considered. Fuel

production and consumption are not as time constraining as meeting electric loads (even BEV charging) so that this cross-sectoral type of scenario provides a strong opportunity to evaluate the value of flexible GW-scale electrolyzer systems and how these can balance load-supply mismatch in a deep renewable power generation sector. At the same time, these large-scale electrolytics hydrogen production capabilities provide seasonal storage of grid electricity and transportation electrification attributes.

The exception to the electrolyzer CF ceiling would be the availability of onshore wind generation and lifting the limitation on OOS imports to supplement local solar power generation. This is important because reducing the cost of hydrogen consequently affects the opportunity to dispatch hydrogen powered fuel cells, promoting capacity deployment to meet load that would otherwise be met by natural gas power plants. However, due to the nature of bulk energy transmission it would be more likely for OOS to produce and import hydrogen than to build additional electric transmission capacity to deliver feedstock electricity specifically for hydrogen production. To this end, the key assumptions that are worth re-evaluating in future work from this study would be the assumption that 1) 10% CF and the resulting cash flow is the marginal economically viable deployment, as opposed to higher or lower and 2) the availability of hydrogen imports from OOS.

Transmission between inter-state regions is fairly congested with most of the challenge arising from meeting evening and late-night loads. If the solution for this is not to increase transmission line capacity to deliver PV+BESS electricity, it may be the usage of hydrogen pipelines for fuel cell power systems closer to load centers. In this study, fuel cell capacities were distributed

proportionally to utility-scale solar and BESS deployment, however it may be possible to skew deployment towards major load centers to circumvent electric transmission.

Future studies that may investigate the LCOH sensitivities may also want to account for the value of being able to defer electric transmission upgrades in favor of lower cost hydrogen pipelines as well as the latest government subsidies (e.g., the Inflation Reduction Act of 2022). Future work can also build upon the results of the congested transmission lines to evaluate the trade-off between upgrading electric transmission lines and siting utility-scale solar closer to loads despite lower capacity factors. Statistical studies to account for interannual variabilities in renewable generation is strongly recommended to evaluate the reliability of the provided solution when confronted with once-in-a-century weather phenomena.

7.4 Chapter Summary and Conclusions

To conclude, an hourly annual optimization is carried out for four different scenarios representing two levels of hydrogen demand for applications outside of the power generation sector. Half of the scenarios model 21 GW of offshore wind capacity resulting in lower total generation and cost for each respective level of hydrogen demand. A carbon price of 50 $/tonne price is sufficient to offset the increased cost of hydrogen fuel production and conditioning for transportation applications to be at parity with nonrenewable fuel costs. The total cost of power generation is 8% and 11% higher in the high hydrogen demand scenarios at the benefit of decreasing CO2 emissions by 19 MMT in the solar scenario and by 22 MMT in the wind scenario compared to the low demand scenarios. This is a 45% and 73% carbon emissions reduction from the scenarios that utilize less hydrogen equivalent to an emission reduction costing 45 and 34 $/MTCO2 for the solar and wind scenarios, respectively.

Increased electrolytic hydrogen production for applications outside of the power generation sector reduces carbon emissions but results in an order of magnitude smaller increase in carbon emissions within the power generation sector due to the shrinking opportunity for fuel cell systems to operate economically with a higher level of solar generation. If there is not a surplus of renewable generation from midnight to dawn either due to increased future overnight loads or lack of renewable capacity, electrolyzer systems will be operated to strongly follow PV generation profiles, which produces a relatively low ceiling on CF at a value of roughly 25%. Despite this, the LCOH is more sensitive to the price of feedstock electricity than it is to the capital cost or CF of the electrolyzer system. This in turn affects the level of dispatch of fuel cell power systems using hydrogen and the remaining flexible needs that are met by natural gas power plants driving up power generation sector costs.

Massive amounts of gas storage are required for hydrogen for seasonal storage amounting to between 72 and 149 TBtu for the scenarios considered. Hydrogen gas storage requirement and consumption is lower in the wind scenarios due to complementary seasonal generation of solar and offshore wind but also because wind can meet more nighttime loads reducing hydrogen consumption for power generation outside of solar generation hours. BESS operation in the solar scenarios is relatively static throughout the year but is more active in winter months when significant wind capacity is deployed. Surprisingly, BESS and electrolyzer electricity consumption is somewhat inversely related, with BESS operating relatively lower in the middle of the year corresponding to peak electrolyzer operation.

8 Dissertation Summary, Conclusions, and Future Work

The goal of this dissertation was to comprehensively evaluate the application of power-to-gas, (i.e., electrolytic hydrogen) to facilitate a deep renewable future. This was achieved by carrying out a cost-benefit analysis in the wholesale sector (Chapter 3), an integrated microgrid analysis in the retail sector (Chapter 4), a feasibility analysis through the killer application of freight transportation (Chapter 5), a geospatial analysis injecting electrolyzers enhancing gas grid renewable contents (Chapter 6), and finally optimizing a system-wide unit-commitment problem to evaluate synergistic interactions between sectors (Chapter 7). The main takeaways from this work, separated by chapter are as follows:

Chapter 3 investigates an increasingly common challenge with utility-scale PV power plants encountering curtailment due to excess generation and transmission congestion. Some notable conclusions from this analysis were:

- With congestion, current price signals best indicate that BESS should be deployed to manage congestion and continue to enable further utility-scale PV deployments.
- Current price signals do not incentivize seasonal storage using P2G despite the requirement of seasonal storage at higher renewable penetration levels.
- Utilizing current state renewable fuel incentives is the only economically viable path for electrolyzer projects in this setting.
- Acceptance of novel fuel pathways that are contingent upon injecting hydrogen alleviate electric transmission, promote further utility-scale PV deployments, and bolster gas grid renewable content.
- Policies or incentives promoting seasonal storage are required to enable P2G system deployments as a complementary technology to BESS.

Chapter 4 investigates the role of energy storage in a distributed microgrid setting in which the maximum geospatially limited rooftop PV is deployed. Some notable conclusions from this analysis were:

- Only 20% of PV could directly meet load, with an additional 12% of load being met through energy storage either by BESS or P2G2P via a fuel cell, slightly limited by the minimum operating constraint of the on-site gas turbine power plant.
- Even without an onsite gas-turbine combined-cycle power plant, over half of the total electric load would have to be met through grid electricity.
- Due to the limitation of space in the distributed setting, electric or gas renewable market commodities must be procured to balance the distributed energy resources to achieve carbon neutrality.
- Current policy and tariffs establish price signals that suggest using market commodities to reach carbon neutrality rather than incentivizing distributed local resources for reliability and acting as an asset to the system at large.

Chapter 5 investigates the question of how much hydrogen would be required to meet the difficult-to-decarbonize freight transportation sector. Some notable conclusions from this analysis were:

- The hydrogen fuel demand is massive at 9-20 MMT/yr with similar contributions from both HDV and ships.
- To meet the high of this demand, 2,112 km^2 or 5939 km^2 of solar or offshore wind generation site area, respectively, is required.
- The major benefits of this approach are the complete decarbonization of a heavy polluting sector, being extensible, and resistant to volatile fossil-based fuels prices.
- The magnitude of electrolyzer capacity deployed for this application would drive cost reductions, unlocking P2G use for other marginal applications.

Chapter 6 investigates the feasibility and balance of deploying distributed and transmission electrolyzers injecting into the gas grid. Some notable conclusions from this analysis were:

- The statewide total distributed potential is estimated to be roughly 2 GW constrained by hydrogen blend limits and land-use designations.
- Distributed electrolyzers are only optimistically sited to inject in 10% of total system high-pressure distribution pipeline mains.
- To maximize transmission hydrogen injection potential, solar sites would have to be co-located throughout the northern half of the state, likely co-located with sub-optimal solar PV locations rather than depending on electric transmission availability.

Chapter 7 investigates a 2050 spatially-resolved hourly annual statewide power generation model co-optimized to meet massive hydrogen fuel demand. Some notable conclusions from this analysis were:

- Meeting massive electrolytic hydrogen demand increases total cost but reduces emissions from the transportation sector equivalent to a carbon abatement cost as low as 34 $/MTCO2e.
- The levelized cost of hydrogen is limited by the availability of low-cost feedstock electricity. This results in electrolyzer systems operating with a capacity factor ceiling akin to solar PV in California.
- Despite the relatively higher cost of offshore wind, the overall system cost is roughly 16% lower than a solar dominant portfolio.
- 115 TBtu of seasonal storage is required for a 90% RES power generation sector with conservative hydrogen adoption for the transportation sector.

Overall, the role of P2G largely complements those that cannot be met through BESS technologies to achieve carbon neutrality. These applications typically end up being seasonal storage and hard-to-decarbonize applications, with one of the largest markets being for freight.

While the short-term challenges of decarbonization can be addressed with BESS (e.g., increasing power generation RES%, electrification of passenger transportation, electrification of some heating demands), further looking challenges will require an alternative approach due to self-discharge and the coupled power-energy capacity nature of BESS. Early investment in the hydrogen vector will allow flexibility in decarbonizing various applications with synergistic effects. For example, electrolyzers in both distributed and transmission settings could enable higher levels of local PV generation--- increasing electric grid renewable content and injecting renewable hydrogen into the gas grid otherwise. Garnering experience in deploying and integrating P2G systems will pay dividends when tackling the hardest to decarbonize applications. Significant investments and policies are required to generate momentum for long-term success.

While the analyses of this work are conducted with sensitivities for many changing variables, the roles that hydrogen would fill in the power generation and transportation sectors is unlikely to change. Future work should consider exploring various policies and incentives that would significantly affect the economic viability of deploying P2G systems. In addition, interconnected regional analyses are recommended with a focus on hydrogen effectively replacing the existing natural gas grid system between states.

9 References

[1] M. A. Qaisrani, J. Wei, and L. A. Khan, “Potential and transition of concentrated solar power: A case study of China,” *Sustainable Energy Technologies and Assessments*, vol. 44, Apr. 2021, doi: 10.1016/j.seta.2021.101052.

[2] R. Wiser, M. Bolinger, B. Hoen, and et al., “Land-Based Wind Market Report: 2022,” 2022. [Online]. Available: https://escholarship.org/uc/item/48j7s9v1

[3] T. N. Russo, “Rethinking Low Impact Hydropower and Renewable Energy Certificates,” *Climate and Energy*, vol. 37, no. 9, pp. 26–32, Apr. 2021, doi: 10.1002/gas.22225.

[4] L. Rybach, “Geothermal Power Growth 1995–2013—A Comparison with Other Renewables,” *Energies 2014, Vol. 7, Pages 4802-4812*, vol. 7, no. 8, pp. 4802–4812, Jul. 2014, doi: 10.3390/EN7084802.

[5] B. Tarroja, F. Chiang, A. AghaKouchak, and S. Samuelsen, “Assessing future water resource constraints on thermally based renewable energy resources in California,” *Appl Energy*, vol. 226, pp. 49–60, Sep. 2018, doi: 10.1016/j.apenergy.2018.05.105.

[6] M. Temiz and I. Dincer, “Enhancement of a nuclear power plant with a renewable based multigenerational energy system,” *Int J Energy Res*, vol. 45, no. 8, pp. 12396–12412, Jun. 2021, doi: 10.1002/ER.6582.

[7] A. T. Bouma, Q. J. Wei, J. E. Parsons, J. Buongiorno, and J. H. Lienhard, “Energy and water without carbon: Integrated desalination and nuclear power at Diablo Canyon,” *Appl Energy*, vol. 323, p. 119612, Oct. 2022, doi: 10.1016/J.APENERGY.2022.119612.

[8] J. Peng and L. Lu, “Investigation on the development potential of rooftop PV system in Hong Kong and its environmental benefits,” *Renewable and Sustainable Energy Reviews*, vol. 27, pp. 149–162, 2013, doi: 10.1016/j.rser.2013.06.030.

[9] L. Novoa, R. Flores, and J. Brouwer, “Optimal renewable generation and battery storage sizing and siting considering local transformer limits,” *Appl Energy*, vol. 256, no. September, p. 113926, 2019, doi: 10.1016/j.apenergy.2019.113926.

[10] D. Assouline, N. Mohajeri, and J. L. Scartezzini, “Large-scale rooftop solar photovoltaic technical potential estimation using Random Forests,” *Appl Energy*, vol. 217, no. September 2017, pp. 189–211, 2018, doi: 10.1016/j.apenergy.2018.02.118.

[11] J. Melius, R. Margolis, and S. Ong, “Estimating Rooftop Suitability for PV: A Review of Methods , Patents , and Validation Techniques,” *NREL Technical Report*, no. December, p. 35, 2013.

[12] S. Freitas, C. Catita, P. Redweik, and M. C. Brito, “Modelling solar potential in the urban environment: State-of-the-art review,” *Renewable and Sustainable Energy Reviews*, vol. 41, pp. 915–931, 2015, doi: 10.1016/j.rser.2014.08.060.

[13] J. Schallenberg-Rodríguez, “Photovoltaic techno-economical potential on roofs in regions and islands: The case of the Canary Islands. Methodological review and methodology proposal,” *Renewable and Sustainable Energy Reviews*, vol. 20, pp. 219–239, 2013, doi: 10.1016/j.rser.2012.11.078.

[14] A. Strzalka, N. Alam, E. Duminil, V. Coors, and U. Eicker, “Large scale integration of photovoltaics in cities,” *Appl Energy*, vol. 93, pp. 413–421, 2012, doi: 10.1016/j.apenergy.2011.12.033.

[15] S. Kucuksari *et al.*, “An Integrated GIS, optimization and simulation framework for optimal PV size and location in campus area environments,” *Appl Energy*, vol. 113, pp. 1601–1613, 2014, doi: 10.1016/j.apenergy.2013.09.002.

[16] S. Barua, R. A. Prasath, and D. Boruah, “Rooftop Solar Photovoltaic System Design and Assessment for the Academic Campus Using PVsyst Software,” *International Journal of Electronics and Electrical Engineering*, vol. 5, no. 1, pp. 76–83, 2017, doi: 10.18178/ijeee.5.1.76-83.

[17] J. Hofierka and J. Kaňuk, “Assessment of photovoltaic potential in urban areas using open-source solar radiation tools,” *Renew Energy*, vol. 34, no. 10, pp. 2206–2214, 2009, doi: 10.1016/j.renene.2009.02.021.

[18] C. Helm and K. Burman, “Kauai , Hawaii : Solar Resource Analysis and High-Penetration PV Potential Kauai , Hawaii : Solar Resource Analysis and High-Penetration PV Potential,” *Contract*, no. April, 2010.

[19] J. C. Feng, J. Yan, Z. Yu, X. Zeng, and W. Xu, “Case study of an industrial park toward zero carbon emission,” *Appl Energy*, vol. 209, no. November 2017, pp. 65–78, 2018, doi: 10.1016/j.apenergy.2017.10.069.

[20] Y. Yamagata and H. Seya, “Simulating a future smart city: An integrated land use-energy model,” *Appl Energy*, vol. 112, pp. 1466–1474, 2013, doi: 10.1016/j.apenergy.2013.01.061.

[21] J. Byrne, J. Taminiau, L. Kurdgelashvili, and K. N. Kim, “A review of the solar city concept and methods to assess rooftop solar electric potential, with an illustrative application to the city of Seoul,” *Renewable and Sustainable Energy Reviews*, vol. 41, pp. 830–844, 2015, doi: 10.1016/j.rser.2014.08.023.

[22] M. H. Kabir, W. Endlicher, and J. Jägermeyr, “Calculation of bright roof-tops for solar PV applications in Dhaka Megacity, Bangladesh,” *Renew Energy*, vol. 35, no. 8, pp. 1760–1764, 2010, doi: 10.1016/j.renene.2009.11.016.

[23] J. Zhang *et al.*, "Impact of urban block typology on building solar potential and energy use efficiency in tropical high-density city," *Appl Energy*, vol. 240, no. January, pp. 513–533, 2019, doi: 10.1016/j.apenergy.2019.02.033.

[24] L. K. Wiginton, H. T. Nguyen, and J. M. Pearce, "Quantifying rooftop solar photovoltaic potential for regional renewable energy policy," *Comput Environ Urban Syst*, vol. 34, no. 4, pp. 345–357, 2010, doi: 10.1016/j.compenvurbsys.2010.01.001.

[25] A. Lopez, B. Roberts, D. Heimiller, N. Blair, and G. Porro, "U.S. Renewable Energy Technical Potentials: A GIS-Based Analysis," *National Renewable Energy Laboratory Document*, vol. 1, no. 7, pp. 1–40, 2012, doi: NREL/TP-6A20-51946.

[26] J. A. Rosas-Flores, E. Zenón-Olvera, and D. M. Gálvez, "Potential energy saving in urban and rural households of Mexico with solar photovoltaic systems using geographical information system," *Renewable and Sustainable Energy Reviews*, vol. 116, no. May, 2019, doi: 10.1016/j.rser.2019.109412.

[27] R. Vardimon, "Assessment of the potential for distributed photovoltaic electricity production in Israel," *Renew Energy*, vol. 36, no. 2, pp. 591–594, 2011, doi: 10.1016/j.renene.2010.07.030.

[28] L. Bergamasco and P. Asinari, "Scalable methodology for the photovoltaic solar energy potential assessment based on available roof surface area: Application to Piedmont Region (Italy)," *Solar Energy*, vol. 85, no. 5, pp. 1041–1055, 2011, doi: 10.1016/j.solener.2011.02.022.

[29] P. Denholm, R. Margolis, and National Renewable Energy Laboratory, "Supply Curves for Rooftop Solar PV-Generated Electricity for the United States," *National Renewable Energy Laboratory*, no. November, pp. 1–23, 2008.

[30] G. Lobaccaro *et al.*, "A cross-country perspective on solar energy in urban planning: Lessons learned from international case studies," *Renewable and Sustainable Energy Reviews*, vol. 108, no. February, pp. 209–237, 2019, doi: 10.1016/j.rser.2019.03.041.

[31] J. Kanters and M. Wall, "A planning process map for solar buildings in urban environments," *Renewable and Sustainable Energy Reviews*, vol. 57, pp. 173–185, 2016, doi: 10.1016/j.rser.2015.12.073.

[32] International Energy Agency IEA, "Potential for building integrated photovoltaics," *IEA-PVPS Task*, vol. 2002, pp. 2–4, 2002.

[33] J. Paidipati, L. Frantzis, H. Sawyer, and A. Kurrasch, "Rooftop photovoltaics market penetration scenarios," *Renewable Energy Grid Interaction: The Business of Photovoltaics*, no. February, pp. 1–26, 2009.

[34] M. Karteris, T. Slini, and A. M. Papadopoulos, “Urban solar energy potential in Greece: A statistical calculation model of suitable built roof areas for photovoltaics,” *Energy Build*, vol. 62, pp. 459–468, 2013, doi: 10.1016/j.enbuild.2013.03.033.

[35] CEC, “Electric Generation Capacity and Energy,” 2021. https://www.energy.ca.gov/data-reports/energy-almanac/california-electricity-data/electric-generation-capacity-and-energy (accessed Oct. 07, 2021).

[36] “Bill Text - SB-100 California Renewables Portfolio Standard Program: emissions of greenhouse gases.” https://leginfo.legislature.ca.gov/faces/billTextClient.xhtml?bill_id=201720180SB100 (accessed Oct. 07, 2021).

[37] E. G. J. Brown, *Executive Order B-16-12*. 2012.

[38] Executive Order N-79-20. 2020.

[39] Gavin Newsom, *Executive Order N-19-19*. 2019, pp. 1–4. Accessed: Oct. 06, 2021. [Online]. Available: https://www.gov.ca.gov/wp-content/uploads/2019/09/9.20.19-Climate-EO-N-19-19.pdf

[40] Bill Text - SB-129 Budget Act of 2021. 2021.

[41] E. B. Jr. Brown, *Executive Order B-48-18*. 2018.

[42] G. N. Tiwari and S. Dubey, *Fundamentals of Photovoltaic Modules and their Applications*. 2009. doi: 10.1039/9781849730952.

[43] W. R. Smythe, “Static and dynamic electricity,” p. 623, 1989.

[44] W. Gorman, A. Mills, and R. Wiser, “Improving estimates of transmission capital costs for utility-scale wind and solar projects to inform renewable energy policy,” *Energy Policy*, vol. 135, no. May, p. 110994, 2019, doi: 10.1016/j.enpol.2019.110994.

[45] Southern California Edison, “2021 General Rate Case Load Growth , Transmission Projects and Engineering,” 2019.

[46] A. Arabkoohsar and H. Nami, “Chapter Four - Pumped hydropower storage,” in *Mechanical Energy Storage Technologies*, Academic Press, 2020, pp. 73–100. doi: 10.1016/B978-0-12-820023-0.00004-3.

[47] B. Tarroja, K. Forrest, F. Chiang, A. AghaKouchak, and S. Samuelsen, “Implications of hydropower variability from climate change for a future, highly-renewable electric grid in California,” *Appl Energy*, vol. 237, no. December 2018, pp. 353–366, 2019, doi: 10.1016/j.apenergy.2018.12.079.

[48] Y. Zheng and M. Sahraei-Ardakani, “Leveraging existing water and wastewater infrastructure to develop distributed pumped storage hydropower in California,” *J Energy Storage*, vol. 34, p. 102204, Feb. 2021, doi: 10.1016/J.EST.2020.102204.

[49] X. Luo, J. Wang, M. Dooner, and J. Clarke, “Overview of current development in electrical energy storage technologies and the application potential in power system operation,” *Appl Energy*, vol. 137, pp. 511–536, 2015, doi: 10.1016/j.apenergy.2014.09.081.

[50] E. Drury, P. Denholm, and R. Sioshansi, “The value of compressed air energy storage in energy and reserve markets,” *Energy*, vol. 36, no. 8, pp. 4959–4973, Aug. 2011, doi: 10.1016/J.ENERGY.2011.05.041.

[51] A. Foley and I. Díaz Lobera, “Impacts of compressed air energy storage plant on an electricity market with a large renewable energy portfolio,” *Energy*, vol. 57, pp. 85–94, Aug. 2013, doi: 10.1016/J.ENERGY.2013.04.031.

[52] S. Donadei and G. S. Schneider, “Compressed Air Energy Storage in Underground Formations,” *Storing Energy: With Special Reference to Renewable Energy Sources*, pp. 113–133, Jan. 2016, doi: 10.1016/B978-0-12-803440-8.00006-3.

[53] Z. Heydarzadeh, D. McVay, R. Flores, C. Thai, and J. Brouwer, “Dynamic Modeling of California Grid-Scale Hydrogen Energy Storage,” *ECS Trans*, vol. 86, no. 13, p. 245, Jul. 2018, doi: 10.1149/08613.0245ECST.

[54] J. Cho, S. Jeong, and Y. Kim, “Commercial and research battery technologies for electrical energy storage applications,” *Prog Energy Combust Sci*, vol. 48, pp. 84–101, Jun. 2015, doi: 10.1016/J.PECS.2015.01.002.

[55] C. Zhang, Y. L. Wei, P. F. Cao, and M. C. Lin, “Energy storage system: Current studies on batteries and power condition system,” *Renewable and Sustainable Energy Reviews*, vol. 82, pp. 3091–3106, Feb. 2018, doi: 10.1016/J.RSER.2017.10.030.

[56] A. R. Dehghani-Sanij, E. Tharumalingam, M. B. Dusseault, and R. Fraser, “Study of energy storage systems and environmental challenges of batteries,” *Renewable and Sustainable Energy Reviews*, vol. 104, pp. 192–208, Apr. 2019, doi: 10.1016/J.RSER.2019.01.023.

[57] T. Terlouw, T. AlSkaif, C. Bauer, and W. van Sark, “Multi-objective optimization of energy arbitrage in community energy storage systems using different battery technologies,” *Appl Energy*, vol. 239, no. January, pp. 356–372, 2019, doi: 10.1016/j.apenergy.2019.01.227.

[58] S. Varghese and R. Sioshansi, “The price is right? How pricing and incentive mechanisms in California incentivize building distributed hybrid solar and energy-storage systems,” *Energy Policy*, vol. 138, no. January, p. 111242, 2020, doi: 10.1016/j.enpol.2020.111242.

[59] A. Vafamehr, R. Moslemi, and R. Sharma, “Aggregation of BTM Battery Storages to Provide Ancillary Services in Wholesale Electricity Markets,” *Proceedings of 2019 the 7th International Conference on Smart Energy Grid Engineering, SEGE 2019*, pp. 162–166, 2019, doi: 10.1109/SEGE.2019.8859939.

[60] B. Cheng and W. B. Powell, “Co-Optimizing Battery Storage for the Frequency Regulation and Energy Arbitrage Using Multi-Scale Dynamic Programming,” *IEEE Trans Smart Grid*, vol. 9, no. 3, pp. 1997–2005, 2018, doi: 10.1109/TSG.2016.2605141.

[61] F. Wankmüller, P. R. Thimmapuram, K. G. Gallagher, and A. Botterud, “Impact of battery degradation on energy arbitrage revenue of grid-level energy storage,” *J Energy Storage*, vol. 10, pp. 56–66, 2017, doi: 10.1016/j.est.2016.12.004.

[62] K. Bradbury, L. Pratson, and D. Patiño-Echeverri, “Economic viability of energy storage systems based on price arbitrage potential in real-time U.S. electricity markets,” *Appl Energy*, vol. 114, pp. 512–519, 2014, doi: 10.1016/j.apenergy.2013.10.010.

[63] J. A. Dowling *et al.*, “Role of Long-Duration Energy Storage in Variable Renewable Electricity Systems,” *Joule*, pp. 1–22, 2020, doi: 10.1016/j.joule.2020.07.007.

[64] A. Narayanan, K. Mets, M. Strobbe, and C. Develder, “Feasibility of 100% renewable energy-based electricity production for cities with storage and flexibility,” *Renew Energy*, vol. 134, pp. 698–709, 2019, doi: 10.1016/j.renene.2018.11.049.

[65] Z. Abdin and W. Mérida, “Hybrid energy systems for off-grid power supply and hydrogen production based on renewable energy: A techno-economic analysis,” *Energy Convers Manag*, vol. 196, no. January, pp. 1068–1079, 2019, doi: 10.1016/j.enconman.2019.06.068.

[66] R. Walawalkar, J. Apt, and R. Mancini, “Economics of electric energy storage for energy arbitrage and regulation in New York,” *Energy Policy*, vol. 35, no. 4, pp. 2558–2568, 2007, doi: 10.1016/j.enpol.2006.09.005.

[67] R. L. Fares and M. E. Webber, “What are the tradeoffs between battery energy storage cycle life and calendar life in the energy arbitrage application?,” *J Energy Storage*, vol. 16, pp. 37–45, 2018, doi: 10.1016/j.est.2018.01.002.

[68] B. Gundogdu, D. Gladwin, and D. Stone, “Battery energy management strategies for UK firm frequency response services and energy arbitrage,” *The Journal of Engineering*, vol. 2019, no. 17, pp. 4152–4157, 2019, doi: 10.1049/joe.2018.8226.

[69] P. L. Denholm and R. M. Margolis, “The Potential for Energy Storage to Provide Peaking Capacity in California Under Increased Penetration of Solar Photovoltaics,” 2018. [Online]. Available: http://www.osti.gov/servlets/purl/1427348/

[70] J. Eichman, A. Townsend, and M. Melaina, “Economic Assessment of Hydrogen Technologies Participating in California Electricity Markets Economic Assessment of Hydrogen Technologies Participating in California Electricity Markets,” *National Renewable Energy Laboratory*, no. February, p. 31, 2016.

[71] L. Göransson and F. Johnsson, “Dispatch modeling of a regional power generation system - Integrating wind power,” *Renew Energy*, vol. 34, no. 4, pp. 1040–1049, 2009, doi: 10.1016/j.renene.2008.08.002.

[72] O. Babacan, E. L. Ratnam, V. R. Disfani, and J. Kleissl, “Distributed energy storage system scheduling considering tariff structure, energy arbitrage and solar PV penetration,” *Appl Energy*, vol. 205, no. July, pp. 1384–1393, 2017, doi: 10.1016/j.apenergy.2017.08.025.

[73] K. Bassett, R. Carriveau, and D. S. K. Ting, “Energy arbitrage and market opportunities for energy storage facilities in Ontario,” *J Energy Storage*, vol. 20, no. April, pp. 478–484, 2018, doi: 10.1016/j.est.2018.10.015.

[74] R. H. Byrne, T. A. Nguyen, D. A. Copp, R. J. Concepcion, B. R. Chalamala, and I. Gyuk, “Opportunities for Energy Storage in CAISO: Day-Ahead and Real-Time Market Arbitrage,” *SPEEDAM 2018 - Proceedings: International Symposium on Power Electronics, Electrical Drives, Automation and Motion*, pp. 63–68, 2018, doi: 10.1109/SPEEDAM.2018.8445408.

[75] X. Yan, C. Gu, F. Li, and Z. Wang, “LMP-Based Pricing for Energy Storage in Local Market to Facilitate PV Penetration,” *IEEE Transactions on Power Systems*, vol. 33, no. 3, pp. 3373–3382, 2018, doi: 10.1109/TPWRS.2017.2785286.

[76] J. Zarnikau, C. H. Tsai, and C. K. Woo, “Determinants of the wholesale prices of energy and ancillary services in the U.S. Midcontinent electricity market,” *Energy*, vol. 195, p. 117051, 2020, doi: 10.1016/j.energy.2020.117051.

[77] N. Parker, R. Williams, R. Dominguez-Faus, and D. Scheitrum, “Renewable natural gas in California: An assessment of the technical and economic potential,” *Energy Policy*, vol. 111, pp. 235–245, Dec. 2017, doi: 10.1016/J.ENPOL.2017.09.034.

[78] L. R. C. Assunção, P. A. S. Mendes, S. Matos, and S. Borschiver, “Technology roadmap of renewable natural gas: Identifying trends for research and development to improve biogas upgrading technology management,” *Appl Energy*, vol. 292, p. 116849, Jun. 2021, doi: 10.1016/J.APENERGY.2021.116849.

[79] B. C. Murray, C. S. Galik, and T. Vegh, “Biogas in the United States: An Assessment of Market Potential in a Carbon-Constrained Future,” Feb. 2014.

[80] B. Lane, J. Reed, B. Shaffer, and S. Samuelsen, “Forecasting renewable hydrogen production technology shares under cost uncertainty,” *Int J Hydrogen Energy*, vol. 46, no. 54, pp. 27293–27306, Aug. 2021, doi: 10.1016/J.IJHYDENE.2021.06.012.

[81] UC Irvine Advanced Power and Energy Program, "Roadmap for the Deployment and Buildout of Renewable Hydrogen Production Plants in California Prepared for: California Energy Commission Prepared by: UC Irvine Advanced Power and Energy Program," Jun. 2020.

[82] D. Haeseldonckx and W. D'haeseleer, "The use of the natural-gas pipeline infrastructure for hydrogen transport in a changing market structure," *Int J Hydrogen Energy*, vol. 32, no. 10–11, pp. 1381–1386, 2007, doi: 10.1016/j.ijhydene.2006.10.018.

[83] A. Hormaza Mejia, J. Brouwer, and M. Mac Kinnon, "Hydrogen leaks at the same rate as natural gas in typical low-pressure gas infrastructure," *Int J Hydrogen Energy*, vol. 45, no. 15, pp. 8810–8826, Mar. 2020, doi: 10.1016/j.ijhydene.2019.12.159.

[84] Z. Hafsi, S. Elaoud, and M. Mishra, "A computational modelling of natural gas flow in looped network: Effect of upstream hydrogen injection on the structural integrity of gas pipelines," *J Nat Gas Sci Eng*, vol. 64, no. January, pp. 107–117, 2019, doi: 10.1016/j.jngse.2019.01.021.

[85] B. Wang, Y. Liang, J. Zheng, R. Qiu, M. Yuan, and H. Zhang, "An MILP model for the reformation of natural gas pipeline networks with hydrogen injection," *Int J Hydrogen Energy*, vol. 43, no. 33, pp. 16141–16153, 2018, doi: 10.1016/j.ijhydene.2018.06.161.

[86] I. A. Gondal, "Hydrogen integration in power-to-gas networks," *Int J Hydrogen Energy*, vol. 44, no. 3, pp. 1803–1815, 2019, doi: 10.1016/j.ijhydene.2018.11.164.

[87] A. Ekhtiari, D. Flynn, and E. Syron, "Investigation of the Multi-Point Injection of Green Hydrogen from Curtailed Renewable Power into a Gas Network," *Energies (Basel)*, vol. 13, no. 22, p. 6047, 2020, doi: 10.3390/en13226047.

[88] G. Guandalini, P. Colbertaldo, and S. Campanari, "Dynamic modeling of natural gas quality within transport pipelines in presence of hydrogen injections," *Appl Energy*, vol. 185, pp. 1712–1723, 2017, doi: 10.1016/j.apenergy.2016.03.006.

[89] C. J. Quarton and S. Samsatli, "Should we inject hydrogen into gas grids? Practicalities and whole-system value chain optimisation," *Appl Energy*, vol. 275, no. May, p. 115172, 2020, doi: 10.1016/j.apenergy.2020.115172.

[90] S. Samsatli and N. J. Samsatli, "The role of renewable hydrogen and inter-seasonal storage in decarbonising heat – Comprehensive optimisation of future renewable energy value chains," *Appl Energy*, vol. 233–234, no. June 2018, pp. 854–893, 2019, doi: 10.1016/j.apenergy.2018.09.159.

[91] N. Gray, S. McDonagh, R. O'Shea, B. Smyth, and J. D. Murphy, "Decarbonising ships, planes and trucks: An analysis of suitable low-carbon fuels for the maritime, aviation and haulage sectors," *Advances in Applied Energy*, vol. 1, no. January, p. 100008, 2021, doi: 10.1016/j.adapen.2021.100008.

[92] X. Mao, D. Rutherford, L. Osipova, and B. Comer, “Refueling assessment of a zero-emission container corridor between China and the United States: Could hydrogen replace fossil fuels?,” *International Council on Clean Transportation*, no. March, 2020.

[93] J. W. Pratt and L. E. Klebanoff, “Feasibility of the SF-BREEZE : a Zero-Emission , Hydrogen Fuel Cell , High-Speed Passenger Ferry,” no. September, 2016.

[94] NCE, “Norwegian future value chains for liquid hydrogen,” *NCE Maritime CleanTech*, p. 84, 2019.

[95] OECD, “Decarbonising Maritime Transport. Pathways to zero-carbon shipping by 2035,” *International Transport Forum*, p. 86, 2018.

[96] A. Patonia and R. Poudineh, Ammonia as a storage solution for future decarbonized energy systems, no. November. 2020.

[97] Z. Liu, K. Kendall, and X. Yan, “China progress on renewable energy vehicles: Fuel cells, hydrogen and battery hybrid vehicles,” *Energies (Basel)*, vol. 12, no. 1, pp. 1–10, 2019, doi: 10.3390/en12010054.

[98] F. Mariani, “Cost Analysis of LNG refuelling stations,” no. 321592, p. 62, 2016.

[99] J. Hu, S. You, M. Lind, and J. Østergaard, “Coordinated charging of electric vehicles for congestion prevention in the distribution grid,” *IEEE Trans Smart Grid*, vol. 5, no. 2, pp. 703–711, 2014, doi: 10.1109/TSG.2013.2279007.

[100] P. Staudt, M. Schmidt, J. Gärttner, and C. Weinhardt, “A decentralized approach towards resolving transmission grid congestion in Germany using vehicle-to-grid technology,” *Appl Energy*, vol. 230, no. September, pp. 1435–1446, 2018, doi: 10.1016/j.apenergy.2018.09.045.

[101] F. van Triel and T. E. Lipman, “Modeling the future California electricity grid and renewable energy integration with electric vehicles,” *Energies (Basel)*, vol. 13, no. 20, pp. 1–20, 2020, doi: 10.3390/en13205277.

[102] T. Fletcher and K. Ebrahimi, “The Effect of Fuel Cell and Battery Size on Efficiency and Cell Lifetime for an L7e Fuel Cell Hybrid Vehicle,” *Energies (Basel)*, vol. 13, no. 22, p. 5889, 2020, doi: 10.3390/en13225889.

[103] P. Colombo, A. Saeedmanesh, M. Santarelli, and J. Brouwer, “Dynamic dispatch of solid oxide electrolysis system for high renewable energy penetration in a microgrid,” *Energy Convers Manag*, vol. 204, no. May, p. 112322, 2020, doi: 10.1016/j.enconman.2019.112322.

[104] M. Di Salvo and M. Wei, “Synthesis of natural gas from thermochemical and power-to-gas pathways for industrial sector decarbonization in California,” *Energy*, vol. 182, pp. 1250–1264, 2019, doi: 10.1016/j.energy.2019.04.212.

[105] A. H. Sanstad, S. McMenamin, A. Sukenik, G. L. Barbose, and C. A. Goldman, “Modeling an aggressive energy-efficiency scenario in long-range load forecasting for electric power transmission planning,” *Appl Energy*, vol. 128, pp. 265–276, 2014, doi: 10.1016/j.apenergy.2014.04.096.

[106] L. Göransson, J. Goop, T. Unger, M. Odenberger, and F. Johnsson, “Linkages between demand-side management and congestion in the European electricity transmission system,” *Energy*, vol. 69, pp. 860–872, 2014, doi: 10.1016/j.energy.2014.03.083.

[107] Z. Yang, K. Xie, J. Yu, H. Zhong, N. Zhang, and Q. X. Xia, “A General Formulation of Linear Power Flow Models: Basic Theory and Error Analysis,” *IEEE Transactions on Power Systems*, vol. 34, no. 2, pp. 1315–1324, 2019, doi: 10.1109/TPWRS.2018.2871182.

[108] M. Dashtdar, M. Najafi, and M. Esmaeilbeig, “Calculating the locational marginal price and solving optimal power flow problem based on congestion management using GA-GSF algorithm,” *Electrical Engineering*, vol. 102, no. 3, pp. 1549–1566, 2020, doi: 10.1007/s00202-020-00974-z.

[109] Q. Li, D. W. Gao, L. Cheng, F. Zhang, and W. Yan, “Fully Distributed DC Optimal Power Flow Based on Distributed Economic Dispatch and Distributed State Estimation,” pp. 1–8, 2019.

[110] M. Cain, R. O’Neill, and A. Castillo, “History of Optimal Power Flow and Formulations (OPF Paper 1),” *FERC Staff Tech. Pap.*, no. December, pp. 1–36, 2012.

[111] E. Litvinov, T. Zheng, G. Rosenwald, and P. Shamsollahi, “Marginal loss modeling in LMP calculation,” *IEEE Transactions on Power Systems*, vol. 19, no. 2, pp. 880–888, 2004, doi: 10.1109/TPWRS.2004.825894.

[112] K. Purchala, L. Meeus, D. Van Dommelen, and R. Belmans, “Usefulness of DC power flow for active power flow analysis,” *2005 IEEE Power Engineering Society General Meeting*, vol. 1, pp. 454–459, 2005, doi: 10.1109/pes.2005.1489581.

[113] A. Castillo and D. F. Gayme, “Evaluating the effects of real power losses in optimal power flow-based storage integration,” *IEEE Trans Control Netw Syst*, vol. 5, no. 3, pp. 1132–1145, 2018, doi: 10.1109/TCNS.2017.2687819.

[114] C. F. Heuberger, E. S. Rubin, I. Staffell, N. Shah, and N. Mac Dowell, “Power capacity expansion planning considering endogenous technology cost learning,” *Appl Energy*, vol. 204, no. July, pp. 831–845, Oct. 2017, doi: 10.1016/j.apenergy.2017.07.075.

[115] T. Mai *et al.*, "The role of input assumptions and model structures in projections of variable renewable energy: A multi-model perspective of the U.S. electricity system," *Energy Econ*, vol. 76, pp. 313–324, 2018, doi: 10.1016/j.eneco.2018.10.019.

[116] N. Johnson and J. Ogden, "A spatially-explicit optimization model for long-term hydrogen pipeline planning," *Int J Hydrogen Energy*, vol. 37, no. 6, pp. 5421–5433, 2012, doi: 10.1016/j.ijhydene.2011.08.109.

[117] P. Kluschke and F. Neumann, "Interaction of a Hydrogen Refueling Station Network for Heavy-Duty Vehicles and the Power System in Germany for 2050," 2019.

[118] J. Goop, M. Odenberger, and F. Johnsson, "The effect of high levels of solar generation on congestion in the European electricity transmission grid," *Appl Energy*, vol. 205, no. July, pp. 1128–1140, 2017, doi: 10.1016/j.apenergy.2017.08.143.

[119] M. Jentsch, T. Trost, and M. Sterner, "Optimal Use of Power-to-Gas Energy Storage Systems in an 85% Renewable Energy Scenario," *Energy Procedia*, vol. 46, pp. 254–261, Jan. 2014, doi: 10.1016/J.EGYPRO.2014.01.180.

[120] P. K. Rose and F. Neumann, "Hydrogen refueling station networks for heavy-duty vehicles in future power systems," *Transp Res D Transp Environ*, vol. 83, no. May, p. 102358, 2020, doi: 10.1016/j.trd.2020.102358.

[121] S. Roy, P. Sinha, and S. I. Shah, "Assessing the techno-economics and environmental attributes of utility-scale PV with battery energy storage systems (PVS) compared to conventional gas peakers for providing firm capacity in California," *Energies (Basel)*, vol. 13, no. 2, 2020, doi: 10.3390/en13020488.

[122] M. A. Cohen and D. S. Callaway, "Effects of distributed PV generation on California's distribution system, Part 1: Engineering simulations," *Solar Energy*, vol. 128, pp. 126–138, 2016, doi: 10.1016/j.solener.2016.01.002.

[123] S. Tian *et al.*, "Environmental Benefit-Detriment Thresholds for Flow Battery Energy Storage Systems : A Case Study in California," no. 949.

[124] J. Coignard, P. Macdougall, F. Stadtmueller, and E. Vrettos, "Will Electric Vehicles Drive Distribution Grid Upgrades?: The Case of California," *IEEE Electrification Magazine*, vol. 7, no. 2, pp. 46–56, 2019, doi: 10.1109/MELE.2019.2908794.

[125] M. A. Cohen, P. A. Kauzmann, and D. S. Callaway, "Effects of distributed PV generation on California's distribution system, part 2: Economic analysis," *Solar Energy*, vol. 128, pp. 139–152, 2016, doi: 10.1016/j.solener.2016.01.004.

[126] N. Zhang, Z. Li, X. Zou, and S. M. Quiring, "Comparison of three short-term load forecast models in Southern California," *Energy*, vol. 189, p. 116358, 2019, doi: 10.1016/j.energy.2019.116358.

[127] S. Wang, B. Tarroja, L. S. Schell, B. Shaffer, and S. Samuelsen, "Prioritizing among the end uses of excess renewable energy for cost-effective greenhouse gas emission reductions," *Appl Energy*, vol. 235, no. June 2018, pp. 284–298, 2019, doi: 10.1016/j.apenergy.2018.10.071.

[128] B. Zhao *et al.*, "Air Quality and Health Cobenefits of Different Deep Decarbonization Pathways in California," *Environ Sci Technol*, vol. 53, no. 12, pp. 7163–7171, 2019, doi: 10.1021/acs.est.9b02385.

[129] D. Shawhan *et al.*, "A detailed power system planning model: Estimating the long-run impact of carbon-reducing policies," *Proceedings of the Annual Hawaii International Conference on System Sciences*, vol. 2015-March, pp. 2497–2506, 2015, doi: 10.1109/HICSS.2015.300.

[130] A. Asadinejad, K. Tomsovic, and M. G. Varzaneh, "Examination of incentive based demand response in western connection reduced model," *2015 North American Power Symposium, NAPS 2015*, 2015, doi: 10.1109/NAPS.2015.7335170.

[131] P. R. Brown and F. M. O'Sullivan, "Spatial and temporal variation in the value of solar power across United States electricity markets," *Renewable and Sustainable Energy Reviews*, vol. 121, no. July, 2020, doi: 10.1016/j.rser.2019.109594.

[132] S. Tierney, "Resource Adequacy and Wholesale Market Structure for a Future Low-Carbon Power System in California," pp. 1–25, 2018.

[133] R. Orvis and S. Aggarwal, "Refining competitive electricity market rules to unlock flexibility," *Electricity Journal*, vol. 31, no. 5, pp. 31–37, 2018, doi: 10.1016/j.tej.2018.05.012.

[134] F. Egli, "Renewable energy investment risk: An investigation of changes over time and the underlying drivers," *Energy Policy*, vol. 140, no. April 2019, p. 111428, 2020, doi: 10.1016/j.enpol.2020.111428.

[135] C. R. Flor and S. L. Hansen, *Technological advances and the decision to invest*, vol. 9, no. 3. 2013. doi: 10.1007/s10436-012-0191-4.

[136] L. He, L. Zhang, Z. Zhong, D. Wang, and F. Wang, "Green credit, renewable energy investment and green economy development: Empirical analysis based on 150 listed companies of China," *J Clean Prod*, vol. 208, pp. 363–372, 2019, doi: 10.1016/j.jclepro.2018.10.119.

[137] L. He, R. Liu, Z. Zhong, D. Wang, and Y. Xia, "Can green financial development promote renewable energy investment efficiency? A consideration of bank credit," *Renew Energy*, vol. 143, pp. 974–984, 2019, doi: 10.1016/j.renene.2019.05.059.

[138] M. Guo, Y. Hu, and J. Yu, “The role of financial development in the process of climate change: Evidence from different panel models in China,” *Atmos Pollut Res*, vol. 10, no. 5, pp. 1375–1382, 2019, doi: 10.1016/j.apr.2019.03.006.

[139] A. Masini and E. Menichetti, “Investment decisions in the renewable energy sector: An analysis of non-financial drivers,” *Technol Forecast Soc Change*, vol. 80, no. 3, pp. 510–524, 2013, doi: 10.1016/j.techfore.2012.08.003.

[140] A. Boute, “Regulatory stability and renewable energy investment: The case of Kazakhstan,” *Renewable and Sustainable Energy Reviews*, vol. 121, no. November 2019, p. 109673, 2020, doi: 10.1016/j.rser.2019.109673.

[141] J. Liu, D. Zhang, J. Cai, and J. Davenport, “Legal Systems, National Governance and Renewable Energy Investment: Evidence from Around the World,” *British Journal of Management*, vol. 00, pp. 1–32, 2019, doi: 10.1111/1467-8551.12377.

[142] L. Liu, M. Zhang, and Z. Zhao, “The application of real option to renewable energy investment: A review,” *Energy Procedia*, vol. 158, pp. 3494–3499, 2019, doi: 10.1016/j.egypro.2019.01.921.

[143] S. R. Sinsel, R. L. Riemke, and V. H. Hoffmann, “Challenges and solution technologies for the integration of variable renewable energy sources—a review,” *Renew Energy*, vol. 145, pp. 2271–2285, 2020, doi: 10.1016/j.renene.2019.06.147.

[144] K. Hansen, C. Breyer, and H. Lund, “Status and perspectives on 100% renewable energy systems,” *Energy*, vol. 175, pp. 471–480, 2019, doi: 10.1016/j.energy.2019.03.092.

[145] J. B. Ang, P. G. Fredriksson, and S. Sharma, “Individualism and the adoption of clean energy technology,” *Resour Energy Econ*, vol. 61, p. 101180, 2020, doi: 10.1016/j.reseneeco.2020.101180.

[146] B. R. Lukanov and E. M. Krieger, “Distributed solar and environmental justice: Exploring the demographic and socio-economic trends of residential PV adoption in California,” *Energy Policy*, vol. 134, no. August, p. 110935, 2019, doi: 10.1016/j.enpol.2019.110935.

[147] J. Rode and A. Weber, “Does localized imitation drive technology adoption? A case study on rooftop photovoltaic systems in Germany,” *J Environ Econ Manage*, vol. 78, pp. 38–48, 2016, doi: 10.1016/j.jeem.2016.02.001.

[148] J. A. Hayward and P. W. Graham, “A global and local endogenous experience curve model for projecting future uptake and cost of electricity generation technologies,” *Energy Econ*, vol. 40, pp. 537–548, 2013, doi: 10.1016/j.eneco.2013.08.010.

[149] J. Huenteler, C. Niebuhr, and T. S. Schmidt, “The effect of local and global learning on the cost of renewable energy in developing countries,” *J Clean Prod*, vol. 128, pp. 6–21, 2016, doi: 10.1016/j.jclepro.2014.06.056.

[150] O. Schmidt, S. Melchior, A. Hawkes, and I. Staffell, “Projecting the Future Levelized Cost of Electricity Storage Technologies,” *Joule*, vol. 3, no. 1, pp. 81–100, Jan. 2019, doi: 10.1016/j.joule.2018.12.008.

[151] A. Hassan, M. K. Patel, and D. Parra, “An assessment of the impacts of renewable and conventional electricity supply on the cost and value of power-to-gas,” *Int J Hydrogen Energy*, vol. 44, no. 19, pp. 9577–9593, 2019, doi: 10.1016/j.ijhydene.2018.10.026.

[152] M. Wei, S. J. Smith, and M. D. Sohn, “Experience curve development and cost reduction disaggregation for fuel cell markets in Japan and the US,” *Appl Energy*, vol. 191, pp. 346–357, 2017, doi: 10.1016/j.apenergy.2017.01.056.

[153] Battelle Memorial Institute, “Manufacturing Cost Analysis of PEM Fuel Cell Systems for 5- and 10-kW Backup Power Applications,” no. October, p. 124, 2016.

[154] J. R. Schmidt-Costa, M. Uriona-Maldonado, and O. Possamai, “Product-service systems in solar PV deployment programs: What can we learn from the California Solar Initiative?,” *Resour Conserv Recycl*, vol. 140, no. December 2017, pp. 145–157, 2019, doi: 10.1016/j.resconrec.2018.09.017.

[155] S. O. Hazboun, M. Briscoe, J. Givens, and R. Krannich, “Keep quiet on climate: Assessing public response to seven renewable energy frames in the Western United States,” *Energy Res Soc Sci*, vol. 57, no. July, p. 101243, 2019, doi: 10.1016/j.erss.2019.101243.

[156] Z. Tzankova, “Public policy spillovers from private energy governance: New opportunities for the political acceleration of renewable energy transitions,” *Energy Res Soc Sci*, vol. 67, no. March, p. 101504, 2020, doi: 10.1016/j.erss.2020.101504.

[157] E. O. Shaughnessy *et al.*, “Community Choice Aggregation: Challenges , Opportunities , and Impacts on Renewable Energy Markets Community Choice Aggregation: Challenges , Opportunities , and Impacts on Renewable Energy Markets,” *National Renewable EnergyLaboratory (NREL)*, no. February, pp. 1–56, 2019.

[158] D. Vogel, “Promoting Sustainable Government Regulation: What We Can Learn From California,” *Organ Environ*, vol. 32, no. 2, pp. 145–158, 2019, doi: 10.1177/1086026619842517.

[159] D. J. Hess and D. Lee, “Energy decentralization in California and New York: Conflicts in the politics of shared solar and community choice,” *Renewable and Sustainable Energy Reviews*, vol. 121, p. 109716, 2020, doi: 10.1016/j.rser.2020.109716.

[160] M. Topcu and C. T. Tugcu, “The impact of renewable energy consumption on income inequality: Evidence from developed countries,” *Renew Energy*, vol. 151, pp. 1134–1140, 2020, doi: 10.1016/j.renene.2019.11.103.

[161] C. G. Monyei, B. K. Sovacool, M. A. Brown, K. E. H. Jenkins, S. Viriri, and Y. Li, "Justice, poverty, and electricity decarbonization," *Electricity Journal*, vol. 32, no. 1, pp. 47–51, 2019, doi: 10.1016/j.tej.2019.01.005.

[162] J. L. Reyna and M. V. Chester, "Energy efficiency to reduce residential electricity and natural gas use under climate change," *Nat Commun*, vol. 8, no. May 2017, pp. 1–12, 2017, doi: 10.1038/ncomms14916.

[163] S. Wang, L. Sun, and S. Iqbal, "Green financing role on renewable energy dependence and energy transition in E7 economies," *Renew Energy*, vol. 200, pp. 1561–1572, Nov. 2022, doi: 10.1016/J.RENENE.2022.10.067.

[164] J. L. Fan, J. X. Wang, J. W. Hu, Y. Yang, and Y. Wang, "Will China achieve its renewable portfolio standard targets? An analysis from the perspective of supply and demand," *Renewable and Sustainable Energy Reviews*, vol. 138, p. 110510, Mar. 2021, doi: 10.1016/J.RSER.2020.110510.

[165] G. Wang, Q. Zhang, Y. Li, B. C. Mclellan, and X. Pan, "Corrective regulations on renewable energy certificates trading: Pursuing an equity-efficiency trade-off," *Energy Econ*, vol. 80, pp. 970–982, May 2019, doi: 10.1016/J.ENECO.2019.03.008.

[166] P. Colbertaldo, S. B. Agustin, S. Campanari, and J. Brouwer, "Impact of hydrogen energy storage on California electric power system: Towards 100% renewable electricity," *Int J Hydrogen Energy*, vol. 44, no. 19, pp. 9558–9576, 2019, doi: 10.1016/j.ijhydene.2018.11.062.

[167] J. Bistline, N. Santen, and D. Young, "The economic geography of variable renewable energy and impacts of trade formulations for renewable mandates," *Renewable and Sustainable Energy Reviews*, vol. 106, no. March, pp. 79–96, 2019, doi: 10.1016/j.rser.2019.02.026.

[168] H. Lo, S. Blumsack, P. Hines, and S. Meyn, "Electricity rates for the zero marginal cost grid," *Electricity Journal*, vol. 32, no. 3, pp. 39–43, 2019, doi: 10.1016/j.tej.2019.02.010.

[169] J. Ossenbrink, S. Finnsson, C. R. Bening, and V. H. Hoffmann, "Delineating policy mixes: Contrasting top-down and bottom-up approaches to the case of energy-storage policy in California," *Res Policy*, vol. 48, no. 10, 2019, doi: 10.1016/j.respol.2018.04.014.

[170] P. Cramton, "Why We Need to Stick with Uniform-Price Auctions in," *The Electricity Journal*, vol. 20, no. 1, pp. 1040–6190, 2007.

[171] "California Electric Transmission Line." https://cecgis-caenergy.opendata.arcgis.com/datasets/california-electric-transmission-line?geometry=-124.776%2C34.753%2C-114.482%2C37.851 (accessed May 11, 2018).

[172] “California ISO - Price Map.” http://www.caiso.com/PriceMap/Pages/default.aspx (accessed Jan. 06, 2020).

[173] Lazard, “Table of Contents目次,” *Nihon Naika Gakkai Zasshi*, vol. 107, no. 1, pp. Contents1–Contents1, 2018, doi: 10.2169/naika.107.contents1.

[174] Z. Chen, B. Xia, C. C. Mi, and R. Xiong, “Loss-Minimization-Based Charging Strategy for Lithium-Ion Battery,” *IEEE Trans Ind Appl*, vol. 51, no. 5, pp. 4121–4129, Sep. 2015, doi: 10.1109/TIA.2015.2417118.

[175] N. Yang, X. Zhang, B. Shang, and G. Li, “Unbalanced discharging and aging due to temperature differences among the cells in a lithium-ion battery pack with parallel combination,” *J Power Sources*, vol. 306, pp. 733–741, Feb. 2016, doi: 10.1016/j.jpowsour.2015.12.079.

[176] J. Reed and S. Samuelsen, “Renewable Hydrogen Production Roadmap Project Results Summary,” 2019.

[177] D. Papageorgopoulos, “Fuel Cells R&D Overview,” 2019.

[178] B. D. James and C. Houchins, “2018 DOE Hydrogen and Fuel Cells Program Review Hydrogen Storage Cost Analysis,” 2018.

[179] J. A. Salva, A. Iranzo, F. Rosa, E. Tapia, E. Lopez, and F. Isorna, “Optimization of a PEM fuel cell operating conditions: Obtaining the maximum performance polarization curve,” *Int J Hydrogen Energy*, vol. 41, no. 43, pp. 19713–19723, Nov. 2016, doi: 10.1016/j.ijhydene.2016.03.136.

[180] T. L. Gibson and N. A. Kelly, “Predicting efficiency of solar powered hydrogen generation using photovoltaic-electrolysis devices,” *Int J Hydrogen Energy*, vol. 35, no. 3, pp. 900–911, Feb. 2010, doi: 10.1016/j.ijhydene.2009.11.074.

[181] “California Average Grid Electricity Used as a transportation fuel in California.”

[182] R. Dominguez-Faus, “The carbon intensity of NGV C8 trucks.”

[183] R. Derwent, P. Simmonds, S. O’Doherty, A. Manning, W. Collins, and D. Stevenson, “Global environmental impacts of the hydrogen economy,” *International Journal of Nuclear Hydrogen Production and Applications*, vol. 1, no. 1, p. 57, 2006, doi: 10.1504/ijnhpa.2006.009869.

[184] M. Mac Kinnon, Z. Heydarzadeh, Q. Doan, C. Ngo, J. Reed, and J. Brouwer, “Need for a marginal methodology in assessing natural gas system methane emissions in response to incremental consumption,” *J Air Waste Manage Assoc*, vol. 00, no. 00, pp. 1–9, 2018, doi: 10.1080/10962247.2018.1476274.

[185] “Argonne GREET Model.” https://greet.es.anl.gov/ (accessed Jul. 05, 2018).

[186] “Gaseous hydrogen: Flammability Safetygram 4.”

[187] USDrive, “Hydrogen Storage Technologies Roadmap Hydrogen Delivery Technical Team Roadmap,” 2013.

[188] C. Yang and J. Ogden, “Determining the lowest-cost hydrogen delivery mode,” *Int J Hydrogen Energy*, vol. 32, no. 2, pp. 268–286, Feb. 2007, doi: 10.1016/J.IJHYDENE.2006.05.009.

[189] L. The Mendota Group, “Benchmarking Transmission and Distribution Avoided by Energy Energy Efficiency Investments,” 2014.

[190] S. Ericson and D. Olis, “A Comparison of Fuel Choice for Backup Generators,” *National Renewable Energy Laboratory, Technical Report NREL/TP-6A50-72509*, no. March, p. 59, 2019.

[191] J. Eichman and F. Flores-espino, “California Power-to-Gas and Business Case Evaluation,” no. December, pp. 1–70, 2016.

[192] D. Aas, A. Mahone, Z. Subin, M. MacKinnon, B. Lane, and S. Price, “The Challenge of Retail Gas in California’s Low-Carbon Future Appendices A-G.”

[193] “California ISO - Annual and quarterly reports.” http://www.caiso.com/market/Pages/MarketMonitoring/AnnualQuarterlyReports/Default.aspx (accessed Aug. 26, 2020).

[194] “Product Catalog,” 2015.

[195] P. C. Ryan, N.E.; Larsen, K.M.; Black, “Smaller, Closer, Dirtier: Diesel Backup Generators in California,” 2002.

[196] California Air Resources Board (CARB), “Risk Management Guidance for the Permitting of New Stationary Diesel-Fueled Engines,” no. October, 2000.

[197] J. Kurtz, G. Saur, S. Sprik, and C. Ainscough, “Backup Power Cost of Ownership Analysis and Incumbent Technology Comparison,” no. September, p. 31, 2014.

[198] D. Painter, “private communication.”

[199] “Manufacturing Cost Analysis of 100 and 250 kW Fuel Cell Systems for Primary Power and Combined Heat and Power Applications,” 2016.

[200] H. S. Das, C. W. Tan, A. H. M. Yatim, and K. Y. Lau, “Feasibility analysis of hybrid photovoltaic/battery/fuel cell energy system for an indigenous residence in East

Malaysia," *Renewable and Sustainable Energy Reviews*, vol. 76, no. March 2016, pp. 1332–1347, 2017, doi: 10.1016/j.rser.2017.01.174.

[201] "DOE Technical Targets for Hydrogen Delivery | Department of Energy." https://www.energy.gov/eere/fuelcells/doe-technical-targets-hydrogen-delivery (accessed Dec. 20, 2019).

[202] Lazard, "Lazard's Levelized Cost of Storage Analysis - Version 6.0," 2020.

[203] K. Mongird *et al.*, "Energy Storage Technology and Cost Characterization Report | Department of Energy," no. July, 2019.

[204] Generac Industrial Power, "TCO Calculator - Total Cost of Ownership (TCO) Calculator." http://roicalc.gastechnology.org/ROICalculator (accessed Jan. 22, 2021).

[205] "Lazard's Levelized Cost of Energy Analysis - Version 11.0." https://www.lazard.com/media/450337/lazard-levelized-cost-of-energy-version-110.pdf (accessed Jan. 22, 2021).

[206] "Climate Action Plan: University of California, Irvine 2016 Update," 2016.

[207] ARC Alternatives, "Deep Energy Efficiency and Cogeneration Study Findings Report," *Deep Energy Efficiency and Cogeneration Study Findings Report*, 2014.

[208] United Nations Conference on Trade and Development, *REVIEW OF MARITIME TRANSPORT 2021.* UNITED NATIONS, 2022.

[209] UNCTAD, "Global Trade Update," 2022. Accessed: Apr. 14, 2022. [Online]. Available: https://unctad.org/system/files/official-document/ditcinf2022d1_en.pdf

[210] International Transport Forum, *ITF Transport Outlook 2019*. OECD, 2019. doi: 10.1787/transp_outlook-en-2019-en.

[211] International Marine Organization Marine Environment Protection Committee, "REDUCTION OF GHG EMISSIONS FROM SHIPS: 4th IMO Greenhouse Gas Study 2020 - Final Report," 2020. doi: 10.1017/CBO9781107415324.004.

[212] J. D. Marshall, K. R. Swor, and N. P. Nguyen, "Prioritizing Environmental Justice and Equality: Diesel Emissions in Southern California," 2014, doi: 10.1021/es405167f.

[213] G. A. Bishop, B. G. Schuchmann, D. H. Stedman, and D. R. Lawson, "Emission Changes Resulting from the San Pedro Bay, California Ports Truck Retirement Program," *Environ. Sci. Technol*, vol. 46, pp. 551–558, 2012, doi: 10.1021/es202392g.

[214] A. P. Ault, M. J. Moore, H. Furutani, and K. A. Prather, “Impact of Emissions from the Los Angeles Port Region on San Diego Air Quality during Regional Transport Events,” *Environ Sci Technol*, vol. 43, no. 10, pp. 3500–3506, 2009, doi: 10.1021/es8018918.

[215] F. W. Geels, “Disruption and low-carbon system transformation: Progress and new challenges in socio-technical transitions research and the Multi-Level Perspective,” *Energy Res Soc Sci*, vol. 37, no. September 2017, pp. 224–231, 2018, doi: 10.1016/j.erss.2017.10.010.

[216] P. J. Loftus, A. M. Cohen, J. C. S. Long, and J. D. Jenkins, “A critical review of global decarbonization scenarios: What do they tell us about feasibility?,” *Wiley Interdiscip Rev Clim Change*, vol. 6, no. 1, pp. 93–112, 2015, doi: 10.1002/wcc.324.

[217] A. G. Boulanger, A. C. Chu, S. Maxx, and D. L. Waltz, “Vehicle electrification: Status and issues,” *Proceedings of the IEEE*, vol. 99, no. 6, pp. 1116–1138, 2011, doi: 10.1109/JPROC.2011.2112750.

[218] Y. Van Fan, S. Perry, J. J. Klemeš, and C. T. Lee, “A review on air emissions assessment: Transportation,” *J Clean Prod*, vol. 194, pp. 673–684, Sep. 2018, doi: 10.1016/j.jclepro.2018.05.151.

[219] C. Yang, D. L. McCollum, R. McCarthy, and W. Leighty, “Identifying Options for Deep Reductions in Greenhouse Gas Emissions from California Transportation: Meeting an 80% Reduction Goal in 2050,” *Institute of Transportation Studies, Working Paper Series*, Sep. 2008.

[220] A. Mahone *et al.*, “Deep Decarbonization in a High Renewables Future.”

[221] M. N. Taptich, A. Horvath, and M. V. Chester, “Worldwide Greenhouse Gas Reduction Potentials in Transportation by 2050,” *J Ind Ecol*, vol. 20, no. 2, pp. 329–340, Apr. 2016, doi: 10.1111/jiec.12391.

[222] F. Creutzig *et al.*, “Transport: A roadblock to climate change mitigation?,” *Science (1979)*, vol. 350, no. 6263, pp. 911–912, 2015, doi: 10.1126/science.aac8033.

[223] S. J. Davis *et al.*, “Net-zero emissions energy systems,” *Science (1979)*, vol. 360, no. 6396, 2018, doi: 10.1126/science.aas9793.

[224] P. Kluschke, T. Gnann, P. Plötz, and M. Wietschel, “Market diffusion of alternative fuels and powertrains in heavy-duty vehicles: A literature review,” *Energy Reports*, vol. 5, pp. 1010–1024, Nov. 2019, doi: 10.1016/j.egyr.2019.07.017.

[225] K. Çağatay Bayindir, M. A. Gözüküçük, and A. Teke, “A comprehensive overview of hybrid electric vehicle: Powertrain configurations, powertrain control techniques and electronic control units,” *Energy Convers Manag*, vol. 52, no. 2, pp. 1305–1313, 2011, doi: 10.1016/j.enconman.2010.09.028.

[226] W. Zhuang *et al.*, "A survey of powertrain configuration studies on hybrid electric vehicles," *Appl Energy*, vol. 262, no. December 2019, p. 114553, 2020, doi: 10.1016/j.apenergy.2020.114553.

[227] J. Osorio-Tejada, E. Llera, and S. Scarpellini, "LNG: an alternative fuel for road freight transport in Europe," vol. 168, pp. 235–246, 2015, doi: 10.2495/sd150211.

[228] J. L. Osorio-Tejada, E. Llera-Sastresa, and S. Scarpellini, "Liquefied natural gas: Could it be a reliable option for road freight transport in the EU?," *Renewable and Sustainable Energy Reviews*, vol. 71, no. December 2016, pp. 785–795, 2017, doi: 10.1016/j.rser.2016.12.104.

[229] J. H. Yuan, S. Zhou, T. D. Peng, G. H. Wang, and X. M. Ou, "Petroleum substitution, greenhouse gas emissions reduction and environmental benefits from the development of natural gas vehicles in China," *Pet Sci*, vol. 15, no. 3, pp. 644–656, 2018, doi: 10.1007/s12182-018-0237-y.

[230] F. Y. Al-Aboosi, M. M. El-Halwagi, M. Moore, and R. B. Nielsen, "Renewable ammonia as an alternative fuel for the shipping industry," *Curr Opin Chem Eng*, vol. 31, p. 100670, 2021, doi: 10.1016/j.coche.2021.100670.

[231] R. C. Armstrong *et al.*, "The frontiers of energy," *Nat Energy*, vol. 1, no. 1, pp. 1–8, 2016, doi: 10.1038/nenergy.2015.20.

[232] A. Brown *et al.*, "Advanced Biofuels – Potential for Cost Reduction," *IEA Bionenergy*, pp. 1–88, 2020.

[233] W. Leighty, J. M. Ogden, and C. Yang, "Modeling transitions in the California light-duty vehicles sector to achieve deep reductions in transportation greenhouse gas emissions," *Energy Policy*, vol. 44, pp. 52–67, May 2012, doi: 10.1016/j.enpol.2012.01.013.

[234] J. Reed *et al.*, "Roadmap for the Deployment and Buildout of Renewable Hydrogen Production Plants in California," 2020.

[235] A. K. Madhusudhanan, X. Na, A. Boies, and D. Cebon, "Modelling and evaluation of a biomethane truck for transport performance and cost," *Transp Res D Transp Environ*, vol. 87, no. September, p. 102530, 2020, doi: 10.1016/j.trd.2020.102530.

[236] N. Yilmaz, "Comparative analysis of biodiesel-ethanol-diesel and biodiesel-methanol-diesel blends in a diesel engine," *Energy*, vol. 40, no. 1, pp. 210–213, 2012, doi: 10.1016/j.energy.2012.01.079.

[237] M. H. Langholtz, B. J. Stokes, and L. M. Eaton, "2016 Billion-ton report: Advancing domestic resources for a thriving bioeconomy, Volume 1: Economic availability of feedstock," *Oak Ridge National Laboratory, Oak Ridge, Tennessee, managed by UT-Battelle, LLC for the US Department of Energy*, vol. 2016, pp. 1–411, 2016.

[238] R. L. Skaggs, A. M. Coleman, T. E. Seiple, and A. R. Milbrandt, “Waste-to-Energy biofuel production potential for selected feedstocks in the conterminous United States,” *Renewable and Sustainable Energy Reviews*, vol. 82, no. April 2017, pp. 2640–2651, 2018, doi: 10.1016/j.rser.2017.09.107.

[239] A. K. Madhusudhanan, X. Na, A. Boies, and D. Cebon, “Modelling and evaluation of a biomethane truck for transport performance and cost,” *Transp Res D Transp Environ*, vol. 87, no. September, p. 102530, 2020, doi: 10.1016/j.trd.2020.102530.

[240] J. Kast, R. Vijayagopal, J. J. Gangloff Jr, and J. Marcinkoski, “Clean commercial transportation: Medium and heavy duty fuel cell electric trucks,” *Int J Hydrogen Energy*, vol. 42, no. 7, pp. 4508–4517, 2017.

[241] J. Minnehan and J. Pratt, “Practical Application Limits of Fuel Cells and Batteries for Zero Emission Vessels,” Albuquerque, NM, and Livermore, CA (United States), Nov. 2017. doi: 10.2172/1410178.

[242] A. S. Martinez, J. Brouwer, and G. S. Samuelsen, “Feasibility study for SOFC-GT hybrid locomotive power part II. System packaging and operating route simulation,” *J Power Sources*, vol. 213, no. x, pp. 358–374, 2012, doi: 10.1016/j.jpowsour.2012.04.023.

[243] A. Saeedmanesh, M. A. Mac Kinnon, and J. Brouwer, “Hydrogen is essential for sustainability,” *Curr Opin Electrochem*, vol. 12, pp. 166–181, 2018, doi: 10.1016/j.coelec.2018.11.009.

[244] O. Lah, “Decarbonizing the transportation sector: policy options, synergies, and institutions to deliver on a low-carbon stabilization pathway,” *Wiley Interdiscip Rev Energy Environ*, vol. 6, no. 6, pp. 1–13, 2017, doi: 10.1002/wene.257.

[245] P. Parthasarathy and K. S. Narayanan, “Hydrogen production from steam gasification of biomass: Influence of process parameters on hydrogen yield - A review,” *Renew Energy*, vol. 66, pp. 570–579, 2014, doi: 10.1016/j.renene.2013.12.025.

[246] A. Muscat, E. M. de Olde, I. J. M. de Boer, and R. Ripoll-Bosch, “The battle for biomass: A systematic review of food-feed-fuel competition,” *Global Food Security*, vol. 25. Elsevier B.V., Jun. 01, 2020. doi: 10.1016/j.gfs.2019.100330.

[247] Z. Abdin, A. Zafaranloo, A. Rafiee, W. Mérida, W. Lipiński, and K. R. Khalilpour, “Hydrogen as an energy vector,” *Renewable and Sustainable Energy Reviews*, vol. 120, no. December 2019, 2020, doi: 10.1016/j.rser.2019.109620.

[248] P. Parthasarathy and K. S. Narayanan, “Hydrogen production from steam gasification of biomass: Influence of process parameters on hydrogen yield - A review,” *Renew Energy*, vol. 66, pp. 570–579, 2014, doi: 10.1016/j.renene.2013.12.025.

[249] S. M. Saba, M. Müller, M. Robinius, and D. Stolten, “The investment costs of electrolysis – A comparison of cost studies from the past 30 years,” *Int J Hydrogen Energy*, vol. 43, no. 3, pp. 1209–1223, 2018, doi: 10.1016/j.ijhydene.2017.11.115.

[250] O. Schmidt, A. Gambhir, I. Staffell, A. Hawkes, J. Nelson, and S. Few, “Future cost and performance of water electrolysis: An expert elicitation study,” *Int J Hydrogen Energy*, vol. 42, no. 52, pp. 30470–30492, Dec. 2017, doi: 10.1016/J.IJHYDENE.2017.10.045.

[251] S. Schiebahn, T. Grube, M. Robinius, V. Tietze, B. Kumar, and D. Stolten, “Power to gas: Technological overview, systems analysis and economic assessment for a case study in Germany,” *Int J Hydrogen Energy*, vol. 40, no. 12, pp. 4285–4294, 2015, doi: 10.1016/j.ijhydene.2015.01.123.

[252] I. Staffell *et al.*, “The role of hydrogen and fuel cells in the global energy system,” *Energy Environ Sci*, vol. 12, no. 2, pp. 463–491, 2019, doi: 10.1039/c8ee01157e.

[253] C. Yang and J. Ogden, “Determining the lowest-cost hydrogen delivery mode,” *Int J Hydrogen Energy*, vol. 32, no. 2, pp. 268–286, 2007, doi: 10.1016/j.ijhydene.2006.05.009.

[254] M. Moreno-Benito, P. Agnolucci, and L. G. Papageorgiou, “Towards a sustainable hydrogen economy: Optimisation-based framework for hydrogen infrastructure development,” *Comput Chem Eng*, vol. 102, pp. 110–127, 2017, doi: 10.1016/j.compchemeng.2016.08.005.

[255] J. Adolf *et al.*, “Shell hydrogen study: Energy of the future?,” *Shell Deutschland Oil GmbH*, p. 72, 2017.

[256] P. Agnolucci, O. Akgul, W. McDowall, and L. G. Papageorgiou, “The importance of economies of scale, transport costs and demand patterns in optimising hydrogen fuelling infrastructure: An exploration with SHIPMod (Spatial hydrogen infrastructure planning model),” *Int J Hydrogen Energy*, vol. 38, no. 26, pp. 11189–11201, 2013, doi: 10.1016/j.ijhydene.2013.06.071.

[257] J. . L. Gillette and R. L. Kolpa, “Overview of interstate hydrogen pipeline systems.,” Argonne, IL, Feb. 2008. doi: 10.2172/924391.

[258] A. H. Mejia, J. Brouwer, and M. Mac Kinnon, “Hydrogen leaks at the same rate as natural gas in typical low-pressure gas infrastructure,” *Int J Hydrogen Energy*, 2020.

[259] Argonne National Laboratory Environmental Science Division, “Overview of Interstate Hydrogen Pipeline Systems”, Accessed: Jan. 09, 2022. [Online]. Available: www.anl.gov.

[260] S. Shiva Kumar and V. Himabindu, “Hydrogen production by PEM water electrolysis – A review,” *Mater Sci Energy Technol*, vol. 2, no. 3, pp. 442–454, Dec. 2019, doi: 10.1016/J.MSET.2019.03.002.

[261] IRENA, Hydrogen: a renewable energy perspective, no. September. 2019.

[262] IRENA, “Hydrogen from Renewable Power: Technology Outlook for the Energy Transition,” 2018.

[263] D. Haeseldonckx and W. D’haeseleer, “The use of the natural-gas pipeline infrastructure for hydrogen transport in a changing market structure,” *Int J Hydrogen Energy*, vol. 32, no. 10–11, pp. 1381–1386, 2007, doi: 10.1016/j.ijhydene.2006.10.018.

[264] I. Staffell *et al.*, “The role of hydrogen and fuel cells in the global energy system,” *Energy Environ Sci*, vol. 12, no. 2, pp. 463–491, 2019, doi: 10.1039/c8ee01157e.

[265] M. Dadfarnia, P. Sofronis, J. Brouwer, and S. Sosa, “Assessment of resistance to fatigue crack growth of natural gas line pipe steels carrying gas mixed with hydrogen,” *Int J Hydrogen Energy*, vol. 44, no. 21, pp. 10808–10822, 2019.

[266] P. A. Kempler, J. J. Slack, and A. M. Baker, “Research priorities for seasonal energy storage using electrolyzers and fuel cells,” *Joule*, Jan. 2022, doi: 10.1016/j.joule.2021.12.020.

[267] Association of American Railroads, “State Rank State,” 2017. https://www.aar.org/wp-content/uploads/2019/05/AAR-State-Rankings-2017.pdf

[268] B. of T. S. U.S. Department of Transportation, “Freight Flows By State | Bureau of Transportation Statistics.” https://www.bts.gov/freight-flows-state (accessed Sep. 21, 2020).

[269] F. Pavley and F. Nunez, *California Assembly Bill No. 32-Global Warming Solutions Act of 2006*, vol. 5, no. 32. 2006, pp. 38500–38599.

[270] N. Bautista, “08/28/18- Senate Floor Analysis for Bill No. SB 100,” Sacramento, 2018.

[271] California Energy Commission, “The Challenge of Retail Gas in California’s Low-Carbon Future,” 2020.

[272] Federal Highway Administration Freight Management and Operations, “Freight Analysis Framework,” 2017.

[273] California Air Resource Board, “Vision 2.1 Scenario Modeling System,” pp. 1–40, 2017.

[274] “Shipping Schedules | Vessel Schedules | Maersk.”

[275] “INVENTORY OF AIR EMISSIONS FOR CALENDAR YEAR 2017,” 2018.

[276] “A Global Presence - Connecting Trade | Maersk.”

[277] IRENA, Hydrogen: a renewable energy perspective, no. September. 2019.

[278] A. Mahone *et al.*, “Deep Decarbonization in a High Renewables Future Updated Results from the California PATHWAYS Model California Energy Commission.”

[279] A. S. Martinez, J. Brouwer, and G. S. Samuelsen, “Comparative analysis of SOFC – GT freight locomotive fueled by natural gas and diesel with onboard reformation,” vol. 148, pp. 421–438, 2015, doi: 10.1016/j.apenergy.2015.01.093.

[280] S. Wang, S. Gao, T. Tan, and W. Yang, “Bunker fuel cost and freight revenue optimization for a single liner shipping service,” *Comput Oper Res*, vol. 111, pp. 67–83, Nov. 2019, doi: 10.1016/j.cor.2019.06.003.

[281] J. J. Corbett, H. Wang, and J. J. Winebrake, “The effectiveness and costs of speed reductions on emissions from international shipping,” *Transp Res D Transp Environ*, vol. 14, no. 8, pp. 593–598, Dec. 2009, doi: 10.1016/J.TRD.2009.08.005.

[282] National Renewable Energy Laboratory, “Solar Resource Data, Tools, and Maps.,” 2018.

[283] National Renewable Energy Laboratory, “Wind Resource Data, Tools, and Maps,” 2017.

[284] B. Zakeri and S. Syri, “Electrical energy storage systems: A comparative life cycle cost analysis,” *Renewable and Sustainable Energy Reviews*, vol. 42, pp. 569–596, 2015, doi: 10.1016/j.rser.2014.10.011.

[285] “National Land Cover Database 2016 (NLCD2016) Legend | Multi-Resolution Land Characteristics (MRLC) Consortium.”

[286] J. A. Schwarz and K. A. G. Amankwah, “Hydrogen storage systems,” *United States Geological Survey*, 1993.

[287] Department of Energy, “DOE H2A Delivery Analysis,” 2006.

[288] U.S. Department of Energy, “Costs of Storing and Transporting Hydrogen.”

[289] J. Reed *et al.*, “Roadmap for the Deployment and Buildout of Renewable Hydrogen Production Plants in California,” 2020.

[290] “PORT OF LOS ANGELES: INVENTORY OF AIR EMISSIONS FOR CALENDAR YEAR 2017,” 2018.

[291] Y. A. Cengel and M. A. Boles, “Thermodynamics: an engineering approach,” *Sea*, vol. 1000, p. 8862, 2002.

[292] M. Vedran, S. Žarković Božica, and P.-O. Jasna, “MARINE SLOW SPEED TWO-STROKE DIESEL ENGINE-NUMERICAL ANALYSIS OF EFFICIENCIES AND IMPORTANT OPERATING PARAMETERS.”

[293] S. F. Sghaier, T. Khir, and A. Ben Brahim, “Energetic and exergetic parametric study of a SOFC-GT hybrid power plant,” *Int J Hydrogen Energy*, vol. 43, no. 6, pp. 3542–3554, Feb. 2018, doi: 10.1016/j.ijhydene.2017.08.216.

[294] “Port Performance Freight Statistics Program.”

[295] O. Merk, B. Busquet, and R. Aronietis, “The Impact of Mega-Ships,” 2015, doi: 10.3399/bjgp14X682705.

[296] W. Murray, “Economies of Scale in Container Ship Costs,” p. 25, 2016.

[297] “Freight Analysis Framework (FAF).”

[298] “Solar Data | Geospatial Data Science | NREL.”

[299] A. C. Tamboli, D. C. Bobela, A. Kanevce, T. Remo, K. Alberi, and M. Woodhouse, “Low-Cost CdTe/Silicon Tandem Solar Cells,” *IEEE J Photovolt*, vol. 7, no. 6, pp. 1767–1772, Nov. 2017, doi: 10.1109/JPHOTOV.2017.2737361.

[300] Lazard, “Lazard’s Levelized Cost of Energy Analysis - version 12.0,” no. November, pp. 0–19, 2018.

[301] J. A. Schwarz and K. A. G. Amankwah, “Hydrogen storage systems,” *United States Geological Survey*, 1993.

[302] O. Schmidt, S. Melchior, A. Hawkes, and I. Staffell, “Projecting the Future Levelized Cost of Electricity Storage Technologies,” *Joule*, 2019, doi: 10.1016/j.joule.2018.12.008.

[303] “National Land Cover Database 2016 (NLCD2016) Legend | Multi-Resolution Land Characteristics (MRLC) Consortium.”

[304] National Renewable Energy Laboratory, “California Wind 50m height,” 2012.

[305] S. Abdelhady, D. Borello, and A. Shaban, “Assessment of levelized cost of electricity of offshore wind energy in Egypt,” *Wind Engineering*, vol. 41, no. 3, pp. 160–173, 2017, doi: 10.1177/0309524X17706846.

[306] “San Pedro Bay Ports Clean Air Action Plan 2017 FINAL,” 2017.

[307] J. Soukup, “Air Quality, GHG, and Human Health Impacts Associated with Fuel Cell Electric Technologies in Port Applications,” University of California, Irvine, 2019.

[308] Califfornia Governor’s Office of Emergency Servies Public Data Hub, “California Electric Transmission Lines | California Energy Commission.” https://cecgis-caenergy.opendata.arcgis.com/datasets/CAEnergy::california-electric-transmission-lines/about (accessed May 16, 2022).

[309] Southern California Association of Governments, “2019 Annual Land Use Dataset (ALU v.2019.2) .” https://gisdata-scag.opendata.arcgis.com/datasets/SCAG::2019-annual-land-use-dataset-alu-v-2019-2/explore?location=34.178870%2C-116.867750%2C8.66 (accessed May 16, 2022).

[310] “California Elevation Map.” https://www.yellowmaps.com/map/california-elevation-map-274.htm#ym-viewmap (accessed Jan. 26, 2023).

[311] United States Census Bureau, “B01001 SEX BY AGE, 2020 American Community Survey 5-Year Estimates,” *U.S. Census Bureau, American Community Survey Office*. https://data.census.gov/cedsci/ (accessed May 16, 2022).

[312] S. Ong, C. Campbell, P. Denholm, R. Margolis, and G. Heath, “Land-Use Requirements for Solar Power Plants in the United States,” 2013. Accessed: May 31, 2019. [Online]. Available: www.nrel.gov/publications.

[313] S. Ong, C. Campbell, P. Denholm, R. Margolis, and G. Heath, “Land-Use Requirements for Solar Power Plants in the United States,” 2013. Accessed: May 29, 2019. [Online]. Available: www.nrel.gov/publications.

[314] Southern California Gas Company, Pacific Gas and Electric Company, San Diego Gas and Electric Company, Southwest Gas Corporation, City of Long Beach Energy Resources Department, and Southern California Edison Company, “2020 California Gas Report,” 2020. Available online: https://www.pge.com/pipeline_resources/pdf/library/regulatory/downloads/cgr20.pdf

[315] California Independent System Operator, “Assessment of the CPUC-Selected 38 MMT Integrated Resource Plan Portfolio.”

[316] California Energy Commission, “Final 2021 Integrated Energy Policy Report Volume IV: California Energy Demand Forecast California Energy Commission,” 2022.

[317] California Energy Commission, “2021 SB 100 Joint Agency Report Achieving 100 Percent Clean Electricity in California: An Initial Assessment,” 2021.

[318] California ISO, “CAISO Board Approved 2018-2019 Transmission Plan,” 2019.

[319] U. Energy Information Administration, “Annual Energy Outlook 2022 Narrative,” 2022. [Online]. Available: www.eia.gov

[320] Lazard, “Lazard’s Levelized Cost of Hydrogen Analysis,” 2021. Accessed: Nov. 08, 2022. [Online]. Available: https://www.lazard.com/media/451922/lazards-levelized-cost-of-hydrogen-analysis-version-20-vf.pdf

[321] IPCC, *Global Warming of 1.5°C*. Cambridge University Press, 2022. doi: 10.1017/9781009157940.

[322] U. Epa and C. Change Division, “Inventory of U.S. Greenhouse Gas Emissions and Sinks: 1990-2020 – Main Text,” 1990. [Online]. Available: https://www.epa.gov/ghgemissions/draft-inventory-us-greenhouse-gas-emissions-

[323] Lazard, “Lazard’s Levelized Cost of Energy Analysis—Version 15.0,” 2021. Available online: https://www.lazard.com/media/451881/lazards-levelized-cost-of-energy-version-150-vf.pdf

[324] International Renewable Energy Agency, *Renewable power generation costs in 2021*. 2022. [Online]. Available: www.irena.org

[325] National Renewable Energy Laboratory, “2018 ATB Cost and Performance Summary.” https://atb.nrel.gov/electricity/2018/summary.html (accessed Apr. 21, 2019).

[326] Lazard, “Lazard’s Levelized Cost of Storage Analysis—Version 7.0”. Available online: https://www.lazard.com/media/451882/lazards-levelized-cost-of-storage-version-70-vf.pdf

[327] P. Beiter *et al.*, “The Cost of Floating Offshore Wind Energy in California Between 2019 and 2032 Cost and Performance Results Data.” [Online]. Available: www.nrel.gov/publications.

[328] California Energy Commission, “Estimated Cost of New Utility-Scale Generation in California: 2018 Update California Energy Commission,” 2019.

[329] “Table 4-43: Estimated National Average Vehicle Emissions Rates per Vehicle by Vehicle Type using Gasoline and Diesel | Bureau of Transportation Statistics.” https://www.bts.gov/archive/publications/national_transportation_statistics/table_04_43 (accessed Nov. 30, 2022).

[330] California Environmental Protection Agency Air Resource Board, “Emission Reduction Offset Transaction Costs Summary Report for 2018,” 2020.

[331] “California Underground Natural Gas Storage Capacity.” https://www.eia.gov/dnav/ng/ng_stor_cap_dcu_SCA_a.htm (accessed Dec. 11, 2022).

10Appendix: Remaining Line Capacity

10.1 L-S Scenario

PG&E_BAY_to_PG&E_VLY												
L-S	Jan.	Feb.	Mar.	Apr.	May.	Jun.	Jul.	Aug.	Sept.	Oct.	Nov.	Dec.
0	924	569	249	63	29	45	40	406	719	911	1066	1012
1	1070	1005	452	82	32	116	242	753	923	1350	1406	1416
2	1438	1206	601	107	40	155	443	917	1328	1558	1877	1728
3	1474	1363	732	87	34	173	291	1025	1232	1502	2293	1857
4	1710	1429	555	80	42	91	241	1050	1127	1487	2225	1888
5	1227	1267	257	54	12	51	132	527	1037	916	1846	1518
6	1407	1287	145	11	2	2	0	42	588	983	1425	1678
7	1336	148	16	187	184	21	15	4	97	111	113	782
8	451	100	124	433	318	51	27	25	36	20	39	334
9	231	210	334	602	326	169	125	84	74	45	31	110
10	126	263	354	489	354	105	47	173	112	76	160	15
11	231	362	275	417	225	80	38	55	67	154	292	140
12	307	498	208	347	253	22	26	0	85	158	287	276
13	206	312	156	307	161	0	0	6	157	79	89	114
14	89	201	66	216	76	61	26	112	337	125	37	35
15	111	73	76	193	121	14	72	174	598	202	17	142
16	445	99	58	63	33	0	193	316	672	389	148	124
17	79	0	0	0	19	0	276	538	277	420	82	316
18	448	97	0	0	0	111	133	767	500	514	75	428
19	376	158	0	0	0	117	215	701	595	492	30	317
20	526	31	0	0	0	91	152	948	808	381	77	406
21	627	81	0	0	0	95	133	1249	1364	404	184	550
22	743	86	0	0	0	4	189	647	792	318	87	440
23	1215	854	1363	1130	1597	1457	1788	1670	1197	1333	872	1070

SCE_to_SDGE												
L-S	Jan.	Feb.	Mar.	Apr.	May.	Jun.	Jul.	Aug.	Sept.	Oct.	Nov.	Dec.
0	2067	2359	2633	2478	2161	2561	1870	1791	2021	2639	1858	2570
1	2215	1951	2596	2394	2086	2390	2899	2757	2588	1778	1846	1709
2	1642	2404	2531	2164	2024	2128	2973	2649	2546	2454	1682	2172
3	1970	2460	2218	1667	2119	2133	2967	2662	2147	2163	1649	1563
4	2247	1999	2847	2069	2071	1846	2738	2312	1838	1790	1843	1713
5	2003	2130	2565	2393	2461	2413	3053	2220	2151	1995	2152	1881
6	2025	2094	2567	2330	2105	1584	2703	2458	2333	1581	2039	1818
7	1703	2902	2464	2118	2429	2008	2110	2078	1891	2805	2858	2183
8	2620	2337	2552	2487	2930	2767	2250	2201	2308	2101	2164	3025
9	2252	1862	2124	1710	2458	1918	2051	2453	1924	2004	1808	2567
10	2059	1809	1876	1761	2037	1725	2202	1895	2013	1890	1684	1706
11	1850	1727	1880	1406	1969	1794	1955	1974	2125	2001	1815	1901
12	1646	2147	1527	1861	1872	2096	1846	2126	1809	1895	2073	2165
13	2058	2125	2344	2692	2356	2028	2254	2242	2261	2033	1893	1726
14	1971	1821	2039	2278	2687	2271	2116	2388	1861	1798	1952	1711
15	1935	1670	1912	2369	2415	2185	1978	1757	1654	1892	1564	1984
16	2764	1352	1935	1661	1950	1674	2184	2488	1919	2825	3033	2993
17	2687	3163	3041	2495	2036	1551	1229	2108	2391	2031	2689	2146
18	2505	2567	2023	1762	1273	714	1450	1538	1999	1920	2377	2316
19	2696	2725	2032	1454	1249	1235	1923	1533	2023	2129	2626	2205
20	3011	3127	2210	1414	1108	979	1707	1453	1924	1936	2962	2548
21	2885	3019	2583	2105	1325	705	1603	1709	2024	2826	2980	2228
22	2825	3048	2696	2455	1733	1253	1283	2051	2332	3057	3089	2873
23	1816	1418	2184	2417	2186	2438	2051	1706	1696	1885	2003	2340

PG&E_VLY_to_SCE												
L-S	Jan.	Feb.	Mar.	Apr.	May.	Jun.	Jul.	Aug.	Sept.	Oct.	Nov.	Dec.
0	2479	2907	2238	1882	1519	425	494	1415	2318	2959	2693	2344
1	2164	2919	2818	2261	1855	810	1147	2221	2567	2864	2357	2077
2	1901	2092	2988	2228	2120	1091	1718	2577	2553	2109	1621	1766
3	1934	1968	2696	2126	2037	1039	1580	2824	2276	2022	1074	1261
4	1586	1552	2334	1891	1711	784	1394	2712	1998	2328	959	1491
5	1607	1898	1699	965	1514	1015	1699	2465	2115	2162	1507	1316
6	1860	1823	1622	321	95	0	0	44	550	1790	1590	1488
7	1883	218	59	372	656	165	0	0	0	0	184	1411
8	109	0	155	241	142	0	0	0	0	0	0	121
9	62	58	101	41	186	0	0	0	0	0	0	0
10	0	0	0	7	166	0	0	0	0	0	0	0
11	11	0	0	0	98	0	0	0	0	0	0	0
12	6	20	0	53	49	0	0	0	0	0	0	9
13	0	0	0	44	115	0	0	0	0	0	0	0
14	22	0	0	154	173	0	0	0	0	0	0	0
15	0	16	91	155	150	6	0	0	0	0	0	0
16	135	102	0	179	219	0	0	0	0	0	0	435
17	274	241	989	340	17	0	0	0	0	26	0	230
18	207	97	269	893	866	119	0	0	128	1	0	218
19	474	114	99	385	130	0	0	137	0	220	0	244
20	512	81	98	401	43	0	0	76	61	179	0	263
21	231	156	481	974	600	14	0	152	246	289	0	660
22	663	154	679	1029	783	251	76	198	237	176	0	666
23	1199	1074	1314	1870	1395	1286	1201	1875	1294	1671	960	1366

SCE_East_to_SCE												
L-S	Jan.	Feb.	Mar.	Apr.	May.	Jun.	Jul.	Aug.	Sept.	Oct.	Nov.	Dec.
0	16	52	0	93	63	122	0	51	0	0	8	79
1	136	54	2	0	116	72	0	52	0	16	54	113
2	151	69	1	1	76	100	0	53	0	62	143	113
3	130	76	5	0	19	67	0	51	5	62	182	111
4	158	86	2	0	71	47	0	50	4	3	234	114
5	130	80	0	96	22	57	1	59	0	0	177	180
6	129	139	0	455	361	690	524	143	0	0	156	187
7	54	45	120	304	484	590	533	239	247	166	3	9
8	98	118	390	284	160	26	131	225	244	428	51	142
9	185	548	287	171	138	4	3	263	113	394	315	267
10	228	407	379	78	108	48	32	39	20	196	485	231
11	246	409	432	82	49	0	31	75	122	281	534	528
12	168	374	183	98	32	0	0	36	173	148	416	356
13	193	274	96	69	142	0	29	42	15	196	393	211
14	436	413	257	111	123	12	45	0	36	444	495	398
15	416	741	516	284	271	65	84	189	374	519	518	181
16	28	712	725	614	525	504	178	37	70	82	0	62
17	66	66	0	190	442	344	0	0	0	0	0	43
18	22	70	0	0	0	0	0	0	66	0	0	64
19	78	71	0	0	0	0	0	0	34	0	0	42
20	106	48	0	0	0	0	0	0	65	0	0	64
21	61	52	0	0	0	0	0	0	0	0	0	64
22	62	56	0	27	7	0	0	0	62	0	0	44
23	210	234	213	163	216	274	93	99	120	158	253	300

SCE_EoL_to_SCE												
L-S	Jan.	Feb.	Mar.	Apr.	May.	Jun.	Jul.	Aug.	Sept.	Oct.	Nov.	Dec.
0	3318	3334	2477	2170	1813	1220	1661	2359	3028	3296	3663	3510
1	3710	3553	2817	2415	2007	1508	1978	2744	3390	3695	4206	4093
2	3938	3808	3010	2537	2290	1576	2280	2934	3529	3967	4508	4203
3	3998	4030	3138	2519	2218	1665	2248	3020	3607	4113	4542	4329
4	4202	4204	3069	2262	1993	1531	2158	3023	3936	4015	4608	4464
5	4128	4190	2478	1661	1956	1704	2224	3152	3836	3914	4484	4443
6	4031	4178	2343	1088	1590	1317	652	711	1678	3386	4465	4473
7	3395	1349	1558	2424	2854	2973	2282	1526	1562	1159	1407	2979
8	1046	1670	2547	2270	2411	2004	2708	2532	2222	1793	1819	1198
9	1333	1945	2714	2752	2530	2372	2462	1943	2288	1908	2088	1306
10	1639	2844	2843	2664	2515	2698	2288	2535	2530	2773	2244	1302
11	1579	3470	3137	2809	2703	2428	1903	2262	2602	2546	2783	2160
12	2038	3334	3268	2984	2365	1941	1800	2137	2021	1915	2793	2366
13	1609	3043	2696	2368	2208	2105	1800	2205	2055	1844	2390	2054
14	1779	2697	2705	2324	2110	1597	1670	2190	1606	1770	1791	1562
15	764	2124	2860	2798	2500	1747	2093	1550	1569	1254	1571	858
16	1376	965	2203	2306	2485	2726	475	196	16	538	514	1313
17	962	711	1348	920	526	761	0	92	303	611	60	929
18	802	505	666	1411	1558	1021	136	261	389	604	45	715
19	1054	513	545	993	1058	874	167	557	476	775	56	879
20	1046	464	498	993	1043	889	158	423	510	608	92	901
21	1222	484	859	1489	1368	898	174	445	477	960	120	979
22	1367	661	1192	1708	1555	1053	282	431	596	967	370	1097
23	4670	4661	4674	4702	4659	4646	4680	4769	4679	4659	4637	4671

SCE_Metro_to_SCE												
L-S	Jan.	Feb.	Mar.	Apr.	May.	Jun.	Jul.	Aug.	Sept.	Oct.	Nov.	Dec.
0	2699	2168	915	579	392	87	260	1348	1436	1994	2153	2735
1	4582	2048	1034	924	574	233	221	1511	1912	2900	3395	4714
2	3885	2238	1424	1079	530	274	593	1414	1647	3389	4507	4032
3	4449	2895	1382	942	714	275	376	1274	2567	3960	3906	4256
4	4948	3594	1510	1062	701	289	608	1675	3486	3453	3860	4963
5	5549	3864	1449	776	715	286	685	2000	3474	3838	4097	4708
6	5421	4319	1501	829	1890	733	554	209	1174	3036	4339	4940
7	2978	1404	1618	2416	2930	1492	1149	946	1278	1403	1342	2503
8	1239	2360	1516	2895	2185	1789	1451	1649	2683	2649	2542	1657
9	1708	2319	2796	3936	3149	2435	1669	2481	2368	3274	2210	2129
10	2613	2970	3253	4240	3191	2860	1767	1886	3037	3279	2864	3214
11	2485	3752	3941	4889	3088	2221	1304	2371	2838	3090	3411	3497
12	2618	3854	4269	4893	3371	1731	1363	2129	2834	4160	4066	2689
13	3666	3554	3773	4189	3333	1773	952	1321	1948	2367	3036	3845
14	3715	3522	3665	3611	3173	1942	1005	1284	1702	2166	3183	3257
15	2412	2634	3235	3541	2308	666	942	1211	1201	1881	1745	1706
16	1478	2193	3052	2224	1718	1085	1160	403	323	83	152	1144
17	1121	654	316	379	301	34	0	98	609	1229	0	1432
18	853	371	9	86	106	0	230	596	831	1388	5	1404
19	1404	500	15	25	0	0	346	912	863	976	12	1005
20	1343	194	6	15	0	0	354	865	846	1029	40	1009
21	1466	425	3	46	1	0	465	697	892	1087	23	1311
22	1478	506	101	165	126	0	330	538	847	1306	219	1528
23	7192	7048	4660	4988	4137	4363	3966	5554	5372	6595	6942	6943

SCE_NoL_to_SCE												
L-S	Jan.	Feb.	Mar.	Apr.	May.	Jun.	Jul.	Aug.	Sept.	Oct.	Nov.	Dec.
0	1021	1027	1153	1160	1157	1134	1094	1079	1046	1089	1012	1013
1	1055	1059	1177	1203	1205	1195	1163	1136	1092	1105	1050	1049
2	1103	1098	1190	1194	1218	1208	1187	1147	1094	1117	1082	1085
3	1113	1104	1190	1163	1195	1180	1156	1140	1094	1113	1095	1103
4	1105	1099	1163	1142	1160	1147	1124	1116	1074	1084	1085	1115
5	1088	1063	1106	1087	1135	1137	1097	1075	1016	1027	1048	1087
6	1015	1018	1066	1088	1137	1124	1084	1052	1001	987	999	1032
7	978	1000	1085	1108	1136	1124	1075	1040	1019	998	1006	1006
8	996	1027	1118	1127	1146	1134	1053	1026	1015	1018	1023	1007
9	1008	1054	1131	1150	1140	1120	1045	1011	1004	1013	1042	1029
10	1046	1083	1137	1149	1155	1092	1001	982	980	1006	1065	1045
11	1054	1100	1133	1154	1138	1062	981	938	964	1025	1075	1075
12	1069	1114	1129	1128	1121	1026	916	900	923	1005	1072	1093
13	1064	1106	1129	1117	1102	992	879	851	888	996	1055	1072
14	1058	1107	1120	1118	1090	968	845	803	846	976	1034	1065
15	1032	1072	1126	1140	1120	976	850	806	829	980	1005	1030
16	1009	1041	1113	1110	1082	942	816	766	807	939	968	989
17	952	960	1030	1047	1012	886	778	738	799	906	900	939
18	916	931	968	987	966	858	768	738	747	898	904	905
19	946	911	965	966	937	850	790	743	792	950	921	965
20	962	954	973	983	941	842	810	778	809	941	941	962
21	966	939	1020	1030	1004	930	886	871	890	1027	955	961
22	1008	999	1074	1081	1043	1004	960	940	963	1043	999	989
23	1015	1022	1100	1102	1094	1065	1027	994	992	1053	1007	1009

SCE_TabCC_to_SCE												
L-S	Jan.	Feb.	Mar.	Apr.	May.	Jun.	Jul.	Aug.	Sept.	Oct.	Nov.	Dec.
0	971	496	101	53	233	382	262	723	396	833	178	1070
1	1727	472	153	198	202	404	158	494	499	821	723	1478
2	1102	310	320	409	182	427	294	420	565	644	624	1245
3	1361	500	334	455	309	382	138	458	562	756	193	978
4	1437	887	269	397	212	413	107	505	1068	750	402	1268
5	1895	894	401	462	507	547	254	860	1344	1359	830	1381
6	2532	1439	662	962	1472	564	1325	582	904	1211	880	1671
7	1358	1273	2087	1514	1756	832	1235	1319	1248	1345	1013	1196
8	1544	2418	1768	3337	2889	3434	2213	1267	1756	1608	2475	1629
9	1834	1499	3163	4349	4094	4167	2969	2485	2477	1781	1864	2003
10	1719	1797	3101	4688	4413	4087	3378	2391	2859	1956	1208	1521
11	1616	1492	3179	4784	4434	4229	3197	2970	2609	2309	1020	1295
12	1643	1892	3363	4720	4293	4151	3342	2505	3046	2729	2259	1304
13	1986	2381	3833	4187	4102	3879	2581	1752	2414	1989	2107	1817
14	1764	2143	2970	3766	3386	3150	2411	1456	2640	1468	1999	1288
15	1622	1251	2629	2895	2197	2117	2074	1897	1061	1486	1204	1448
16	1122	1417	1518	1243	780	744	174	26	29	265	159	573
17	644	221	276	898	874	309	0	67	352	341	2	537
18	583	166	122	81	106	126	171	268	167	251	0	389
19	813	215	147	167	105	107	124	362	190	371	0	508
20	783	87	151	175	137	99	121	278	200	463	12	306
21	989	212	109	61	107	119	65	395	272	438	15	624
22	704	241	86	64	124	142	187	379	515	369	48	655
23	3137	3179	1944	2442	1834	2001	1587	2688	2506	3274	3090	3327

10.2 L-W Scenario

PG&E_BAY_to_PG&E_VLY												
L-W	Jan.	Feb.	Mar.	Apr.	May.	Jun.	Jul.	Aug.	Sept.	Oct.	Nov.	Dec.
0	1102	823	1357	1134	590	904	491	676	919	541	1387	1394
1	1100	880	1382	986	478	753	294	438	814	389	1425	1463
2	1093	821	1138	997	401	777	255	306	755	493	1497	1505
3	1199	905	1232	1130	411	857	311	291	933	514	1408	1431
4	1229	780	1571	1202	502	882	358	389	825	751	1382	1292
5	1191	737	1594	1259	599	665	399	633	935	779	1287	1040
6	1191	866	1295	1028	888	624	697	735	901	762	1321	1140
7	1031	937	1385	920	911	639	688	662	1127	873	1022	1277
8	1083	1263	1383	937	1135	739	902	726	1054	956	1351	996
9	1203	1027	1427	1002	853	712	797	938	1193	873	1424	1016
10	1328	1000	1258	908	737	768	996	1000	1285	839	1132	1068
11	1040	871	1098	708	676	657	1151	1062	1301	937	1135	977
12	1116	750	956	764	806	720	1450	1448	1474	903	1259	841
13	992	711	1103	712	565	582	1192	1455	1322	868	1002	999
14	918	786	1204	971	539	762	1084	1368	1401	1004	1128	843
15	701	870	1126	904	440	759	1010	1337	1048	1250	1184	819
16	877	677	1094	1057	767	738	1293	1269	1434	865	1036	862
17	1028	689	1011	1025	808	756	1122	1440	1435	963	1135	1069
18	903	802	1238	900	841	954	1266	1575	1486	1127	993	1045
19	894	871	1446	950	1039	952	1147	1691	1588	1122	828	961
20	687	833	1293	958	1035	984	1266	1670	1415	1068	916	1074
21	703	886	1408	1021	888	761	1270	1642	1513	947	762	1114
22	715	898	1470	962	936	715	1135	1351	1194	712	959	1181
23	1168	876	1494	1250	1015	976	544	1038	947	947	1597	1462

SCE_to_SDGE												
L-W	Jan.	Feb.	Mar.	Apr.	May.	Jun.	Jul.	Aug.	Sept.	Oct.	Nov.	Dec.
0	1873	1851	2042	2263	1901	1728	1054	1061	1315	1879	1891	1567
1	2244	2197	2479	2239	1883	2085	1357	1368	1716	2480	2322	1987
2	1865	2670	2147	2090	1908	1971	1663	1646	1828	2198	2102	2231
3	1981	1936	1988	1947	1886	1891	1802	1680	1791	2390	1774	1922
4	1469	2388	2339	1981	1820	1796	1849	1618	1833	2326	1951	2292
5	2054	2212	2324	2119	1969	1908	1633	1178	1458	2073	2193	1962
6	1813	2265	1821	2541	2973	2933	2594	1231	1444	1559	2339	1753
7	1306	2316	2744	2095	1933	2033	1663	2315	2121	2849	2667	1387
8	2302	1976	2034	2442	2719	2464	1643	889	1256	1421	1795	2498
9	1548	1114	1626	2158	2208	2105	1603	1031	837	1508	602	1393
10	599	1396	1327	2020	1872	1519	1243	1071	755	1780	555	721
11	810	1711	1452	1938	2193	1622	969	1135	672	1720	484	893
12	763	1939	2188	2074	2067	1493	1536	697	1063	2040	901	611
13	1404	1888	1976	2158	2098	1878	924	1153	1485	1795	1785	1159
14	2143	2101	2116	2151	2393	1718	1551	1266	1438	1885	2239	1898
15	2356	2468	2295	2636	2593	2330	1462	1476	1663	2666	2807	2642
16	2154	2794	2383	2068	1976	1513	1203	710	1148	1271	1963	2033
17	1587	1686	1621	2209	2230	1118	120	128	355	828	1426	1142
18	1159	1284	1165	996	692	172	30	181	241	527	1326	894
19	1311	1212	1111	722	326	181	22	113	281	612	1535	1049
20	1465	1460	1138	636	336	158	4	82	409	551	1811	1301
21	1498	1404	1460	1109	438	278	228	498	1169	1202	1840	1163
22	1892	1772	1751	1428	924	565	132	560	1240	1377	2095	1896
23	831	994	1124	946	760	334	86	38	448	611	1182	912

PG&E_VLY_to_SCE												
L-W	Jan.	Feb.	Mar.	Apr.	May.	Jun.	Jul.	Aug.	Sept.	Oct.	Nov.	Dec.
0	1244	1425	1502	1637	1732	1643	1393	1460	1569	811	1742	1488
1	998	867	1022	1291	1220	1785	1112	1188	1273	598	878	810
2	707	725	697	1256	1167	1613	564	867	996	422	523	482
3	591	644	794	1274	1367	1775	610	767	1076	395	656	470
4	645	622	890	1506	1582	1774	1042	989	1095	669	510	439
5	1006	714	1830	1721	1832	1420	1116	1523	1614	1757	1169	599
6	1434	1482	1931	1686	1809	875	1438	2372	2097	1619	2004	914
7	1790	1944	1692	1788	1173	1311	1191	785	1204	1406	1625	1711
8	1193	1152	1372	1667	2200	2034	2247	1405	953	1114	1143	1452
9	1056	1290	1422	1550	1657	1952	1656	1403	858	1571	909	1301
10	1006	1341	1405	1850	1594	1848	1935	1110	973	1640	812	929
11	1114	1743	1373	1761	1924	1562	2000	1042	964	1662	1122	1006
12	1099	1645	1750	2061	1654	1840	1820	1135	565	1527	1357	757
13	891	1944	1386	2002	1518	2025	1793	1079	791	1457	1164	803
14	1254	1765	1418	1777	1749	1762	1838	1019	813	1643	1027	868
15	1235	1237	1532	1623	2140	1701	1681	624	730	1496	1595	1017
16	1426	859	1293	1038	1487	1431	987	416	243	2024	1739	1536
17	1672	1794	1964	1850	1667	1495	1077	392	673	1458	1176	1579
18	1546	1272	1672	1496	1250	1054	1061	140	342	1394	1384	1460
19	1508	1396	1574	1479	1164	1144	1032	64	423	1853	1397	1613
20	1539	1628	1248	1388	1193	1277	959	207	539	1811	1275	1811
21	1461	1651	1730	1679	1057	1224	1562	619	717	1780	1414	1826
22	1368	1816	1491	1405	1053	1039	1451	1537	1632	1491	1610	1783
23	344	86	180	174	224	370	113	334	391	172	248	300

SCE_East_to_SCE												
L-W	Jan.	Feb.	Mar.	Apr.	May.	Jun.	Jul.	Aug.	Sept.	Oct.	Nov.	Dec.
0	321	820	973	860	647	450	724	535	480	1298	262	167
1	626	1287	1202	849	726	751	994	1004	803	1540	760	423
2	875	1243	1298	869	764	717	1283	1317	987	1544	930	549
3	849	1202	1150	728	631	638	1299	1394	1034	1559	846	645
4	856	1173	837	563	572	678	951	995	820	1284	857	626
5	819	1091	404	358	423	496	778	692	348	439	634	601
6	402	358	240	97	397	275	136	28	30	322	154	353
7	330	30	236	530	935	901	606	412	248	219	0	152
8	76	353	299	312	167	117	482	440	398	405	185	43
9	185	446	368	257	242	126	452	328	274	320	443	202
10	401	436	412	246	317	166	208	371	380	485	465	322
11	438	570	693	365	301	107	224	198	499	255	461	419
12	338	550	484	269	237	91	89	132	199	323	467	475
13	381	330	408	345	301	23	54	50	146	150	549	492
14	354	424	348	169	123	18	0	6	68	364	676	273
15	196	675	583	272	222	68	47	228	335	590	264	100
16	114	224	412	418	681	904	449	273	344	75	117	171
17	3	251	269	131	206	203	246	26	0	30	9	16
18	2	8	206	580	971	539	45	14	0	22	1	21
19	55	28	206	427	673	437	56	0	0	63	24	22
20	21	58	279	422	598	292	113	13	0	64	37	20
21	40	92	358	574	961	716	67	0	0	179	67	24
22	93	206	673	703	1074	1009	773	135	168	477	88	51
23	274	598	700	856	1201	1112	1115	415	479	580	366	337

SCE_EoL_to_SCE												
L-W	Jan.	Feb.	Mar.	Apr.	May.	Jun.	Jul.	Aug.	Sept.	Oct.	Nov.	Dec.
0	3888	3965	3692	3284	2587	2448	3021	3239	3672	4182	3770	3904
1	4172	4445	4044	3522	2937	2746	3504	3635	4048	4497	4276	4345
2	4404	4383	4194	3533	3037	2558	3843	4032	4374	4536	4514	4493
3	4485	4378	4073	3524	2865	2627	3978	4196	4401	4577	4451	4528
4	4464	4353	3792	3238	2607	2523	3580	3848	4210	4330	4508	4573
5	4361	4291	3325	2862	2545	2506	3290	3498	3510	3493	4201	4393
6	3814	3333	2889	2218	2150	1656	1673	2246	2908	2972	3571	4079
7	3519	2719	1524	1835	3161	2737	2781	1769	1928	1732	2167	3516
8	2038	2650	2898	3001	2925	2957	3181	2400	2800	2878	2671	2062
9	2550	3588	3075	3468	3123	3004	3185	2759	2902	3285	3415	2676
10	3111	3568	3279	3275	2992	2865	2992	2790	2695	2970	3549	3241
11	3115	3385	3392	3490	3186	3106	3199	2832	2220	3281	3351	3419
12	2905	3667	3301	3243	3217	2885	2739	2557	2137	2885	3208	3459
13	3116	3414	3259	3145	3296	2985	2481	2565	2331	3095	2845	3204
14	3085	3217	3186	3062	3132	3008	2739	2584	2135	2757	2599	2698
15	2196	2602	3375	2660	2776	2820	2655	2074	1745	1940	1352	1922
16	2957	1487	1536	1744	2349	2460	1073	537	532	2354	2541	2729
17	1820	2937	3188	2510	2053	1218	843	653	745	1867	1327	1770
18	1732	1909	2323	3275	3628	2495	1176	363	511	1758	1331	1789
19	1845	1935	2150	2865	3183	2191	988	315	515	2074	1484	1790
20	1921	2111	2294	2799	2922	1883	792	430	683	2063	1597	1880
21	1991	2234	2620	3347	3658	2942	1626	834	1040	2521	1668	1958
22	2509	2946	3117	3498	3841	3399	3311	2141	2410	3017	2255	2371
23	4655	4656	4677	4706	4666	4653	4716	4815	4693	4661	4636	4671

SCE_Metro_to_SCE												
L-W	Jan.	Feb.	Mar.	Apr.	May.	Jun.	Jul.	Aug.	Sept.	Oct.	Nov.	Dec.
0	506	175	609	712	339	140	0	20	190	170	657	812
1	862	612	861	1063	568	145	11	45	402	439	928	1103
2	1539	650	1238	1348	512	220	35	87	854	1131	1714	1504
3	1724	1546	1426	1513	730	214	58	94	968	915	1898	2026
4	2331	1379	1003	1349	842	190	94	73	668	809	1974	1871
5	1279	1056	414	766	508	228	177	116	482	171	1435	1660
6	905	369	545	682	1603	1317	306	221	401	374	1000	949
7	814	988	1582	2013	2289	1003	887	539	1002	1001	1369	1345
8	1280	2143	2284	3173	1871	1204	572	806	1215	1612	2388	1311
9	1889	3248	2690	3512	2729	1957	340	850	1593	2148	3490	2093
10	3044	3714	3797	4005	2857	1715	530	824	1894	2382	4197	3102
11	3332	3758	4183	4297	2932	1558	513	765	2033	2293	4986	3703
12	3479	4145	3481	3538	2793	1436	242	437	1295	2036	4949	4174
13	3050	4031	4108	4276	2619	964	227	448	1097	2179	3924	3485
14	2991	3649	3868	3210	2325	1104	249	252	597	1969	3768	3029
15	1963	4051	3957	2937	1627	838	174	204	478	1750	1152	1346
16	755	1973	3035	2042	1656	1038	81	0	63	122	206	452
17	99	52	447	418	262	42	0	0	0	0	5	229
18	39	0	0	170	7	0	0	0	0	0	0	199
19	48	0	0	115	0	0	0	0	0	0	17	219
20	91	0	0	87	0	0	0	0	0	0	10	200
21	120	0	2	2	0	0	0	0	0	0	1	266
22	227	19	63	100	0	0	0	0	0	0	99	280
23	1120	701	684	638	383	139	6	171	341	668	1032	1052

SCE_NoL_to_SCE												
L-W	Jan.	Feb.	Mar.	Apr.	May.	Jun.	Jul.	Aug.	Sept.	Oct.	Nov.	Dec.
0	1021	1025	1152	1160	1156	1133	1093	1078	1046	1087	1011	1010
1	1055	1059	1176	1202	1204	1195	1161	1136	1092	1104	1050	1047
2	1103	1098	1189	1193	1217	1208	1186	1146	1094	1116	1082	1085
3	1112	1104	1189	1163	1194	1180	1154	1139	1093	1113	1096	1103
4	1105	1099	1162	1141	1160	1146	1123	1115	1072	1083	1085	1115
5	1086	1063	1106	1089	1135	1138	1097	1073	1014	1021	1049	1086
6	1011	1007	1067	1090	1138	1126	1088	1053	1002	987	1001	1029
7	977	1001	1087	1110	1139	1125	1078	1044	1022	1001	1008	1005
8	998	1031	1122	1131	1149	1137	1053	1029	1019	1022	1027	1009
9	1011	1057	1134	1156	1162	1124	1048	1015	1009	1027	1045	1032
10	1050	1086	1141	1157	1161	1097	1005	1000	996	1032	1069	1048
11	1059	1104	1137	1162	1146	1069	985	955	967	1040	1079	1077
12	1074	1116	1135	1153	1128	1033	933	904	926	1030	1075	1095
13	1076	1112	1133	1140	1108	999	884	855	891	998	1057	1072
14	1061	1108	1120	1124	1094	974	850	807	848	977	1037	1066
15	1035	1075	1127	1143	1122	981	853	809	832	984	1009	1031
16	1009	1044	1115	1112	1083	945	817	766	806	941	967	984
17	923	941	1030	1048	1014	889	777	737	767	888	899	904
18	901	896	967	988	964	858	767	722	748	871	902	900
19	922	907	963	983	935	849	766	726	768	910	920	924
20	956	934	972	983	940	841	785	746	805	926	940	945
21	950	936	1019	1030	1002	929	883	843	887	997	954	939
22	1003	995	1072	1080	1041	1002	956	928	940	1029	997	982
23	1021	1025	1101	1104	1096	1072	1021	996	1011	1051	1015	1016

SCE_TabCC_to_SCE												
L-W	Jan.	Feb.	Mar.	Apr.	May.	Jun.	Jul.	Aug.	Sept.	Oct.	Nov.	Dec.
0	35	20	0	136	72	66	95	1	30	42	1	64
1	146	82	84	178	100	43	146	14	17	161	18	93
2	267	344	195	200	180	171	259	137	100	279	124	181
3	449	577	232	265	188	69	279	149	111	252	191	301
4	381	499	131	200	291	131	188	54	47	121	97	394
5	219	211	20	142	175	113	83	39	21	59	46	355
6	56	95	2	430	978	1401	834	269	33	55	26	121
7	115	322	1435	1340	1168	1048	930	1119	862	830	586	119
8	1015	1413	2256	2964	2653	2699	1370	1887	1640	1278	1805	1304
9	1645	2390	3048	3802	3753	3282	2018	2278	2573	1691	2710	1692
10	2514	3004	3771	4210	3801	3631	2403	2602	2894	2767	3191	2396
11	2760	2993	3981	3975	3699	3679	2839	2285	3333	2680	3949	2990
12	2959	2807	3611	3896	3887	3407	3101	2867	3232	2614	4232	3157
13	2484	3498	4127	4221	3338	3111	3066	2682	2681	2563	3216	2611
14	2038	3206	3841	3519	3124	2782	2461	2008	2007	1807	2446	2149
15	1243	2666	2943	3073	2433	2349	1876	1471	997	747	1188	1579
16	121	1557	1596	1335	977	1000	1272	550	144	89	2	92
17	14	0	10	119	247	649	378	122	13	0	16	36
18	23	13	64	92	63	139	85	22	29	2	3	59
19	52	8	73	99	105	65	8	34	17	3	2	52
20	41	6	81	98	69	93	52	52	0	3	0	58
21	19	3	38	21	88	43	67	19	22	3	21	62
22	11	0	6	41	113	50	73	0	14	0	0	12
23	378	565	322	263	267	148	225	205	354	431	403	299

10.3 H-S Scenario

PG&E_BAY_to_PG&E_VLY												
H-S	Jan.	Feb.	Mar.	Apr.	May.	Jun.	Jul.	Aug.	Sept.	Oct.	Nov.	Dec.
0	1172	371	265	75	6	45	109	356	577	945	751	1172
1	935	1016	417	86	32	137	211	745	1390	1184	1313	1103
2	1659	1002	565	121	66	136	450	949	1182	1401	1868	1442
3	1828	1205	628	104	52	186	320	1030	1242	1484	2313	1706
4	1712	1538	515	84	20	113	336	803	1286	1216	2170	1714
5	1727	1505	359	51	15	48	81	855	1062	935	1699	1770
6	1333	1043	223	9	21	17	0	108	194	742	1221	1520
7	1062	31	18	175	192	26	0	0	58	137	146	791
8	325	79	112	436	363	50	32	10	57	44	23	304
9	268	200	306	556	448	150	131	104	96	56	34	112
10	188	377	395	515	363	87	45	175	169	88	163	43
11	265	292	305	396	169	49	27	136	123	190	302	195
12	340	372	148	334	162	44	8	0	61	178	281	263
13	276	271	164	289	158	46	0	0	134	58	94	122
14	88	110	105	130	116	26	3	21	279	47	15	35
15	102	55	82	283	199	50	72	117	463	200	47	92
16	147	34	55	71	71	0	254	647	629	510	134	571
17	258	0	0	0	11	24	258	562	717	141	66	561
18	470	14	0	0	0	0	249	1108	884	305	0	494
19	474	0	0	0	0	110	237	883	1062	382	21	620
20	479	0	0	0	0	96	436	1238	1234	306	16	576
21	561	0	0	0	0	54	370	1232	1072	396	129	558
22	347	6	0	0	0	4	174	480	591	336	90	534
23	1324	1794	1631	1452	1937	1941	1899	1688	1195	1340	1687	1144

SCE_to_SDGE												
H-S	Jan.	Feb.	Mar.	Apr.	May.	Jun.	Jul.	Aug.	Sept.	Oct.	Nov.	Dec.
0	1409	1854	2984	2550	2416	2273	1663	2386	2341	2299	2042	1784
1	2047	1812	2230	2425	2438	3043	3161	2807	2823	1669	1838	2301
2	1996	1918	2108	2194	2383	2724	3100	2898	2074	2229	2208	2125
3	1988	2236	2170	2377	2127	2574	2989	2547	2224	2202	1970	2459
4	1784	2235	2485	2190	2306	2472	2818	2658	1782	2285	1542	1829
5	2140	1904	2498	2742	2429	2544	3104	2442	2123	1805	2333	1622
6	1429	1837	2633	2126	2209	2025	2404	2555	2502	2204	1756	1999
7	2217	2538	2657	1969	2094	1556	1832	2273	1967	2841	2744	2452
8	2609	2036	2287	2350	2461	2429	1975	1596	1828	1881	1858	2662
9	2051	1846	1934	1742	1984	1878	1738	2036	2102	2348	1552	2090
10	1674	2126	1154	1482	1581	1201	1907	2220	2160	2098	2256	2105
11	2311	1545	1626	1103	1868	1337	1556	1974	2179	1726	2131	1652
12	2154	1970	1749	1794	1573	1375	1580	1594	1894	1630	2322	1909
13	1841	1616	1650	1557	1949	1696	1761	2168	1987	1705	1587	1729
14	1418	1630	1861	1935	2094	2071	1767	2002	1473	1368	1559	1421
15	1772	1401	2498	2190	2071	2120	1790	1403	1435	1438	1615	1994
16	2363	1828	1344	1914	1483	1325	1242	1288	1852	2394	2963	2817
17	2859	3214	2850	1956	1603	1348	2454	2325	2543	2204	2464	2539
18	2506	2502	1953	1749	1451	1012	1713	2364	1886	1852	2177	2318
19	2584	2668	1954	1629	1375	627	1886	2219	2001	2193	2547	2541
20	2966	2995	2177	1536	1176	634	2271	1967	2044	1842	2871	2711
21	2790	3011	2490	1955	1363	899	1234	1506	1977	2584	3073	2731
22	3010	3159	2727	2472	1865	1289	1262	1748	2833	2906	2936	2858
23	1712	1846	2308	2061	2098	1962	2154	1435	1819	1856	1810	1833

PG&E_VLY_to_SCE												
H-S	Jan.	Feb.	Mar.	Apr.	May.	Jun.	Jul.	Aug.	Sept.	Oct.	Nov.	Dec.
0	2488	3027	2357	2406	1906	1153	491	1088	2175	2643	2452	2625
1	2218	2790	2746	2879	1981	1732	856	2207	2909	2489	2843	2285
2	2431	2500	2991	2989	2163	2069	1550	2504	2441	2285	1913	1958
3	1886	1911	2811	2939	2155	1691	1603	2524	2342	1885	1170	1391
4	1951	1476	2637	2519	1999	1396	1408	2296	2202	2379	1292	1549
5	1434	1727	1788	1602	1833	1154	1270	2293	2055	2197	1686	1787
6	2330	2176	1184	93	79	0	0	7	105	1518	1802	1504
7	1102	1	41	372	587	107	0	0	0	0	98	743
8	0	0	185	181	588	404	0	0	0	0	0	8
9	0	0	125	84	315	65	0	0	0	0	0	0
10	0	74	70	9	240	0	0	0	0	32	0	0
11	0	0	32	197	204	36	0	0	0	0	0	0
12	0	20	0	140	207	51	0	0	0	0	0	0
13	0	0	0	45	215	0	0	0	0	0	0	0
14	0	0	0	134	147	118	0	0	0	0	0	0
15	0	0	73	457	659	324	0	0	0	0	0	0
16	4	2	0	142	187	0	0	0	0	0	133	399
17	85	163	396	21	0	0	0	0	57	90	0	104
18	178	1	181	926	862	99	10	0	69	30	0	104
19	10	0	137	290	115	0	0	0	0	0	0	68
20	150	30	124	220	26	0	0	92	93	147	0	153
21	174	0	507	911	499	0	51	0	106	138	31	165
22	154	69	706	1043	777	191	0	162	9	88	0	288
23	1013	1762	1589	1864	1267	1376	1354	1040	1333	1536	1320	940

SCE_East_to_SCE												
H-S	Jan.	Feb.	Mar.	Apr.	May.	Jun.	Jul.	Aug.	Sept.	Oct.	Nov.	Dec.
0	0	0	0	19	150	6	0	0	0	56	0	77
1	23	5	19	9	79	15	0	0	16	72	39	180
2	62	13	27	34	44	21	0	0	39	99	78	170
3	62	17	27	0	40	0	28	0	26	88	117	185
4	42	23	13	0	28	53	0	0	61	36	231	189
5	92	44	7	0	3	112	0	0	15	41	200	197
6	80	169	11	359	459	645	664	374	106	1	102	208
7	3	152	200	741	931	287	725	643	813	397	89	0
8	250	535	595	444	609	640	457	488	519	683	603	316
9	601	588	333	279	427	128	245	180	270	345	446	532
10	533	572	555	421	358	47	200	167	241	473	679	502
11	451	759	493	426	216	56	15	279	137	313	592	506
12	484	596	421	300	158	52	8	5	139	196	426	591
13	565	373	544	430	230	57	106	77	172	474	575	600
14	384	639	637	444	361	34	275	435	217	628	453	627
15	430	640	838	836	807	584	748	715	799	587	635	296
16	83	506	830	446	518	587	461	118	250	283	0	18
17	0	0	230	734	616	585	0	0	0	0	0	13
18	0	0	0	0	0	0	0	0	0	0	0	21
19	0	0	0	0	0	0	0	0	0	0	0	29
20	0	0	0	0	0	0	0	0	0	0	0	29
21	63	0	0	0	0	0	0	0	0	0	0	29
22	0	0	0	1	6	0	0	18	0	0	0	50
23	211	223	213	163	216	274	102	113	118	158	253	287

SCE_EoL_to_SCE												
H-S	Jan.	Feb.	Mar.	Apr.	May.	Jun.	Jul.	Aug.	Sept.	Oct.	Nov.	Dec.
0	3451	3214	2493	2382	1995	1868	1637	1986	3017	3306	3549	3538
1	3674	3446	2796	2692	2166	2074	1872	2462	3213	3722	4101	3943
2	3979	3637	2998	2858	2374	2145	2238	2717	3362	4013	4342	4093
3	4163	3854	3075	2861	2397	2136	2323	2777	3453	4153	4563	4197
4	4268	4117	3026	2657	2251	1916	2215	2568	3629	4055	4569	4377
5	4248	4158	2577	2133	2107	1716	1969	2678	3720	3869	4510	4323
6	4286	4250	1959	848	1001	1161	1145	560	759	2749	4419	4387
7	2663	766	1076	1149	1100	1421	968	1160	832	1051	1242	2094
8	1057	907	2115	2727	3029	3438	3086	1869	2207	1443	1215	1091
9	878	2096	2991	3265	3094	2939	3289	2563	2130	2162	1714	943
10	1214	2157	3504	3276	2964	2742	2386	2988	2778	2513	2417	1355
11	1191	2465	2881	3358	2918	2919	2087	2468	2941	2245	1632	1804
12	1975	3217	2909	2756	3012	2539	2400	2169	2727	2251	2452	1798
13	1479	2575	3364	3114	2729	2590	2134	2828	2739	2011	1993	1363
14	778	2700	3108	3058	2945	2515	2872	2172	2005	2102	1324	867
15	1179	904	2570	3278	3108	3252	3054	2285	1246	849	1103	1618
16	670	1665	1220	924	1471	1618	552	267	347	363	671	1117
17	348	365	728	733	466	630	0	29	87	471	179	634
18	322	154	707	1411	1490	991	90	96	246	323	187	795
19	360	188	545	937	951	782	151	151	49	468	186	650
20	353	166	544	889	899	817	141	279	129	476	200	941
21	525	181	968	1548	1275	836	153	149	120	414	234	909
22	476	309	1340	1734	1529	1075	302	272	291	544	476	998
23	4660	4660	4674	4702	4659	4646	4681	4812	4679	4658	4636	4668

SCE_Metro_to_SCE												
H-S	Jan.	Feb.	Mar.	Apr.	May.	Jun.	Jul.	Aug.	Sept.	Oct.	Nov.	Dec.
0	3168	2131	776	661	414	178	515	873	1815	2274	2165	3485
1	3657	1920	1111	791	596	291	248	777	1576	2942	3154	4300
2	3182	2350	960	837	693	461	693	863	1675	2750	3221	3907
3	3395	2597	1630	1138	551	317	557	780	2294	3181	3348	3652
4	4224	3298	1009	960	775	444	825	950	2765	3588	4462	4314
5	4419	3601	1184	751	649	281	362	1375	3388	3318	4202	5086
6	5427	5005	1052	1067	1705	1601	456	195	282	2026	4674	4437
7	2632	1217	1284	1416	1462	2101	1631	1738	958	1460	1258	1839
8	840	2852	1505	2364	2646	1697	2847	1882	1992	2841	2928	1745
9	1064	2687	2043	3380	3090	2863	1698	2659	2508	2372	4371	2214
10	2410	2065	2808	3610	3969	2714	1561	2668	2282	3474	3098	3948
11	3553	3537	3701	4684	3790	2595	1307	2654	2464	4731	3204	3457
12	3800	3792	4116	4513	3594	2568	1492	1361	2209	3003	4779	5055
13	4279	3874	4479	4660	3211	2113	1481	1438	2270	4033	5402	4272
14	3921	3462	4005	3403	2836	2246	1915	1742	1463	4748	3941	3559
15	3772	4025	2736	3716	2899	2237	3146	2876	1972	2973	3122	3584
16	812	3292	2435	2507	1991	2457	2607	1472	1131	454	305	1286
17	496	126	321	791	1222	660	106	0	42	583	471	1175
18	408	0	4	19	39	0	104	205	155	791	165	1212
19	559	21	0	0	0	0	84	338	44	1051	95	1463
20	391	40	0	8	0	0	345	178	86	707	179	1311
21	565	20	24	43	0	0	240	133	154	501	464	1446
22	551	177	74	184	110	0	232	256	165	465	418	1750
23	5423	6424	4406	4683	3804	3696	3792	4322	4653	5563	5867	6118

SCE_NoL_to_SCE												
H-S	Jan.	Feb.	Mar.	Apr.	May.	Jun.	Jul.	Aug.	Sept.	Oct.	Nov.	Dec.
0	1024	1025	1153	1159	1157	1132	1094	1080	1048	1101	1013	1029
1	1057	1060	1177	1203	1205	1195	1163	1137	1094	1106	1052	1062
2	1105	1098	1190	1194	1218	1208	1187	1147	1096	1118	1082	1086
3	1113	1105	1190	1163	1195	1180	1156	1140	1096	1115	1095	1103
4	1105	1099	1163	1142	1159	1145	1125	1116	1074	1085	1085	1115
5	1088	1063	1106	1087	1134	1137	1097	1075	1014	1041	1050	1087
6	1014	1006	1066	1086	1132	1116	1081	1048	999	988	1018	1036
7	978	994	1079	1104	1132	1119	1068	1029	1013	995	1003	1006
8	989	1020	1114	1128	1140	1132	1049	1020	999	1003	1016	1000
9	1002	1048	1128	1148	1150	1112	1041	993	999	1024	1035	1025
10	1037	1083	1134	1147	1147	1084	984	988	986	998	1061	1038
11	1052	1097	1127	1148	1132	1058	975	944	959	1015	1061	1062
12	1067	1110	1128	1141	1114	1025	925	893	916	1014	1068	1077
13	1070	1109	1127	1127	1095	988	877	845	881	977	1058	1056
14	1050	1103	1113	1119	1086	964	844	787	843	963	1032	1059
15	1025	1066	1124	1139	1118	977	836	802	825	978	1000	1026
16	1009	1039	1110	1107	1075	938	812	762	804	936	969	987
17	926	943	1029	1045	1010	886	776	736	767	925	901	916
18	904	897	968	987	965	857	768	723	748	875	922	911
19	925	909	965	966	937	850	781	746	770	932	938	930
20	958	936	973	983	941	842	787	765	833	963	943	952
21	951	938	1020	1030	1004	931	895	860	888	1000	957	962
22	1005	997	1074	1081	1043	1004	966	931	943	1045	1000	1003
23	1014	1020	1100	1102	1094	1065	1021	992	991	1050	1008	1008

SCE_TabCC_to_SCE												
H-S	Jan.	Feb.	Mar.	Apr.	May.	Jun.	Jul.	Aug.	Sept.	Oct.	Nov.	Dec.
0	945	517	57	17	108	185	364	445	685	539	370	1257
1	1355	166	164	79	152	202	227	207	284	513	801	1427
2	829	203	293	238	212	216	424	102	363	570	394	1221
3	727	305	408	226	251	241	244	83	589	460	384	1048
4	1307	566	240	181	216	265	398	230	620	910	651	1205
5	1263	882	93	235	510	559	244	416	1236	1040	1058	1660
6	2165	2172	543	1274	2090	1323	731	621	486	747	1393	1318
7	1172	1276	1415	908	677	1158	1025	862	793	936	991	999
8	937	1287	965	1860	1727	1358	990	644	538	841	1601	1389
9	517	1127	1124	3330	3553	3950	1617	1939	2097	949	1382	947
10	1062	1149	1876	3398	4143	4607	2386	2160	1900	1406	812	1236
11	323	1196	2993	3933	4252	4156	3381	3395	2163	1561	1133	1072
12	774	864	3449	4574	4662	4752	2931	2743	2591	2200	1337	1000
13	875	2114	2882	4268	3876	3808	3470	1657	2309	2142	1474	1103
14	1679	896	1992	2696	3518	3592	2310	1895	1975	1764	1890	1657
15	1714	1185	728	1480	1212	1443	1490	1346	997	1458	1600	1663
16	1144	1710	943	1465	1014	1106	476	442	89	379	161	818
17	122	18	329	836	1497	697	0	0	9	361	76	320
18	276	14	99	62	88	158	80	151	99	221	43	399
19	118	15	134	207	129	164	9	133	19	240	41	381
20	203	35	126	234	186	141	149	25	0	376	61	454
21	235	10	52	42	86	158	177	29	28	256	164	582
22	297	8	31	55	133	156	192	186	80	254	98	643
23	2072	3048	1711	2121	1549	1387	1523	1385	2018	2771	2178	2147

10.4 H-W Scenario

PG&E_BAY_to_PG&E_VLY												
H-W	Jan.	Feb.	Mar.	Apr.	May.	Jun.	Jul.	Aug.	Sept.	Oct.	Nov.	Dec.
0	1176	808	1272	1070	649	742	514	663	938	553	1359	1372
1	1053	894	1326	993	431	889	327	440	810	398	1367	1440
2	1051	849	1196	996	334	813	271	348	849	464	1439	1418
3	1242	933	1239	1147	309	863	308	338	924	541	1442	1349
4	1327	805	1531	1198	535	791	368	436	774	783	1379	1216
5	1224	756	1587	1395	711	976	387	657	898	792	1263	1048
6	1167	795	1306	1281	1030	757	545	859	768	775	1313	991
7	980	1147	1345	1189	1055	770	736	895	1176	1109	1138	1077
8	1192	1351	1300	939	993	765	835	876	1087	1121	1277	892
9	1174	1330	1373	933	876	631	900	887	1097	819	1312	1039
10	1367	988	1047	862	693	773	1105	1057	1286	586	1408	1211
11	1089	941	974	828	594	663	1036	1363	1345	1033	1463	1236
12	1235	701	827	838	780	792	1122	1312	1311	751	1364	997
13	1164	788	807	921	608	644	1270	1317	1253	843	1011	927
14	622	636	1274	914	724	782	1113	1638	1069	803	1077	828
15	672	755	942	955	535	739	1207	1359	1014	982	1124	919
16	850	952	1092	1138	925	564	1264	1304	1429	927	991	814
17	735	646	997	1149	642	853	1144	1401	1574	970	1064	819
18	632	828	1228	896	743	948	1095	1564	1489	1132	990	672
19	657	875	1434	965	1039	952	1269	1704	1507	1119	821	742
20	560	869	1296	959	1060	985	1298	1672	1353	1068	897	711
21	593	971	1405	948	907	761	1196	1531	1531	947	789	532
22	614	920	1490	932	877	715	1114	1299	1167	712	959	744
23	1271	909	1483	1229	1067	949	522	1005	1027	952	1580	1474

SCE_to_SDGE												
H-W	Jan.	Feb.	Mar.	Apr.	May.	Jun.	Jul.	Aug.	Sept.	Oct.	Nov.	Dec.
0	1920	2011	2064	2033	1690	1673	1118	1155	1539	1757	1930	1866
1	2276	2354	2204	1858	2089	1897	1468	1376	1739	2204	2443	1655
2	2168	2222	1961	2087	1785	1968	1679	1688	1920	2406	2365	2265
3	1950	1941	2114	1791	2164	1979	1792	1764	2090	2504	2137	2200
4	2278	1979	2524	2088	1929	1745	1716	1634	2142	2134	2263	2037
5	2068	2541	2263	2050	1949	2107	1729	1253	1929	2016	2005	2295
6	2062	1982	2025	2584	2749	2771	2822	2503	1978	1651	2129	1852
7	1820	2598	2540	1939	1560	1674	1614	2614	2670	3064	2764	1735
8	2687	2225	1396	2025	2444	2346	1311	1083	1265	1667	1962	2852
9	2364	1150	1226	2259	2074	2049	1411	1113	1877	1541	1268	1873
10	1426	1748	1210	1756	2020	1858	1437	1182	1152	1828	1464	1590
11	1390	1379	1664	1954	2104	1834	1222	1734	1289	1927	1448	1314
12	1722	1899	2097	2230	1897	1703	1391	1175	1353	2012	1636	1397
13	2187	1995	2308	2171	2049	1684	1051	1244	1818	1762	1475	2087
14	2091	1766	2444	2147	2457	2029	1519	1592	2020	1677	2005	2455
15	2342	2175	1802	2281	2479	2083	1568	1891	1824	2764	2346	2341
16	2425	2454	2411	1826	1604	1931	2445	2119	1514	1798	2034	2344
17	1639	1665	2272	2188	2132	2034	782	358	353	753	1522	1366
18	1202	1227	1205	988	684	241	40	123	256	505	1463	1056
19	1310	1269	1143	840	325	143	10	77	291	618	1550	1298
20	1612	1449	1216	774	265	73	0	114	306	625	1801	1539
21	1635	1328	1427	1092	421	247	181	350	1174	1194	1759	1546
22	2076	1798	1753	1416	825	514	148	513	1197	1288	2147	2171
23	870	1062	1001	1144	710	220	87	129	472	926	1435	946

PG&E_VLY_to_SCE												
H-W	Jan.	Feb.	Mar.	Apr.	May.	Jun.	Jul.	Aug.	Sept.	Oct.	Nov.	Dec.
0	1898	1364	1404	1299	1237	1520	1386	1613	1643	828	2144	1938
1	1551	934	953	1067	1255	1999	1221	1173	1340	582	1411	1614
2	1051	760	695	1322	1205	1729	932	837	1102	439	774	994
3	953	711	733	1159	1243	1639	694	777	1026	413	713	869
4	940	682	965	1708	1092	1366	1247	1057	1265	750	710	709
5	1295	768	1684	1580	1976	2057	1633	1590	1663	1737	1355	911
6	1662	1540	1891	1498	1344	1448	1625	1556	1556	1892	2170	1419
7	1906	1495	1453	1731	1052	1192	1630	1399	1039	1297	1464	1956
8	574	1497	1206	1491	1703	2114	945	1135	746	1726	1259	1131
9	505	1422	1562	1639	2432	1974	1734	1320	893	1871	1174	1167
10	634	1150	1645	1687	1942	1790	1888	1463	897	1784	1461	958
11	609	1561	1602	1587	1860	1786	2019	1567	1067	1636	1126	626
12	957	1562	1538	1702	1701	2030	2076	1493	970	1735	1785	740
13	1088	1201	1815	1709	1901	1920	1708	1245	1036	1542	1738	867
14	894	1536	1574	1781	1897	1656	1852	1165	1118	1705	1450	1111
15	936	1987	1568	1100	1399	1288	1617	1067	1054	1637	1052	1088
16	1584	1333	1531	1304	1133	722	1184	462	746	1084	1699	1276
17	1353	1700	2168	1812	1629	998	741	41	632	1440	968	1095
18	1215	1333	1654	1588	1348	1262	1096	143	411	1417	1347	1019
19	1189	1443	1460	1485	1187	1166	878	64	428	1735	1261	1165
20	1216	1679	1362	1434	1262	1380	847	114	580	1825	1396	1279
21	1157	1869	1706	1694	1066	1248	1666	657	671	1751	1338	1195
22	1350	1799	1634	1436	1127	1048	1338	1564	1513	1549	1525	1303
23	329	115	175	190	288	377	95	315	367	180	254	288

SCE_East_to_SCE												
H-W	Jan.	Feb.	Mar.	Apr.	May.	Jun.	Jul.	Aug.	Sept.	Oct.	Nov.	Dec.
0	305	832	1099	794	854	545	747	534	475	1361	215	137
1	636	1303	1347	949	965	745	965	936	765	1570	741	454
2	860	1223	1388	831	864	763	1252	1270	1031	1586	950	638
3	834	1155	1234	840	865	803	1254	1367	1112	1572	946	761
4	851	1157	962	619	833	666	999	1005	855	1335	943	747
5	781	1073	540	353	335	305	480	563	315	510	622	744
6	269	351	76	614	752	690	1108	611	69	127	165	296
7	79	62	282	543	587	549	554	1092	525	497	69	25
8	142	504	546	460	519	491	681	189	673	452	375	197
9	527	398	428	363	365	148	345	670	271	445	624	380
10	525	528	491	418	274	149	264	349	406	389	395	498
11	272	727	574	413	276	29	230	60	231	517	518	811
12	564	504	595	347	219	26	136	27	173	358	674	766
13	479	747	676	412	339	38	74	10	90	408	804	824
14	756	729	731	414	244	53	57	47	514	574	622	601
15	562	816	649	722	671	539	530	588	516	572	719	571
16	227	640	560	660	607	559	605	354	410	372	92	113
17	3	203	73	450	881	770	550	248	0	30	47	16
18	2	38	181	547	697	171	50	15	0	22	1	19
19	17	24	213	429	651	419	50	25	0	49	24	22
20	20	98	180	404	532	192	72	19	0	63	37	20
21	41	62	338	591	935	723	61	0	0	180	33	24
22	98	210	670	748	1085	1001	745	165	183	492	104	41
23	273	568	697	916	1182	1125	1064	418	513	584	372	341

SCE_EoL_to_SCE												
H-W	Jan.	Feb.	Mar.	Apr.	May.	Jun.	Jul.	Aug.	Sept.	Oct.	Nov.	Dec.
0	3544	3978	3811	3106	2984	2255	2895	3102	3555	4301	3539	3538
1	3956	4461	4192	3511	3135	2502	3488	3525	3948	4548	4135	4025
2	4161	4378	4339	3492	3209	2711	3782	3925	4287	4596	4433	4340
3	4268	4349	4176	3422	3196	2755	3934	4121	4351	4580	4437	4456
4	4306	4349	3908	3044	2915	2198	3489	3688	4157	4371	4463	4486
5	4166	4289	3393	2630	2759	2111	2972	3233	3389	3527	4145	4350
6	3409	3358	2607	1076	924	836	757	728	1596	2589	3477	3838
7	2704	1396	1314	2121	2769	2667	2141	1023	1487	1586	1189	2637
8	1277	1620	2645	3360	3354	3009	4011	3256	2426	1346	1983	1419
9	1639	2856	2939	3493	3296	2930	3215	3130	2789	2946	1786	1169
10	1426	3411	3288	3610	3218	3025	3060	2961	3094	3234	1983	1742
11	2241	3578	3678	3492	3039	2821	3111	3168	2875	2818	2451	2068
12	1702	3708	3403	3389	3273	2956	2950	2755	2945	3175	3342	1920
13	1996	3680	3227	3339	3257	2704	2901	2454	3017	2471	2516	1792
14	1622	3122	2763	3341	3137	2953	2979	2717	2646	2301	1946	1918
15	1645	2182	2428	2953	3391	3004	3369	3004	1858	1752	1620	1166
16	1633	774	889	1849	2182	2355	2420	668	627	1073	2515	2133
17	1533	2828	2173	948	388	491	519	214	774	1906	1358	1149
18	1391	1930	2282	3137	3394	2190	1071	350	506	1775	1317	1128
19	1453	1970	2145	2754	3176	2192	861	260	544	2022	1450	1156
20	1527	2223	2147	2652	2877	1962	789	321	691	2101	1615	1230
21	1553	2339	2644	3301	3643	2968	1598	899	991	2562	1603	1307
22	2131	2974	3178	3491	3885	3423	3235	2205	2337	3056	2213	1608
23	4659	4656	4676	4705	4666	4653	4717	4814	4695	4661	4637	4674

SCE_Metro_to_SCE												
H-W	Jan.	Feb.	Mar.	Apr.	May.	Jun.	Jul.	Aug.	Sept.	Oct.	Nov.	Dec.
0	338	83	523	357	314	67	0	41	186	219	690	401
1	725	622	1094	1181	681	135	24	19	370	597	884	1324
2	1618	1403	1542	1057	878	176	12	73	583	905	1299	1437
3	1592	2110	1449	1384	636	237	61	152	638	1020	1505	1739
4	1352	1839	693	1042	516	245	12	43	375	780	1681	1663
5	1543	1045	422	676	1103	235	141	64	133	241	1416	1220
6	791	439	600	1094	1452	1323	597	166	199	442	1037	812
7	581	921	616	2041	2016	1374	1249	143	1715	1236	1084	619
8	1110	1199	2411	2721	1880	1842	2151	1984	2026	1772	2390	1346
9	1531	2369	2884	3023	2504	2190	790	2345	1913	1938	3259	1368
10	1394	2611	3049	4106	3087	1859	621	752	1853	2642	3993	1808
11	2139	3627	3444	4167	2947	1940	290	728	2088	2713	2940	2508
12	2053	3541	3394	3814	3329	1532	185	590	1548	3300	3651	2728
13	2723	4221	3622	3935	2835	1477	350	640	1566	2500	3754	3454
14	3068	4050	2497	2869	2675	1369	83	528	1827	2894	4813	3355
15	2205	2999	2652	2639	2621	2070	1693	1890	2599	2584	3444	2002
16	704	3045	1819	1797	1111	1402	1195	698	692	181	289	149
17	19	88	183	417	564	505	0	0	0	0	4	13
18	0	0	0	15	20	0	0	0	0	0	7	11
19	0	0	0	0	0	0	0	0	0	0	0	3
20	17	0	0	0	0	0	0	0	0	0	8	16
21	0	0	2	4	0	0	0	0	7	0	28	8
22	33	19	74	111	9	0	0	0	0	4	30	18
23	1024	658	714	479	308	249	7	101	157	454	782	1004

SCE_NoL_to_SCE												
H-W	Jan.	Feb.	Mar.	Apr.	May.	Jun.	Jul.	Aug.	Sept.	Oct.	Nov.	Dec.
0	1021	1025	1151	1158	1154	1133	1093	1079	1046	1087	1012	1009
1	1055	1059	1176	1202	1202	1192	1161	1136	1092	1104	1050	1047
2	1103	1098	1189	1193	1216	1207	1186	1146	1094	1116	1082	1085
3	1113	1104	1189	1162	1193	1179	1154	1139	1093	1113	1096	1103
4	1105	1099	1162	1141	1159	1144	1123	1115	1072	1083	1086	1115
5	1086	1063	1106	1087	1133	1134	1097	1074	1014	1021	1049	1086
6	1010	1007	1066	1085	1137	1121	1085	1050	1000	987	1001	1027
7	976	999	1084	1104	1135	1122	1072	1037	1017	997	1006	1004
8	995	1027	1118	1127	1143	1131	1051	1028	1014	1017	1022	1005
9	1006	1054	1132	1147	1154	1117	1041	1012	1001	1024	1039	1026
10	1047	1082	1135	1148	1151	1088	995	994	988	1025	1064	1043
11	1055	1096	1130	1153	1136	1059	977	945	960	1033	1072	1073
12	1073	1110	1129	1144	1117	1023	925	896	918	1026	1071	1093
13	1072	1108	1127	1130	1099	989	875	847	883	995	1056	1072
14	1059	1108	1116	1118	1086	967	842	802	844	974	1035	1063
15	1034	1074	1122	1141	1117	978	850	805	828	978	1006	1030
16	1009	1042	1113	1108	1077	940	811	764	806	937	967	983
17	923	941	1029	1047	1010	886	774	734	766	888	899	904
18	901	896	967	986	964	856	766	722	748	871	902	899
19	922	907	963	964	935	848	766	726	768	910	920	923
20	956	934	972	982	939	841	785	745	805	926	940	945
21	950	936	1019	1028	1002	929	882	843	887	997	954	939
22	1003	995	1072	1080	1041	1002	956	928	940	1029	997	982
23	1021	1027	1101	1103	1096	1071	1021	996	996	1050	1013	1017

SCE_TabCC_to_SCE												
H-W	Jan.	Feb.	Mar.	Apr.	May.	Jun.	Jul.	Aug.	Sept.	Oct.	Nov.	Dec.
0	24	35	37	223	144	269	172	0	20	41	0	32
1	43	91	152	244	163	145	174	14	11	145	23	20
2	146	360	288	290	273	206	263	134	72	353	123	104
3	251	572	253	232	265	113	287	118	61	352	170	149
4	216	483	120	183	250	324	180	63	34	135	54	200
5	84	264	11	179	177	164	0	25	21	33	35	129
6	59	146	127	798	787	1424	602	540	110	65	16	50
7	153	720	882	1379	980	652	695	784	820	467	890	138
8	1284	1064	1428	2265	1778	2517	1311	1301	1457	1316	1933	1391
9	1367	959	2601	3146	3351	3389	2066	2089	1937	1096	1240	1365
10	1434	1229	3053	4102	3851	3492	2563	2144	2087	2103	1646	1256
11	1104	2599	3064	4241	3728	4125	2628	2126	2864	2343	1531	1264
12	1542	2839	3270	4304	4029	3605	2784	2782	3010	2428	1538	1096
13	1481	2329	3630	3919	3464	3614	2764	2944	2730	2046	1311	1481
14	1735	2031	2213	2773	3074	3272	2059	2062	2174	1362	1033	1506
15	1110	790	1575	1783	1699	2159	1560	1543	1220	766	1891	1239
16	318	2271	1100	1172	834	1072	796	340	375	235	6	52
17	30	0	104	726	632	737	263	143	8	0	13	55
18	52	20	59	51	72	126	156	54	38	2	3	75
19	59	8	53	38	77	47	150	67	17	2	2	37
20	58	6	84	49	60	73	111	64	0	2	0	45
21	38	4	21	24	71	36	61	22	28	3	22	57
22	5	0	3	44	82	53	95	3	7	0	8	3
23	387	563	332	241	234	145	281	242	353	430	399	302